National Research Council Canada
Conseil national de recherches Canada

Division of Physics
Division de physique

NRC Workshop on Water Calorimetry

June 6 and 7 1988

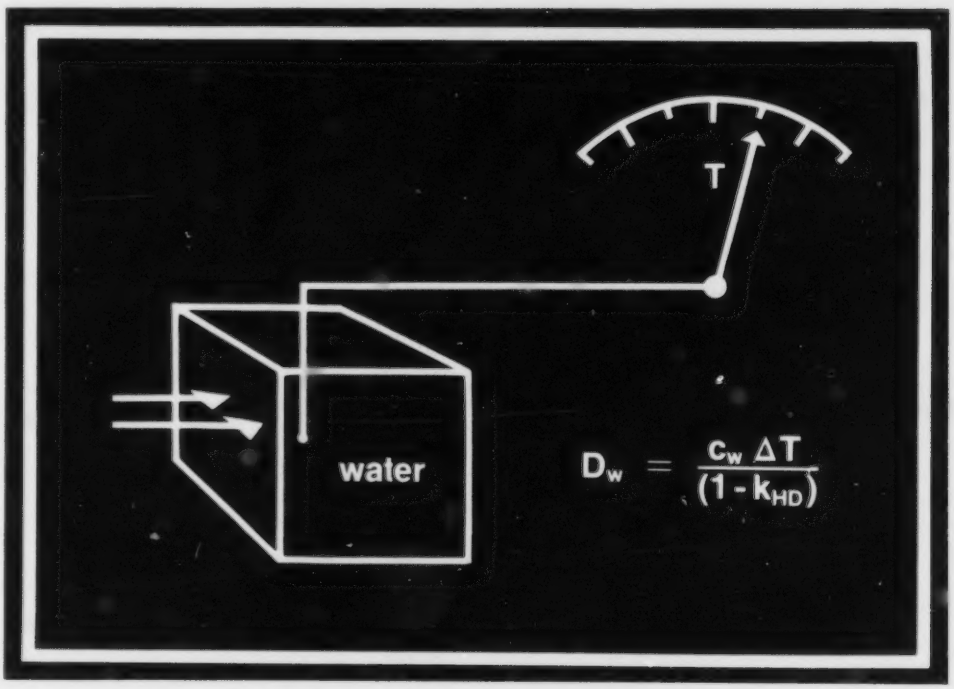

Canada

NRC-29637

89-03243/

Price: $15.00
ISBN no. 0-660-12942-6
DSS catalogue no.: NR15-35/1988E
NRC publication no.: 29637

Sold by:

Publication Sales and
Distribution Section
National Research Council
Ottawa, Ontario
K1A 0R6

Prix: $15.00
N° ISBN: 0-660-12942-6
N° de catalogue du MAS: NR15-35/1988E
N° de publication du CNRC: 29637

En vente par:

Le Service de vente et diffusion
des publications
Conseil national de recherches
Ottawa Ontario
K1A 0R6

NRC WORKSHOP ON WATER CALORIMETRY

Proceedings of a workshop
held at the
National Research Council of Canada
in Ottawa on June 6-7, 1988

Edited by

C.K. Ross
N.V. Klassen
Division of Physics
National Research Council
Ottawa, Canada K1A 0R6

Contents

Preface v

Group photograph vii

List of participants ix

The Role of the Water Calorimeter in High-Energy Medical Radiation Dosimetry
R. Loevinger 1

The Current Status of Water Absorbed Dose Calorimetry in the PTB
M. Roos 9

Water Calorimetry at Radiation Physics Department Göteborg
O. Mattsson 17

Recent Developments in Graphite and Water Calorimeters for Electron Beam Dosimetry at NPL
D.T. Burns and W.T. Morris 25

Water Calorimetry in Edinburgh
T.M. Kehoe and G. Galloway 31

The Direct Determination of Dose-to-Water Using a Flexible, Temperature-Regulated, Sealed-Core Water Calorimeter
R.J. Schulz, C.S. Wuu and M.S. Weinhous 39

The Chemical Heat Defect of Water
N.V. Klassen, C.K. Ross, K.R. Shortt and G.D. Smith 55

Determination of the Heat Defect of Water by Total Absorption of Soft X-Rays
K. Hohlfeld, H.M. Kramer and H.J. Selbach 61

Water Calorimetry, with Emphasis on the Heat Defect
C.K. Ross, N.V. Klassen, K.R. Shortt and G.D. Smith 69

Measurement of the Heat Defect of Water Caused by High-Energy Electrons
M. Roos 77

The Role of Water Purity, Convection and Heat Conduction in a New Calorimeter Design
S.R. Domen 85

Calorimetry in 1913
D.V. Cormack 93

The Radiation Chemistry of Water at High LET
N.V. Klassen and C.K. Ross 95

Concepts to Improve Water Calorimeter Sensitivity and Accuracy
J.W. Fletcher 99

Water Calorimetry in Medium Energy X-Ray Beams
J. Seuntjens, H. Thierens, A. Poffyn and O. Segaert 101

Brief Report on the New NPL Calibration Service in Absorbed Dose to Water for High-Energy X- and Gamma-Radiation
D.T. Burns, J.E. Burns and B. Owen 109

Construction of a Prototype High Sensitivity Pulsed Calorimeter
H. Kubo 111

Measurement of the Thermal Defect of Water Exposed to Protons in the Range 0.9-40 MeV
R.J. Schulz and N. Venkataramanan 115

Ferrous Sulfate Dosimetry and its Role in Establishing an Absorbed Dose to Water Standard for the National Research Council of Canada
K.R. Shortt, N.V. Klassen, C.K. Ross and G.D. Smith 121

Concluding remarks
C.K. Ross 127

General discussion 129

After dinner talk, Monday, June 6:

Detection of Individual Variation in Radiosensitivity in Human Populations: Possible Consequences for Radiogenic Cancer Risk and for Radiotherapeutic Tumour Management
N.E. Gentner and D.P. Morrison 135

Preface

The need for improved high energy absorbed dose standards for photon and electron beams used for radiation therapy has been recognized for a long time. For radiation therapy purposes, the reference material for specifying the absorbed dose is usually water, and so the most direct way of establishing a suitable absorbed dose standard is with a water calorimeter. Throughout the 1980s a number of laboratories have actively pursued the possibility of constructing a practical water calorimeter. By 1988, a considerable body of expertise, both published and anecdotal, had been built up and it seemed a useful time in the development of water calorimetry to bring together the workers in the field to pool their expertise, to assist in solving each other's problems, to describe their current research activities, to examine the best ways to proceed in the future and to encourage each other in their endeavours. This Workshop has, indeed, brought together most of those active in the field.

In order that this Workshop act as an authorative reference of the state-of-the-art in 1988, all the presentations made during the Workshop are included in these Proceedings. Included as well, is a comprehensive resume of the discussion periods, transcribed from tapes made during the Workshop. The editors wish to thank all the participants for supplying manuscripts of their talks so promptly. The editors take responsibility for the transcription of the tapes.

After the banquet on Monday night, Dr. Gentner from Chalk River gave a lively and informative presentation on the variation in the response of biological systems to ionizing radiation. He has kindly provided us with a manuscript based on his talk for inclusion in the Proceedings.

We would like to thank all those who participated in the Workshop, and hope you find these Proceedings a useful permanent record.

C.K. Ross
N.V. Klassen

BACK ROW: Gerry van Dyk, Wally Fletcher, Dave Rogers, Olof Mattsson, Joe McDonald, Leo Heistek, Eugenio Cecatti, Martin Roos, Bill Henry, George Yelle.
MIDDLE ROW: David Burns, Mireille Boutillon, Alex Bielajew, Steve Domen, Klaus Hohlfeld, Joanna Cygler, Len Van der Zwan, Dale Kubo, Josiane Daures, Bob Loevinger, Bob Schulz.
FRONT ROW: Rob Barnett, Doug Cormack, George Smith, Norman Klassen, Carl Ross, Ken Shortt, Jan Seuntjens, Terry Kehoe.

List of Participants

R. Barnett, Toronto-Bayview Regional Cancer Centre, 2075 Bayview Avenue, Toronto, Ontario M4N 3M5 CANADA

A.F. Bielajew, Division of Physics, National Research Council of Canada, Montreal Road, Ottawa, Ontario K1A 0R6 CANADA

M. Boutillon, BIPM, Pavillon de Breteuil, F-92310, Sèvres, FRANCE

D.T. Burns, Division of Radiation Science and Acoustics, National Physical Laboratory, Teddington, Middlesex, UNITED KINGDOM

E. Cecatti, Comissao Nacional de Energia Nuclear, Instituto de Radioprotecao E Dosimetria, Av des Americae, Km 115 - Barra da Tijuca, Cx.P. 37025 - Rio de Janairo, BRAZIL

D.V. Cormack, Tom Baker Cancer Centre, 1331 - 29th Street N.W., Calgary, Alberta T2N 4N2 CANADA

J. Cylger, Medical Physics Department, Ottawa Regional Cancer Centre, Civic Division, 190 Melrose Avenue, Ottawa, Ontario K1Y 4K7 CANADA

J. Daures, Laboratoire de Métrologie des Rayonnements Ionisants, BP 6-91192, Gif-sur-Yvette, Saclay, FRANCE

S. Domen, Center for Radiation Research, National Bureau of Standards, Gaithersburg, MD 20899 U.S.A.

G. van Dyk, Atomic Energy of Canada Ltd., Radiochemical Research Company, 413 March Road, P.O. Box 13500, Kanata, Ontario K2K 1X8 CANADA

J.W. Fletcher, Atomic Energy of Canada Ltd., Chalk River Nuclear Laboratories, Chalk River, Ontario K0J 1J0 CANADA

W.H. Henry, 580 Thessaly Circle, Ottawa, Ontario K1H 5W5 CANADA

K. Hohlfeld, Physikalisch-Technische Bundesanstalt, D-3300 Braunschweig, Bundesallee 100, FEDERAL REPUBLIC OF GERMANY

T. Kehoe, Department of Medical Physics and Medical Engineering, Western General Hospital, Edinburgh, EH4 2XU, SCOTLAND

N.V. Klassen, Division of Physics, National Research Council of Canada, Montreal Road, Ottawa, Ontario K1A 0R6 CANADA

H. Kubo, University of Rochester Cancer Center, 601 Elmwood Avenue, P.O. Box 647, Rochester, N.Y. 14642 U.S.A.

R. Loevinger, Center for Radiation Research, National Bureau of Standards, Gaithersburg, MD 20899 U.S.A.

O. Mattsson, Radiation Physics Department, Sahlgren Hospital, University of Göteborg, S-41345 Göteborg, SWEDEN

J. McDonald, P7-03, Battelle Northwest Laboratory, P.O. Box 999, Richland, Washington 99352 U.S.A.

K. Metha, Atomic Energy of Canada Ltd., Whiteshell Nuclear Research Establishment, Pinawa, Manitoba ROE 1L0 CANADA

D.W.O. Rogers, Division of Physics, National Research Council of Canada, Montreal Road, Ottawa, Ontario K1A 0R6 CANADA

M. Roos, Physikalisch-Technische Bundesanstalt, D-3300 Braunschweig, Bundesallee 100, FEDERAL REPUBLIC OF GERMANY

C.K. Ross, Division of Physics, National Research Council of Canada, Montreal Road, Ottawa, Ontario K1A 0R6 CANADA

R.J. Schulz, Department of Therapeutic Radiology, Yale University School of Medicine, New Haven, CT 06510 U.S.A.

J. Seuntjens, Dosimetry Laboratory, Ghent State University, Proeftuinstraat 86, B-9000 Ghent, BELGIUM

K.R. Shortt, Division of Physics, National Research Council of Canada, Montreal Road, Ottawa, Ontario K1A 0R6 CANADA

G.D. Smith, Division of Physics, National Research Council of Canada, Montreal Road, Ottawa, Ontario K1A 0R6 CANADA

L. van der Zwan, Division of Physics, National Research Council of Canada, Montreal Road, Road, Ottawa, Ontario K1A 0R6 CANADA

THE ROLE OF THE WATER CALORIMETER IN HIGH-ENERGY MEDICAL RADIATION DOSIMETRY

Robert Loevinger
Center for Radiation Research, National Bureau of Standards
Gaithersburg, MD 20899. U.S.A.

ABSTRACT - The water calorimeter is a direct, energy-independent method of measuring absorbed dose in tissue-like material. It is proposed that the roles of the water calorimeter are to stimulate research, and to provide a reliable primary standard and convenient secondary standard of water absorbed dose for high-energy radiation.

Le calorimètre à eau est un instrument de mesure directe, indépendante de l'énergie, de la dose absorbée par une matière de type tissulaire. On propose que le calorimètre à eau joue trois rôles: stimuler la recherche et devenir un étalon primaire fiable et un étalon secondaire pratique de la dose absorbée par l'eau sous des rayonnements très énergétiques.

Introduction

It is the goal of medical radiation dosimetry to determine the absorbed dose at suitable points in a material that serves as a "phantom" (i.e., substitute) for human or other biological tissue. Water is generally accepted as the reference phantom material, for several reasons:

It is available and has a composition known to anyone in any country, now and in the future.

It has absorption properties and mass density close to those of soft tissue, for photons and electrons.

Because it is a fluid, it can be adapted to a variety of purposes.

Many other phantom materials have been used, of which I will have occasion to mention only two: graphite and polystyrene. While assuredly water has some disadvantages, it remains the standard phantom material for medical radiation dosimetry.

Modern radiation therapy, when practiced with curative intent, utilizes high-energy radiations, i.e., primarily photon and electron beams with energies from 1 MeV to perhaps 30 or 35 MeV. The uncertainty of the dosimetry associated with such high-energy radiations is due in a good part to the problems of energy dependence of the detectors and of the physical factors that enter the calculations.

The choice of water as the phantom material, absorbed dose as the physical quantity, and high-energy radiation as the modality, cry out together for a water calorimeter. There are several ways of measuring absorbed dose, but clearly the calorimeter is the most nearly direct, and is by its very nature energy independent. Water calorimetry in one form or another has actually been used in radiation measurements for more than 50 years.

Because this meeting is concerned with current developments in water calorimetry, and because this talk is concerned with the present and future role of the water calorimeter, no historical review is attempted. Consideration is directed to a water calorimeter capable of determining absorbed dose at a point in stagnant water, and to the problems associated with such a calorimeter. The modern history of such an absorbed-dose water calorimeter starts with the 1980 paper by S. R. Domen in the journal Medical Physics.

It is my view that the absorbed-dose water calorimeter has three roles to play in medical radiation dosimetry:

Role I. To stimulate research.

Role II. To provide a reliable primary standard of water absorbed dose for high-energy radiations.

Role III. To provide a convenient secondary standard of water absorbed dose for high-energy radiations.

Before discussing these roles, I wish to comment on four problems. Of course, there are many experimental problems that must be solved in creating and operating a water calorimeter, but these four seem to be inherent in water calorimetry. They are heat defect, convection, heat conduction, and excess heat from nonwater materials.

Heat Defect

There are a variety of reactions to ionizing radiation in water that could in principle give rise to a heat defect, positive or negative, depending on circumstances. Ross et al. (1988) have examined the matter and concluded that radiation-induced chemical reactions are the most likely mechanism giving rise to a heat defect in

water. Among the earliest work in absorbed dose water calorimetry appears to be that of Pettersson (1967), who assumed zero heat defect in air-saturated water after an irradiation of 1.2 kGy, and Lovell and Shen (1976), who calculated a value of 0.3% in aerated water using very high doses. Essentially all subsequent publications on water calorimeters have at least mentioned the matter.

The basis for our present insight comes from Fletcher (1982), who used the Boyd-Carver-Dixon (1980) model for the radiolysis of water. Ross et al. (1984, 1988), in a series of sophisticated experiments, have used this model to study the effects of dissolved gases, and found good agreement between theory and experiment. It seems likely to me that we now have adequate knowledge of the heat defect of ultra-pure water handled in a sealed, noncontaminating system using appropriate dissolved gases. Schulz et al. (1987) were the first to describe the use of such a system.

In what we might call the real world, we seldom have ultra-pure water and a noncontaminating system. Domen (1982) found what he believed to be a negative heat defect of 3.5%, comparing the water calorimeter to the NBS graphite calorimeter. A similar result has been obtained by several subsequent investigators (Barnett, 1986; de Marles, 1981; Kubo, 1983, 1985; Mattsson, 1984) who found values from 2 to 5%. These latter results were obtained by comparison of water calorimeter measurements with ionization chamber measurements, so they contain any uncertainty inherent in the ionization chamber protocols, and are only secondarily traceable to graphite calorimeters. It is difficult to judge whether these differences reflect differences in water quality, or simply experimental variation, or real errors in the ionization-chamber protocols. A safe generalization is this: the heat defect of water is dose dependent, dose-rate dependent, and very sensitive to impurities. Bewley (1984) suggested that the use of a solution with a known heat defect, however large, is preferable to an unknown heat defect, even if it is small.

It has not yet been decided whether ordinary distilled water in an open system, using appropriate dissolved gases, gives everywhere the same heat defect. I believe that this is an important matter that deserves further investigation, as I shall point out later.

Convection

In his original paper on the water calorimeter, Domen (1980) believed that he had detected convection, and he suggested the use of thin, non-perturbing barriers to eliminate it. He was perhaps mistaken in his interpretation (the thermistor power was 300 μW!), but the suggestion of convection barriers was valid, and he has repeated the suggestion in subsequent papers. Of course, the polyethylene films, used by Domen to support the thermistors, themselves constituted a convection barrier.

The first clear observation of convection in a water calorimeter was made by Schulz and Weinhous (1985). There has been some small published controversy between Schulz (1986) and Domen (1986, 1988b) concerning the exact interpretation of the Schulz and Weinhous observations, but no controversy about the existence of convection, which was also clearly demonstrated by Barnett (1986).

It is readily shown that convection can arise in a large water calorimeter. Domen (1987), starting with the Rayleigh number, showed that the onset of convection at room temperature is to be expected when the product of the absorbed dose difference between two positions times the cube of their vertical separation, is greater than 4×10^5 Gy mm^3. For a horizontal beam with a 100-mm diameter and a dose of only one gray, the product becomes 10^6 Gy mm^3, clearly well into the convection region. It does not necessarily follow that the thermistor reading will be in error, because if the water velocity is slow enough the water passing the thermistor will be at a very nearly constant temperature. Domen (1988a) has studied the effect of convection velocity on thermistor reading.

A thermistor operated at high power is particularly sensitive to convection. The temperature rise in water is 0.24 mK/Gy, and Domen (1982) measured a temperature rise in the thermistor of 2.6 mK/μW of power dissipation. From this it follows that the ratio of the equilibrium thermistor temperature rise to the water temperature rise is approximately 10 times the power in microwatts divided by the dose in grays. Thus, for 80 μW and 20 Gy (approximately the Schulz and Weinhous values), the equilibrium thermistor temperature rise is 40 times that of the water. It is evident that a small change in the equilibrium thermistor temperature due to convection can easily give a significant measurement error.

Convection effects can be controlled or eliminated in a variety of ways, for example by stirring the water, by circulation of the water between runs, by the use of convective barriers and low thermistor powers, or by operation at 4°C. I believe that convection need no longer be considered a problem.

Heat Conduction

It is self-evident that conduction will eventually distort the isothermal surfaces that we interpret as isodose surfaces. The trick in using a water calorimeter is to complete the measurement before this happens. Domen (1987) has described use of the Schmidt method of numerical calculation of heat conduction, and Roos (1987) has presented calculations for some extreme circumstances that illustrate considerable error due to heat conduction. Barnett (1986) has presented calculations showing the effect of conduction on depth-dose profiles for cobalt-60, 15-MV x rays, 10-, 12-, 15-, and 18-MeV electrons. Heat conduction in a water calorimeter is well understood, and if the dose gradient is not too great, and the dose rate not too low, conduction does not present a problem to measurement of absorbed dose at a point.

In the presence of a steep dose gradient or a dose rate so low that it requires very long irradiation times, it appears to be impossible at this time to use a water calorimeter to measure absorbed dose at a point. However, Domen (1982) has suggested that it may be possible to circumvent the steep gradient problem. He suggest placing a heat conduction barrier on the distal side of the measurement point. This barrier could be made of nonwater material that serves as an excess heat source. This suggestion has not been put into practice, so far as I know, but Domen informs me that calculations will be made in the near future.

Excess heat from nonwater materials

The correction for nonwater materials may involve the atomic number, mass density, and specific heat of the foreign materials, the last being normally the most important. The high specific heat of water means that all nonwater materials likely to be used in a water calorimeter will contribute unwanted heat. Polyethylene has about one-half, and both graphite and Pyrex glass have about one-sixth the specific heat of water, and other materials of interest here fall in between. Thus nonwater materials show a temperature rise between two and six times that of water.

The excess heat must be accounted for, or shown to be negligible. Domen (1982) has discussed this problem with respect to the polyethylene films that enclosed his thermistors. Barnett (1986) has presented detailed calculations for the excess heat in the polyethylene films and the thermistors. Ross et al. (1988) have given a detailed account of their meticulous treatment of this problem for a calorimeter for which all parts were within the radiation beam. I believe that the correction for excess heat from foreign, nonwater materials is adequately understood, and need not be considered a problem.

Role I. To stimulate research.

The modern water calorimeter has stimulated many talented persons to carry out further work on the radiolysis of water, and on energy transport in water by conduction and convection. By challenging the conventional ionometric and chemical methods, it has stimulated a renewed look at their reliability.

Even if we never have a reliable absorbed dose water calorimeter as a primary standard in our national laboratories, even if we never have a convenient absorbed dose water calorimeter as a secondary standard in our hospitals, the work that has already been devoted to the absorbed dose water calorimeter will have been worthwhile because of the information that has resulted from the research that has been stimulated in these fields. We can be very satisfied with what has already been accomplished, and the work has only just begun.

Role II. To provide a reliable primary standard of water absorbed dose for high-energy radiation.

I use the phrase primary standard to mean a standard that realizes the unit of a physical quantity in terms of its definition. In this sense ionization chambers and chemical dosemeters cannot serve as primary standards of absorbed dose, since they require an empirically determined yield (the well-known W-value or G-value) that is obtained from the literature. A cavity ionization chamber can however serve as a primary standard of exposure: the energy per ion pair is not required since the quantity exposure is defined in terms of charge. There are always empirically determined factors that are used in realizing the unit from its definition, but these are correction factors of the order of unity, experimentally evaluated by the laboratory establishing the standard, and are not considered to vitiate the statement that the unit has been determined in terms of the definition of the quantity.

For the purpose of this talk, I assume that the primary standard of absorbed dose is used to establish the absorbed dose rate at a point in an open water phantom at a national standardizing laboratory. The matter of disseminating the magnitude of the unit so established is not considered here. For simplicity, I limit consideration to beams of photons and electrons.

I consider here five methods of establishing a primary standard of water absorbed dose for high-energy radiations, four based on a water calorimeter and, for comparison, a fifth based on a graphite calorimeter. I will describe each very briefly, and then comment on what appear to me to be its advantages and disadvantages. These evaluations of advantage and disadvantage are made with respect to contributions to the overall uncertainty in absorbed dose determination, without regard to whether the method is more or less complicated, or more or less time-consuming. Complexity in construction or operation is not here considered a disadvantage.

National Research Council (Ross et al., 1988). This is a three-step procedure. 1) Mean absorbed dose rate will be determined in a sealed glass vessel with about 100 cm^3 of stirred, ultra-pure water and appropriate dissolved gases. The entire water volume will be irradiated. 2) Fricke solution will be irradiated in the same vessel, and thus calibrated in all beams of interest. 3) The Fricke solution will be used separately to determine the absorbed dose rate at a point in an open water phantom.

Advantages are that the method uses a heat defect supported by theory, and convection is irrelevant. Disadvantages are the indirect nature of the dose determination, involving a second dosemeter, and the necessity for detailed determination of heat excess from all parts of the vessel.

National Bureau of Standards (Domen, 1988c). This is a single-step procedure. 1) Absorbed dose rate at a point will be determined in a sealed, thin-walled glass vessel with about 100 cm^3 of stagnant, ultra-pure water and a dissolved gas. The entire vessel is irradiated, while suspended in an open water phantom.

Advantages are that the method gives absorbed dose rate at a point, it uses a heat defect supported by theory, convection will be negligible in the small vessel, and it will not be necessary to determine heat excess from all parts of the glass vessel, since not all the excess heat from the vessel will reach the measurement point.

Physikalisch-Technische Bundesanstalt (Hohlfeld et al., 1987; Roos, 1987; Roos and Hohlfeld, 1987). This is a two-step procedure. 1) Absorbed dose rate at a point will be determined in an open water phantom using thermistors supported between thin films. The calorimeter will be operated at 4°C in a horizontal beam using distilled water. Gas will be bubbled from the bottom to provide the chosen dissolved gas, and to remove temperature gradients. 2) The heat defect of the water used will be determined in separate experiments.

Advantages are that the method gives absorbed dose rate at a point, the applicable heat defect will be used, there will be no convection, and calculations for excess heat will be concerned only with material in the neighborhood of the measurement point. A disadvantage is that the heat defect used will apply only to the local procedure, presumably without theoretical support.

Yale University (Schulz et al., 1987). This is a three-step procedure. 1) Absorbed dose rate at a point has been determined in a sealed glass vessel of about 800 cm^3 with ultra-pure water and dissolved gas, operated at 4°C. The entire vessel is covered by the beam. 2) An ion chamber is calibrated in a dummy calorimeter under identical conditions. 3) That chamber can be used to give absorbed dose rate at a point in an open water phantom. (Step 3 has been added for the comparison, but was not used at Yale.)

Advantages are that the method measures absorbed dose rate at a point, it uses a heat defect supported by theory, there is no convection, and the correction for excess heat is concerned only with material in the neighborhood of the measurement point. A disadvantage is that it is an indirect method of obtaining absorbed dose rate in an open phantom.

National Physical Laboratory (Burns et al., 1988). This is a four-step procedure. 1) The absorbed dose rate is determined in a graphite calorimeter. 2) Ionization chambers are calibrated in terms of graphite absorbed dose in a graphite phantom, and then 3) used in a water phantom to determine graphite absorbed dose in water, which is then 4) converted by calculation to water absorbed dose at a point in the open water phantom.

Advantages are the electrical calibration of the calorimeter core, and the absence of a significant heat defect in graphite (Bewley and Page, 1972; Sæbel et al., 1973, 1974; Weimer, 1973). Disadvantages are the necessity for energy-dependent conversion steps from one material to another, and for energy-dependent corrections for the vacuum gaps in the graphite calorimeter.

These obviously inadequate descriptions of five methods of obtaining primary standards of water absorbed dose for high-energy beams are intended to compare and contrast the several approaches, the details of which you will be hearing presently. Obviously we look forward to comparisons between these standards, which will have to be carried out by means of transfer instruments. Such a comparison could be started in the near future, since three of the laboratories are essentially ready at this time, but it will be a little longer before the other two are ready. The comparison should cover at least the photon energy range from cobalt-60 to 20 MeV or so. The methods are so different that, if adequate agreement is obtained, it becomes unlikely that there are major systematic errors. This is particularly so if the graphite calorimeter method is in good agreement with the water calorimeter methods.

I consider it particularly fortunate that one of the primary absorbed dose standards is based on the graphite calorimeter. Nevertheless, I think the advantages of the water calorimeter are sufficient that other national laboratories would be well advised to use a water calorimeter for developing high-energy primary standards. Very likely other national laboratories are already doing so, but I have of necessity limited my comments to those projects of which I have some knowledge.

There are other kinds of water calorimeters: Sundara Rao and Naik (1980), Witzani et al. (1985), and Domen (unpublished), have constructed graphite-in-water calorimeters that have some potential advantages. They are electrically calibrated, assume zero graphite heat defect, and are immune to the problems of convection and radiolysis of water. Domen (1983) and Kubo (1986) have also studied polystyrene-in-water calorimeters, which also are immune to convection and radiolysis of water, but which have the disadvantage of needing a determination of the specific heat of polystyrene. These two types of calorimeters have not received the extensive study of the usual water calorimeter, and so are mentioned here only in passing.

The problems of dissemination of dosimetry units from primary standards are very different from one country to the next, and I have here only one suggestion, in the comments that follow.

Role III. To provide a convenient secondary standard of water absorbed dose for high-energy radiation.

Three of the four types of primary water calorimeters mentioned above use ultra-pure water and special dissolved gases, while the fourth determines the appropriate heat defect by separate experiments. Such procedures are too demanding for a water calorimeter to be used in institutions such as hospitals. It will be necessary for such water calorimeters to use ordinary distilled water in an open phantom, and common, non-explosive gases. But there is a problem. Because the heat defect of water is very sensitive to impurities, it will be very difficult to be sure that the results are everywhere the same. I suggest that we consider water calorimeters using ordinary distilled water as secondary standards, and that they be related to primary standard water calorimeters in somewhat the way that secondary standard ionization chambers are related to primary standards at present.

The secondary water calorimeters would be compared with the primary water calorimeter using transfer ionization chambers. This could be considered a calibration, or perhaps simply a measurement-assurance test. Probably it would be adequate to do this at only one or two energies, and the secondary calorimeter would thereafter serve as an energy-independent local secondary standard. Such a test would not need to be repeated often, because the constancy of a secondary calorimeter would be maintained in the same way that any dosimetry secondary standard is maintained: by redundant constancy checks. The response of the secondary water calorimeter should be checked periodically in one or two stable radiation beams, and with one or two stable ionization chambers. With such 3- or 4-fold redundancy, the constancy of the calorimeter could be confidently assured, and comparisons with a primary calorimeter would rarely need to be repeated.

In order to carry out such a plan, it is necessary to simplify the operation and maintenance of the water calorimeter. I suggest that further development work on secondary water calorimeters be clearly differentiated from development work on primary water calorimeters, and that increased attention be given to simplifying the water calorimeter so that it can conveniently be used in a hospital as a standard for high-energy beams. Such an instrument, supported by an ordinary personal computer, could become the next generation of instruments for high-energy, absorbed-dose determination. Kubo and Mento (1984) have taken the first step in this direction, describing what they called an instant dose, *in situ* water calorimeter.

References

Barnett, R.B. (1986). Water calorimetry for radiation dosimetry. Ph.D. Thesis, Faculty of Graduate Studies, Univ. of Calgary, Calgary, Alberta.

Bewley, D.K. and Page, B.C. (1972). Heat defect in carbon calorimeters for radiation dosimetry. Phys. Med. Biol. 17, 584-589.

Bewley, D.K. (1984). Letter: Absorbed dose determination with a water calorimeter. Phys. Med. Biol. 29, 604.

Boyd, A.W., Carver, M.B., and Dixon, R.S. (1980). Computed and experimental product concentrations in the radiolysis of water. Radiat. Phys. Chem. 15, 177-185.

Burns, J.E., Dale, J.W.G., Du Sautoy, A.R., Owen, B., and Pritchard, D.H. (1988). New calibration service for high-energy x-radiation at NPL. IAEA-SM-298/56, in Internat. Symp. on Dosimetry in Radiotherapy (1987), International Atomic Energy Agency, Vienna.

de Marles, A.E.M. (1981). Comparison of measurements of absorbed dose to water using a water calorimeter and ionization chambers for clinical radiotherapy photon and electron beams. Ph.D. Thesis, Graduate School of Biomedical Sciences, Univ. of Texas, Houston, Texas.

Domen, S.R. (1980). Absorbed dose water calorimeter. Med. Phys. 7, 157-159.

Domen, S.R. (1982). An absorbed dose water calorimeter: Theory, design, and performance. J. Res. Nat. Bur. Stand. (U.S.) 87, 211-235.

Domen, S.R. (1983). A polystyrene-water calorimeter. J. Res. Nat. Bur. Stand. (U.S.) 88, 373-387.

Domen, S.R. (1986). Letter: Comment on 'Convection currents in a water calorimeter'. Phys. Med. Biol. 31, 1166-1168.

Domen, S.R. (1987). Advances in calorimetry for radiation dosimetry. Chapter 4 in The Dosimetry of Ionizing Radiation, Vol. II, K.R. Kase, B.E. Bjärngard, and F.H. Attix, eds., Academic Press, Orlando, Florida.

Domen, S.R. (1988a). Convective velocity effects on a thermistor in water. J. Res. Nat. Bur. Stand. (U.S.), in press.

Domen, S.R. (1988b). Letter: Further comments on convection currents in a water calorimeter. Phys. Med. Biol., in press.

Domen, S.R. (1988c). The role of water purity, convection, and heat conduction in a new calorimeter design. Proceedings of this Workshop.

Fletcher, J.W. (1982). Radiation chemistry of water at low dose rates. Emphasis on the energy balance: A computer study. AECL-7834, Chalk River Nuclear Laboratories, Chalk River, Ontario.

Hohlfeld, K., Kramer, H.M., Roos, M., and Selbach, H.-J. (1987). Two experimental methods for determining the heat defect of water. IAEA-SM-298/29, in Internat. Symp. on Dosimetry in Radiotherapy (1987), International Atomic Energy Agency, Vienna.

Kubo, H. (1983). Absorbed dose determination with a water calorimeter in comparison with an ionisation chamber. Phys. Med. Biol. 28, 1391-1399.

Kubo, H. (1985). Water calorimetric determination of absorbed dose by 280 kVp orthovoltage x-rays. Radiother. Oncol. 4, 275-281.

Kubo, H. (1986). Comparison of absorbed dose determinations between water and polystyrene-water calorimeters. Phys. Med. Biol. 31, 251-266.

Kubo, H. and Mento, D. (1984). An instant dose obtainable *in situ* calorimeter. Phys. Med. Biol. 29, 1433-1436.

Lovell, S. and Shen, H. (1976). A flow calorimetric method of determining electron beam energy. Phys. Med. Biol. 21, 198-208.
Mattsson, O. (1984). Application of the water calorimeter, Fricke dosimeter and ionization chamber in clinical dosimetry. Ph.D. Thesis, Department of Radiation Physics, Univ. of Göteborg, Göteborg, Sweden.
Pettersson, C. (1967). Calorimetric determination of the G-value of the ferrous sulphate dosimeter with high-energy electrons and Co-60 gamma-rays. Arkiv för Fysik 34, 385-400.
Roos, M. (1987). A water calorimetric determination of absorbed dose to water. Thermochimica Acta 119, 81-93.
Roos, M. and Hohlfeld, K. (1987). A measurement of the heat defect of water caused by high energy electrons. Thermochimica Acta 119, 95-101.
Ross, C.K., Klassen, N.V., and Smith, G.D. (1984). The effect of various dissolved gases on the heat defect of water. Med. Phys. 11, 653-658.
Ross, C.K., Klassen, N.V., Shortt, K.R., and Smith, G.D. (1988). A direct comparison of water calorimetry and Fricke dosimetry. Phys. Med. Biol., in press.
Sȕbel, M., Schmidt, Th., and Pauly, H. (1973). Heat defect of low energy x-rays absorbed in carbon and various plastics. Health Physics 25, 519-521.
Sȕbel, M., Schmidt, Th., and Pauly, H. (1974). Heat defect of low energy x-rays in some materials of interest in absorbed dose calorimetry. Rad. and Environ. Biophys. 11, 259-264.
Schulz, R.J. (1986). Letter: Reply to comments on 'Conveotion currents in a water calorimeter'. Phys. Med. Biol. 31, 1168-1169.
Schulz, R.J. and Weinhous, M.S. (1985). Convection currents in a water calorimeter. Phys. Med. Biol. 30, 1093-1099.
Schulz, R.J., Wuu, C.S., and Weinhous, M.S. (1987). The direct determination of dose-to-water using a water calorimeter. Med. Phys. 14, 790-796.
Sundara Rao, I.S. and Naik, S.B. (1980). Graphite calorimeter in water phantom and calibration of ionization chambers in dose to water for ^{60}Co gamma radiation. Med. Phys. 7, 196-201.
Weimer, V.G. (1973). Dependence of heat defect on absorbed dose in plastics. Atomkernenergie 20, 327-328. (In German)
Witzani, J., Duftschmid, K.E., Strachotinsky, Ch., and Leitner, A. (1985). Abstract: A portable graphite-water calorimeter. 3rd Int. Symp. Radiat. Phys., Ferrara, Italy.

Discussion

Rogers: Why do you consider a heat defect based on theory to be an advantage and one based on experiment to be a disadvantage? I consider it an advantage that it be based on an experimental measurement, preferably with theoretical confirmation.

Loevinger: Advantages and disadvantages are in the eye of the beholder. I used the phrase, "the heat defect is supported by theory". Now, the theory has to be tested in various ways and it will continue to be tested, so that theory and experiment will work back and forth, as it must. No theory can stand by itself. The PTB is determining the heat defect for their water but you can't generalize their results to the water used in other laboratories. It takes extreme care with the water before you get to a situation where theory is applicable. But maybe they are going to use ultrapure water.

Hohlfeld: The first idea behind our work is that we want to evaluate a method. The next thing is to apply this method to water which is pure and which can be maintained in the same composition for a long time. This water we will use in the calorimeter. At the same time we will develop our method, and investigate the heat defect for different dissolved gases in the water, so that, later on, we can make changes in the water.

Loevinger: I wasn't criticising this method. I mentioned five very different methods, which makes the comparison very interesting.

-

Shortt: If you determine the heat defect by using a beam of 5 MeV electrons the energy and the current being determined in a separate experiment, is the subsequent detector a primary standard?

Loevinger: That is what the PTB is doing. I did say it was not a primary standard if an empirically determined factor entered. This raises a slight logical inconsistency which could be gotten out of by erasing the definition.

Domen: But if you don't measure the heat defect directly like the PTB what do you assign for it? People may wonder whether it is 3.5% or what? That would more likely be defined at present as a secondary standard. You have to wait for time to really judge this type of calorimeter.

Loevinger: There is no law which says primary and secondary must mean.

-

Domen: Do the radiation chemists feel more comfortable with a primary standard based on a high purity system? What about once distilled water? I think that they would be more comfortable with a high purity system where you can make a calculation of the heat defect.

-

Klassen: I am concerned about your suggestion of a secondary standard using ordinary distilled water. You seem to want to avoid a great deal of preparation of the water. This gives one very little control over the quality of the water. Being open to the air, it may be contaminated between calibrations.

Loevinger: We need to investigate the properties of an instrument which is simple to make and to use and determine what precautions must be taken. Can you use ordinary distilled water; can you change it every day and so on?

Domen: I will have more to say about this tomorrow.

Fletcher: I see no reason why you shouldn't be able to make a completely sealed secondary standard with pure water which will stay pure year in and year out.

Loevinger: If that is shown, then that is the answer. One needs three- or four-fold redundancy. I am suggesting that there should be two lines of research, one for the high class instrument and one for the everyday sort of instrument to be used in hospitals.

Hohlfeld: At this moment I do not see the need for a secondary standard water calorimeter because, if we succeed in calibrating ionization chambers in a water phantom against a primary absorbed dose water calorimeter, we can use these ionization chambers, which are easier to use. The uncertainty we will get with this transfer will be smaller than by using a water calorimeter for which we don't know what factors may change the heat defect. But a research water calorimeter will be very useful, not as a primary standard, but to determine energy dependencies, etc.

Loevinger: In the United States there are approximately 2000 places where radiation therapy is performed and at least half of these use high energy radiation. At the moment, there is no calibration capability at energies above ^{60}Co. Some day NBS may offer high energy calibrations. The secondary calibration labs have no such calibration facilities and it is hard to see how they will establish it, and NBS can't calibrate all of them.

Kehoe: Can anyone define what is meant by pure water?

Ross: This question will be discussed in detail over the next two days.

THE CURRENT STATUS OF WATER ABSORBED DOSE CALORIMETRY IN THE PTB

M. Roos
Physikalisch-Technische Bundesanstalt
D-3300 Braunschweig, Federal Republic of Germany

ABSTRACT - The current status of water absorbed dose calorimetry in the PTB is outlined with emphasis on the description of a calorimeter type enabling the calibration of dosimeters for horizontally directed beams. Heat conduction calculations are presented showing that the extension of the application to electron beams might cause problems - particularly in the case of not too high energies.

L'état actuel de la calorimétrie des doses absorbées dans l'eau au PTB est décrit, et l'accent est mis sur la description d'un type de calorimètre permettant d'étalonner des dosimètres dans des faisceaux pointés à l'horizontale. Les calculs de conduction thermique montrent qu'il pourrait être difficile d'étendre l'application aux faisceaux d'électrons, notamment aux faisceaux d'énergie relativement peu élevée.

INTRODUCTION

For many years - at least since the seventies - calorimetric methods have been involved in the realization and dissemination of the unit of water absorbed dose in PTB.

A graphite calorimeter was built and compared with other graphite calorimeters at the BIPM. These results were used for W-value determinations in air. However, the transfer of the absorbed dose to graphite determination in the graphite phantom to the absorbed dose to water in the water phantom proved to be inferior to another method developed at the PTB.

Today the national standard for the unit of the water absorbed dose for high energy photon and electron radiation is based on ferrous sulfate dosimetry. The response of the solution is determined by total absorption of high energy electrons with a known radiant energy. The energy dependence of the chemical yield of the solution at high energies is assumed to be zero within acceptable uncertainties. So the calibrated Fricke solution allowed the beam of a cobalt source to be measured and serve as a PTB standard for the quantity water absorbed dose under specified conditions.

In addition, Fricke dosemeters are generally used at PTB to determine the response of ionization chambers to high energy photon and electron beams (Kuszpet et al. 1982).

In principle, a water calorimeter can accomplish the same task and without the restriction to high energies, and, Steve Domen showed in his pioneering papers that a water calorimeter can be easily built (Domen 1980, 1982, 1983). Since - from a puristical point of view - the calorimeter allows the dose to be measured according to its definition, and possibly with lower uncertainties, some time ago we began water calorimetric work at PTB.

Our first task is the development of a water absorbed dose calorimeter for calibration of dosimeters for Co60-gamma radiation appropriate to our irradiation facilities.

To establish the calorimeter as a primary standard for water absorbed dose, the heat defect must be determined using a method which does not include the absorbed dose. We therefore elaborated two methods to accomplish this, one for soft X- rays (Hohlfeld 1988) and one for high-energy electrons (Roos 1988).

In the following the main features of our water absorbed dose calorimeter are outlined, and the extension of its applicability to other types of radiation discussed.

CALORIMETER SET UP

As far as possible we tried to follow Steve Domen's well-proven design (Domen 1982). Deviations are necessary, however, to fit our special irradiation conditions - which means primarily horizontal beams. Fig. 1 shows its main features.

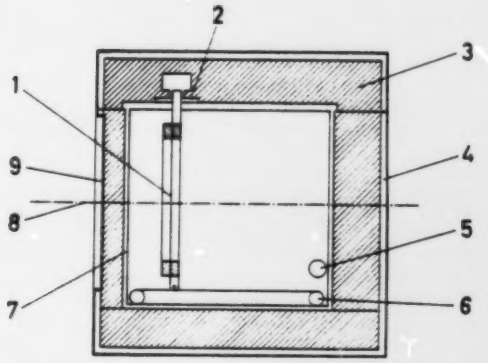

Figure 1

Schematic diagram of the water calorimeter. (1) exchangeable detector assembly fixed in support (2), (3) expanded polystyrene, (4) outer enclosure, (5) immersion heater, (6) perforated silicon tube, (7) acrylic tank filled with water, (8) beam axis, (9) entrance window.

It consists of an acrylic (polymethylmethacrylate) tank (7) (21 cm length, 30 cm width, 25 cm height) filled with distilled water. This is thermally isolated from its surroundings by polystyrene layers (3) and wooden enclosure (4) covered with aluminium foil.

The rise in temperature at the point of measurement, caused by a broad radiation beam entering through the entrance window (9), is measured using thermistors in the detector assembly (1). The water tank contains an immersion heater (5), a cooler as well as a perforated silicon tube (6) around its bottom edges. By bubbling gas (usually nitrogen) through the tube the water can be agitated to remove internal temperature gradients and to saturate it with the gas.

In order to avoid building a new water phantom we used the same phantom as in the Fricke calibration service. So we can use the available supports for several ionization chambers and for Fricke dosimeters. They can be replaced by the calorimeter detector shown in fig. 2, facilitating comparison measurements, or - later on - calibrations of dosimeters.

Figure 2

Detector assembly with acrylic rings, thermistors, polyethylene foils and support.

We also use a second wire configuration with length equal to the four electrical connections. The detector support allows the connection with copper wires or coaxial cables for DC or AC measurements.

Figure 3 shows that our DC bridge is sensitive enough for calorimetric measurement at the dose rates available at PTB (about 0.5 Gy per minute).

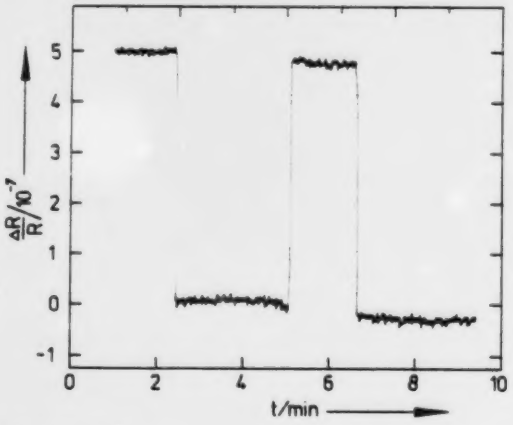

Figure 3

Recorder trace showing fractional changes in resistance $\Delta R/R$ of about $5 \cdot 10^{-7}$ in each case, corresponding to temperature changes of about 10^{-3} K.

The bridge was balanced and the bridge voltage recorded. The sudden changes were caused by relative changes in resistance of about $5 \cdot 10^{-7}$, corresponding to temperature changes of about 10^{-5} K. However, this trace refers to ideal conditions, that means short wires and Zeranin resistors instead of the thermistors.

We ran our first measurements with Co60-radiation without protection against convection. Figure 4 shows a typical recorder trace; the time increases from the right hand side to the left hand side. At times a and c irradiation commenced, at times b and d it ended. The sudden changes inbetween were caused by manual resistance changes. Each irradiation time was 4 minutes, the temperature rise amounting to about 0.5 mK.

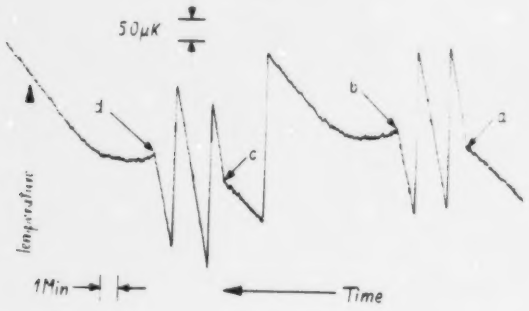

Figure 4

Time dependence of temperature for a typical calorimeter run at room temperature.

At the end of irradiation the trace reveals pronounced cooling drifts caused by convection currents (the underlying heating drift, caused by nonuniformities in the background temperature, are less important here).

To avoid convection we now use the same method as Schulz and Weinhous (Schulz and Weinhous 1985, Schulz, Wuu and Weinhous 1987), that means we operate the calorimeter at 4 °C. Fig. 5 shows how we accomplish this. The calorimeter is surrounded by a temperature stabilized enclosure, the lid being removed. The air is cooled down by two heat exchangers, each sandwiched between the cooling plates of two Peltier aggregates on the left hand side. The temperature is stabilized by heating with two bulbs in front of the heat exchangers.

Ventilators behind the heat exchangers cause the cooled air to circulate around the calorimeter.

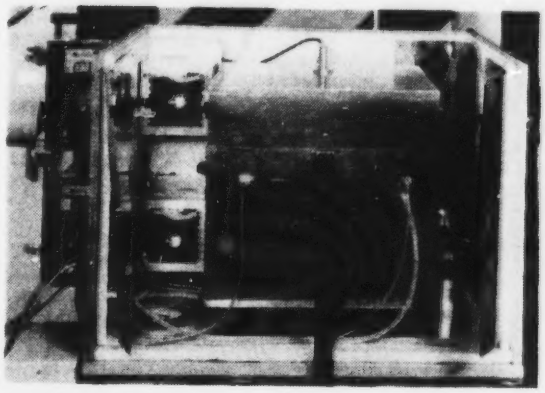

Figure 5

Calorimeter surrounded by a temperature stabilized enclosure, the lid being removed.

The air is guided around the corners by metal sheets. The aggregates are operated at a constant power level which would result in a temperature below 4 °C. The temperature is then controlled by heaters in the circulating air in front of the heat exchangers. When the water is agitated by gas - for instance nitrogen - this is guided through the heat exchangers several times to avoid heating the water.

The lid of the calorimeter contains a supply for a secondary standard thermometer for the calibration of the thermistors. We use a platinum thermometer, the constancy being checked with a triple point cell. An additional heat exchanger allows the water to be cooled down separately in order to accelerate the cooling-down procedure.

Fig. 6 shows that the convection problem does indeed now seem solved.

Even in the case of a very long irradiation time of more than 400 s the recorder trace shows straight lines, pre period and post period being parallel without any cooling drift. The increased noise is caused by a too small isolation resistance between the thermistors and the surrounding water.

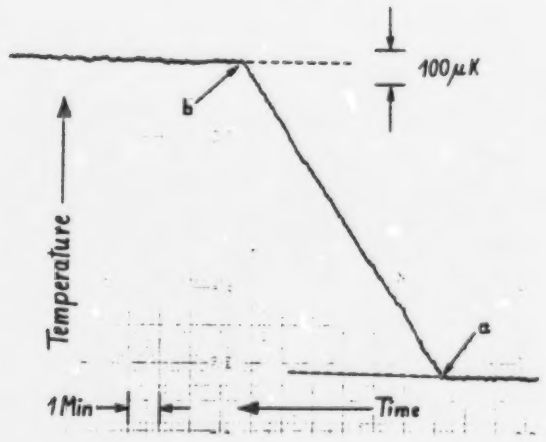

Figure 6

Time dependence of temperature for a calorimeter run at 4 °C. At time a Co60-gamma irradiation commenced, about 400 seconds later - at time b - it ended.

Of course the operation of the calorimeter at 4 °C has the disadvantage that the calibration of ionization chambers is more difficult. So it is not possible to just remove the lid of the calorimeter and replace the detector by the chambers because it would be difficult to determine the air temperature in the sensitive volume. To avoid that problem, one can continue to calibrate the chambers at room temperature. The calorimeter permits the warming up - and also the cooling down - procedures in reasonable times.

But - particularly in the case of the most important reference radiation field of the cobalt source - one could follow Steve Domen's suggestion and use foils as convection barriers and then verify that procedure by comparison with the results at 4 °C.

IRRADIATION AT DIFFERENT BEAM QUALITIES

Because of the importance of the quantity water absorbed dose, we are interested in the application of the water calorimeter not just for Co60-gamma radiation but also for X-rays and for high energy electron, photon and neutron beams.

Since the convection problem does not seem to limit the applicability of the calorimeter, we tried to find out as to how far the influence of heat conduction restricts the measurements.

To study the influence of conduction heat transfer on the measured temperature rise, we calculated the broadening of radiation induced temperature profiles during and after irradiation.

The application of almost homogeneous radiation fields extending over the whole phantom front surface permits the simplification of the calculations as a numerical solution of the one dimensional unsteady-state heat conduction equation (see for instance Holman 1981). It was further assumed that there is no heat transfer through the water surface. Since the radiation-induced temperature rise is proportional to the absorbed dose, the temperature distributions in the water were determined from depth dose curves. The calculations were performed for a water temperature of 22 °C.

Fig. 7 shows the results for 8 MV Bremssstrahlung

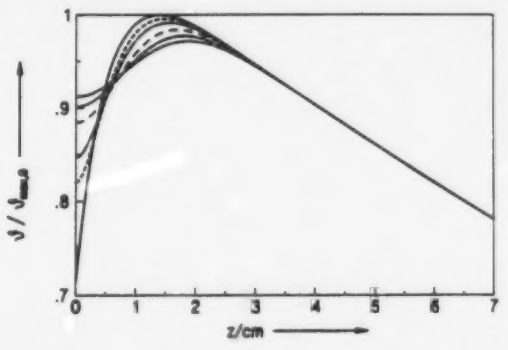

Figure 7

Depth distributions of temperature in the water phantom irradiated with 8 MV Bremsstrahlung for various times after starting the irradiation. The distributions are normalized to the "true" temperatures for dose maximum $\vartheta_{max,o}$.

——— immediately after irradiation commenced
– – – – – after 60 s
—·—·— after 120 s (at the end of the irradiation period)
— — — — after 180 s
—— —— after 240 s
—·—·—·— after 300 s

In the region of maximum dose the deviations are rather large, whereas at greater depths the heat transfer at even greater depths is almost (nearly) balanced by heat transfer from greater regions.

This can be inferred quantitatively from Fig. 8. For depths around the reference depth of 5 cm the deviations are smaller than 0.1 %.

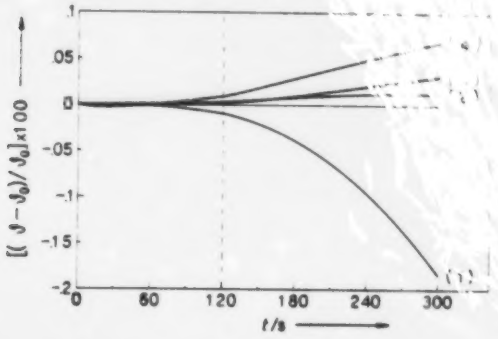

Figure 8

Calculated deviation of the temperature ϑ from the "true" value ϑ_0 in percent as a function of time t after beginning 8 MV photon irradiation for depths of (1) 3 cm, (2) 4 cm, (3) 5 cm and (4) 10 cm. The end of the irradiation period is indicated by a dashed line.

Similarly advantageous is the situation in the case of neutron beams.

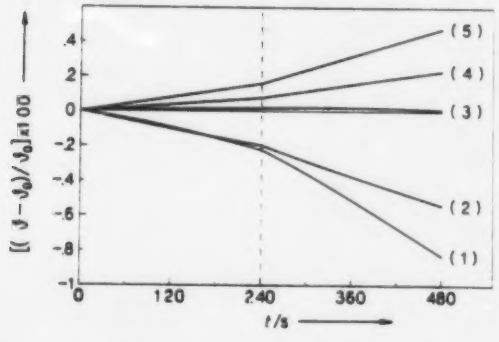

Figure 9

Deviation of the temperature ϑ from the "true" value ϑ_0 in percent as a function of time t after starting (d(15) + Be) neutron irradiation for depths of (1) 1 cm, (2) 3 cm, (3) 5 cm, (4) 8 cm and (5) 15 cm. The end of the irradiation period is indicated by a dashed line.

Fig. 9 shows as an example the results for d(15) + Be neutron radiation. The underlying depth dose curve (SSD = 150 cm, FS = 20 cm x 20 cm) is taken from Br. J. Radiol. Suppl. 17, (1983). The depth of 5 cm is especially well suited for calorimetric purposes. The heat transfer is nearly balanced so that the temperature deviation is smaller than 0.1 %.

The situation in the case of electron beams is quite different, as can be seen in Fig. 10 and Fig. 11.

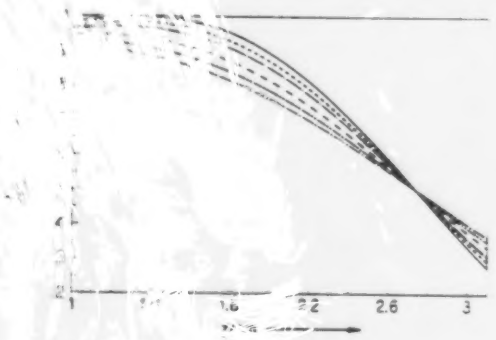

Figure 10

Depth distributions of temperature in the water phantom irradiated with 7 MeV electrons for various times after starting the irradiation. The times and the corresponding symbols are the same as in Fig. 7. The distributions are again normalized to the "true" temperatures for maximum dose.

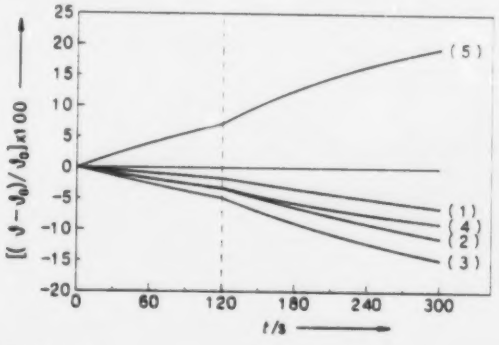

Figure 11

Deviation of the temperature ϑ from the "true" temperature ϑ_0 in percent as a function of time t after starting 7 MeV electron irradiation for depths of (1) 1 cm, (2) 1.38 cm - the depth of maximum dose -, (3) 2 cm, (4) 2.5 cm and (5) 3 cm. The end of the irradiation period is indicated by a dashed line.

It can be seen that the reference depth for dosimetry in radiation therapy - the depth of the dose maximum - is not well suited for water calorimeters since the error in the measured temperature rise is particularly large, amounting to 3.4 % at the end of the irradiation period. For a temperature of 4 °C the deviation decreases slightly to 3.2 %. But again depths exist where the heat transferred to greater depth is roughly compensated by the heat transferred from shallower regions. Fig. 12 shows that the deviations are essentially smaller at depths around 2.7 cm.

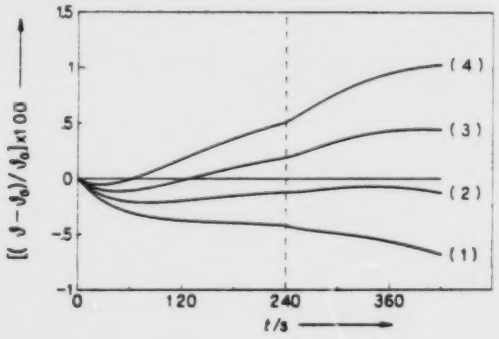

Figure 12

Deviation of the temperature ϑ from the "true" temperature ϑ_0 in percent as a function of time after starting 7 MeV electron irradiation for depths of (1) 2.73 cm, (2) 2.74 cm, (3) 2.75 cm and (4) 2.76 cm. The end of the irradiation period is indicated by the dashed line.

To get the same temperature rise the irradiation periods were doubled from 2 minutes to 4 minutes. In the range from 2.73 cm to 2.76 cm the deviations are now smaller than about +0.5 % and -0.5 % but the time dependence is critically dependent on the depth.

CONCLUSION

We hope to be able to establish the water calorimeter as a primary standard for water absorbed dose for Co60-radiation the determination of the heat defect being included.

The extension to high-energy Bremsstrahlung and to X-rays should cause no problems. That enables the calibration of dosemeters and especially the determination of the type specific correction factors k_Q and k_E for the energy dependence of the ionization chambers. The knowledge of the dependence of the response on the radiation quality is of vital importance in the course of the dissemination of the unit of the water absorbed dose.

The calculations have shown, however, that the extension to electron beams might cause problems - at least in the case of not too high energies.

REFERENCES

1. Boutillon, M. and Perroche-Roux, A.M. 1987. Re-evaluation of the W-value for electrons in dry air. Phys. Med. Biol. 32, 2 pp. 213-219.

2. Domen, S.R. 1980. Absorbed dose water calorimeters. Med. Phys. 7, pp. 157-159.

3. Domen, S.R. 1982. An absorbed dose water calorimeter: theory, design and performance. Journal of Research of the NBS 87, pp. 211-235.

4. Domen, S.R. 1983. A polystyrene-water calorimeter. Journal of Research of the NBS 88, pp. 373-387.

5. Feist, H. 1982. Determination of the absorbed dose to water for high-energy photons and electrons by total absorption of electrons in ferrous sulfate solution. Phys. Med. Biol. 27, 12, pp. 1435-1447.

6. Hohlfeld, K. 1988. Determination of the heat defect of water by total absorption of soft X-rays. In this volume.

7. Holman, J.P. 1981. Heat transfer. Mc Graw-Hill, New York.

8. ICRU-Report 31 (1979). Average energy required to produce an ion pair. ICRU, Washington D.C..

9. Kuszpet, M.E., Feist, H., Collin, W. and Reich, H. 1982. Determination of C and C_E conversion factors and stopping power ratios using calibrated ferrous sulphate dosemeters. Phys. Med. Biol. 27, 12, pp. 1419-1433.

10. Roos, M. 1988. Measurement of the heat defect of water caused by high-energy electrons. In this volume.

11. Schulz, R.J. and Weinhous, M.S. 1985. Convection currents in a water calorimeter. Phys. Med. Biol. 30, pp. 1093-1099.

12. Schulz, R.J., Wuu, C.S. and Weinhous, M.S. 1987. The direct determination of dose-to-water using a water calorimeter. Med. Phys. 14, 5, pp. 790-796.

Discussion

Ross: Did you use AC bridges or DC or both?

Roos: Both.

-

Domen: You presented your results for these low energy electron beams as the errors caused right at the instant the beam is turned off. At the instant the beam is turned off there is a temperature drop, and the after-drift will show a downward drift. Taking the after-drift and extrapolating to the midrun, as is usually in practice, would tend to decrease the errors.

Roos: We have started to do that, but not for all cases, and the results are rather different, because the curvature of the post-periods is rather different. In many cases the deviations will be smaller, but they can also increase.

Domen: The main thing, if one has a high dose rate, is to make the run short.

Roos: That's true.

-

Schulz: Have you actually used 8 MeV electrons with your calorimeter?

Roos: Not up to now. We have only tried to see if the method can be used with electrons without problems or not.

Schulz: We have used 16 MeV electrons, where there is a fairly broad flat peak in the depth-dose curve, and the rating periods are quite flat before and after. The water calorimeter will probably never be good for low energy electrons.

Roos: That's true. If the curvature is not very large, and the radiation periods are short, there should not be too large problems.

Domen: Loevinger mentioned my 1982 report. In it, in Figure 1, I show an 11 MeV curve and behind that I show a material other than water. I indicate an indefinite thickness and an indefinite position. With a computer, I want to vary the thickness, and also the position and see what effect that has on the measurement of a run of a definite duration and after-drift. It could extend it down to lower energies.

-

Klassen: In your calculations, how close do you have to get to the surface before the higher temperature at the surface has an effect on the temperature changes that you measure?

Roos: It depends on whether one uses a very thin entrance window or rather thick lucite. Using ^{60}Co and very thin windows and a depth of 5 cm there will be nearly no influence. In the case of electrons, one has to modify the calculations if one has a horizontal beam and a depth around 1 cm.

Klassen: When you bubble with gases do you presaturate the gases with water, and if not, do you notice any cooling of the water due to evaporation by the gas?

Roos: The temperature rise around the thermistor is broken down by the gas bubbling so one has to wait until the water no longer moves and then one can see if one has the same, higher or lower temperature.

-

McDonald: Do you plan to look at the thermal defect for the charged particles produced by neutrons? There might be some difference between the thermal defect for neutron beams and for electron or photon beams.

Roos: I have no information on the heat defect for neutrons. We have developed two methods for the determination of the heat defect and one or other might be used for neutrons to give an idea of the heat defect for high LET radiation. We have not done such experiments.

-

Ross: How long do you have to wait for thermal stability for runs at 4 C in a large calorimeter?

Roos: The water is always kept in the calorimeter, so we can start immediately.

Domen: Do you use my temperature drift balancer that I mentioned in my reports?

Roos: Yes, we use it and it is a fine method.

WATER CALORIMETRY AT RADIATION PHYSICS DEPARTMENT GÖTEBORG

Olof Mattsson
Radiation Physics Department, Sahlgren Hospital
S-413 45 Göteborg, Sweden

ABSTRACT - The aim with this study was to investigate the possibility to use a Domen type water calorimeter for measurements in clinically used photon and electron beams and to make a comparison with ionization chamber and Fricke dosimetry. A difference in calorimeter behaviour in photon and electron beams was found. In general the calorimeter was more stable in the photon beams. In the high energy beams the agreement between the different systems is within approximately ± 1 percent and in the orthovoltage beams differences up to 4 percent was observed.

RÉSUMÉ - Le but de l'étude était d'examiner la possibilité d'effectuer des mesures dans des faisceaux de photons et d'électrons d'usage médical au moyen d'un calorimètre à eau de type Domen et de comparer les résultats avec ceux d'une chambre d'ionisation et d'un dosimètre Fricke. On a constaté que le calorimètre se comporte différemment dans les faisceaux de photons et d'électrons. Il est en général plus stable dans les faisceaux de photons. Dans les faisceaux de haute énergie, l'accord entre les différents systèmes est meilleur qu'un pour-cent environ et atteint 4 % dans les faisceaux orthovoltés.

INTRODUCTION

The radiation physics department at Sahlgren Hospital in Göteborg has been involved in research projects in radiation dosimetry for several years. For a long time a main interest have been ionization chamber dosimetry. The department was very active in the revision of the NACP dosimetry protocol which was published in 1980 and -81. An important part of the introduction of a new protocol is to check the complete dosimetric procedure using an independent dosimetry system. Preferably such a system should be less dependent on the radiation beam quality than the ionization chamber dosimetry. If any, the quality dependence should be well known. When this check was made for the NACP protocol the best alternative available was the ferrous sulphate dosimeter (Fricke). Fricke is almost water equivalent and the beam quality dependence is therefore very small. However, it has a very low sensitivity and is, as used here, not an absolute dosimetry method. When Domen presented his work on the absorbed dose water calorimeter in 1980 it was therefore with great interest we studied his results. In theory the water calorimeter is an absolute dosimeter with an acceptable sensitivity and with a small beam quality dependence for low LET radiation. It was decided to investigate the possibility to use the instrument as a reference for absorbed dose to water in clinical photon and electron beams. This included a comparison between the water calorimeter and the exsisting dosimetry systems i.e. ionization chamber and ferrous sulphate dosimetry. The result of the comparison has previously been reported by Mattsson (1984, 1985 and 1985). The emphasis in the water calorimeter project at the university of Göteborg is thus more on the use of the system in clinical radiation beams than on the development of the instrument itself.

WATER CALORIMETRY

The calorimeter

The water calorimeter in Göteborg is of the same type as that described by Domen (1980, 1982) (see Figure 1, 2 and 3). Domens design was studied on site at the National Bureau of Standards (NBS) in Washington. During this visit Domen very kindly supplied all information necessary for the construction of the instrument. The choice of materials and components are in most cases the same as used by Domen. Our interest have been the absorbed dose water calorimeter therefore no attempts have been made to modify the instrument into a polystyrene- or graphite-water calorimeter.

As the instrument was to be used in an ordinary radiation therapy department with no or very poor temperature control in the treatment rooms, the thermal insulation of the calorimeter was improved compared to the original design. This was done by adding a layer of aluminized polyurethane around the calorimeter (Figure 3). With this design the calorimeter could be used in most of the treatment rooms. However, when measurements were made in orthovoltage X-ray beams the thermal conditions in the treatment room were too poor to keep the instrument under control for a sufficient period of time. The thermal insulation had to be improved further. The entire calorimeter was surrounded by a thermal shield of polyurethane covered on both sides with aluminium foils. The lid of this structure was polyurethane with a cutout for the beam entrance covered with a polyethylene film.

Due to the limited access to the irradiation equipment for dosimetry work, common for most therapy departments, it is essential that the measuring equipment is simple to set up and take down. To assure reproducible measuring conditions and predictable instrument performance this requires high quality cables and connectors and also a well design electrical grounding system. In addition the choice of materials and methods for connecting the different units are important. The influence of thermal electromotive forces (emfs) along the connecting paths must be minimized. This was achieved by following the recommendations given by Domen (1982). With the present design the measurements could be made in the evenings after the normal working hours and be completed on the same evening. The instrument could be used at the medical accelerators where the electronic noise levels are very high which is a good test of the electrical shielding and grounding of the system.

Detector

The two 0.25 mm diameter thermistors used in the detector, manufacured by Victory Engineering Corporation, have a nominal resistance of 3 kΩ at a temperature of 25 C. The thermistor sensitivity was determined as described by Domen (1982). The sensitivity of a thermistor is given as

$$S = - \beta / T^2$$

where T is the absolute temperature. The values for β for the two thermistors differed by 0.6 percent with a mean value β of 3201 K. For the same type of thermistors Domen (1982) used a mean value β of 3202 K.

The thermistors were sandwiched between two 20 μm polyethylene films stretched between two polystyrene rings.

All measurements were made with a nominal thermistor power dissipation of 5 μW. Corrections to zero thermistor power were made according to Domen (1982).

The Wheatstone bridge

A simplified drawing of the Wheatstone bridge is given in Figure 4. The bridge power supply was two 1.35 V mercury cells. The dc output of the bridge was fed into a 20 m signal cable connected to a chopper amplifier. The output of the amplifier was fed into a chart recorder. All components of the bridge including all connectors were provided with thermal insulation to reduce the effects of thermal emfs. The stability of the system was tested before each measurement. The observed changes in the amplifier output during the tests were very slow and predictable.

Water preparation

The water used in the calorimeter was once destilled water. A still made of Pyrex glass was used. On most occasions 25 l pyrex glass jugs were used as intermediate storage containers. However,occasionally, due to practical reasons, a polyethylene jug was used. The influence on the calorimeter measurents of the different storage containers was not analysed in detail. No obvious difference could however be observed.

Calorimeter set up

The evening before the day of measurements the calorimeter including electronics and cables was taken into the treatment room and stored on a trolley. At the same time the jugs with water were taken into the room and stored on the floor approximately 1 m below the calorimeter. With this procedure, adapted from Domen, the water temperature was always slightly lower than the calorimeter temperature. On the measuring day, after the ordinary patient treatments, the calorimeter was positioned on the treatment table, connected to the electronics, filled with water and the lid was snapped on. The water was then agitated for about 30 minutes with air from an aquarium pump. After a period of about 10 minutes when the water had come to rest the measurements could be started.

Determination of absorbed dose to water

The principles for the determination of absorbed dose to water for this type of calorimeter has been discussed in detail by Domen (1982). The same procedure was followed here. An exothermic chemical defect of 3.5 % (Domen 1982) was assumed for all beam qualities (i.e. the instrument gives a larger signal than that corresponding to the absorbed dose).

IRRADIATION CONDITIONS

Measurements were made in two orthovoltage X-ray beams, 100 kV, HVT= 3.9 mm Al and 200 kV, HVT=1.3 mm Cu, in a Co-60 gamma beam and electron and photon beams from three linear accelerators, a Clinac 4/100 (4 MV photons), a Philips SL 75/14 (6 MeV electrons), a Philips SL 75/20 (16 MV photons, 10 and 20 MeV electrons) and a microtron Scanditronix MM22 (10 MeV electrons).

The field size was 20 cm x 20 cm, except for the measurements in the orthovoltage X-ray beams where the maximum possible field size was 17.5 cm x 17.5 cm.

The nominal dose rates in the orthovoltage X-ray beams were 0.5 and 0.8 Gy min^{-1} for the 100 and 200 kV beams, respectively. In the Co-60 beam the dose rate was 0.9 Gy min^{-1} and in the accelerator produced beams dose rates between 2 and 5 Gy min^{-1} were used.

In the high energy photon and electron beams the measurements were made at or very close to the normal treatment distance. In the orthovoltage X-ray beams a SSD of 50 cm was used.

IONIZATION CHAMBER DOSIMETRY

For the measurements in the orthovoltage X-ray beams a 0.6 cm^3 Farmer type chamber, type NE 2505/3, was used. For the measurements in the high energy photon beams and in the 20

MeV electron beams a 5 mm diameter cylindrical homogeneous graphite chamber was used . In the 6 and 10 MeV electron beams a NACP plane parallel chamber was used. The cylindrical chambers were calibrated at the Swedish National Standards Laboratory in Stockholm. The plane parallel chamber was calibrated in a 20 MeV electron beam as described in NACP (1981). All measurements were made in a 30 cm x 30 cm x 40 cm water phantom. To obtain the same measuring conditions during the ionization chamber and Fricke measurements as during the water calorimeter measurements a slab of expanded polystyrene covered with an aluminium foil of the same construction as the calorimeter lid, was positioned on top of the phantom.

For the determination of the absorbed dose to water from the ionization chamber measurements the new IAEA code of practice (1987) has been used for the high energy beams. In the orthovoltage beams the ICRU Report 24 (1976) was used.

FERROUS SULPHATE DOSIMETRY

The ferrous sulphate system has previously been described by Mattsson et. al.(1982). $\epsilon_m G = 352\ 10^{-6}\ m^2\ kg\ J^{-1}$ (ICRU 35, 1984) was used for the absorbed dose calculation for all beams.

RESULTS AND DISCUSSION

Calorimeter performance

In high energy photon beams the calorimeter performance was essentially the same as reported by Domen (1982) for Co-60 beams. After the initiating procedure, described above, the thermal drift rates were stable and predictable. No drastic changes in the calorimeter performance was observed even after several hours of measurements and high accumulated absorbed doses. An example of a chart recording from a measurement in the 16 MV beam is shown in figure 5. When the irradiation starts, indicated with an arrow, a spike can be seen on the recording. This could be seen in most of the measurements. The magnitude was however different in different beams, being smallest in the Co-60 beam and largest in the electron and high energy photon beams. The height of the spike seems to be correlated to the dose rate. A possible explanation is that the initial temperature increase in the thermistors is faster than in the surrounding water but after a short time this effect will disappear due the cooling effect of the water on the small thermistors. A linear temperature increase can then be observed until the beam was turned off. The finial temperature drift was approximately the same as before the irradiation.

In electron beams the calorimeter performance was different. In general the behavior was less stable than in photon beams. This was seen as larger changes in the thermal drifts with accumulated absorbed dose. In the beginning of a measurment there was a general tendency for the drifts to turn upward(the thermistors sensed an increasing temperature). But after several runs the drifts turned downward(cooling). Finally the control of the calorimeter was lost. The number of runs before the calorimeter control was lost was depending on the beam energy, being less for low energies than for high. To regain control it was nesessary to agitate the water again.

The explanation for this can be that in electron beams only a limited volume of the water is heated due to the peaked depth dose curve. With decreasing energy the irradiated volume decreases. After some time and accumulated absorbed dose the influence of the "cool water" outside the heated region will be sensed by the thermistors. Eventually this influence becomes too large and the calorimeter control is lost.

A chart recording from a 10 MeV electron beam is shown in figure 6. After the initial spike when the beam was turned on a linear temperature increase can be seen. Comparing figures 5 and 6 some differences can be observed. For the photon beam the extrapolated linear part of the curve intersects the initial drift curve at the point where the beam was turned on. For the electron beam this is not the case. The linear part of the curve seems to be shifted downward. This can also be seen when the beam was turned off as a corresponding upward pen deflection. A downward pen deflection indicates that the termistors senses a decreasing temperature. In this case it can not be caused by a decreasing water temperature. As the effect is observed only during irradiation and only in electron beams it can be a direct effect of the negatively charged electrons being stopped in the thermistors or the wires in the detector. However, no proved explanation has been found for this behavior. Another difference between the performance in photon and electron beams is that the chart recordings have an "overshot" immediately after the beam was turned off in electron beams (figures 6 and 7). After the overshot a constant temperature drift was restored. The overshot could be explained by a heat source positioned close to the thermistors. If this heat source has a fairly small heat capacity and if its temperature rise during irradiation is faster than that of the surrounding water it could produce an "overshot". Why this would happen only in electron beams is not clear. Possible heat sources could be the polyethylene films or the thermistor leads. To prove the theory further investigaitons are needed.

For the determination of $\Delta R/R$, needed for the absorbed dose determination, the extrapolation to mid run procedure described by Domen (1982) has been used. This requires well defined and constant temperature drifts before and after a run. The uncertainty in the extrapolation due to the "overshot" can probably result in uncertainties in the absorbed dose value of the order 2-3 percent. For the determination of the $\Delta R/R$ in this report the constant temperature drift after the "overshot" was used.

For the 200 kV beam and the high energy photon and electron beams the standard deviation (±1 S.D.) for a set of measurements varied between 0.6 and 2 percent. For the 100 kV beam the standard deviation varied from 3.5-4.5 percent. An explanation for these larger values can be the low dose rate. An attempt was made to increase the dose rate by reducing the source to phantom surface distance. However, this also reduced the field size to 14 cm x 14 cm. After succesive irradiations the temperature drift turned downward followed by a loss of calorimeter control as described above for electron beams. This can probably be explained by the influence of the cold unirradiated water outside the radiation beam.

There thus seems to be some limitations in the measuring conditions under which this water calorimeter can used.

Absorbed dose comparison

The result of the absorbed dose comparison in high energy photon and electron beams using the different methods is given in table 1. The differences between the ionization chamber and Fricke dosimetry are within approximately 1 percent, which is within the uncertainty of the measurements. Also the differences between the water calorimeter and Fricke are within 1 percent. However, the three methods can probably not be considered as being independent as all three in different ways are based on graphite calorimetry. Graphite calorimetry has been used to determine the (W/e)-value for the ionization chamber, the ε_m G-value for the Fricke and the value of the chemical defect for the water calorimeter. Correctly used all three should thus give the same absorbed dose values.

The result of the comparison in orthovoltage X-ray beams is given in table 2. No measurements were made with Fricke. The differences are here larger than in high energy beams. However, also the standard deviations are larger. The result is in the same direction as that reported by Kubo (1985), i.e. the water calorimeter gives higher absorbed dose values than ionization chamber dosimetry.

CONCLUSION

The aim with the water calorimeter project at Sahlgren Hospital in Göteborg was to investigate the possibility to use the instrument in clinical photon and electron beams and to make a comparison with other dosimetry methods. The investigations show that the water calorimeter can be used in clinical beams under normal clinical conditions. The calorimeter behaviour was found to be different in photon and electron beams. In general the calorimeter performance was more stable in photon beams. Further investigations are needed to explain the observed differences.

In high energy photon and electron beams the agreement between the different dosimetry methods is within approximately ± 1 percent, which must be considered as satisfactory.

In orthovoltage X-ray beams the absorbed dose value determined with the water calorimeter is 2 to 4 percent higher than values determined with ionization chamber dosimetry.

REFERENCES

1. Domen, S.R. 1980. ABSORBED DOSE WATER CALORIMETER. Med.Phys. Vol. 7, p. 157.

2. Domen, S.R. 1982. AN ABSORBED DOSE WATER CALORIMETER: THEORY, DESIGN AND PERFORMANCE. Journal of Research of the NBS. Vol. 87, p. 211.

3. International Atomic Energy Agency (IAEA) 1987. ABSORBED DOSE DETERMINATION IN PHOTON AND ELECTRON BEAMS, AN INTERNATIONAL CODE OF PRACTICE. Vienna.

4. International Commission on Radiation Units and Measurements (ICRU) 1976. Report No. 24. DETERMINATION OF ABSORBED DOSE IN A PATIENT IRRADIATED BY BEAMS OF X OR GAMMA RAYS IN RADIOTHERAPY PROCEDURES. Washington, D.C.

5. International Commission on Radiation Units and Measurements (ICRU) 1984. Report No. 35. ELECTRON BEAMS WITH ENERGIES BETWEEN 1 AND 50 MeV. ICRU Publications, Bethesda, MD.

6. Kubo H. 1985. WATER CALORIMETRIC DETERMINATION OF ABSORBED DOSE BY 280 kVp ORTHOVOLTAGE X-RAYS. Radiotherapy and Oncology, Vol. 4, p. 275.

7. Mattsson L.O. 1984. APPLICATION OF THE WATER CALORIMETER, FRICKE DOSIMETER AND IONIZATION CHAMBER IN CLINICAL DOSIMETRY. Thesis, University of Göteborg.

8. Mattsson L.O. 1982. FERROUS SULPHATE DOSIMETER FOR CONTROL OF IONIZATION CHAMBER DOSIMETRY OF ELECTRON AND ^{60}Co GAMMA BEAMS. Acta Radiol. Oncol. Vol. 21, p. 139.

9. Mattsson L.O. 1985. COMPARISON OF VARIOUS DOSIMETRY PROTOCOLS FOR HIGH ENERGY PHOTON AND ELECTRON BEAMS. Invited paper at the VII International Conference on Medical Physics (ICMP), Espoo, Finland.

10. Mattsson L.O. 1985. COMPARISON OF WATER CALORIMETRY AND IONIZATION CHAMBER DOSIMETRY IN 100 AND 200 kV X-RAY BEAMS. Report prepared for the CCEMRI meeting in Paris.

11. Nordic Association of Clinical Physics (NACP) 1980. PROCEDURES IN EXTERNAL RADIATION THERAPY DOSIMETRY WITH ELECTRON AND PHOTON BEAMS WITH MAXIMUM ENERGIES BETWEEN 1 AND 50 MeV. Acta Radiol. Oncol. Vol. 19, p. 55.

12. Nordic Association of Clinical Physics (NACP) 1981. ELECTRON BEAMS WITH MEAN ENERGIES AT THE PHANTOM SURFACE BELOW 15 MeV. Acta Radiol. Oncol. Vol. 20, p. 401.

Table 1. Results of the measurements made in high energy photon and electron beams using the ionization chamber, the Fricke and the water calorimeter.

Beam quality		$D_{w,ioniz.}$	$D_{w,Fricke}$	$D_{w,cal.}$	% Difference $\frac{D_{w,ioniz.}}{D_{w,Fricke}}$	% Difference $\frac{D_{w,cal.}}{D_{w,Fricke}}$
Co-60		2.000	2.018	2.022	-0.9	0.2
4 MV	X-ray	2.001	2.017	2.019	-0.8	0.1
16 MV	X-ray	1.990	1.996	2.014	-0.3	0.9
6 MeV	Electron	1.989	2.010	2.018	-1.1	-0.4
10 MeV	Electron[1)]	1.986	2.008	2.027	-1.1	1.0
10 MeV	Electron[2)]	1.986	1.964	1.966	+1.1	0.1
18.8 MeV	Electron	1.983	2.002	2.007	-1.0	0.2

1) Thick scattering foil, applicator scattered electrons

2) Thin scattering foil, no applicator scattered electrons

Table 2. Results of the measurements made with the water calorimeter and ionization chamber for the 100 kV and 200 kV X-ray beams.

Beam quality		Absorbed dose to water		% Difference
Potential	HVT	$D_{w,cal.}$	$D_{w,ioniz.}$	$\frac{D_{w,cal.}}{D_{w,ioniz.}}$
kV		Gy min^{-1} $\pm$ 1 SD	Gy min^{-1} $\pm$ 1 SD	
100	3.9 mm Al	0.428 $\pm$ 0.006	0.412 $\pm$ 0.004	3.9
200	1.2 mm Cu	0.799 $\pm$ 0.014	0.783 $\pm$ 0.006	2.0

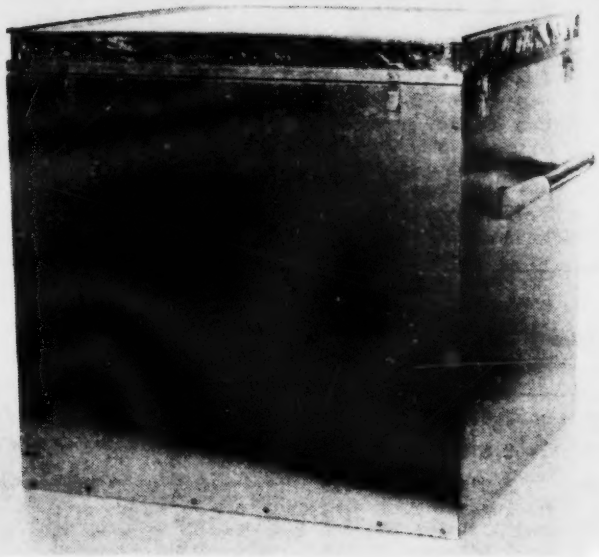

Figure 1. Photograph of the calorimeter external details.

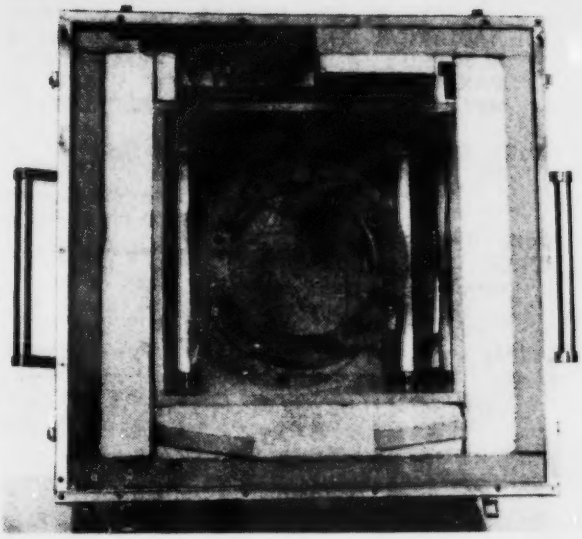

Figure 2. Photograph of the calorimeter internal details.

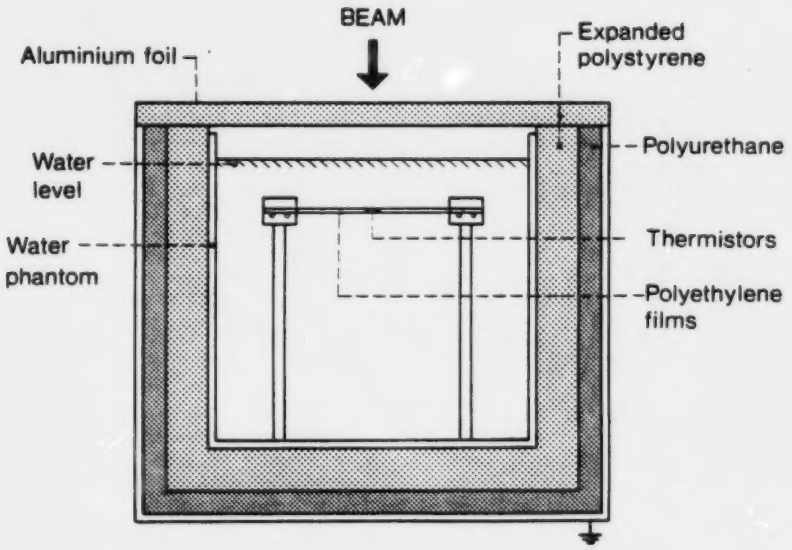

Figure 3. Schematic diagram of the water calorimeter.

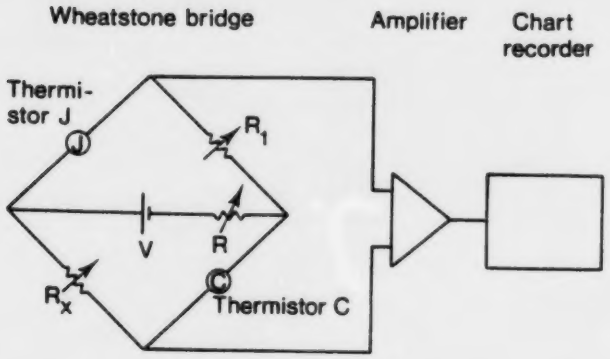

Figure 4. Electronic circuit diagram of the water calorimeter.

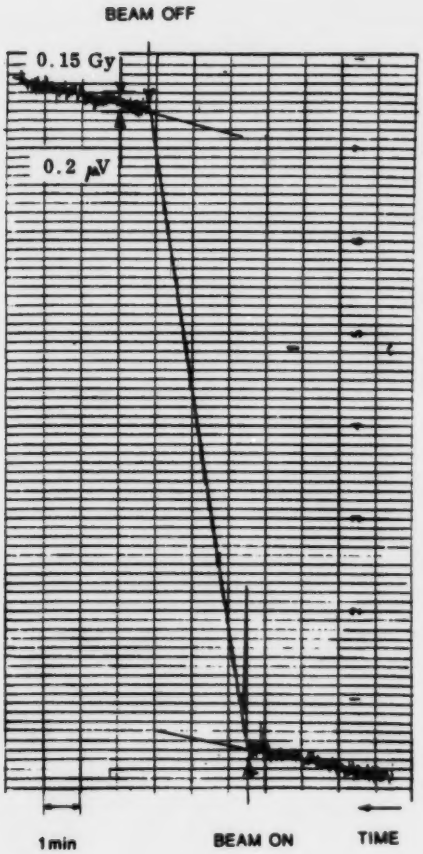

Figure 5. An example of a chart recording for the 16 MV photon beam obtained with the water calorimeter.

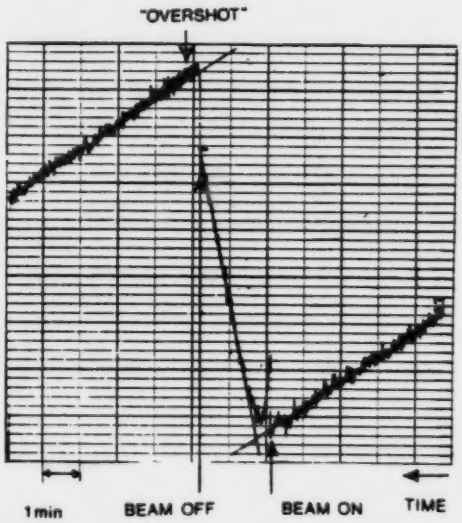

Figure 6. An example of a chart recording for the 10 MeV electron beam obtained with the water calorimeter.

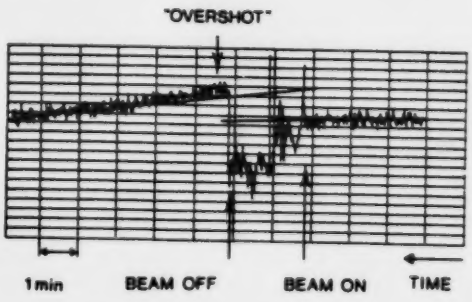

Figure 7. A chart recording for the 10 MeV electron beam illustrating the "overshot" problem.

Discussion

[During Mattsson's talk, there was a detailed discussion of anomalies in thermistor response. We have paraphrased the main elements of this discussion.]

Mattsson: I would like to draw your attention to a spike at the beginning of the irradiations with photon beams.

Domen: I have seen a similar effect from time to time. It had no effect on the measured absorbed dose. I think it has something to do with the electrical resistivity of the water.

Schulz: Are you sure it is not electrical noise? We have seen a similar effect when our calorimeter was out of the beam and the accelerator turned on.

Mattsson: For the accelerators I use, the RF power comes on 15 to 20 seconds before the beam. There is no spike at this time. I think the effect is produced somehow by the irradiation.

-

Mattsson: With electron beams, after several irradiations, the temperature drift would become too large. The problem was worse with low energy electrons; I could make fewer runs with low energy electrons than with high.

Kubo: What happened if you waited a long time between runs?

Mattsson: The only way I could re-establish a reasonable drift rate was to agitate the water again.

-

Mattsson: With electron beams, I observe a different anomaly in the thermistor response than with photons.

Seuntjens: Is it because the radiation beam consists of charged particles?

Mattsson: Yes, I believe that is the reason.

Domen: Was the water grounded?

Mattsson: Yes.

Barnett: Was the dose rate significantly different for the photon and electron beams?

Mattsson: No.

-

Schulz: You assumed a 3.5% exothermicity for your calorimetry?

Mattsson: Yes.

-

Schulz: What was your thermistor power level?

Mattsson: About 6 W.

Schulz: A higher thermistor power would have given you less noisy rating periods.

-

Domen: Did Schulz and Kubo observe similar overshoot anomalies in electron beams as you did?

Kubo: I did.

Schulz: We did not.

Domen: Perhaps the polyethylene films cause trouble. I suggested in my original report to put some cement between the films.

Kubo: This might be part of the answer. I noticed that the effect depends on detector fabrication.

Domen: What size thermistors did you use?

Mattsson: They were the same as what you used.

Rogers: Is the absorbed dose in the thermistors different in electron and photon beams?

Mattsson: I don't know.

-

Kubo: Has there been any intercomparisons of orthovoltage x-ray measurements?

Mattsson: In Scandinavia, there have been exposure intercomparisons, but not absorbed dose.

Kubo: Why has the IAEA come up with a different number now?

Hohlfeld: The IAEA figures go down to only 200 keV. These values are based on measurements of absorbed dose in a phantom using extrapolation chambers. The ICRU method in report 23 is the direct application of an ionization chamber.

Mattsson: What is introduced in the IAEA protocol is a replacement correction. I have not understood the physics behind the value of this correction. I think it is in the wrong direction. This is the factor that leads to the difference between the ICRU and the IAEA.

RECENT DEVELOPMENTS IN GRAPHITE AND WATER CALORIMETERS FOR ELECTRON BEAM DOSIMETRY AT NPL

D T Burns & W T Morris
National Physical Laboratory
Teddington, Middlesex, UK

ABSTRACT – This paper describes the design and testing of the new NPL electron beam graphite calorimeter, with some recent results of comparisons with existing absorbed-dose standards. The proposed design for an electron beam water calorimeter, based on the graphite calorimeter, is discussed and the possibility of using this water calorimeter as a transfer standard between X-ray and electron beams is presented.

RÉSUMÉ – Cette communication décrit la conception et l'essai au NPL d'un nouveau calorimètre à graphite dans un faisceau d'électrons, et des résultats récents de comparaisons avec des étalons existants de la dose absorbée. Nous examinons la conception proposée pour un calorimètre à eau pour un faisceau d'électrons qui se fonde sur le calorimètre à graphite, et nous présentons la possibilité de l'emploi de ce calorimètre à eau comme un étalon de transfert entre des faisceaux de rayons X et d'électrons.

1. INTRODUCTION

In the field of high-dose electron beam dosimetry, the primary standard in routine use at NPL is a graphite calorimeter with a thermocouple sensor (Burns and Morris 1988). Thermocouples were chosen for their convenience, ready availability and ease of use, although their relatively low sensitivity results in a lower dose limit to the calorimeter of a few kilograys.

With the possibility of food irradiation being permitted in the UK, a more sensitive graphite calorimeter employing a thermistor bridge has recently been developed, and has been shown to have a lower dose limit of only a few grays. It is also usable in electron beams up to high dose levels. The new calorimeter has the advantage of simplicity: there is no vacuum system, no temperature control, no calibrating heaters and no bridge balancing, nor is a high degree of operator expertise required. However, it is still subject to the uncertainties inherent in the derivation of absorbed dose to water from the measured absorbed dose to graphite, in particular the electron collision stopping-power ratio of water to graphite.

Current interest in water calorimetry and recent progress towards an understanding of the heat defect in water have led to a proposal for an NPL water calorimeter, for use in horizontal electron beams down to a few tens of grays. Such a calorimeter would eliminate not only the stopping-power correction, but also the relatively large uncertainty in the specific heat of graphite. By comparing the water calorimeter with the new NPL X-ray primary standard of absorbed dose to water (based on the graphite microcalorimeter and the photon-fluence scaling theorem (Burns *et al* 1987)), valuable information should be gained on the heat defect of the water. The water calorimeter could also be usable as a transfer standard for absorbed dose to water between X-ray and electron beams (Owen 1988).

2. NEW GRAPHITE CALORIMETER

The design of the new, more sensitive graphite calorimeter is based upon that of the existing NPL high-dose electron beam calorimeter. It is intended to cover the dose range from industrial level calibrations of typically 25 kGy down to the lower end of food irradiation around 50 Gy.

2.1 Calorimeter Construction

The absorbing element is a disc of graphite, 50 mm in diameter and 7.16 mm in thickness. A 1½mm diameter, 1 cm deep hole is drilled radially into the absorber to accommodate a glass bead thermistor. Thermal contact with the graphite is improved by using a small amount of heat-sink compound at the thermistor bead.

This absorber is inset into the surface of a larger block of graphite, 9 cm high by 9 cm wide by 2.5 cm deep, which is thermally isolated from the absorber by a nominal ½mm air gap. Small expanded polystyrene beads suspend the absorber in this air gap. The dimensions of the larger block have been chosen to be sufficiently large to ensure complete scattering of electrons into the absorber, but at the same time small enough to ensure relatively uniform heating of the whole block, in area and depth, in a scattered 10 MeV electron beam from the NPL linear accelerator (LINAC).

The absorber and block are completely enclosed in 1 cm of expanded polystyrene. If this assembly is allowed to reach equilibrium in an environment which is temperature controlled to ±1 K, then the measured absorber temperature drift is linear over a period of tens of minutes and is always less than 1 mK/min. Dose rates down to about 10 Gy/min are therefore measurable without the need for further temperature control. In particular, no vacuum system or controlling heaters are necessary.

2.2 Thermistor Calibration and Specific Heat Measurements

Figure 1 shows the temperature measurement system. The temperature sensor is a 1½mm diameter, 50 kΩ glass bead thermistor. A simple DC Wheatstone bridge employing low noise, low temperature-coefficient precision resistors is supplied by a 5 V reference voltage i.c. with long-term stability to better than ±50 μV. Power dissipation in the thermistor is around 120 μW. The out-of-balance voltage from the bridge is read by an IEEE-488-controlled digital voltmeter (DVM) with excellent noise rejection, so eliminating the need for an AC bridge arrangement at these dose rates. The overall noise from the system is typically ±10 μK.

The out-of-balance voltage V is calibrated directly in terms of absorber temperature T. This calibration was carried out by Temperature Standards section at NPL against a secondary standard platinum resistance thermometer accurate to ±1 mK. The calibration data in 0.2 K steps between 19 °C and 24 °C was fitted with a function $T(V)$ of the bridge parameters and each point was fitted to better than ±1 mK. This function is programmed into the controlling computer which therefore calculates the absolute

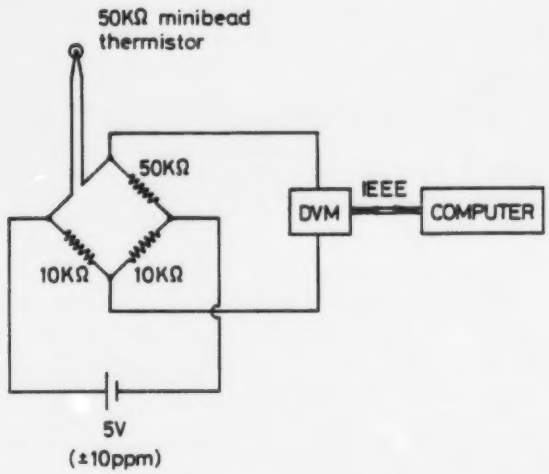

Figure 1 – Temperature measurement system

absorber temperature directly from the bridge out-of-balance voltage. The uncertainty in the gradient dT/dV at any temperature within the limits of the fit is estimated to be less than 0.1%.

The specific heat $c_g(T)$ of a sample taken from the graphite used in the calorimeter was measured at NPL as a continuous function of temperature over the range 0 °C to 50 °C using the technique of differential scanning calorimetry (Richardson 1984). The results are shown in Figure 2, the overall uncertainty in the measured values being quoted as ± 1%. From these it can be seen that the specific heat varies significantly even over the restricted temperature range 20 °C to 25 °C within which the calorimeter is normally operated. It is evident that taking a constant value for the specific heat, for example the commonly tabulated 25 °C value, can lead to a systematic error of several percent. In practice a linear fit to the data is programmed into the controlling computer:

$$c_g(T) = 642 + 2.9\,T(°C) \quad \text{J/kg/K} \qquad (2.1)$$

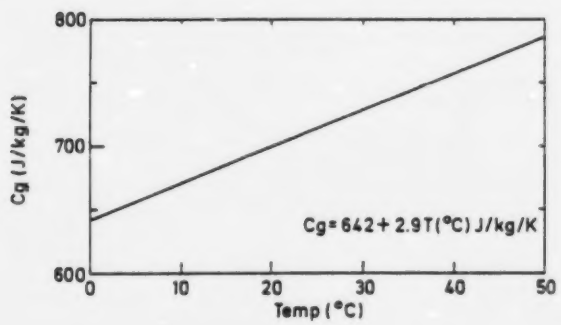

Figure 2 – Specific heat of graphite used in calorimeter

2.3 Data Analysis and Beam Monitoring

The bridge out-of-balance voltage V is read every second by the DVM under computer control. After each reading, the absorber temperature is calculated using the temperature calibration function $T(V)$ and the result is plotted on a temperature/time graph throughout the irradiation.

Figure 3 shows the actual computer printout for a typical

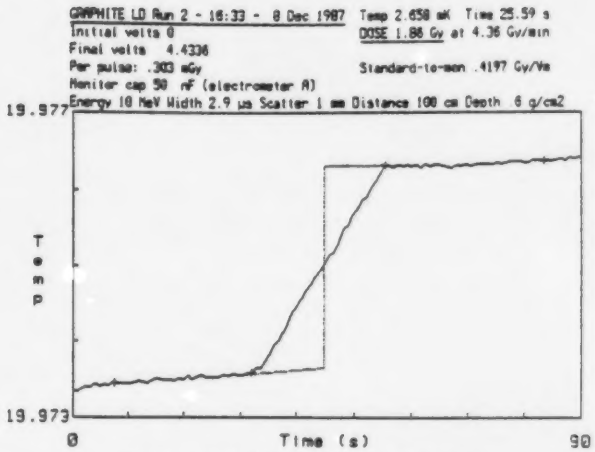
GRAPHITE LO Run 2 - 16:33 - 8 Dec 1987 Temp 2.658 mK Time 25.59 s
Initial volts 0
DOSE 1.86 Gy at 4.36 Gy/min
Final volts 4.4336
Per pulse: .303 mGy
Standard-to-mon .4197 Gy/Vs
Monitor cap 50 nF (electrometer A)
Energy 10 MeV Width 2.9 µs Scatter 1 mm Distance 100 cm Depth 6 g/cm2
19.977
19.973
Temp
0
Time (s)
90

Figure 3 – Typical irradiation of less than 2 Gy

low-dose irradiation. The temperature/time data is analysed to correct for background temperature drift during the irradiation by extrapolation of the pre- and post-irradiation data sets (using linear fits) to the midpoint of the irradiation period. The corrected temperature rise ΔT_c is taken as the difference between these extrapolated temperatures. The mid-irradiation temperature T_{mid} is calculated from the actual temperatures recorded immediately before and after the irradiation. The points labelled + defining the boundaries between which the linear fits are made are chosen by the operator — the remainder of the analysis is automated and takes only a few seconds. The absorbed dose to graphite is then given by

$$D_g = c_g(T_{mid})\,\Delta T_c \qquad (2.2)$$

The electron beam current output from the LINAC is subject to short-term variations of a few percent, and the reproducibility of calorimeter results from one irradiation to the next cannot be reliably determined without monitoring these changes in beam current. At the low dose-rate end of the calorimeter operation, a transmission ionisation chamber can be used. For higher dose rates, an automated charge monitoring system has been installed on the LINAC (Burns 1985), shown schematically in Figure 4.

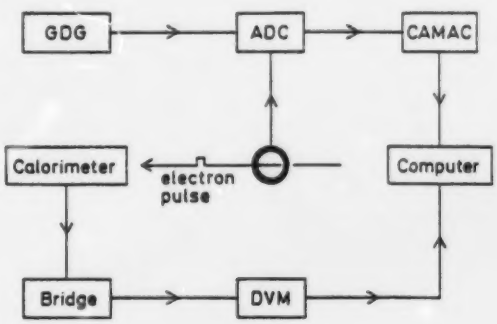

Figure 4 – Electron beam charge monitoring system

Current signals from a pulse-transforming coil wound toroidally around an insulating section of the accelerator flight tube are passed to a fast current-integrating ADC and the resulting charge reading digitised in approximately 100 μs and read (via CAMAC interfacing) by the controlling computer. A gate and delay generator (GDG) allows this integration to take place only for the

duration of each beam pulse so that any noise picked up between beam pulses, for example radio-frequency pickup in the pulse-transforming coil or in the coaxial cabling, is ignored.

Correlation of the charge information with the absorbed-dose measurement takes account of any drift in the LINAC output.

2.4 Correction to Absorbed Dose to Water

The present method of determining the absorbed dose to water in a water phantom from the measured absorbed dose to graphite in a graphite phantom involves two correction factors.

(i) Electron collision stopping powers take account of the different energy absorption characteristics of different materials for a given mean energy incident at the point of measurement. These are taken from Berger and Seltzer (1982). Correcting from graphite to water for an incident energy of 10 Mev and a measurement depth of 0.60 g/cm^2:

$$\frac{S_w^{col}}{S_g^{col}} = 1.134$$

with an estimated uncertainty of ± 1.5% at the 99% confidence level.

(ii) The above correction does not take account of the possibility of a different electron fluence and spectral distribution of energies incident at the measurement position. The effect of different build-up materials on the electron fluence at a given depth has been measured on the NPL LINAC using a specially designed, water-immersible ionisation chamber (Morris 1988a). The results for water, graphite and aluminium in the 10 MeV electron beam are shown in Figure 5. For the fluence ratio water/graphite at 1 g/cm^2, these yield the (null) result:

$$\frac{F_w}{F_g} = 0.997 \pm 0.005$$

It is evident that, in the particular case of correcting from graphite to water, the stopping power correction is sufficient.

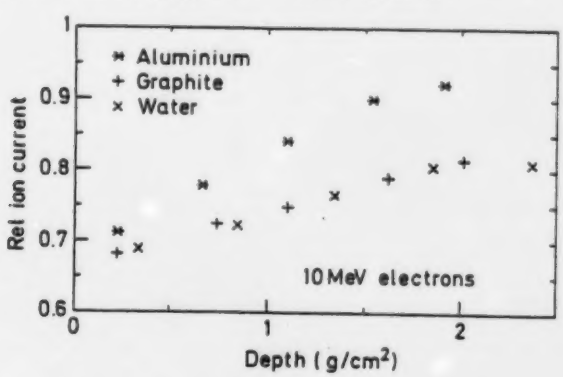

Figure 5 – Electron fluence build-up in various media

2.5 Calorimeter Performance and Uncertainties

The random uncertainty in the calorimeter/monitoring system can be estimated by evaluating the standard deviation in the calorimeter dose per unit monitor charge for a series of irradiations. This is typically 0.4% and is generally better at the low-dose end of the operating range.

There are two major components of non-random uncertainty. The larger is the uncertainty in correcting for background temperature drift during an irradiation, ie the uncertainty in the linear fits and extrapolations of Figure 3. For high doses, this is estimated to be as large as ± 2%, although for small doses the post-irradiation region is more linear and the correction is normally better than ± 1%. The other major component is the uncertainty in the measurement of the specific heat of graphite, which has been estimated to be ± 1%.

The total non-random uncertainty in the absorbed dose to graphite at lower doses, including the smaller uncertainties in the thermistor calibration, impurity correction, change in thermistor power, etc., is estimated to be ± 2% at the 99% confidence level. In addition, correction to absorbed dose to water must include the uncertainties given in Section 2.4. The total non-random uncertainty in the measurement of absorbed dose to water is estimated to be ± 2.5%.

The new calorimeter was compared with the existing high-dose graphite calorimeter in a 10 MeV electron beam at a dose rate of 3.5 kGy/min. The mean ratio of four separate comparisons is

$$\frac{\text{high-dose calorimeter}}{\text{new calorimeter}} = 0.984 \qquad \text{sd } 0.9\%$$

This agreement is within the non-random uncertainty of both systems and relates the new calorimeter response to a previous intercomparison between the high-dose graphite calorimeters of NPL, NBS and Risø (Morris *et al* 1988b), which gave satisfactory agreement between all three calorimeters.

The new calorimeter has also been compared with the NPL potassium dichromate reference dosimeter (Sharpe *et al* 1985). This dosimeter is supplied in 2 ml glass ampoules, 12 mm in diameter, and can be used in electron beams of 8 MeV and above to doses between 10 and 40 kGy. Calibration in terms of absorbed dose to water is based upon the NPL 2 MV primary standard of exposure and the accuracy of this calibration is quoted as ± 4% at the 99% confidence level.

The ampoules were irradiated in pairs with their centres 2 cm apart in a graphite phantom. The electron beam was scattered using a 2 mm aluminium plate and the graphite front face was positioned at 1 m from this plate. Irradiations were carried out at 10 MeV at a depth of 1.5 g/cm^2 in graphite and at a dose rate of 7 kGy/min. The raw results are shown in Table 1, giving the mean ratio dichromate/calorimeter = 0.980 (standard deviation 0.3%).

Dichromate dose estimate (kGy)	Calorimeter dose estimate (kGy)	Ratio dichromate/ calorimeter
19.44	19.83	0.980
19.46	19.83	0.981
12.10	12.33	0.981
12.12	12.33	0.983
27.65	28.27	0.978
27.56	28.27	0.975

Table 1 – Comparison of graphite calorimeter with dichromate

This result closely confirms a previous result (Burns and Morris 1988); the 2% under-reading of the dichromate dosimeter seems to be consistent and reproducible and is likely to be due to the perturbation of the graphite by the dichromate ampoule. The magnitude of this effect has been estimated, using the electron fluence build-up data shown in Figure 5, to be 2.4%. The corrected ratio is then

$$\frac{\text{dichromate dose}}{\text{calorimeter dose}} = 1.003$$

This agreement is well within the overall non-random uncertainty for both systems.

3. WATER CALORIMETER PROPOSAL

One advantage of the new graphite calorimeter is the simplicity of both the calorimetric body and the measurement system, and it is hoped that this will also be a feature of the water calorimeter. The temperature measurement system of the graphite calorimeter can be used in a water calorimeter with only a slight modification to make the thermistor leads watertight. Initial tests were conducted in a 20 cm by 20 cm by 20 cm Perspex container filled with tap water. These showed that, with as little as 1 cm of expanded polystyrene insulation, the temperature stability at a distance of 2 cm from the thin-film entrance window is better than 30 μK/min (Figure 6). With such stability, a dose rate as low as 10 Gy/min to water can be measured without the need for further temperature control/insulation.

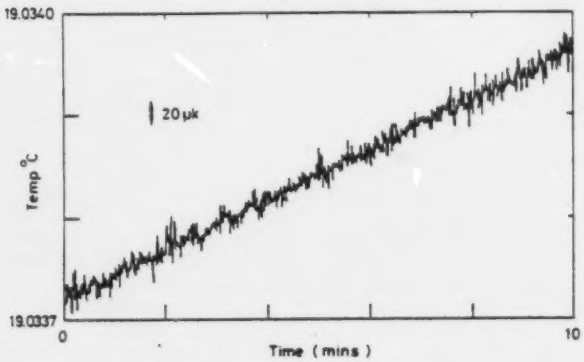

Figure 6 – Stability of water temperature (showing noise level)

Three problem areas are envisaged: the presence of convection currents generated by the horizontal electron beam; the excess temperature rise produced in the sensor/mounting/container arrangement, all parts of which have a lower specific heat than that of water; and the heat defect of the system.

3.1 Convection Considerations

The use of a water calorimeter in a horizontal electron beam is the worst case from the point of view of possible convection effects. Schulz and Weinhous (1985) have shown that the temperature distribution set up by irradiation with a 19 MeV horizontal electron beam led to pronounced convection currents for doses as low as 20 Gy (at 30 °C). In their calorimeter, water circulation was not restricted and no attempt was made to minimise temperature gradients.

The present proposal is to introduce a vertical film barrier to convection beyond the sensor at a depth of around 3 cm. Depth-ionisation measurements at the NPL LINAC have shown that, for the 16 MeV electron beam, the dose in the first 3 g/cm^2 of Perspex changes by only 2%. Assuming a similar depth-ionisation distribution for water, a dose of 10 Gy therefore induces a temperature gradient of less than 20 μK/cm, some 50 times less than that of Schulz and Weinhous (1985).

In the radial direction, the scattered NPL electron beam at 16 MeV is reduced in intensity at the measurement depth by around 2% at a radius of 5 cm. Therefore an isolated disc of water, 10 cm in diameter by 3 cm deep, would at no point have a temperature gradient greater than 20 μK/cm. Such an arrangement is not likely to induce convection currents.

3.2 Correction for Materials other than Water

The materials of the thermistor, bead and supporting structure have a specific heat typically 5 times lower than that of water, so that the temperature rise in the water tends to be overestimated. The fractional correction for this effect is a function of the time allowed for equilibration following an irradiation, and the effective volume of water 'seen' by the thermistor.

Assume, as in the initial tests, that the thermistor is supported by a 4 mm diameter glass tube with 0.4 mm thick walls and that the thermistor protrudes by 1 cm from the end of the tube. If the measurement time after irradiation is sufficiently long that there is equilibration throughout the 10 cm diameter disc of water (assuming thin-film convection barriers with the thermistor at the centre of the disc), then the correction for the different masses, specific heats and stopping powers of the materials to the measured temperature rise is calculated to be much less than 0.1%. However, for such times, conductive heat transfer from outside the disc may not be negligible, particularly to the rear of the disc. Behaviour is more predictable if the effective equilibration radius is limited to 1.5 cm (half the disc thickness). The correction to the measured temperature rise is then –0.25% to an uncertainty of less than 0.1%

3.3 Heat Defect

There is growing evidence, both experimental (Ross *et al* 1984, Schulz *et al* 1987, Domen 1982) and theoretical (Ross *et al* 1984, Fletcher 1982), to suggest that a constant, in some cases non-zero heat defect can be obtained by saturation of highly purified water with a suitable gas mixture. Pre-irradiation to a dose of up to 100 Gy may be required to use up any remaining organic impurities.

In the initial stability tests at NPL, tap water was used and effort has been concentrated on designing a simplified system which may be used particularly in horizontal electron beams. It is envisaged that the prototype will be a sealed container of highly purified water with perhaps the provision for bubbling though particular gases, depending upon the outcome of measurements being made presently at various laboratories.

An alternative approach planned at NPL is to use the water calorimeter as a transfer standard between X-ray and electron beams. This will make use of the new NPL calibration service in absorbed dose to water based upon the primary standard graphite microcalorimeter (Burns *et al* 1987, Owen 1988) The transfer between graphite and water in X- and gamma-radiation has been carried out by two independent methods; one experimentally-biased and making use of the photon-fluence scaling theorem, and the other using cavity ionisation theory. Agreement between the two methods is excellent, typically 0.2% (Burns and Owen 1988).

The transfer from X-rays to electrons would involve comparing the water calorimeter in X-radiation with existing secondary or working standard ionisation chambers calibrated in absorbed dose to water. This would yield absolute information on the heat defect by a novel method. By assuming that the heat defect for electrons is the same as that for X-rays, the calorimeter could then be used as a transfer standard in electron beams for calibration of secondary standard electron chambers. Intercomparison with the new electron beam graphite calorimeter would provide a confirmation route and yield information on the relative stopping powers of graphite and water.

4. SUMMARY AND CONCLUSIONS

The new graphite calorimetric system performs consistently and with sufficient accuracy to suit the calibration needs of the majority of industrial users of electron beams at high and intermediate dose levels. The simple and rugged construction of the calorimeter makes it easily portable and suitable for use over a very wide range of doses and dose rates. The calorimeter agrees with the existing NPL high-dose calorimeter, and good agreement with the potassium dichromate reference dosimeter relates the calorimeter response to the NPL 2 MV X-ray primary standard of exposure.

A prototype water calorimeter has been constructed with a thin-film entrance window suitable for use in horizontal electron beams, using the same temperature measurement system as the graphite calorimeter. Initial tests have shown that minimal thermal insulation can produce excellent thermal stability and doses of around 10 Gy can be measured. A film-barrier arrangement has been introduced to minimise convection currents, and the correction for the presence of materials other than water has been calculated. Further work is necessary on the heat defect.

Both the graphite and water calorimeters have been shown to be sensitive enough to work at dose rates below 20 Gy/min. At such rates, the dose per beam pulse can be made sufficiently low that the calorimeters may be compared directly with ionisation chambers (with a small recombination correction). This can therefore be used to relate the water calorimeter response in X-rays directly to the NPL primary standard graphite microcalorimeter, *via* the photon-fluence scaling theorem. If the heat defect in electron beams is the same as that for X-rays, the water calorimeter can then be used to transfer a measurement of absorbed dose to water from X-rays to electrons. This would enable absorbed dose to water calibrations for electrons to be based on the same primary standard as has been established for X-rays.

REFERENCES

M J Berger & S L Seltzer 1982, *Stopping Powers and Ranges of Electrons and Positrons*, NBSIR 82-2550 (National Bureau of Standards, Washington, D.C.)

D T Burns 1985, *An Automated Charge Monitoring System for the NPL Linear Accelerator*, NPL Report RS(EXT)80 (National Physical Laboratory, Teddington, Middlesex)

D T Burns & W T Morris 1988, *High-Dose Calorimetric Standard for Electron Beams*, NPL Report RS(EXT)101 (National Physical Laboratory, Teddington, Middlesex)

J E Burns *et al* 1987, *New Calibration Service for High-Energy X-Radiation at NPL*, IAEA-SM-298/56 in Proceedings of the International Symposium on Dosimetry in Radiotherapy, Vienna, Austria, 31 Aug – 4 Sep 1987; to be published

J E Burns & B Owen 1988, to be published

S R Domen 1982, J Res Natl Bur Stand **87** p 211

J W Fletcher 1982, *Radiation Chemistry of Water at Low Dose Rates with Emphasis on the Energy Balance: A Computer Study*, AECL-7834 (Chalk River Nuclear Laboratories, Chalk River, Ontario)

W T Morris 1988, to be published

W T Morris, D T Burns, A Miller & W L McLaughlin 1988, to be published

B Owen 1988, private communication

M J Richardson 1984, Chapter 17 in *Compendium of Thermophysical Property Measurement Methods Vol 1: Survey of Measurement Techniques*, edited by K D Maglić, A Cezairliyan & V E Peletsky (Plenum Press, New York)

C K Ross, N V Klassen & G D Smith 1984, Med Phys **11** p 653

R J Schulz & M S Weinhous 1985, Phys Med Biol **30** p 1093

R J Schulz, C S Wuu & M S Weinhous 1987, Med Phys **14** p 790

P H G Sharpe, J H Barrett & A M Berkley 1985, Int J Appl Radiat Isot **36** p 647

Discussion

Ross: We have attempted to have the specific heat of graphite measured and the best we could do absolutely was 2%.

Burns: They quote 1% on the measurement we had done.

Rogers: In your automated system, can you sample the DVM once per pulse from the linac?

Burns: Yes. The maximum pulse frequency is 240 pps.

Klassen: If you want to use the water calorimeter as a transfer instrument in the way you described you will have to make sure that the dose rates are the same since the heat defect depends on the dose rate. As well, if the calorimeter is not irradiated uniformly, the concentration of products will not be the same in different parts of the vessel and they will diffuse later on.

McDonald: Do you have to worry about having thermal barriers isolating the radiolytic products?

Klassen: They will have an effect.

Burns: We have to find out more about using thermal barriers. We don't know what we will use. We have done some work with Kapton but we don't know what kind of impurities you can get into the water from Kapton.

McDonald: What kind of voltmeter did you use?

Burns: It's a Datron.

Ross: Have you had electrons on your calorimeter, and did you see any of the thermistor effects discussed earlier?

Burns: The only measurements we've made so far have had pronounced convection effects. I have seen that effect with electron beams in graphite.

Domen: What's the physical size of your water calorimeter?

Burns: The tank is 20 × 20 × 20 cm.

Domen: How close were you to the vertical beam entrance wall?

Burns: 2 cm.

McDonald: How was the thermistor supported in the water bath?

Burns: It was supported by a capillary tube of 4 mm outside diameter and 1/3 mm wall thickness and the thermistor protruded about 1 cm from the end.

Domen: What was your thermistor power?

Burns: About 100 microwatts.

Domen: That's very large.

WATER CALORIMETRY IN EDINBURGH

T.M. Kehoe and G. Galloway, Dept. Medical Physics, Western General Hospital, Edinburgh

The measurement of absorbed dose to ICRU muscle by a water calorimeter in neutron beams has been compared to that measured with an Exradin A-150 ionisation chamber. The doses were measured using the ECNEU protocol. The calorimeter measurements were lower than the ionisation chamber by 4.4% and 2.2% in low and high energy beams. Measurements in 4 & 9 MV photon and 10 Mev electron beams have also been done and compared to other workers.

La mesure de la dose absorbée par le muscle ICRU au moyen d'un calorimètre à eau dans des faisceaux de neutrons a été comparée à celle mesurée au moyen d'une chambre d'ionisation Exradin A-150. Les doses ont été mesurées à l'aide du protocole ECNEU. Les mesures calorimétriques étaient inférieures à celles de la chambre d'ionisation de 4,4 % et de 2,2 % dans des faisceaux de faible énergie et d'énergie élevée. Des mesures dans des faisceaux de photons de 4 et 9 MV et dans un faisceau d'électrons de 10 MeV ont aussi été effectuées et comparées aux résultats d'autres travailleurs.

INTRODUCTION

As some of you are aware, a neutron trial took place between '77 and '83 at Edinburgh. Radiation beams via a fixed head or isocentric head were used to treat bladder, head and neck tumours. The reaction providing the neutrons was 16 MeV deuterons impinging onto a Be target, this gave a beam of similar penetrating capability to orthovoltage x-rays.

International neutron dosimetry protocols recommend the use of A-150 ionisation chambers flushed with TE gas for absorbed dose estimates in fast neutron beams (AAPM 1980, Broerse et al 1981). Unfortunately, the uncertainty in a converted ionisation chamber reading in a beam such as that at Edinburgh is approx. 6.5% (Mijnheer et al 1981). The largest component of which is the kerma ratio used to convert the dose in A-150 to ICRU muscle the reference medium for neutrons (ICRU 1964). In the '80s the first water calorimeter was built by Domen (1980) with significantly less uncertainty than 6.5%. It is against this background that Gordon Galloway, in Edinburgh, built a water calorimeter to compare to dose estimates in the neutron beam using the recommended ionisation method. The results quoted here are in the main those of Galloway (1986).

As the calorimeter measures absorbed dose to water it is necessary to convert this to absorbed dose to ICRU muscle. This is done via the kerma ratio whose value is 0.93 based on data of Caswell (1980), with an uncertainty of approx. 0.4% for the Edinburgh beam. However the water calorimeter has one additional uncertainty and this is the heat defect.

THE CALORIMETER

The design is basically a copy of Domens', see fig. 1. The calorimeter is seen from the front. In the centre is a large perspex tank of base area 34 cm square and 30 cm height. Surrounding this is 7 cm of expanded polystyrene and a plywood box, this affords some insulation.

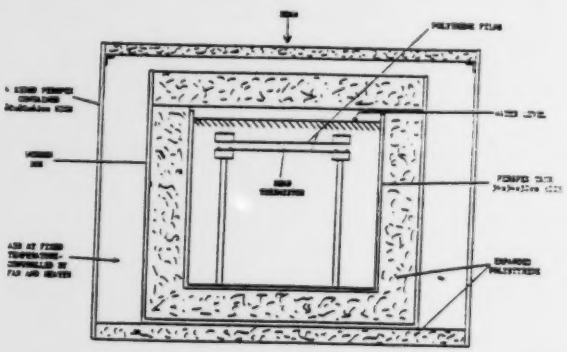

Fig. 1

Aluminium foil coats the inner surface of the plywood and polystyrene to cut down radiation losses and is earthed to act as an electrostatic shield. The plywood box is positioned inside a 80 cm square by 62 cm high perspex tank with a polystyrene lid and base. The temperature of the air in this outer tank is controlled to within 0.05 K. The air is contiuously circulated by a fan in front of which are two, 9 ohm heating coils. The voltage supplied to the heating coils is proportional to the difference between a set temperature on a control box and the air temp. monitored at one site in the tank by a thermistor.

Background drifts of less than 50 uK/min were easily achieved, but the smaller drifts of less than 10 uK/min necessary for neutron measurements were more difficult, but attainable.

The leakage modulus of the calorimeter has been calculated at 4×10^{-6} per sec. So even for long irradiation runs the convention of extrapolating linear initial and final drifts to mid-run is still valid.

THE DETECTOR

In common with other workers the detector is a

thermistor, an ITT U23UD bead, 0.5 mm diameter made of Pt-Ir with a nominal 2 kohm resistance at 20 °C. It has 25 μm diameter leads which were soldered to 80 μm diameter laquered copper wire.

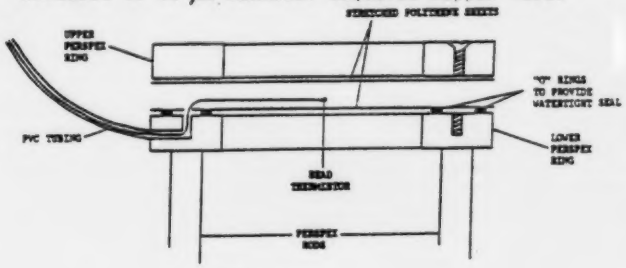

Fig. 2

Fig. 2 shows the thermistor sandwiched between two, 25 μm thick sheets of polyethylene. The sheets are pulled and clamped taught by two perspex rings 15 cm inside diameter, the rings are 3 cm wide and 1.25 cm thick. During assembly silicon grease was smeared radially in between the layers to help with adhesion and the removal of air pockets from the vicinity of the bead. More grease was smeared between the O-rings which completed the "water-tight" arrangement. Foreign materials at the point of measurement are unwanted, however, the bead, wires and sheets occupy only about 0.8% of the volume of a sphere of 10 mm diameter.

When in use the detector was screwed onto three permenant perspex legs so that its position was reproducible. As a direct comparison of dose estimates was made, a second jig has been built for the A-150 ionisation chamber. The chamber used was an Exradin, of volume 0.5 cubic cm. There were no air gaps at the tip where the wall thickness was 1 mm of perspex. A flexible plastic tube isolated the chamber and its cable from the water and was taken out of the calorimeter through the lid. The ionisation chamber jig occupies 50 cc more than the thermistor jig, so when in use this amount of water was removed to keep the depth of measurement constant.

THE BRIDGE

The neutron doserate was only 25 cGy/min, about 1/10th that of a typical linear accelerator photon doserate. This corresponds to a temp. rise of about 60 μK/min and consequently the detection system had to able to measure such a rise with accuracy. An a.c. bridge designed by Calverd (1982) specifically for calorimetry work was used. This type of bridge removes the problem with thermoelectric emf's observed with d.c bridges, and adequate sensitivity can be obtained with one thermistor. This together with a phase sensitive detector allows small signals to be picked out of a noise component permitting the power levels to be reduced without losing sensitivity. The bridge essentially has unequal impedance arms, with a large balance detector impedance, and a balance resistance box approx. 10x the thermistor resistance, the sensitivity approaches twice that of equal impedance arms. The circuit is shown in fig. 3, T1 is the transformer giving unequal arms, S1 is the themistor. A further amplification of the signal can be obtained by coupling the bridge output to the phase sensitive detector via a step-up transformer T2, without compromising bridge linearity. The gain factor is governed by the turns ratio, here this is 6.

The bridge is operated remotely from the calorimeter and is connected by 12.5 m cables. Any temperature changes in the leads introduce a resistance change indistinguishable from a thermistor resistance change. Because of the asymmetry in the arms simply adding the lead resistance in series with R6 and S1 will still result in a contaminated signal. To overcome this the transformer T2 has a third winding, a centre winding closely matched to the primary but in antiphase. By setting R7 to a particular value the voltage fed to the secondary and hence the phase sensitive detector is independent of lead resistance for symmetrical changes. The four leads are microphone quality coax. cables. The bridge is excited at 375 Hz well away from mains harmonics.

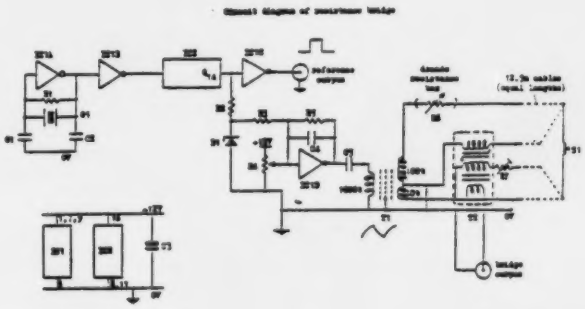

Fig. 3

The phase sensitive detector, a Brookdeal 9503 had a time constant of 1 sec and bandpass filters of 30 Hz and 1 kHz. The output voltage from the detector was fed to a chart recorder and a Cromemco microcomputer. The chart recorder is calibrated in ohms/mm, and the ADC in ohms/V by manual changes in the bridge balance resistance box. The chart recorder resolution is much poorer than the computer, but it does provide a visual check during the runs. The computer automatically stores the incoming data in 3 arrays, initial drift, and final drift are tracked for a minimum of 1 min., and the beam on array. Voltage samples were taken every 2 secs. A linear regression was performed on the drifts which are extrapolated back to mid length of the beam-on array, and the voltage difference calculated.

The bridge performance has been checked by replacing the thermistor with a 2 kohm resistor. The peak-to-peak noise level was 200 μohms, equivalent to 3 μK. With the thermistor in place, The noise level is approx. 5 μK. The sensitivity of the bridge, i.e the output voltage/unit temp.

rise is 23 mV/K at a power level of 9 μW. With this sensitivity temperature changes of 10 μK are detectable.

DETECTOR CALIBRATION

The thermistor had a B value of 3000 K. As a change of 1 K results in only 0.7% change in sensitivity a linear relationship between resistance and temperature was assumed. Even over a period of successive runs there is an overall rise in temperature of typically 0.02 K which results in a sensitivity change of only 0.01%. The sensitivity was regularly checked for signs of radiation damage. No change was seen over 2 kGy of absorbed dose.

The self-heating of the thermistor needs to be corrected for. The power dissipated in the thermistor was altered by tuning the voltage on the primary of the bridge transformer. A linear relationship between resistance and power was observed see fig. 4 and hence the excess temp. of the thermistor is also linear with power.

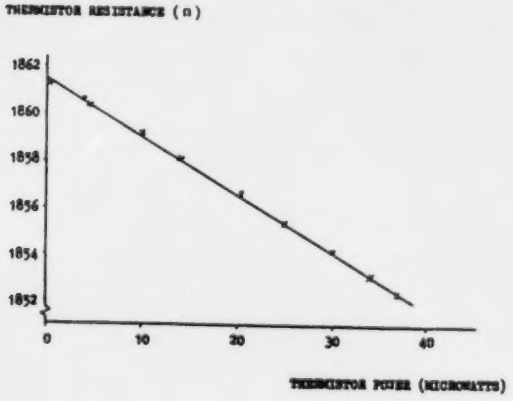

Thermistor resistance as a function of power dissipation

Fig. 4

Therefore the fractional change in thermistor power is equal to the magnitude of the fractional change in thermistor resistance during a run. A typical overestimate value was 0.2 - 0.3%.

The thermistor was calibrated absolutely against an NPL traceable mercury in glass thermometer capable of reading 0.01 K in a constant temperature bath. When a drift rate of less than 1 mK/min was seen on the bridge the resistance of the thermistor along with the temperature was noted. As stated before this is essentially linear over the small temperature range of interest, see fig. 5.

During an irradiation run, the absorbed dose in the polyethylene sheets is greater than the surrounging water and a correction must be applied for this. The overestimate of temperature is time dependent and reduces by conduction from the sheets to water. The appropriate correction can be determined mathematically if we replace

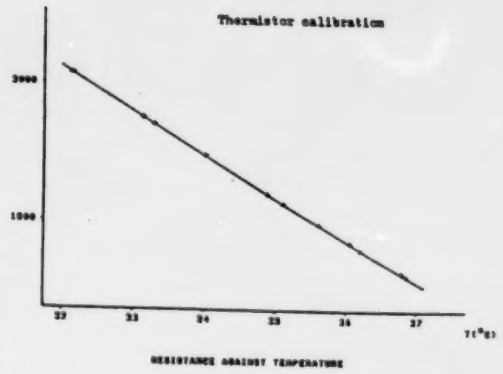

Fig. 5

the polyethylene with a water layer containing the same equivalent excess temperature. In this way effectively there is a homogeneous medium in which a thin layer observes a higher doserate. Fig. 6 illustrates the actual situation in the calorimeter. The conduction is symmetrical about the x axis, which is a good approximation to the

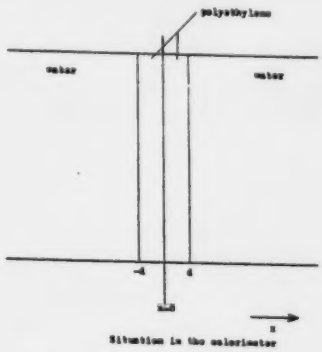

Fig. 6

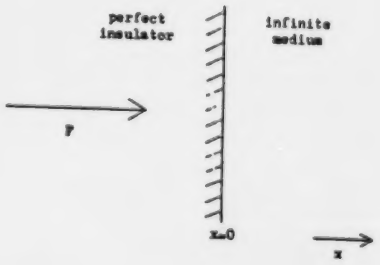

Fig. 7

theoretical situation tackled by Carslaw and Jaeger (1959). The excess temperature rise in this equivalent layer of water for the Edinburgh neutron beam of mean energy 6 MeV corresponds to an excess doserate of approx. 70% over the surrounding water. (For photons and electrons the excess doserate is 46%). The solution provides a

graphical plot of excess temperature expressed as a percentage of the temperature at the time of beam off, tracked over a post irradiation time see fig. 8. As the final drift, tracked over 1 to

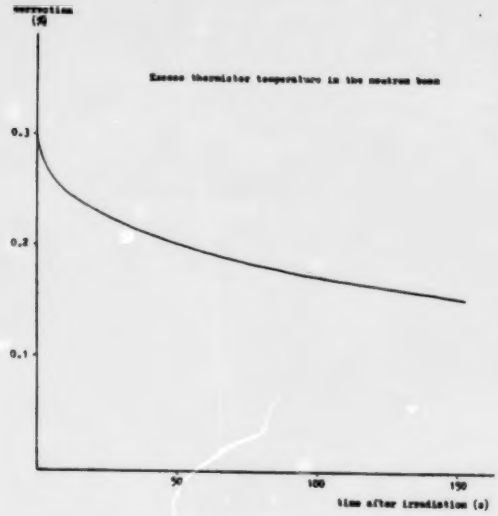

Fig. 8

5 mins, is projected back to the mid run position there is a slight overestimate in the observed resistance change. However the plot shows that a standard correction of 0.2% is applicable with an uncertainty of 0.1%.

A similar analysis for the effect of excess temperature in the bead and leads results in a correction an order of magnitude lower, and is therefore ignored.

RESULTS

In all the radiation runs that follow the water used was triply deionised and had dissolved organics removed by filter. At the start of each radiation session the water was preheated to remove oxygen and hence reduce the formation of gas bubbles underneath the lower polyethylene sheet. Before concentrating on the neutron runs, the calorimeter was used in two photon beams of 4 and 9 MV, and a 10MeV electron beam. As with the neutron irradiation, the dose estimates by the calorimeter and the Exradin were compared.

In the 4 MV beam, the thermistor was at 5 cm deep, at 100 cm from the source, in a field 30 cm square. The doserate was typically 220 cGy/min. Table 1 summarises the 4 MV data. N is the no. of runs per measurement, Rs is the balance resistor value before beam on, ΔRs is the change in balance and ΔT the equivalent temperature rise. The next column is the power dissipation in the thermistor, the standard deviation of each group of runs. The next two columns show the relative readings of the calorimeter and the Exradin chamber normalised to a seperate reference chamber positioned inside the

1	350	16	17887	0.464	0.90	31	0.7	0.4468	0.4666	1.057
2	300	16	16861	0.467	0.79	30	0.6	0.4360	0.4540	1.036
3	300	16	16939	0.435	0.79	19	1.0	0.4375	0.4557	1.039
4	300	16	17398	0.440	0.79	19	1.0	0.4327	0.4466	1.037
5	950	9	16480	0.237	0.62	30	1.0	0.4480	0.4651	1.038
6	70	10	17000	0.0950	0.10	30	0.9	0.4368	0.4579	1.048

mean = 1.040

Table 1

calorimeter. Finally, the ratio of the calorimeter to Exradin absorbed doses to water. The mean ratio is 1.040. Table 2, illustrates the data for 9 MV photons in a similar set-up, the mean ratio of

1	100	15	17239	0.135	0.27	16	1.0	0.4390	0.4561	1.039
2	100	10	16861	0.138	0.27	17	0.6	0.4379	0.4557	1.036
3	100	10	16899	0.138	0.27	17	0.6	0.4387	0.4566	1.033
4	400	10	16860	0.583	1.09	17	0.8	0.4388	0.4558	1.064
5	400	10	16869	0.588	1.09	17	0.7	0.4439	0.4617	1.058
6	1000	10	17274	1.36	2.69	16	0.6	1.195	1.244	1.040
7	1000	9	17794	1.38	2.68	16	0.8	1.210	1.258	1.040
8	1000	5	17997	1.35	2.66	16	0.5	0.4380	0.4556	1.040
9	500	6	17997	0.69	1.23	16	1.0	0.4376	0.4550	1.040
10	1000	6	17279	1.39	2.66	16	0.8	0.4388	0.4573	1.042
11	500	6	17279	0.67	1.36	16	1.3	0.4376	0.4573	1.045
12	500	6	17279	0.68	0.86	16	1.0	0.4377	0.4573	1.045
13	800	10	17837	0.27	0.53	31	1.3	0.4383	0.7577	1.036

mean = 1.045

Table 2

dose estimates is 1.045.

For 10 MeV electrons, the thermistor was at Dmax, 110 cm from the source in a 35 cm square field The doserate was typically 290 cGy/min. A correction has been applied to the Exradin readings to allow for displacement of the chamber centre. Table 3 shows the electron results. The

1	400	10	16437	0.466	0.98	34	0.8	0.5000	0.5276	1.053
2	400	10	16868	0.567	0.95	35	0.6	0.5000	0.5284	1.056
3	400	9	16883	0.597	1.05	36	0.4	0.5010	0.5289	1.066
4	470	10	15885	0.596	1.10	36	0.7	0.5040	0.5321	1.075
5	400	10	15460	0.588	1.13	35	0.5	0.5047	0.5296	1.050
6	450	10	15899	0.588	1.10	35	0.5	0.5008	0.5443	1.055

mean = 1.055

Table 3

mean ratio was 1.055.

These data are similar to other published work (Domen 1980, Kubo 1983 & 1986). For the low LET runs the typical irradiation time was 1 to 2 mins.

In the neutron runs a typical irradiation time was 5 mins, as the doserate was only 25 cGy/min, at 5 cm deep, at 124 cm from the source in a 25 cm circular beam. A transmission ionisation chamber

situated in the isocentric radiation head was used to normalise for beam variations. A typical sequence during a session was, a calibration run interspersed between radiation runs. Exradin readings were done immediately after the calorimeter runs. The total dose delivered per run was 1.3 to 1.5 Gy. Fig. 9 shows typical radiation

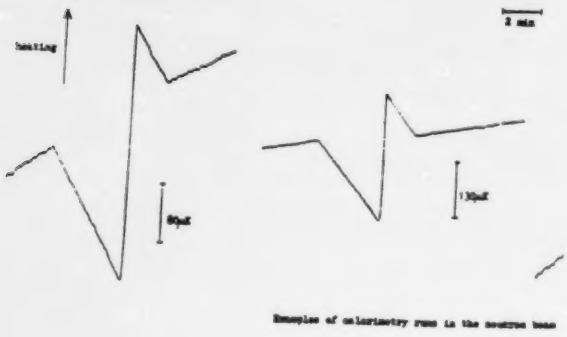

Fig. 9

runs in the Edinburgh neutron beam, because of the low doserate only one manual resistance change was necessary. Table 4 shows the neutron

1	100	10	14425	0.170	0.380	95	1.0	1.360	1.380	0.960
2	100	10	14436	0.171	0.384	95	0.6	1.375	1.380	0.980
3	100	8	14519	0.168	0.380	94	1.0	1.360	1.380	0.964
4	100	13	14423	0.170	0.383	94	1.3	1.380	1.350	0.981
5	99	14	14486	0.163	0.387	13	0.1	1.395	1.360	0.976
6	99	13	15000	0.158	0.394	11	1.3	1.380	1.405	0.947
7	99	9	14470	0.159	0.388	13	0.6	1.370	1.405	0.959
8	100	11	14418	0.160	0.366	15	0.0	1.360	1.414	0.966
9	110	13	14488	0.166	0.379	14	1.0	1.450	1.350	0.959

mean = 0.956

Table 4

results suitably corrected from dose to water to ICRU muscle. The mean ratio of absorbed dose is 0.956.

At a later date another collegue performed similar measurements in a more energetic neutron beam from 62 MeV protons bombarding a Be target at Clatterbridge (Wiliams et al 1987). The bead was at 5 cm deep, 150 cm from the source where the doserate was 50 cGy/min. The dose received by the thermistor was 1.1 Gy over 2 mins. For these measurements a different bead was used which was significantly noisier at about 15 μK peak-to-peak. Due to the lack of available time this noise could not removed, the resulting experimental uncertainty for this data is somewhat larger. Table 5 summarises the data from 40 radiation runs over a two-day period, the

Results of absorbed dose to tissue measurements (in cGy/monitor unit) with the water calorimeter and ionisation chamber.

Run number	Calorimeter	Ionisation chamber	Ratio
I	1.376 ± 0.056	1.438	0.957 ± 0.039
II	1.495 ± 0.033	1.497	0.999 ± 0.025
Average ratio			0.978 ± 0.033

Table 5

average ratio was 0.978. Tables 6 and 7 list the overall uncertainty in the low LET and high LET results respectively. The uncertainty quoted in $\Delta R_s/R_s$ is 3x the standard error of the mean of a set of calorimetry runs.

Quantity	Uncertainty (%)
$\Delta R_s/R_s$	1.0
Thermistor sensitivity	0.2
Correction for power dissipation	0.05
Correction for polyethylene films	0.1
c	-
Overall uncertainty	1.0

Uncertainties in calorimetry measurements.

Table 6

Quantity	Uncertainty (%)
$\Delta R_s/R_s$	1.6
Thermistor sensitivity	0.2
Correction for power dissipation	0.05
Correction for polyethylene films	0.1
c	-
Kerma ratio	0.4
Overall uncertainty	1.7

Uncertainties in a calorimetric measurement in the neutron beam.

Table 7

To-date ther are no other published data for neutrons in a water calorimeter, although calorimeters made of A-150 plastic have been built (Bewley et al 1974). If the ionisation chamber readings are assumed correct, then these results suggest a positive heat defect due to endothermic reactions of magnitude 4.4% for low energy, and 2.2% for high energy neutron beams.

Most calorimeters of similar design indicate

an exothermic heat defect for low LET radiation, one obvious possible conclusion is that the heat defect for high LET is different from that for low LET. This may be the case as the interactions for neutrons are very different from those for electrons. Essentially there is no difference in the operation of the calorimeter in either high or low LET radiation beams. Perhaps it is unlikely though, that we would expect to see a 9% difference in the calorimetry dose estimates to ionisation chamber dose estimates for the different types of radiation. This may illustrate a discrepancy in the applied kerma ratios from A-150 to ICRU muscle. The uncertainty in the kerma ratio has been estimated at approx. 2.6% for the low energy beam, and nearer 10% for the high energy beam (Bewley 1980).

We await further high LET irradiation work to clarify the situation.

REFERENCES

AAPM 1980. Protocol for Neutron beam dosimetry, Report no. 7 (New York: AIP for AAPM)

Bewley, D.K., McCullough, E.C., Page, B.C. and Sakata, S. 1974 Phys. Med. Biol. 19, 831

Bewley, D.K. 1980 Proc. Workshop on Ion Chambers for Neutron Dosimetry (Brussels: CEC) p 209

Broerse, J.J., Mijnheer, B.J. and Williams, J.R. 1981 Br. J. Radiol. 54, 882

Calverd, A.M. 1982 J. Phys. E: Sci. Instrum. 15, 414

Carslaw, H.S. and Jaeger, J.C. 1959 Conduction of Heat in Solids. 2nd Ed. (Oxford: Clarendon Press)

Caswell, R.S., Coyne, J.J. and Randolph, M.L. 1980 Radiat. Res. 83, 217

Domen, S.R. 1980 Med. Phys. 7, 157

Galloway, G. 1986 Ph.D. Thesis. University of Edinburgh

ICRU 1964 Rep. 10b (NBS Handbook, Washington, DC)

Kubo, H. 1983 Phys. Med. Biol. 28, 1391

Kubo, H. 1986 Phys. Med. Biol. 31, 251

Mijnheer, B.J. and Williams, J.R. 1981 Phys. Med. Biol. 26, 57

Williams, J.R., Galloway, G. and Greening J.R. 1987 Phys. Med. Biol. 32, 403

Discussion

Ross: Do you do only neutron therapy?

Kehoe: No, this was just a trial that was performed to assess whether it had any benefits over photon therapy.

-

Kehoe: Has anybody done anything with neutrons?

Klassen: A computer simulation says that for your neutron beam on air-saturated water there would be a heat defect of +2.9% in the absence of any effects of impurities in the water.

Kehoe: What about protons?

Klassen: The situation is the same as far as the computer is concerned.

-

McDonald: Have you thought of using a TE liquid mixture for which the Kerma correction would be very small indeed as compared to ICRU muscle tissue? It would be more complicated to use.

Kehoe: Perhaps that's the way to go in the future. At Edinburgh, we have no chance because the cyclotron isn't there anymore, but that doesn't mean it shouldn't be done elsewhere.

-

Kubo: It is enlightening to know that you used the second dirtiest water, deionized water plus filter, I used only deionized water, and the rest of the people used distilled water and yet the heat defect of those so-called dirty waters is very close to 3.5 - 4%. that seems to support what Bob Loevinger was saying that "dirty water" might possibly be usable for a secondary standard.

Kehoe: Yes, we all seem to get the same with the same type of calorimeter. Surely, we can't all have the same type of dirty water.

Klassen: One possibility is that the important factor may be the yield of OH radicals which react with impurities to produce CO_2. The level of extra heat may depend on the yield of OH radicals and not on how much impurity is present, and only when all the impurity is gone do you get what you would call pure water.

Kehoe: So, if we all saturated the water in a particular way it might alleviate a lot of that problem.

Klassen: It might not depend on the concentration of the impurities. It may depend on the rate at which you produce OH radicals.

Ross: It is not strictly true to say that everyone gets exactly the same heat defect. There is at least a 2% difference.

-

Kehoe: We didn't see the overshoot on the electron beams.

Domen: Was there a little bit of silicone grease around the thermistor to make it tight or was there any air gap around it?

Kehoe: I am sure there was but we tried to eliminate that as much as possible. We couldn't see any but that doesn't mean there wasn't any there.

Kubo: Was the thermistor communicating with the air? At 5 cm depth the water pressure would compress the films. I tried that to check those spikes but I can't remember the details.

Kehoe: It is possible that air was trapped in between the two O-ring seals.

Domen: I avoided that by drilling a hole in the 4-pin socket so that the air communicates with the outside, so there is no trapped air and I never had an effect like Rob Barnett reported where he had to wait a day for it to settle down.

Kehoe: This calorimeter was dismantled and reassembled weekly. So, if air were trapped, it would be a different amount for each session.

THE DIRECT DETERMINATION OF DOSE-TO-WATER USING A FLEXIBLE, TEMPERATURE-REGULATED, SEALED-CORE WATER CALORIMETER[a)]

R.J. Schulz, C.S. Wuu, and M.S. Weinhous
Department of Therapeutic Radiology, Yale University
New Haven, Connecticut 06510

ABSTRACT - The response of a flexible, temperature-regulated at 4°C, sealed-glass-core, water calorimeter has been compared to ionization-chamber dosimetry. Using 4 MV x rays, the Cal/Ion ratio for N_2-saturated water is 1.002 ± 0.001, and for O_2-saturated water it is 0.987 ± 0.001.

La réponse d'un calorimètre à eau versatile, à noyau de verre scellé, thermostaté à 4 °C, a été comparée aux résultats dosimétriques d'une chambre d'ionisation. Sous des rayons X de 4 MV, le rapport Cal/Ion est de 1,002 ± 0,001 pour l'eau saturée de N_2 et de 0,987 ± 0,001 pour l'eau saturée de O_2.

INTRODUCTION

Calorimeters that respond to the temperature changes induced by ionizing radiations provide the only means by which absorbed dose to a specific material can be measured without recourse to radiation-dependent parameters such as stopping powers, photon cross sections, G-values, etc. The development of radiation calorimeters has a relatively long history, and instruments made of graphite, aluminum and polystyrene have proven extremely valuable for the dosimetry of the x-ray and electron beams used in radiation therapy. Currently, most dosimetry protocols for radiation therapy (1, 2, 3, 4) require that accelerator calibrations be specified in terms of the dose-to-water, and that the dosimeter be an ionization chamber calibrated for exposure (or air kerma) from ^{60}Co gamma rays or 2 MV x rays. Using the AAPM dosimetry protocol (1), calibration of a 25 MV x-ray beam may require the application of as many as a dozen radiation-dependent parameters to the reading of the ionization chamber to obtain the dose-to-water, and the overall uncertainty in this procedure may be as great as ±3%.

As water is the material in which absorbed dose is to be specified, then it is logical that the reference standard be a water calorimeter. Leaving aside early experiments with water calorimeters, the most significant steps in this aspect of dosimetry were taken by Domen (5,6) who reviewed the theory, constructed instrumentation, and described the operating characteristics of a practical, reproducible water calorimeter. Although it represented a pioneering effort, the Domen-type of calorimeter has one major defect and several drawbacks: a) it records a dose that is 3.5% higher than that predicted by an ionization chamber used in conjunction with a graphite calorimeter (5,7); b) it operates at room temperature and, as described by Rubo (8), takes many hours to equilibrate after a change in room temperature; c) it is subject to perturbations caused by convection currents; d) being open to the atmosphere and containing plastic components, it is not possible to control the quantity or quality of dissolved gases nor to assure the purity of the water; e) it is restricted to measuring beams that are directed vertically downward.

The present paper describes the authors' efforts to develop a water calorimeter that can serve as a reference standard. To this end, we have expanded upon Domen's accomplishments by constructing a flexible, temperature-regulated, sealed-glass-core calorimeter that largely overcomes the drawbacks listed above, and which records doses that are consistent with radiochemical theory and well within the range of uncertainty of the doses determined by ionization chambers.

METHODS AND MATERIALS

A. The calorimeter

A cross sectional plan of the calorimeter is shown in figure 1. The core is a 10 cm x 10 cm right cylinder made of Pyrex glass. The thermistor support assembly is an integral part of the core, and its location is fixed at the time of core fabrication. The core also contains two glass valves with Teflon stems, not shown, for introducing and exchanging water. We estimate that 60mm^2 of Teflon are in contact with the water, and that this is 10^{-4} of the total interior surface area of the core.

The thermistor support assembly is shown in greater detail in figure 2. The tube wall thickness at the thermistors is approximately 0.2 mm. In order to promote good thermal contact as well as to deter movement, the thermistors are secured by silicone grease (G.E. CG-689). The thermistors are 0.25 mm in diameter, have a resistance of about 5K at 4°C, and are obtained with 60 cm nickel-alloy leads to permit flexible movement of the core in relation to the remainder of the calorimeter during assembly and testing.

The jacket of the calorimeter, which surrounds the core, was originally to be filled with stagnant water to make the calorimeter more nearly homogeneous. It was subsequently decided that air in this space would provide better insulation, and greatly simplify the assembly of the calorimeter.

The shield, which surrounds the jacket, is divided into three compartments to assure a uniform distribution of the 4°C circulating water. Cold water is delivered at the rate of 5 l/min from a refrigerated circulator that has a 27 liter reservoir and regulates temperature within ± 0.1°C. The aluminum outer wall of the shield is insulated with foam rubber to reduce condensation and the effects of room-temperature.

In addition to the calorimeter shown in figure 1, which is primarily for use with x rays, a second calorimeter was constructed for use with electron beams. The main differences between the two can be seen by comparing figure 3 with figure 1: the 1.2 cm polycarbonate plates were milled to 0.24 cm, the thickness of the water jacket reduced to 1.2 cm, the flat surface of the glass core milled to a thickness of 0.086 cm, and the thermistor probes advanced to 1.33 cm of the front wall of the core from the 5 cm-depth they are at in the x-ray calorimeter. Discounting the effect of the air gap, the total mass of materials between the front surface of the calorimeter and the thermistors is equal to the depth of the dose maximum, d_{max}, for 16 MeV electrons. In all other respects the electron calorimeter is the same as the x-ray calorimeter.

B. Thermistor calibration and dose determination

The temperature change of the core water surrounding the thermistors is determined from the change in potential across a Wheatstone bridge in which the thermistors are located in opposite legs. These changes are detected by either a Keithley model 180 nanovoltmeter which drives a strip-chart recorder or a Keithley model 181 nanovolmeter connected to a Compaq Plus computer (see following paper on thermal defect measurements). When the bridge is balanced, the pen of the chart recorder is adjusted to midpoint deflection. A pre-irradiation rating curve is obtained by unbalancing the bridge to the right of the midpoint deflection. Irradiation times are selected which bring the pen to an equivalent location to the left of the midpoint. The sensitivity of the system is on the order of 2.6 V/cm of recorder deflection, and typical irradiations result in deflections of 15-20 cm.

The dose-to-water, D_{water}, is given by

$$D_{water} = c\,\Delta T\,(1+D_T) \qquad (1)$$

where c is the specific heat of water at the calorimeter operating temperature, ΔT is the rise in water temperature caused by irradiation, and D_T is the thermal defect. (The thermal defect is defined by $D_T = (E_a - E_h)/E_a$ where E_a is the energy imparted to a material and E_h is the energy appearing as heat.) At the calorimeter operating temperature of 4°C, the value of c is 4.2048×10^{-3} Gy/°C. (All specific heats used in our work are those of Osborne, Stimson and Ginnings (9) and apply to de-aerated water at constant pressure. According to Laby and Hercus (10), the mechanical equivalent of heat is 4.1852 J/cal at 15°C for both aerated and de-aerated water. The value is very close to that currently accepted by NBS, 4.1858 J/cal, so that the experimental techniques of Laby and Hercus must be regarded as having been careful and precise. Based upon the Laby and Hercus finding, we have assumed in the present work that nitrogen- or oxygen-saturated water has the same specific heat as de-aerated water.) The temperature rise, T, is calculated from various bridge parameters including the bridge unbalance as obtained from the chart recorder. The dose-to-water, omitting the thermal defect, is given by

$$D_{water} = -c\Delta V_u/(V_b[R_f m_1/(R_1+R_f)^2] + R_x m_2/(R_2+R_x)^2]). \qquad (2)$$

where ΔV_u is the bridge unbalance as determined from the chart recorder pen deflection, V_b is the voltage applied to the bridge, and m_1 and m_2 are the slopes, dR/dT, of the resistance versus temperature curves for the thermistors R_1 and R_2. The voltage measurements needed for the calculation of R_1, R_2, and R_x are generally made at the beginning and at the end of an experiment; only extremely small changes are seen and these changes have a negligible effect on the calculated dose.

In order to increase the absolute sensitivity and achieve satisfactory signal-to-noise ratios, the thermistors are routinely operated at 100 microwatts. However, to prevent even very small, power-level-dependent differences between calibration curves from affecting the dose calculations, zero-power-level curves obtained by extrapolation are used to determine the temperature change of the water.

Thermistors are calibrated after being secured in the glass capillary tubes within the core. The core is submerged in the reservoir of a refrigerated water circulator (Haake model A81). In addition to the cold water outside of the core, cold water is also circulated through the core by connections to the optional external inlet and outlet of the circulator. The temperature of this circulating water is maintained constant to better than ± 0.01°C. During calibration the thermistors are connected to the same Wheatstone bridge as is used at the time of irradiation. A typical calibration involves the determination of thermistor resistance at ten water temperatures in the range 2-7°C and five power levels in the range 15-200 microwatts.

A typical thermistor resistance versus power level curve, for water at 4°C, is shown in figure 4. Extrapolation of the curve to zero power is made by a linear, least-squares fit. The approximate temperature of the thermistors, as obtained from the slope of the R versus T curves in figure 5, is shown on the right-side ordinate. A resistance versus temperature curve at zero-power level is obtained from the zero-power resistance and the water temperatures at which they were obtained. A typical zero-power R versus T curve as well as similar curves obtained at 100 and 200 microwatts is shown is figure 4. These data are related by a function of the form

$$1/T = a_0 + a_1 \ln R, \qquad (3)$$

where a_0 and a_1 are obtained from a least-squares curve-fitting program. The slope of this curve as a function of resistance is given by

$$m = \frac{-dR}{dT} = \frac{R}{a_1} (a_0 + a_1 \ln R)^2. \qquad (4)$$

At the time of irradiation, the various bridge potentials are measured, and the resistance of each thermistor calculated. These resistances are then used with equation (4) to calculate the slopes, m, at zero power, and it is these values of m that are used in equation (2) to calculate the dose-to-water. By using the slopes that obtain at zero power, the change in thermistor resistance, ΔR, accurately reflects the change in water temperature, ΔT_w, independent of the power level actually employed.

During the course of irradiation, the resistance of the thermistor decreases with a concomitant decrease in the power level. This, in turn, leads to a decrease in the thermistor's temperature which would not have occured had the power level been maintained constant. Using data similar to those in figure 3, the temperature decrease that results from the power-level decrease is calculated, and the dose-to-water as determined by equation (2) corrected accordingly. For a dose of 600 cGy, this correction increases the dose recorded by the calorimeter by about 0.1%.

C. Core water

All of the water used in the present study was purified by an ion-exchange system (Millipore Milli-Q) which, according to the manufacturer, provides water having less than 0.03 ppm of dissolved inorganics, less than 0.01 ppm of silicates, less than 1 ppm of heavy metals, less than 1 ppm of dissolved organics, and a resistivity greater than 18 MΩ-cm at 25°C. As a thermal defect in water may depend upon dissolved gases, it is essential that their purity and constancy be carefully controlled. The gassing system shown in figure 6 is installed in a 4°C cold room. The gas flow rate is about 4 liters per minute, and this is maintained for at least three hours prior to filling the core.

To fill the core, the bubbler bottle is simply inverted, and the slight gas pressure forces the water into and out from the core. Generally, the core is flushed to the extent of 2-3 volumes by this method before the inlet and outlet valves are closed. Current procedure is to assemble the calorimeter in the 4°C cold room immediately after the core is filled, and to maintain the core at 4°C henceforth.

D. Irradiation conditions

The principal measurements were made using a Varian Clinac 4S accelerator. Ionization-ratios, measured in accordance with the AAPM protocol, yield a nominal accelerating potential of 3.9 MV. To obtain a dose rate of 3 Gy-min^{-1}, an SSD of 53 cm was used for all measurements; this places the thermistors or ion chamber at 65 cm from the source. A field size of 12 x 12 cm^2 at this distance completely encompasses the cores of the water and dummy calorimeters. The irradiation distance is established by a mechanical pointer which can be mounted to the front of the monitor ionization chamber.

To assure that reproducible x-ray exposures are delivered, the operation of the accelerator is carefully monitored, and an independent monitor ionization chamber is employed. Magnetron current and dose rate are maintained constant during each experiment. Reflected RF power was occasionally checked with an oscilloscope but this proved unnecessary if the AFC was adjusted to obtain maximum dose rate prior to use. A monitor ionization chamber consisting of parallel plates of aluminized Kaptan plastic 10 cm in diameter was constructed in a way such that it mounts to the accelerator using the same mechanism that normally holds the shadow tray. This chamber intercepts the entire x-ray beam. Because of the thinness and uniformity of the Kaptan plates, the chamber does not perturb the beam in any detectable way. When biased to +500V, the collection efficiency of this chamber is 0.96 when the nominal dose rate is 1.5 Gy-min^{-1} at 100 cm. This chamber is connected to a Keithley 6169 electrometer operating on the 10^{-7}C range.

In addition to the 4 MV x rays, trial irradiations were made with the x-ray and electron calorimeters using 25 MV x rays, and 16 and 28 MeV electrons produced by the Sagittaire accelerator. This accelerator operates at a fixed pulse repetition rate of 100/sec with a pulse width of 5×10^{-6} sec. Each x-ray pulse covers the entire treatment field, however, instead of using scattering foils to produce homogeneous electron fields, the electron beam is made to scan the treatment field by

electromagnets located close to where the beam exits the vacuum window. The dose per pulse in this scanning electron beam depends upon electron energy and the selected average dose rate which is a direct function of the beam current. Pertinent physical parameters for the Sagittaire that apply to these calorimeter experiments are given in Table I.

E. Reference dosimetry

The methodology of the AAPM dosimetry protocol (1) was employed to determine the dose-to-water from 4 MV x rays. A Farmer-type ionization chamber having an acrylic wall and buildup cap (PTW model 30-351) is employed. The cavity gas calibration factor for this chamber was calculated using an exposure calibration factor for ^{60}Co gamma rays traceable to NBS. The data used in equation (5) of the protocol, and the calculated value of N_{gas}, are listed in Table II. Note that the stopping-power ratios used in this calculation are those of Andreo and Brahme (11).

A dummy calorimeter, figure 7, of construction identical to the water calorimeter was used for ionization-chamber measurements in water. An acrylic build-up cap is secured into the core by a water-tight adapter so as to provide precise repositioning of the chamber. A thermistor temperature probe (Yellow Springs model 416) is mounted at the rear of the core. The attenuation and scattering of the x-ray beam in the dummy calorimeter is nearly identical to that which occurs in the water calorimeter. To confirm the depths of the thermistors in the calorimeter and the ion chamber in the dummy calorimeter, measurements using a laser mounted to a scanning platform are made during assembly, and radiographs made of the devices after assembly. Corrections for differences in absorption and inverse-square attenuation between the dummy calorimeter and any of the several water calorimeters constructed so far have not exceeded 0.2%. The parameters required by equations (9) and (10) of the AAPM protocol for the determination of dose-to-water from 4 MV x rays and the values employed are also listed in Table I.

III. RESULTS

The data presented in this section were obtained with the fifth in a series of glass cores whose designs were similar to that shown in figure 1. The results achieved with these earlier cores are essentially the same as those reported below, however, due to our failure to allow for expansion when brought back to room temperature, breakage prevented long-term evaluation of their performance.

A typical chart recording obtained with our calorimeter exposed to 4 MV x rays is shown in Fig. 8. The straight and parallel rating periods suggest that thermal equilibrium between the 100-microwatt thermistors and the core water has been achieved, and that temperature differences between the core and the water jacket are very small. The straight-line recording during irradiation indicates that the dose rate was constant and that there were no convection currents set up by dose gradients in the core. The insets show enlargements of the tracing when the beam was turned on and off. The almost instantaneous deflection with beam on is due to the effect of stray RF fields on the bridge circuit as well as the heating of the glass capillary tubing surrounding the thermistors. The rapid fall of the tracing which lasts for a few seconds after beam off is due to removal of the RF fields and the cooling of the glass by the surrounding water. In trial irradiations with 250 kV x rays, these instantaeous deflections were much larger due to the larger mass energy-absorption coefficient of glass compared with water at this energy. This blip at the beginning of the post-irradiation rating period is ignored in the extrapolation to the midpoint as it is equal to the instantaneous deflection observed with beam on. The equilibration of the glass and water temperatures is seen to be complete in about eight seconds post-irradiation; this observation is in close agreement with calculations made by Domen (12).

Detailed summaries of the results obtained with the present core filled first with nitrogen-saturated and then with oxygen-saturated water are given in Table III and Fig. 9. When filled with nitrogen-saturated water, the calorimeter response, i.e., the ratio of the dose-to-water from the calorimeter to that from the ionization chamber (Cal/Ion ratio), to 4 MV x rays has been very steady. The present core was first filled with hypoxic water and irradiated in mid July '86. In order to check the thermistor calibration, it was emptied and refilled with hypoxic water at the end of July, and that filling was retained until January '87. In the period January-February '87, the same core was twice filled with oxygenated water. As can be seen in Fig. 9, the patterns of response are consistent, and 38 of 47 Cal/Ion ratios fall between 1.000 and 1.010. In experiments 4 and 5, the response to the first irradiation is high whereas the subsequent responses were clustered within a narrow range. This behavior suggests the accumulation of some contaminant which is consumed by radiochemical reactions during the first dose, or the achievement of chemical equilibrium after the first irradiation. Excluding the two spikes in experiments 4 and 5, the grand mean (13) and the standard deviation of the grand mean for the five experiments with nitrogen-saturated water is 1.002 ± 0.001.

When filled with oxygen-saturated water, the Cal/Ion ratio is initially about 1.015, and then decreases to a stable value of about 0.99 after an accumulated dose of 60 Gy. Although the data in Fig. 9 are for two fillings of the present core, the same pattern was observed in an earlier core which received an accumulated dose of 440 Gy. The grand mean and its standard deviation for the four experiments depicted in Fig. 9, excluding Cal/Ion ratios for accumulated doses less than 60 Gy, is 0.987 ± 0.001.

Once, using the same core as used in the other 4 MV x-ray experiments described above, the water was saturated with laboratory air. This was accomplished with the apparatus shown in figure 6 but the tank of compressed gas was replaced by a centrifugal blower which was cleaned thoroughly to prevent oil and accumulated contaminants from affecting the quality of laboratory air. The response of this calorimeter as a function of accumulated dose is shown in figure 10. The five indicated experiments were performed over a period of one month. The letter P signifies that priming doses were delivered to more rapidly increase the accumulated dose than would have been practical using the single, 600 cGy doses delivered for each calorimetric determination. The initial, exothermic rise of the Cal/Ion ratio to slightly over 1.04 (and its subsequent fall to 1.006 is completely at odds with radiation chemical theory for N_2- and O_2-saturated water. We speculate that organic contaminants, such as automobile exhaust, is responsible for this pattern, and that these contaminants are mainly consumed by doses in excess of 600 Gy.

The results shown in figure 10 stimulated us to review data obtained with our first glass-core calorimeter which had a removable, glass, thermistor assembly like that shown in figure 2. This calorimeter gave the responses shown in figure 11 with N_2-saturated water. What is remarkable about these five experimental runs is the consistent rise and fall in the dose-response curves. We believe, but have no objective evidence for support, that air was leaking into the core between runs. As shown in figure 9, this type of response disappeared after the thermistor support was made integral with the glass core.

The results achieved with the nitrogen-saturated water calorimeter exposed to 25 MV x rays and 16 and 28 MeV electrons are listed in Table IV. These results are preliminary, and do no more than suggest agreement between ionization-chamber and calorimeter dosimetry for 25 MV x rays and 16 MeV electrons. What is significant in these data is the steadily decreasing Cal/Ion ratio with increasing dose per pulse for 28 MeV electrons. As it is unlikely that the response of the water calorimeter decreases with increasing dose rate, when the accumulated dose exceeds 100 Gy, the fault must be with the ionization chamber, and specifically with the correction for ion collection efficiency (P_{ion}). This was subsequently demonstrated in a comparison of the ionization chamber with the Fricke dosimeter. If the Cal/Ion ratio is taken to be unity, approximate values for P_{ion} can be readily calculated. These are shown in the last column of Table IV where it is seen that P_{ion} obtained by the two-voltage technique may be in error by as much as 14% when the dose per pulse is about 14 cGy.

IV. DISCUSSION

Two problems arise in assessing the accuracy of the water calorimeter for low LET radiation: first, is there a thermal defect, what is its magnitude, and does it depend upon dose rate and accumulated dose; second, to what method of dosimetry is the calorimeter compared, and what is its range of uncertainty.

There have been no direct measurements of the thermal defect in water, however, there is theoretical and experimental evidence that for hypoxic water it approaches zero for accumulated doses in excess of 70 Gy, and that dose-rate dependence also disappears above this dose level. Using a radiochemical model developed by Boyd, Carver and Dixon (14), Fletcher (15) calculated the effects various dissolved gases would have on the thermal defect of water as a function of dose and dose rate. For deoxygenated water, assumed equivalent to nitrogen-saturated water, Fletcher's data show a monotonically decreasing endothermicity starting at near 5% for very small doses, and approaching 0% at 100 Gy for dose rates in the range 1-10 Gy-min^{-1}. For oxygen-saturated water, the pattern is similar but 1% endothermicity is still obtained for a dose of 2000 Gy. In highly refined experiments, Ross, Klassen and Smith (16) compared the response of a calorimeter filled with N_2- and O_2-saturated water for doses in the range 50-500 Gy delivered at the rate of 25 Gy-min^{-1}. Their experimental results agree very closely with the predictions of the Boyd-Carver-Dixon model for the dose rate employed, i.e., a mean endothermicity of 1.9% for oxygenated water compared with 0.4% for nitrogen-saturated water, i.e., a mean separation of 1.5%. Our data in figure 8 for nitrogen- and oxygen-saturated water are similar to those of Ross et al in that they follow similar paths with accumulated dose and also have a mean separation of 1.5%. In view of the near impossibility of achieving the degree of chemical purity that is inherent to models, and the uncertainties introduced into calorimetric measurements by temperature probes and containment vessels, it does not appear likely that better agreement between predictions and experimental results will be attained in the near future.

Because of the wide application of ionization chambers to radiation dosimetry, the large and ever-improving store of data that relate to their use, and the half dozen or more dosimetry protocols that are based upon ionization measurements, it was both logical and of general interest to compare the water calorimeter to ionization-chamber dosimetry. The main problem in determining the dose-to-water from ionization measurements is the large number of radiation-dependent parameters used in the dose calculations, each of which has some degree of uncertainty. In the present application of the AAPM dosimetry protocol (1), there are ten radiation-dependent parameters used in the calculations of the cavity-gas calibration factor and the dose-to-water from 4 MV x rays. Based upon the conversations with knowledgable persons and the authors' experience, an estimate of the uncertainty in the dose-to-water is presented in table IV. Included in table IV are estimates of the uncertainties for the water calorimeter assuming that the thermal defect for water is zero. Based upon these data and those in table III, it appears that the two methods of dosimetry yield essentially the same result; either both systems yield the correct dose or both are in error to the same extent and direction.

V. CONCLUSIONS

The very close agreement between the present results for nitrogen- and oxygen-saturated water with those of Roés et al (16), and with the predictions of the model of Boyd et al (14) and the calculations of Fletcher (15), as well as the agreement with ionization-chamber dosimetry, suggest that the water calorimeter is gaining ground as a potential standard for the dosimetry of low LET radiations. A direct determination of the thermal defect of water will be required before it can become a standard, and plans for these determinations are underway at PTB in Germany (17) and also in our laboratories. The long sought goal of absorbed dose calibrations of ionization chambers in terms of dose-to-water for a wide range of x-ray and electron energies is closer to achievement.

REFERENCES

a) This work was supported by Grant No. CA38563-02 awarded by the National Cancer Institute

1. AAPM, Med. Phys., 10, 741-772, (1983).
2. NACP, Acta Radiol. Oncol., 19, 55-79, (1980).
3. SEFM, Publication No. 1-1984 Sociedad Espanola de Fisica Medica, Madrid, Spain.
4. HPA, Phys. Med. Bio. 28, 1097-1104, (1983).
5. Domen, S.R., J. Res. NBS, 87, 211, (1982).
6. Domen, S.R., Med. Phys. 7, 157-159, (1980).
7. Pruitt, J.S., Domen, S.R. and Loevinger, R., J. of Res., NBS, 86, 495-502 (1981).
8. Kubo, H., Phys. Med. Bio., 28, 1391-1399, (1983).
9. Osborne, N.S., Stimson, H.F. and Ginnings, D.C., NBS J. of Res., 23, 197 (1939).
10. Laby, T.H. and Hercus, E.O., Proc, Phys. Soc. (London), 47, 1003 (1935).
11. Andreo, P. and Brahme, A., Phys. Med. Bio., 31, 839-858, (1986).
12. Domen, S., NBS Gaithersburg, MD., personal communication.
13. Paratt, L.G., Probability and Experimental Errors in Science, Dover, New York (1961).
14. Boyd, A.W., Carver, M.B. and Dixon, R.S., Radiat. Phys. Chem., 15, 177 (1980).
15. Fletcher, J.W., AECL-7834, Chalk River Nuclear Laboratories, Chalk River, Ontario, Canada.
16. Ross, C.K., Klassen, N.V., and Smith, G.D. Med. Phys. 11, 653, (1984).
17. Hohlfeld, K., Physikalisch-Technische Bundesanstalt, Braunschweig, Fed. Rep. of Germany, personal communication.
18. Rogers, D.W.O. and Ross, C.K., submitted to Medical Physics.
19. AAPM, Med. Phys., 13, 755-759, (1986).
20. Schulz, R.J., Almond, P.R., Kutcher, G., Loevinger, R., Nath, R., Rogers, D.W.O., Suntharalingam, N., Wright, K.A. and Khan, F.M., Med. Phys. 13, 755 (1986).
21. Rogers, D.W.O. and Ross, C.K., Med. Phys., 15, 40 (1988).

ACKNOWLEDGEMENTS

The authors express their appreciation to Mr. E. Brosious of Yale University for his great skill and patience in constructing the glass components of the calorimeter, to Mr. George Saportin for machining the metal and plastic components, and to Mrs. K. Maturo for typing and retyping the manuscript.

Table I. Physical Characteristics of the Sagittaire accelerator.

Beam	Beam Diameter (FWHM)	Average Dose Rate*	Dose/Pulse*	Instantaneous Dose Rate*
1. 25 MV x rays	——	660 cGy/min	0.11 cGy	0.22×10^5 cGy/sec
2. 16 MeV electrons	10.6 cm	335	1.1	2.2×10^5
3. 23 MeV electrons	5.8	190	1.8	3.7×10^5
4. 28 MeV electrons	5.8	520	5.0	10×10^5
5. 28 MeV electrons	5.8	1500	14.0	28×10^5

*Assuming the water calorimeter to be correct.

Table II. Values of parameters used in equations (5), (9) and (10) of the AAPM protocol to calculate N_{gas} and D_{water}.

N_{gas}		D_{water} (4MV x rays)	
Parameter	Value	Parameter	Value
k	2.58×10^{-4} C/kg/R	Ionization ratio (water)	0.640
W/e	33.77 J/C	Nominal accelerating potential	3.9 MV
A_{icn}	1.00	$(\bar{L}/\rho)^{water}_{air}$	1.127
A_{wall}	0.990	$\bar{L}/\rho)^{acrylic}_{air}$	1.095
$(\bar{L}/\rho)^{acrylic}_{air}$	1.102	$(\bar{\mu}_{en}/\rho)^{water}_{acrylic}$	1.031
$(\bar{\mu}_{en}/\rho)^{air}_{acrylic}$	0.925	$\propto$ (wall and buildup cap, 0.59 g/cm^2)	0.96
K_{humid}	1.001[a]		
N_x	5.538×10^9 R/C[b]	P_{icn}	1.002
N_{gas}	4.712×10^7 Gy/C	P_{repl}	0.9925

[a]Combines corrections for humidity as described in references 20 and 21.

[b]Calibrated at the National Bureau of Standard (NBS), November 4, 1982. The calibration was reduced by 1.1% on 1 January 1986 in accordance with NBS recommendations.

Table III. Cal/Ion ratios for nitrogen- and oxygen-saturated water (All data obtained with core #5).

Experiment	Date	Irradiations*	Cal/Ion Ratio	
1	7/18/86	10	1.004 ± 0.002	
2	7/30/86	10	1.001 ± 0.003	
3	8/19/86	10	0.997 ± 0.004	N_2
4	11/4/86	10	1.002 ± 0.002	
5	1/20/87	8	1.001 ± 0.003	
			Grand Mean 1.002 ± 0.001	
6	1/27/87	7	0.988 ± 0.001	
7	1/30/87	10	0.987 ± 0.001	O_2
8	2/4/87	15	0.987 ± 0.002	
			Grand Mean 0.987 ± 0.001	

*About 5.9 Gy/irradiation.

Table IV. Cal/Ion ratios for nitrogen-saturated water exposed to high-energy x rays and electrons.

Beam	Cal/Ion Ratio	P_{ion} (2V)*	P_{ion}(Cal/Ion=1.00)
1. 25 MV x rays (2)	1.014	1.007	1.021
2. 16 MeV electrons (4)	0.989	1.018	1.007
3. 28 MeV electrons (2)	0.972	1.023	0.994
4. 28 MeV electrons (3)	0.958	1.054	1.010
5. 28 MeV electrons (1)	0.885	1.172	1.037

*Potentials were 500 V. and 100 V.

Table V. Estimates of uncertainties (95% confidence intervals) of parameters critical to the assessment of the water calorimeter.

		Uncertainty
Ionization-chamber dosimetry (4 MV x rays).		
1. Cavity-gas calibration factor N_{gas}.		0.5%
2. Stopping-power ratios, $(\bar{L}/\rho)^{water}_{air}$, $(\bar{L}/\rho)^{acrylic}_{air}$, for 4 MV x rays.		0.2% each
3. Ratio of mass energy-absorption coefficients, $(\bar{\mu}_{en}/\rho)^{water}_{acrylic}$		0.1%
4. Fraction of ionization due to electrons arising in chamber wall, α (effect on dose calculation).		0.05%
5. Correction for ion recombination, P_{ion}		0.1%
6. Replacement factor, P_{repl}.		0.2%
	Over-all	0.6%
Water calorimeter.		
1. Thermistor calibration, dR/dT.		0.3%
2. Thermistor resistance at time of experiment.		0.05%
3. Bridge unbalance caused by irradiaton (midpoint recorder deflection).		0.3%
4. Perturbation of the water temperature by the thermistor probes.		0.05%
	Over-all	0.4%
Common factors.		
1. Distance and attenuation corrections of ion chamber relative to calorimeter.		0.3%
2. Consistency of external monitor chamber and beam energy; ionization/calorimeter measurements.		0.2%
	Over-all	0.4%
Calorimeter/Ion Chamber Ratio	Over-all	0.8%

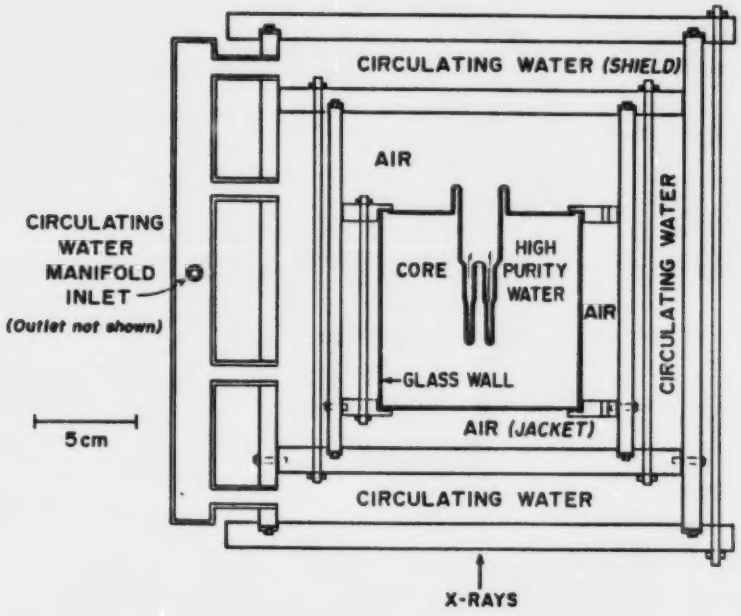

FIGURE 1

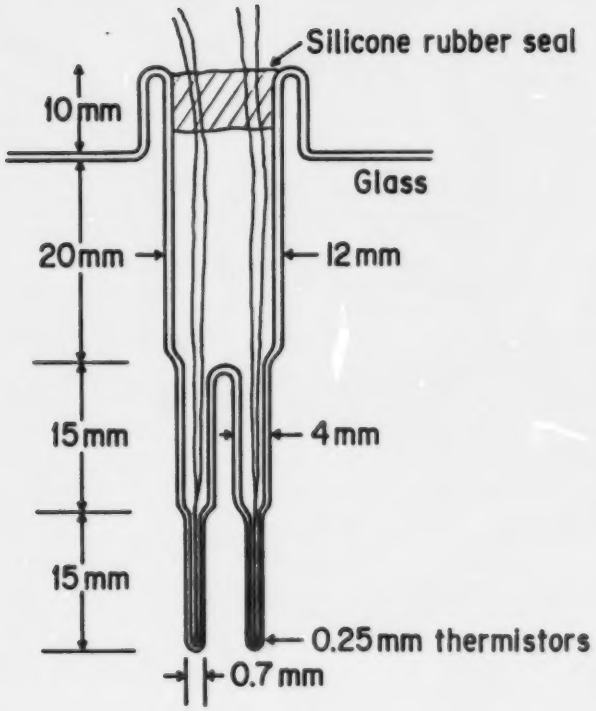

FIGURE 2

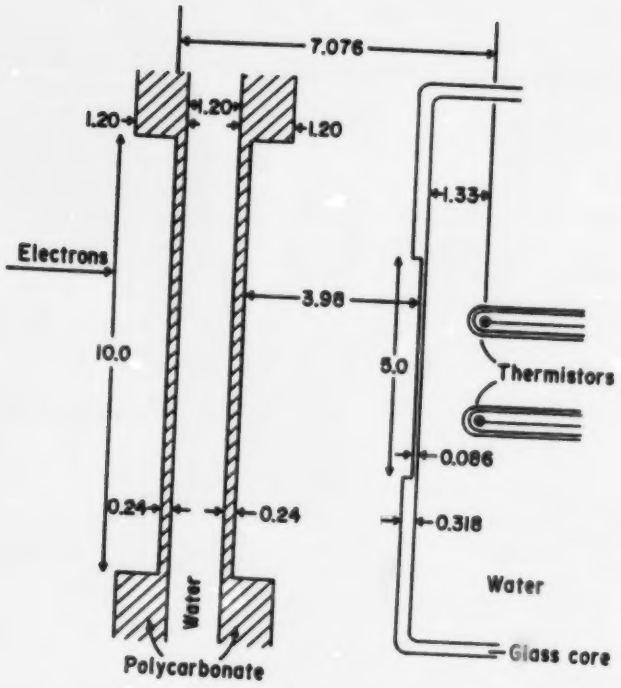

FIGURE 3

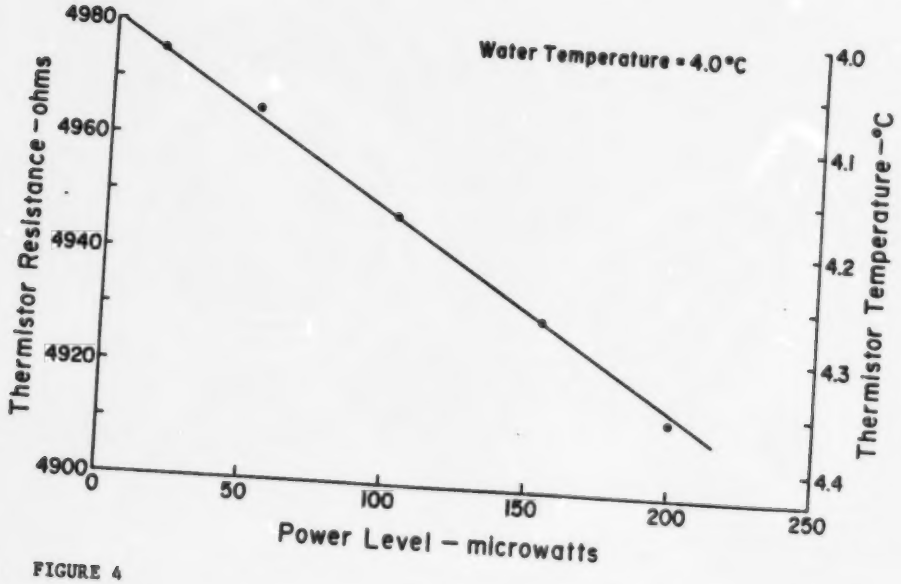

FIGURE 4

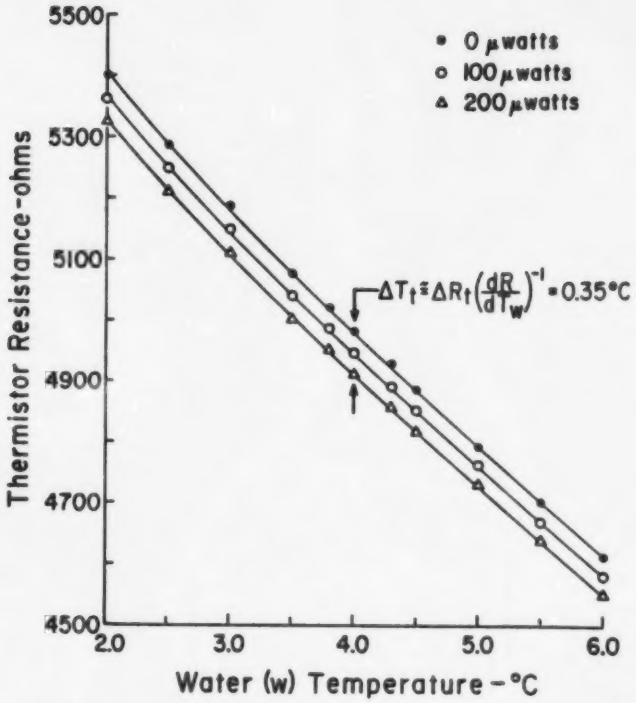

FIGURE 5

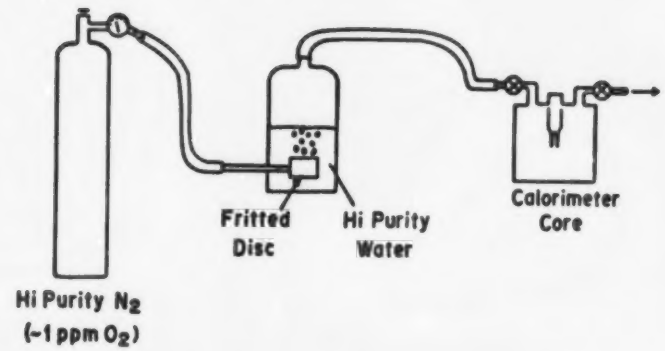

FIGURE 6

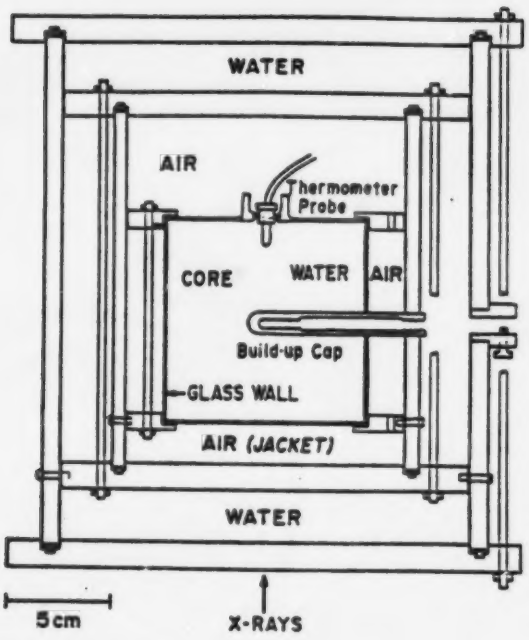

FIGURE 7

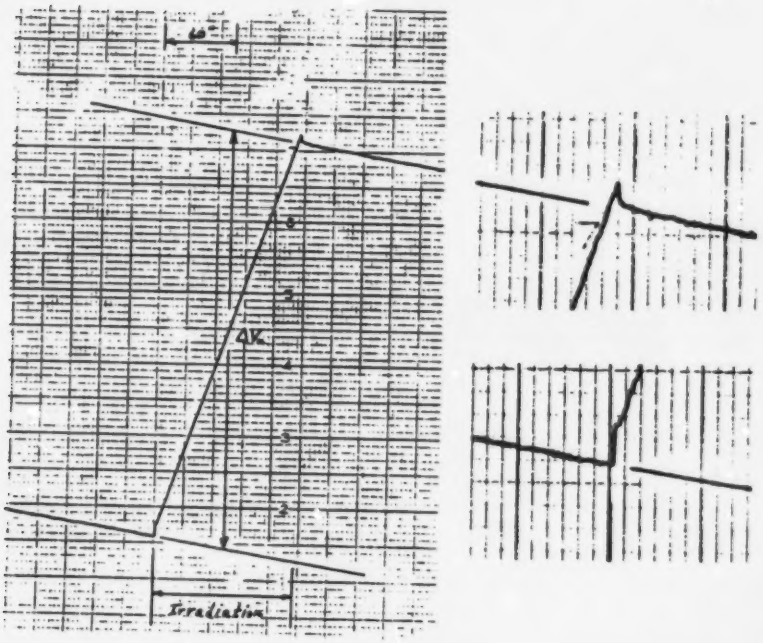

FIGURE 8

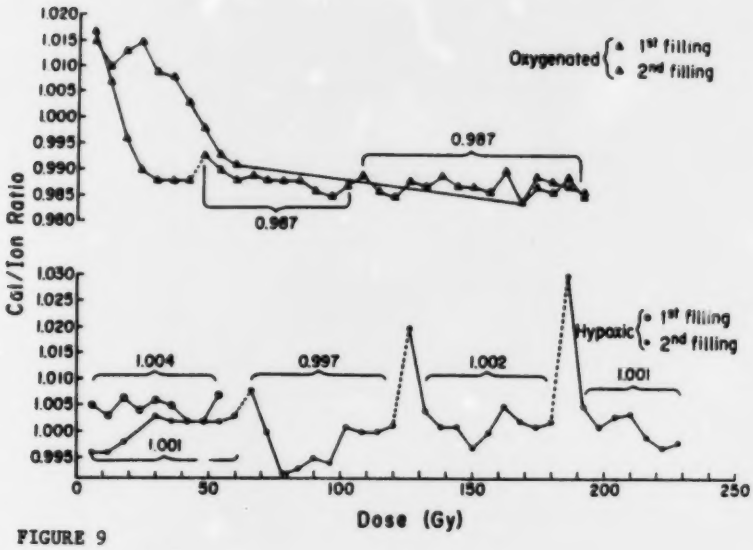

FIGURE 9

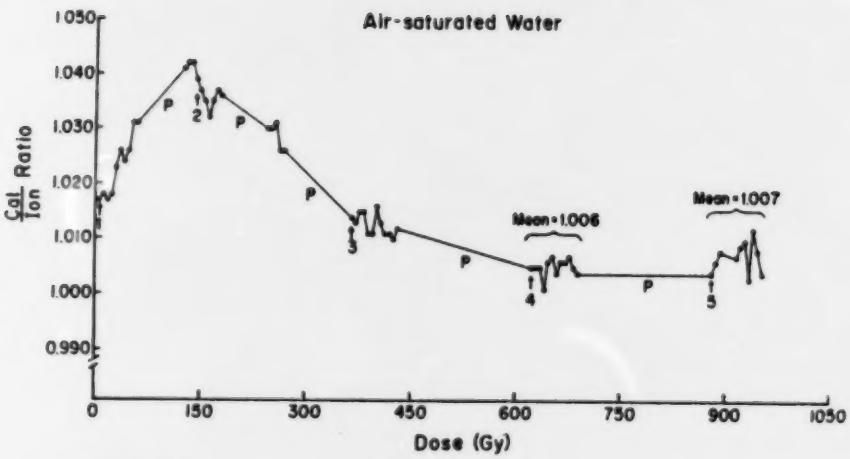

FIGURE 10

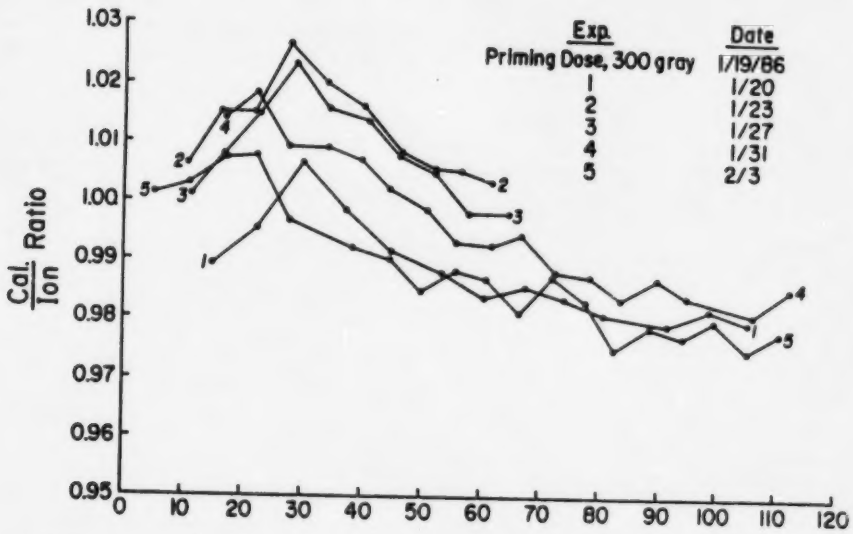

FIGURE 11

Discussion

Klassen: What tubing do you use?

Schulz: Tygon.

Klassen: Tygon tubing is supposed to be bad for water quality.

Schulz: I wouldn't be surprised. We wanted to get going and tygon is readily available and tough.

-

Rogers: Is everything at 4°C when you fill it?

Schulz: It used to be. We used to fill the core in a 4°C room and keep the calorimeter at 4°C. Otherwise, the core would break when it was warmed to room temperature. Most of the results I will describe were done in this way. Now we have a glass bubble on the core to take care of expansion and contraction and now we fill it at room temperature and cool it to 4°C. We would like to take the calorimeter on the road at some time and it would be difficult to keep it at 4°C.

Shortt: Did you notice any difference between the results with a calorimeter completely filled with water and one with an expansion bubble?

Schulz: No. Presumably, the expansion bubble is filled with nitrogen and would not change the hypoxic aspects of the water.

-

Kubo: Do you have any condensation problems with a chamber at 4°C?

Schulz: No. The ion chamber measurements were done at room temperature. With the calorimeter running at 4°C the polycarbonate end plates are sometimes dripping with condensation on a humid day but this hasn't stopped us from working.

Rogers: How thick is the lucite?

Schulz: It is somewhat thinner than the cap supplied with the chamber.

Rogers: So you have a 3-component P_{wall}?

Schulz: No, the chamber wall is lucite.

-

Rogers: Are your values of P_{ion} based on Weinhous' recent numbers?

Schulz: They are based on Boag's two-voltage technique. There are problems when the dose per pulse is too high.

Rogers: The AAPM says not to use the two-voltage technique if the correction is greater than 5%.

-

Rogers: Please comment on how big a perturbation you expect the glass and the core and everything to have on the dose to water that you actually measure. Is your thermistor imbedded in glass?

Schulz: Yes.

Rogers: With an air gap behind it?

Schulz: It is quite a ways behind it except for the air in the capillary tube. The air is pretty well downstream. I don't think the main body of air affects it. The excess heat in the glass, and the heat conduction along the capillary tube, turns out to be a very small correction which we haven't made. We do correct for the change in thermistor power before and after irradiation, as pointed out by Domen as a correction to be made, but it's a very small correction.

-

Rogers: As I understand it air-saturated should be the same as oxygen-saturated water, except for the dirt.

Schulz: That's what is bothersome about this. I don't know what is in most air. Maybe it's just a few hydrocarbons from a bus that passed by, but the result is the opposite to theory, it's exothermic. That's why I think calorimeters should have a controlled gaseous content and I think nitrogen is probably the best.

-

Loevinger: The two spikes that you got after the calorimeter was unused for an extended period and which you blamed on gas leakage, would be worrisome if you transported the calorimeter. You might get a spike at the end of the transportation.

Schulz: Yes, maybe.

Loevinger: This is something that needs to be investigated.

Schulz: The valves are all glass except for some teflon. Whatever it is that has gotten in, it disappears after ℓ Gy.

Loevinger: Oxygen wouldn't disappear.

Schulz: I said, whatever it is.

Loevinger: If you suspect a leak, you might have to put a small pump on the two valves to keep the air away.

-

Fletcher: Had you considered saturating with hydrogen rather than nitrogen?

Schulz: No. I am a little nervous about hydrogen. In the next year we plan to fill the device with a variety of tissue equivalent liquids with the ultimate goal of using this device for neutron beam dosimetry. We will have to concurrently look at the thermal defect of tissue equivalent liquids.

THE CHEMICAL HEAT DEFECT OF WATER

N.V. Klassen, C.K. Ross, K.R. Shortt and G.D. Smith
Division of Physics, National Research Council of Canada, M-35, Ottawa, Canada, K1A 0R6

The radiation chemistry of dilute aqueous solutions and the basis of the chemical contribution to the heat defect is described. Certain aqueous solutions, well-characterized from a radiation chemistry standpoint, are discussed. A comparison of the calculated and measured heat defects for these solutions establishes that the uncertainty, due to the chemical heat defect, is about ±0.5% in water calorimetry.

La chimie des radiations de solutions aqueuses diluées et la base de la contribution chimique au déficit thermique sont décrites. Certaines solutions aqueuses, bien caractérisées du point de vue de la chimie des radiations, sont analysées. Une comparaison des déficits thermiques calculé et mesuré pour ces solutions établit que l'incertitude due au déficit thermique chimique est d'environ ± 0,5 % pour la calorimétrie à eau.

RADIATION CHEMISTRY

This talk deals with the radiation chemistry of water subjected to low LET radiation. Regardless of whether the incident radiation is high energy photons or charged particles, the chemistry is almost entirely initiated by the lower energy secondary electrons. Averaged over the track, the secondary electrons from Co-60, 22 MV x-rays and 2 MeV electrons all have LET's of about 0.2 eV/nm. The chemistry initiated by ionizing radiation is not consistent with a continuous slowing down of the secondary electrons. It is consistent with a discontinuous deposition of energy in discrete amounts in discrete volumes. The deposited energy produces chemical species in these volumes. These regions of highly concentrated, reactive species are called spurs for events of 6-100 eV, blobs for events of 100-500 eV, and short tracks for events of 500-5000 eV (Mozumder and Magee, 1966).

espur,	6-100 eV/event	44000 events/MeV
eblob,	100-500 eV/event	444 events/MeV
eshort track,	500-5000 eV/event	98 events/MeV

where the events per MeV refer to a 1 MeV electron slowing down. Events above 5000 eV are not included in this classification because secondary electrons above 5000 eV produce their own tracks with the formation of isolated spurs. The energy of a 1 MeV electron (or a 10 MeV electron) is deposited in the following manner: 65% (76%) in spurs, 15% (8%) in blobs, and 20% (16%) in short tracks.

For simplicity's sake, we shall refer to all events as spurs. In water, most of the oscillator strength lies below 100 eV. The maximum lies at about 22 eV with a long tail to higher energies (LaVerne and Mozumder, 1986). The oscillator strength at 40 eV is about half that at 22 eV so that events of 20 eV and 40 eV contribute almost equally to the absorbed dose. It is commonly assumed that 40 eV is the average energy deposited per event along the trajectory of the secondary electron.

The earliest changes resulting from energy absorption are

$H_2O \rightarrow H_2O^+ + e^-$

$H_2O \rightarrow H_2O^*$

These extremely fast events are followed in less than a picosecond by the earliest chemical reactions,

$e^- \rightarrow e^-_{aq}$

$H_2O^+ + H_2O \rightarrow H_3O^+ + OH$ henceforth, H_3O^+ becomes H^+

$H_2O^* \rightarrow H + OH$

At 1 ps, the H^+ and the OH radical have not had a chance to diffuse so they are next to each other. The solvated electron is about 2 nm away due to its diffusion as a free electron prior to thermalization. H atoms and OH radicals, produced from an excited water molecule are separated by, perhaps, 2 molecular diameters. This is what we think of as a spur.

The high concentrations of species, some very reactive, in close proximity to one another in the spur leads to spur reactions as the species diffuse.

$H + H \rightarrow H_2$

$H + OH \rightarrow H_2O$

$OH + OH \rightarrow H_2O_2$

$e^-_{aq} + OH \rightarrow OH^-$

$e^-_{aq} + H^+ \rightarrow H + H_2O$

Because of the high local concentration of reactive species in the newly formed spur, the spur reactions can only be interfered with by reactive solutes at very high concentrations.

The spurs expand due to the diffusion of the spur species, thereby lowering their local concentration. The average time for the spurs of a single track to overlap is about 1 μs. At times longer than 1 μs, the spurs begin to lose their identity as interspur reactions commence. If there are scavengers (solutes which react with a significant fraction of a particular reactive species) in the water they will compete for the reactive species. Consider the reaction of e^-_{aq} with O_2 to form O_2^-. Initially, e^-_{aq} reacts faster with species in its own spur than it does with dissolved oxygen. In air-saturated water, the half-life for the $e^-_{aq} + O_2$ reaction is 0.1 μs, which is much shorter than the 1 μs required for spurs in the same track to overlap. Hence, by 0.1 μs, the dominant reaction of e^-_{aq} will be with dissolved O_2. In water, the spur is often said to disappear in 0.1 μs. What is really meant by this is that the spurs will have expanded sufficiently in 0.1 μs that most of the radicals etc. which still

exist in the spur will react with scavengers present at concentrations of 10^{-3} M or greater.

In the language of radiation chemistry, G(X) is defined as the number of molecules (or ions, radicals, etc.) of X formed (or destroyed) per 100 eV of energy absorbed. G(X) always refers to some particular set of conditions. For example, $G(H_2)$ could refer to the G-value for the H_2 initially formed in the spur, or for the H_2 which escapes the spur, or to the final yield of H_2 after radiolysis. Studies of water containing $\leq$ millimolar concentrations of scavengers have established the G-values of the species which escape the spur. These species and their G-values are: e^-_{aq} = 2.7, H^+ = 2.8, H = 0.55, H_2 = 0.45, OH^- = 0.1, OH = 2.75, and H_2O_2 = 0.7 (Boyd et al., 1980). For our test solutions, we have chosen dilute solutes in order to use these G-values. These G-values are not applicable to water containing a high concentration of solutes. For example, in 0.4 M sulfuric acid $G(e^-_{aq})$ = 0.0 and G(H) = 3.7 (Bjergbakke et al., 1987.)

CALCULATING THE HEAT DEFECT

In order to calculate the heat defect for a particular irradiated aqueous solution, we simulate the radiolysis using a computer. The computer simulation requires the reactions and rate constants particular to the solution in question, the dose rate, the G-values corresponding to escape from the spur of radiolytically produced species, and the initial concentrations of reactive solutes. The computer then simulates the reactions which would take place in a homogeneous solution containing the initially added solutes with the addition of the radiolytically produced species at the rate defined by the dose rate and their G-values. For air-saturated water, the number of reactions included depends on the pH and can number up to 60. In most cases, a much smaller number of reactions suffices to adequately define the reaction mechanism but, because of the strong interrelatedness of the reactions in water, one must be careful what is excluded. We typically use about 50 reactions which can usually be simulated in less than 30 minutes on a PC.

The simulation programme we use is called MACKSIM. It was written at Atomic Energy of Canada and its application to the radiation chemistry of water has been published (Boyd, Carver and Dixon, 1980; Fletcher, 1982; Ross, Klassen and Smith, 1984). In our publication we used the reaction mechanism, rate constants and G-values of Boyd, Carver and Dixon which we shall now call Model I. Boyd, Carver and Dixon, in their publication, tested the predictions of Model I against a number of experimental results. The agreement was good in some cases, bad in others. We have determined that the most striking disagreement, that with the results of Kabakchi, Shubin and Dolin (1967), was partly due to a failure to correctly simulate the experimental conditions. Since then, we have made changes to the reactions and rate constants in accordance with a recent review (Buxton et al., 1988) to arrive at Model II. This caused some minor changes in the calculated heat defect under certain conditions and these are shown below.

To calculate the heat defect of a particular irradiation we simulate the radiolysis using an appropriate reaction scheme and the irradiation parameters corresponding to the experiment. From the simulation we determine quantitatively the chemical changes which take place between the beginning of the irradiation period to, perhaps, a minute or so after the end of the irradiation. The change in enthalpy due to the radiolysis is then calculated using the heats of formation (Wagman et al., 1982) of the compounds whose concentrations have increased or decreased. The change in enthalpy is then calculated as a percentage of the absorbed energy.

It is beyond the scope of this talk to deal with all the possible reactions in irradiated water. Rather, we shall restrict ourselves to the reactions which are most important for water calorimetry i.e., for water of pH 5-7, and for the solutions we have tested. For these cases, more than 80% of the chemistry flows through a small number of reactions and these abbreviated reaction schemes will be given. These schemes were determined for our radiolysis conditions, i.e., several 48 sec irradiation periods interspersed with 3 min holding periods.

PURE WATER

One of the first concepts one encounters when dealing with the radiolysis of pure water is the stationary state. When pure water is irradiated, H_2O_2, H_2, and O_2 are produced with G-values which depend on the dose rate (because radical-radical reactions are involved). These stable products do not increase in concentration indefinitely with accumulated dose. Rather, they also react with the reactive species produced by radiolysis. The rates of these so-called back-reactions increase as the concentrations of the stable products increases until the production and destruction of the stable products becomes equal, at which point their concentrations cease to change. Not all stable products reach their stationary state at the same dose. When the concentrations of all the stable products cease to change, a stationary state is said to exist. A stationary state is synonymous with a heat defect of zero. Since the back-reactions compete with radical-radical reactions, the concentrations of stable products at the stationary state depends on the dose rate. It should be pointed out that the attainment of a stationary state requires a steady dose rate and that the concentrations will change somewhat when the irradiation is interupted. For initially pure water, after a stationary state has been reached, the radiolysis mechanism is approximated by

$e^-_{aq} + O_2 \rightarrow O_2^-$
$e^-_{aq} + H_2O_2 \rightarrow OH^- + OH$
$e^-_{aq} + H^+ \rightarrow H$
$H + O_2 \rightarrow HO_2$
$HO_2 \rightarrow O_2^- + H^+$
$OH + O_2^- \rightarrow OH^- + O_2$
$OH + H_2 \rightarrow H + H_2O$

The heat defect for initially pure water after the attainment of a stationary state is insensitive to the G-values and to the rate constants used in the simulation.

The depletion of H_2 and O_2, produced by the radiolysis of pure water, by diffusion into the gas space inhibits the attainment of a stationary state. In order to determine the extent of this effect under our conditions, we irradiated water saturated with a flow of argon/H_2/O_2 such that the concentration of H_2 and O_2 were each calculated to be 2.5 μM. Under these conditions, a stationary state should be reached with little change in their concentrations. The measurement with this solution corresponded to 0.3($\pm$0.3)% more exothermic than the measurements with argon- and with N_2-saturated water.

Exothermicity or Endothermicity of Irradiated Aqueous Solutions at 21°C			
Solution	Percent Exothermicity or Endothermicity		
	Calculated[a]		
	Model I	Model II	Measured
pure water (argon sat'd)	0.00	0.00	assumed[b]
pure water (N_2 sat'd)	0.00	0.00	assumed[b]
2.5 μM O_2, 2.5 μM H_2	0.00	0.00	assumed[b]
O_2/H_2 water, 0.70 mM O_2, 0.42 mM H_2	2.1 exo	2.35 exo	2.0 exo
20/2/0.1 argon/N_2O/O_2		2.01 exo	2.0 exo
1.4 mM O_2	1.8 endo	1.85 endo	1.4 endo
1.3 mM O_2, 0.1 mM CO		3.25 exo	3.2 exo
1.4 mM O_2, 1.0 mM sodium formate		2.60 exo	2.6 exo
Fricke dosimeter	14.85 exo[c]		12.0[d] (13.0)[e] exo

[a]refinements are still being made and may result in small changes
[b]the average of these values was assumed to be zero and all others are relative to this.
[c]modelled after Bjergbakke et al. (1987)
[d]based on water calorimeter dosimetry
[e]based on Fricke dosimetry

AIR-SATURATED WATER

Air-saturated water presents a somewhat different situation, mainly because the O_2 concentration is large enough to scavenge all the e^-_{aq}. One noticeable effect is a greater production of H_2O_2 than in pure water. Dissolved nitrogen is considered to be inert.

$e^-_{aq} + O_2 \rightarrow O_2^-$
$H + O_2 \rightarrow HO_2$
$OH + H_2O_2 \rightarrow H_2O + HO_2$
$OH + O_2^- \rightarrow OH^- + O_2$
$HO_2 + O_2^- \rightarrow HO_2^- + O_2$
$H^+ + HO_2^- \rightarrow H_2O_2$

Note that a stationary state is not reached in air-saturated water and that the concentration of H_2 and H_2O_2 continue to increase with increased accumulated dose. The calculated heat defect changes from 2.2 to 1.8% over the course of a complete set of measurements.

O_2/H_2 WATER

We chose to compare all aqueous solutions to O_2/H_2 water (water saturated with a 50/50 mixture of O_2 and H_2 at a total pressure of one atmosphere). It is attractive for several reasons, (1) all the reactive species, e^-_{aq}, OH, and H, are scavenged, thereby reducing the effect of adventitious impurities, (2) the dilute solutes are easily added by bubbling the water with gases, and (3) there is no need to remove O_2 completely from the solution since it is one of the solutes.

$e^-_{aq} + O_2 \rightarrow O_2^-$
$H + O_2 \rightarrow HO_2$
$OH + H_2 \rightarrow H + H_2O$
$HO_2 + O_2^- \rightarrow HO_2^- + O_2$
$H^+ + HO_2^- \rightarrow H_2O_2$

A stationary state is not reached. H_2O, H_2 and O_2 are continuously converted into H_2O_2.

N_2O/O_2

A rather different solution we have studied is water saturated with 20/2/1 argon/N_2O/O_2. In this solution, the water radiolysis reaches a stationary state but N_2O continues to be converted into N_2 and O_2. The major reactions are

$e^-_{aq} + N_2O \rightarrow OH + OH^- + N_2$
$H + O_2 \rightarrow HO_2$
$OH + OH \rightarrow H_2O_2$
$OH + H_2 \rightarrow H + H_2O$
$OH + H_2O_2 \rightarrow H_2O + HO_2$
$HO_2 \rightarrow O_2^- + H^+$
$OH + O_2^- \rightarrow OH^- + O_2$

In this case, the heat defect is only sensitive to one G-value, that of e^-_{aq}.

CO/O_2

It seems probable that the exothermicity often measured with water calorimeters was due to reactions initiated by the reaction of OH radicals with impurities. One way to avoid this would be to deliberately scavenge OH. To this end, we irradiated water saturated with 9/1 O_2/CO. The major reactions in this case are

$e^-_{aq} + O_2 \rightarrow O_2^-$
$H + O_2 \rightarrow HO_2$
$OH + CO \rightarrow COOH$
$COOH + O_2 \rightarrow HO_2 + CO_2$
$COOH \rightarrow CO_2^- + H^+$
$CO_2^- + O_2 \rightarrow CO_2 + O_2^-$
$O_2^- + H^+ \rightarrow HO_2$
$HO_2 + O_2^- \rightarrow HO_2^- + O_2$
$H^+ + HO_2^- \rightarrow H_2O_2$
$CO_2 + H_2O \rightarrow H^+ + HCO_3^-$

FORMATE/O_2

As an alternative to the potentially explosive O_2/H_2 water system and the poisonous CO/O_2 system, we decided to examine a less deadly candidate which might be useful for larger water calorimeters which are open to the air. One criterion is that it should contain a solute to scavenge OH radicals.

The less deadly candidate we chose is a 10^{-3} M solution of sodium formate ($HCOO^-Na^+$) saturated with O_2 (sodium formate in air-saturated water has the same heat defect). Hydroxyl radicals are scavenged by $HCOO^-$ ions and e^-_{aq} and H atoms are scavenged by O_2. Bubbling the solution with O_2 removes dissolved CO_2. Just after distillation, the pH of water is close to 7 but it drops to about 5.2 as the water picks up CO_2 from the air. The major reactions in a formate/O_2 solution are:

$e^-_{aq} + O_2 \rightarrow O_2^-$
$H + O_2 \rightarrow HO_2$
$OH + HCOO^- \rightarrow CO_2^- + H_2O$
$CO_2^- + O_2 \rightarrow CO_2 + O_2^-$
$CO_2 + H_2O \rightarrow H^+ + HCO_3^-$
$O_2^- + H^+ \rightarrow HO_2$
$HO_2 + O_2^- \rightarrow HO_2^- + O_2$
$H^+ + HO_2^- \rightarrow H_2O_2$

FRICKE

As part of our comparison of water calorimetry and Fricke dosimetry, we measured the temperature rise of the Fricke solution to be 12.0% exothermic based on the dose by water calorimetry (13.0% based on the dose by Fricke dosimetry). This is 2.9% less than the calculated value. This may be due to the presence of complexes in the solution.

GENERAL

There is a physical effect which can lead to a substantial heat defect, but which is probably not apparent in most cases. This is due to the movement of gases into, and out of, the liquid. This can happen for two reasons. If a gas, eg. O_2, is consumed during the radiolysis, it will be replaced by O_2 from the gas phase. This is an exothermic process. On the other hand, if H_2 is formed by radiolysis, most of it will eventually be released to the gas phase. This is an endothermic process. For the case of O_2/H_2 water in which both H_2 and O_2 are consumed, the net exothermicity is equivalent to a heat defect of -0.4%. However, this can only influence the results if the gas is transferred in a time comparable to the measurement. In most cases, this is probably not the case and the effect will show up only as a change in the slope of the baseline. If the exchange is rapid, such as bubbles appearing on surfaces, then the observed heat defect will contain this effect. As well, a transfer of gas from the liquid to the gas phase will result from its reduced solubility in water due to the increase in the temperature of the water, caused by the absorption of energy. This transfer is endothermic but the effect is very small.

CONCLUSIONS

Our measured results of the chemical heat defect, based on the assumption that pure water reaches a stationary state and, hence, a heat defect of zero, agree well with the results of model calculations with the exception of the Fricke dosimeter, for which a possible reason is given. There are discrepancies between model I and model II but these are small. For example, the difference is 0.25% for the heat defect for the O_2/H_2 water system. We conclude that the radiation chemistry of the dilute aqueous solutions used in this study can be modelled well enough to assign an uncertainty of ±0.5% to the chemical heat defect. In view of the potential problems associated with water purity, especially when dealing with "pure water", it seems prudent to measure the temperature rise in several aqueous solutions such as these, for which the radiation chemistry is well known. Our studies of these systems, both experimental and modelling, is continuing.

REFERENCES

Bjergbakke, E., Navaratnam, S., Parsons, B.J. and Swallow, A.J., *Radiat. Phys. Chem.*, 30, 59 (1987)

Boyd, A.W., Carver, M.B. and Dixon, R.S., *Radiat. Phys. Chem.*, 15, 177 (1980).

Buxton, G.V., Greenstock, C.L., Helman, W.P. and Ross, A.B., Radiation Chemistry Data Center, Radiation Laboratory, University of Notre Dame, 1988.

Fletcher, J.W., Atomic Energy of Canada Ltd. Document No. AECL7834 (1982).

Kabakchi, S.A., Shubin, V.N. and Dolin, P.I., *High Energy Chemistry*, 1, 127 (1967).

LaVerne, J.A. and Mozumder, A., *J. Phys. Chem.*, 90, 3242 (1986).

Mozumder, A and Magee, J.L., *Radiat Res.*, 20, 203 (1966).

Ross, C.K., Klassen, N.V. and Smith, G.D., *Med. Phys.*, 11, 653 (1984).

Wagman, D.D., Evans, W.H., Barker, V.B., Schumm, R.H., Halow, I., Bailey, S.M., Churney, K.L. and Nutall, R.L., The NBS tables of chemical thermodynamic properties, *Journal of Physical and Chemical Reference Data*, 11, Suppl. 2 (1982).

Discussion

Schulz: Does the sodium not appear in the reaction mechanism of aqueous sodium formate solutions?

Klassen: It's inert.

Schulz: You suggested that at a stationary state the heat defect is zero.

Klassen: Yes, by definition.

Schulz: But that when you turn the beam off something might happen?

Klassen: Yes. The species HO_2 and O_2^- are rather long lived and take some time to react.

Schulz: Does that suggest we should be measuring the rate of temperature change?

Klassen: That would be one way of doing it, but the effect on turning the beam off is not a large effect.

Barnett: You used a temperature of 21°C. Would you expect much of a change in the rate constants that go into the model between 4°C and 21°C?

Klassen: Yes.

Barnett: Does the model allow for different rate constants as a function of temperature?

Klassen: The final heat defects probably wouldn't change much. If all the rate constants change by the same factor, the final result won't be affected. This is not likely since some reactions are first order and some are second order, some reactions are diffusion-controlled and some are not. Where a stationary state is reached, it will be reached at a somewhat different dose at a different temperature.

Barnett: That is consistent with Schulz's results at 4°C.

Rogers: All the calculated results you showed are for the conditions under which your experiments were done, the dose rate, the timing sequence?

Klassen: Yes.

Rogers: How big an effect on these numbers would you get if you went to a considerably different dose rate?

Klassen: I can't tell you from memory, but Wally Fletcher has such information in his report. A change in dose rate is an important change.

Cygler: At extreme dose rates, you get the situation more like high LET because the spurs overlap.

Rogers: Is everyone who is going to have a standard going to have to run this program at their temperature, their dose rate and their timing sequences to get the answer that they need, unless they use one of these pure water systems?

Klassen: Yes.

Fletcher: I calculated that in my report, but I think that there are effects to look at that are larger than the dose rate effect. I think that the impurity effects are still quite major, unless you add something to counteract them.

Klassen: The formate system I described is attractive. You put a pinch of solid in the water and leave the air in.

Rogers: Is the 2.6% likely to still hold at different dose rates?

Klassen: I haven't done the calculations, but the differences would probably be small.

Ross: There might be some concern with using air based on Schulz's results using air-saturated water. Our measurements with air-saturated water were consistent with the model but his are not, so one has to worry about different air quality in different labs.

Schulz: You people are the only ones who have agreement with the model. My results and all the open calorimeters showed the exothermicity.

Klassen: If the problem in open calorimeters arises from the reactions of OH radicals with impurities, a good approach might be to scavenge the OH radicals with millimolar formate and to scavenge electrons and hydrogen atoms with oxygen from the dissolved air as I described. The impurities are bound to be present at much lower concentrations. The formate system seems quite attractive.

Schulz: But you are still looking at 2.6% exothermic.

Klassen: Yes, but in this case, that is what theory predicts. It is not like predicting 2% endothermic and getting 3% exothermic.

Fletcher: The other alternative is to seal your vessel and have a very pure system.

DETERMINATION OF THE HEAT DEFECT OF WATER BY TOTAL ABSORPTION OF SOFT X-RAYS

K. Hohlfeld, H. M. Kramer, H. J. Selbach
Physikalisch-Technische Bundesanstalt
D-3300 Braunschweig, Federal Republic of Germany

ABSTRACT - This paper presents an experimental method for determining the heat defect of water. The heat defect must be known from experiments or theory not involving absorbed determination, if the water absorbed dose calorimeter should be used as a primary standard. The different temperature rises caused by total absorption of soft X-rays in water and in a medium without heat defect, respectively, is the basic principle of the method. The experimental set-up and the evaluation of the necessary correction factors are described.

RESUME -

On présente une méthode expérimentale de détermination du déficit thermique de l'eau. Il faut connaître ce déficit, à partir d'expériences ou d'une théorie ne faisant pas appel à la détermination de la dose absorbée, pour être en mesure de se servir du calorimètre à dose absorbée dans l'eau comme étalon primaire. Le principe fondamental de la méthode repose sur les augmentations de température différentes créés par l'absorption totale de rayons X mous dans l'eau et dans un milieu ne présentant pas de déficit thermique. On décrit dans le rapport le montage expérimental ainsi que la méthode d'évaluation des facteurs de correction nécessaires.

INTRODUCTION

The water absorbed dose calorimeter can be established as a primary standard only, if the heat defect of water, the fraction of radiation energy absorbed not appearing as heat, is determined. This may be achieved by calculation or measurement, but a method has to be used not involving an absorbed dose determination. A method using evidence only that the heat defect chanoes to zero with energy imparted cannot be incorporated into a primary standard measuring method. The result obtained is applicable only, if the same water is used in the absorbed dose calorimeter avoiding contact with material other than present in the set-up for the heat defect determination. The uncertainty in the measurement of the heat defect must be smaller than the total uncertainty in the determination of the absorbed dose to water in a water phantom by other methods which can be used as primary standard methods. As a consequence, the measurands and all correction factors must be known within a few thenths of a percent.

Total absorption of radiation was chosen as basic principle for an experiment to measure the heat defect. Soft X-rays allow the absorption process taking place nearly entirely in water or in a material without heat defect. The increasing uncertainties in the correction factors needed to take into account the different backscatter, sidescatter and penetration of the X-ray beam lead to an useful energy range between about 20 and 30 kV generating potential.

METHOD OF MEASUREMENT AND EXPERIMENTAL SET-UP

The method has been described already elsewhere (Hohlfeld et al., 1988). By means of a beam monitor equal amounts of X-ray energy are given to a water absorber and a metal absorber. For metal the heat defect is assumed to be zero. Comparing the resulting temperature increases enables to evaluate the heat defect. Problems associated with the use of two diffe-

rent absorbers are eliminated by employing a differential method (Fleming and Glass, 1969). To achieve this a metal disc is shifted by magnetic forces in a water-filled absorber vessel from a position at the rear side into close contact with a very thin radiation entrance window (figure 1). Without changing heat capacity and exterior heat transfer conditions this interior modification of the absorber can be made. In the rear position the radiation energy is almost entirely absorbed in water. In the front position of the disc the soft x-ray beam is nearly completely absorbed in the metal.

The absorber consists of a cylindrical stainless steel vessel of 30 mm in diameter and 15 mm length filled with about 10 g of water. Thermal insulation with a decay constant of about 4x10E-5sE-1 has been reached by gold-coating the vessel and suspending it in a vacuum by means of thin nylon threads.

The thickness of the entrance window of the absorber (Mylar 250 um) is the result of a compromise between attenuation of the X-ray beam and the diffusion of water from the vessel through the thin window of low-Z material.

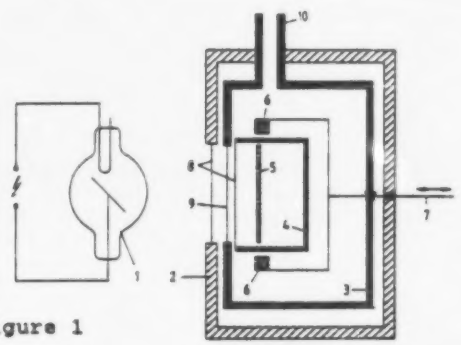

Figure 1

Schematic illustration of the set-up. 1 - X-ray tube; 2 - calorimeter housing; 3 - vaccuum container; 4 - water-filled absorber vessel; 5 - Fe-Ni metal disc; 6 - permanent magnets; 7 - holder to shift the magnets (6); 8 - thin plastic foils; 9 - Be entrance window; 10 - high-vaccuum container.

The water absorber vessel is filled under vacuum avoiding gas bubbles remaining in the vessel and gas load of the water. At present, the procedure to determine the heat defect does not enable to investigate influences of water impurities or gas load.

The water used has the same quality as for the Fricke dosimetry at PTB. It is six times destilled, where one step is on sodium dichromate in acid solution another on potassium permanganat in alkaline solution. The two last steps of the destillation device are made from quartz.

EXPERIMENTS

The low thermal diffusivity of water, enabling the design of the water absorbed dose calorimeter of the Domen-type, prevents thermal equilibrium within the water absorber of the heat defect experiment. Therefore, the metal disc is moved several times in the water volume after the irradiation period. By this, extrapolation of the temperature-time curves to correct for heat transfer can start soon after the end of the irradiation period. A temperature-time curve of the absorber is shown in figure 2. The spikes at the end of the irradiation period are caused by the movement of the metal disc by magnetic forces. Eddy currents are induced in the thin metal wall of the absorber leading to local temperature

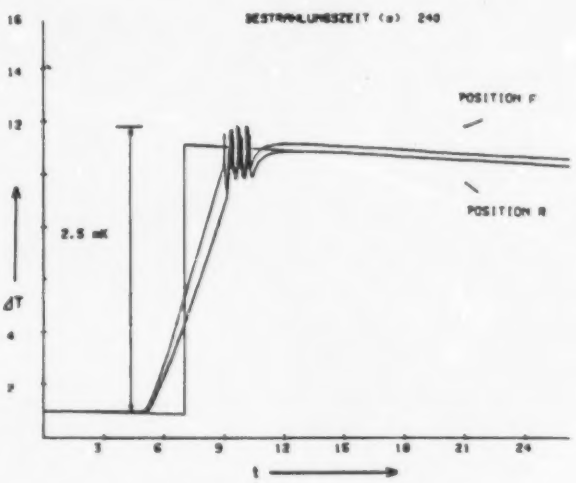

Figure 2

Temperature-time curves. In the diagram two temperature time curves are shown. The upper curve was taken with the metal disc in the front position totally absorbing the radiation without heat defect. The lower curves applies to the metal disc in the rear position. The irradiation starts at t = 5 min and lasts for 4 minutes. The thermistors senses the local temparaturerise in the middle of the side wall of the absorber vessel.

rises. These are detected by the thermistors attached to the side walls of the absorber. The amount of energy involved is small compared with the radiation energy absorbed. By heat transfer into the water the spikes die off rapidly. As they are generated in both parts of the experiment - metal disc in front and in rear position, respectively -, their influence cancels out. The temperature increase by radiation amounts typically to about 2,5x10-3K with an irradiation of 240 s for weakly filtered X-ray of 25 kV generating potential and at a tube current of 50 mA. The exact values of the temperature increase or the energy absorbed is not needed to be known. The specific energy imparted is about 10 Gy per irradiation run.

PRELIMINARY RESULTS

The heat defect is calculated from the relation

$$h = \frac{M_f (1-l_r) - M_r (1-l_f)}{M_f (1-l_r)\, a_{w,r} - M_r (1-l_f)\, a_{w,f}}$$

The symbols have the following meaning:

M_f - reading (temperature increase proportional signal), metal disc in front position
M_r - reading, metal disc in rear position
l_f - fraction of radiation energy lost (by backscatter, sidescatter and penetration), metal disc in front position
l_r - fraction of radiation energy lost, metal disc in rear postion
$a_{w,f}$ - fraction of radiation energy absorbed in water, metal disc in front position
$a_{w,r}$ - fraction of radiation energy absorbed in water, metal disc in rear position

The factors l_f, l_r, $a_{w,f}$, $a_{w,r}$ are needed to take into accout the different amounts of energy lost from backscatter, sidescatter and penetration depending on the position of the metal disc. These correction factors were calculated using the Monte Carlo technique.

In figure 2 temperature-time curves are shown for the metal disc in rear and front position, respectively. From these curves Mf and Mr are evaluated by extrapolation of the initial and final drifts to the mid-point of the irradiation period. The magnitude of this correction for heat transfer is in the order of 2 %. In table 1 the ratios of the readings M_f and M_r are given for 4 different generating potentials of the X-rays. The standard deviation of the mean amounts to 0.3 %, 10 measurements taken for each configuration. Inserting the M_f and M_r values into the relation for the heat defect results in values of h, exhibiting a strong and unexpected energy dependence of the heat defect. This hints to an imperfect correction of the heat transfer, as the temperature distribution within and on the surface of the absorber vessel depends strongly on the radiation quality of the X-rays.

Table 1 Ratio of the temperature increase M_f, M_r and "uncorrected" heat defect h' for 4 different radiation qualities.

Generating voltage in kV	15	20	25	30
Ratio M_f/M_r	1.019	1.012	1.010	1.014
Uncorrected heat defect in %	2.0	0.7	-0.1	-3.5

HEAT LOSS CORRECTION AND TEMPERATURE DISTRIBUTION

The correction for heat losses to the surroundings is applied by extrapolating the initial and final drifts to the midpoint of the irradiation period, the magnitude of the correction beeing about 2 % of the energy absorbed. The absorber and its surroundings are treated as isothermal bodies and the heat transfer between them is assumed proportional to the difference in their temperatures. But as can be concluded from figure 3, this is at best a first-order approximation. The ratio of M_f/M_r should not vary with the irradiation time, if the correction procedure mentioned is appropriate (West, 1963) Therefore, as this seems to be not the case, the temperature distribution and the variation in heat transfer coefficients over the surface must be taken into consideration.

As calculated by Roos (1987), the temperature distribution within the absorber vessel is rather inhomogeneous. As shown in figure 4 for 15kV X-rays, the temperature profile, which at the beginning of the irradiation period is proportional to the depth dose curve, changes with time due to heat flow within the water. From correspondent

curves for different radiation qualities the curves of temperature at the front surface versus time were derived (figure 5). The temperature of the front surface is always considerably higher than the mean (homogeneous) temperature used in correcting heat losses by means of a product of a mean temperature difference and a constant of proportionality, which lumps together all thermal radiation and conduction processes.

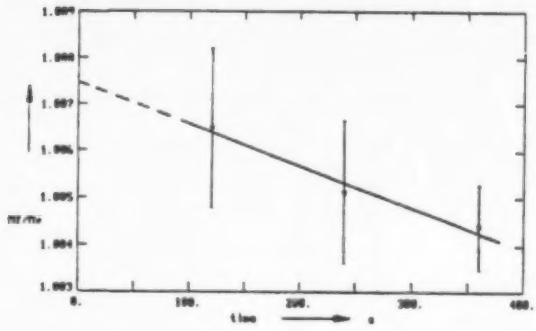

Figure 3

Dependence of M_f/M_r on irradiation time. The slope of the linear regression is an intimation of temperature transients preventing heat loss correction by extrapolating the traces of figure 2 to the mid-time of irradiation. As the extrapolation of the traces starts only a few minutes after the end of the irradiation period, the value of M_f/M_r at t=o does not leat to a correct result. The curve given in figure 3 is valid only for the radiation quality 25 kV.

The results of figures 4 and 5 are based on a one-dimensional solution of the heat conduction equation, where the composition and finite size of the water absorber vessel were neglected.

In order to get more quantitative results the heat generation by local radiation absorption, the spread of the temperature within the absorber vessel and the heat loss of the absorber vessel to the surroundings have been calculated by means of the finite-element method. This numerical method solves the partial differential equation

$$\varrho.c\,\frac{\delta T}{dt} = \mathrm{div}\,(k.\mathrm{grad}T) + H(x,y,t)$$

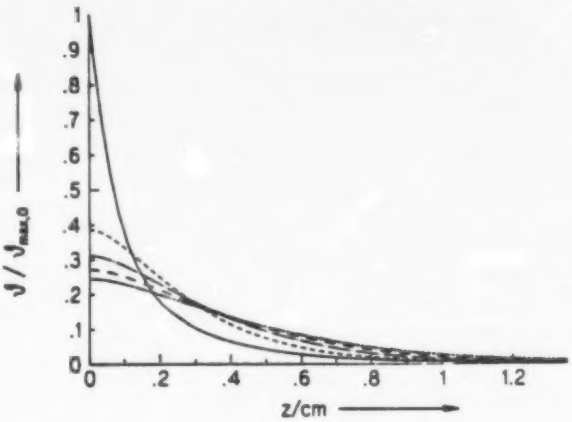

Figure 4

Depth distribution of temperature. Calculated depth distribution of temperature in the water absorber vessel irradiated with 15 kV X-rays for various times after starting the irradiation. They are normalized to the temperature at the surface without falsification by heat conduction at the beginning of the irradiation (solid curve). The solid curve corresponds to the depth-dose distribution. The parameter time for the various curves increases in 30 s steps.

taking into accout the initial and boundary conditions. The grid net representing one half of the symmetrical absorber vessel consists of 144 volume elements, 170 modal points and 32 surface elements.

The specific heat capacities and the thermal conductivity coefficients of the 4 materials (Mylar foil, water, stainless steel and Fe-Cu metal) composing the absorber vessel are attributed to the respective volume elements. The time increases in steps of 0.3 s for the calculation. Heat transfer to the surroundings is assumed to occur only by thermal radiation. As no detailed information on the emissivity coefficients of the actual surface is available, a value of 0.2 was taken for the front surface (aluminized Mylar) and a value of 0.1 for the side walls and the rear (stainless steel). Calculated temperature-time curves for three points of the surface are shown in figure 6 together with measured temperature-time

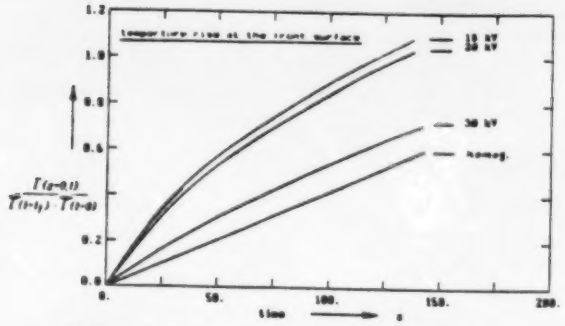

Figure 5

Temperature rise at the front surface. The calculated temperature at the front surface for various radiation qualities is always higher than the homogeneous temperature resulting as the quotient of energy absorbed and heat capacity. The curves are normalized by the homogeneous temperature reaching the value one at the end of the radiation period (240 s).

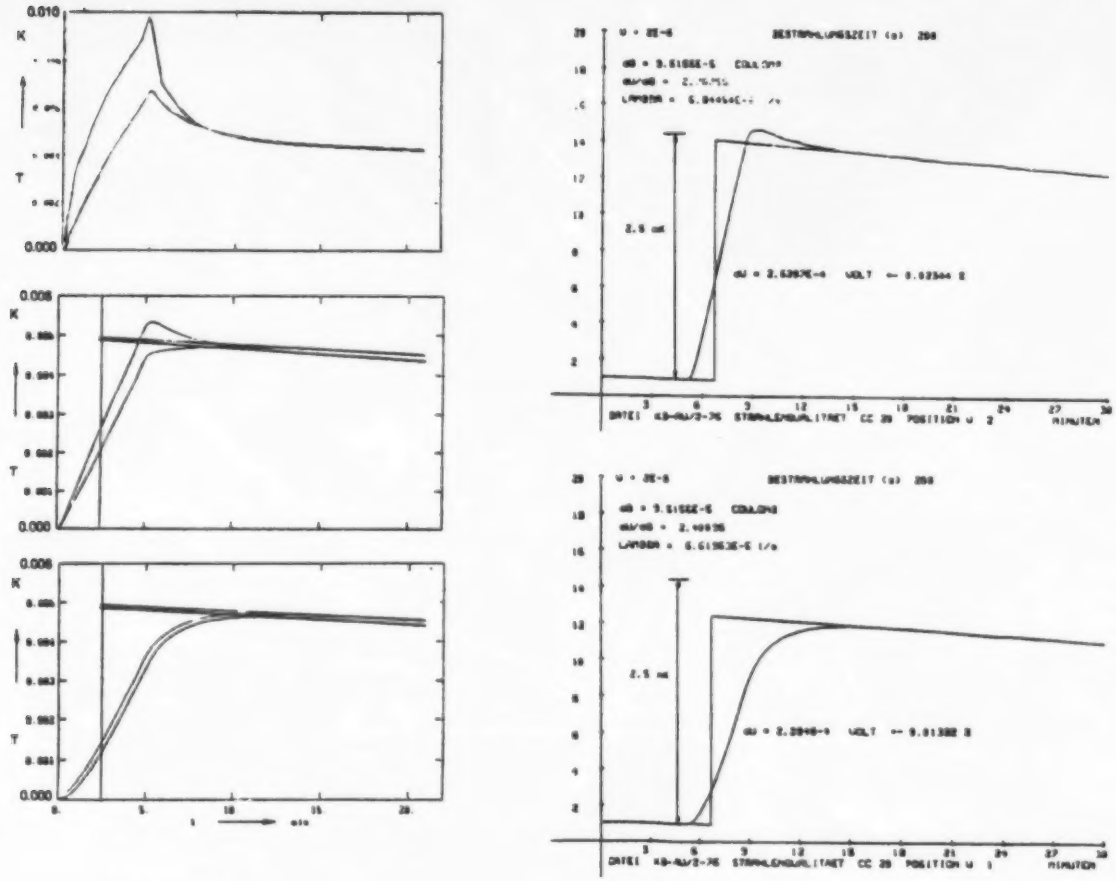

Figure 6

Comparison of calculated and measured temperature-time curves. On the left hand side temperature-time curves calculated by the finite-element method are shown. The temperature is given in arbitrary units, radiation quality 20 kV X-rays. The upper, middle and lower section relate to positions at the center of the front surface, the middle of the side wall and the center of the rear side, respectively. For the upper curve in each of these sections the position of the metal disc was at the front surface. The calculated curves resemble to a great extent those of the right hand side, which are experimentally derived. The corresponding curve to the upper section of the left hand side could not yet be taken.

curves. To calculate the heat loss correction perfectly the temperature distribution on the absorber vessel surface and the heat transfer coefficients for all points of the surface must be known. As especially the later information is not accessible, a variation of the heat transfer coefficients taken for calculation is intended to achieve congruency of the calculated temperature-time curves with those measured at discrete points of the surface. The work is under way.

CONCLUSION

The experimental facilities for determing the heat defect caused by soft X-ray have only been available for a few months. Results begin to emerge, which lead to the conclusion that the method introduced here, will allow to determine the heat defect of water for a specified radiation quality and for a specified water sample. It is clear that more time and investigation are required before the results of the heat defect determination can be adequately used by those working in the primary standard dosimetry area.

REFERENCES

1. Fleming, D. M., Glass, W. A. (1969): Endothermic Processes in Tissue-equivalent Plastic. Rad. Res. 37, 316 - 322

2. Hohlfeld, K., Kramer, H. M., Roos, M., Selbach, H. J., (1988): Two Experimental Methods for Determining the Heat Defect of Water. In: Dosimetry in Radiatherapie, Vol. 2, 145 - 153. IAEA, Vienna.

3. Roos, M. (1987): A Water Calorimetric Determination of Absorbed Dose to Water. Thermochimica Acta, 119, 81 - 93.

4. West, E. D. (1963): Heat Exchange in Adiabatic Calorimeters. J. of. Res. of the National Bureau of Standards, 67A, 331 - 341.

Discussion

Klassen: Do you ever get a bubble of gas in your vessel?

Hohlfeld: With the 200 micron thick foils we did not see any bubbles. We found bubbles when we used much thinner foils, when we had a loss of water of more than 100 micrograms of water per hour.

-

Rogers: What do you assume for your heat losses from the outer surfaces?

Hohlfeld: The heat losses from an element to the surroundings is proportional to the temperature difference and we assign to each element a specific emissivity coefficient.

Domen: What is the emissivity you assign?

Hohlfeld: We can calculate a mean value for the whole absorber which has to be fitted to this 5×10^{-5} per sec.

Domen: Would you say that the emissivity is less than a tenth?

Hohlfeld: Yes. But the gold foil and the mylar foil may be different.

-

McDonald: In the first set of measurements, where was the thermistor located on the absorber?

Hohlfeld: It was attached to the sidewall, towards the front.

-

Rogers: How accurately can you measure the absorption of the low energy x-rays in the window and how uniform is that window? The correction is quite large.

Hohlfeld: We have up to 20% absorption in the 200 micron window with 15 KeV x-rays. But we don't think we should use 15 KeV x-rays where we have only 80% of the signal available. But this absorption doesn't have to be known very accurately because it doesn't enter totally into the heat defect.

Rogers: Because you are going through it in both cases?

Hohlfeld: No, that is not the argument. From the formula for the heat defect, you can see that if these coefficients are not exactly known it affects the heat defect with only, perhaps, one-tenth of this uncertainty, whereas what is really lost to the surroundings enters directly.

-

Schulz: How did you determine the energy loss from the scattered photons and electrons?

Hohlfeld: It was calculated by Monte Carlo.

Schulz: How confident are you of those results? They seem crucial to the entire procedure.

Hohlfeld: The Monte Carlo method is the same for the two cases (water in front and metal disc in front) and most of the errors will cancel. The higher backscatter from water is reflected in the numbers. At higher generating potentials of x-rays this error might be as high as 0.5% and you don't want to incorporate this into the range of energy for which we want to determine the heat defect.

-

Klassen: You might consider that the hydrogen peroxide produced might be decomposing on the metal surfaces so you might find that you produce a stationary state concentration of hydrogen peroxide which then changes as the water stands in the vessel so that the system is no longer at a stationary state.

Hohlfeld: The metal disc is mu metal. The standard deviation of measurements made over several days does not change. If a change occurs it should affect this standard deviation.

-

Rogers: Does your Monte Carlo include Rayleigh scattering or coherent scattering?

Hohlfeld: Yes.

Rogers: Where does it get the form factors of water?

Hohlfeld: I don't have the detailed information on the Monte Carlo calculations. They are done by Michael Kramer.

WATER CALORIMETRY, WITH EMPHASIS ON THE HEAT DEFECT

C.K. Ross, N.V. Klassen, K.R. Shortt and G.D. Smith
National Research Council
Ottawa, Canada

ABSTRACT - Radiation chemistry can be used to predict the heat defect of water containing various additives. We have constructed a small sealed calorimeter containing 100 ml of stirred water in order to test these predictions. Differences between the measured and calculated results are usually less than 0.5%.

La chimie des radiations permet de prévoir le déficit thermique de l'eau contenant divers additifs. Nous avons construit un petit calorimètre scellé contenant 100 mL d'eau agitée pour vérifier ces prévisions. Les écarts entre les mesures et les calculs sont en général inférieurs à 0,5 %.

I Introduction

The modern era of water calorimetry began in the early 1980s when Domen (1982) showed that it was technically possible to construct and operate a large water calorimeter. There had been significant earlier efforts to use water calorimetry (e.g., Pettersson (1967)) but these attempts did not result in an absorbed dose standard traceable to a water calorimeter. Although such a standard still does not exist, current efforts suggest that absorbed dose standards based on water calorimetry are likely to be established within the next few years.

Although Domen was able to operate a water calorimeter, the apparent absorbed dose which he measured in a ^{60}Co field was about 3.5% higher than that expected on the basis of graphite calorimetry. This discrepancy was much larger than the uncertainty associated with the conventional dosimetry, so it has generally been assumed that there was a problem with the water calorimetry. Several others have constructed calorimeters similar to that of Domen (e.g., Kubo (1983), Galloway (1986), Barnett (1986)) and, like Domen, they report apparent absorbed doses which are from 2% to 5% too high.

The motivation for our work was to examine the theoretical predictions regarding the heat defect of water, and to undertake measurements to test these predictions. In Section II we will briefly describe the mechanisms which can give rise to a heat defect in water, and summarize the predicted heat defect of water containing various additives. Our calorimeter is described in Section III, and our measurements to test the relative response of water containing various dissolved gases are summarized in Section IV. We have used Fricke dosimetry to test the absolute absorbed dose scale established with our calorimeter, and these measurements are described in Section V. Finally, some recent measurements will be described in Section VI.

II Heat Defect of Water

We will define the heat defect, k_{HD}, by

$$k_{HD} = \frac{E_a - E_h}{E_a}, \qquad (1)$$

where E_a is the energy absorbed by the irradiated material and E_h is the energy which appears as heat. Note that k_{HD} is greater than zero for endothermic processes and less than zero for exothermic processes.

In general, there are several processes which could give rise to a heat defect. For example, solid state effects, such as lattice dislocations, can lead to a positive heat defect in solids. In the case of a transparent liquid such as water there are at least four mechanisms which might give rise to a heat defect. Since water is transparent over a fairly broad range of wavelengths, any radiation-induced optical emission might escape from the sensitive volume of the calorimeter. The two most likely sources of optical emission are Cerenkov radiation and molecular deexcitation. Simple estimates (Ross et al (1988)) indicate that neither process is expected to make a significant contribution to the heat defect of water. A third possibility is that some energy may be transferred to acoustic modes, but based on available data for protons, we conclude that this mechanism can

also be ignored. Therefore, the most likely process leading to a heat defect in water is radiation-induced chemical reactions.

Fletcher (1982) used the model of Boyd, Carver and Dixon (1980) to calculate the chemical heat defect of water containing various additives. We use the same program (MACKSIM) to calculate the heat defect for systems which are of interest to us.

The first three systems we studied were pure water, water saturated with O_2 gas and water saturated with a 50/50 mixture of H_2 and O_2 gas. For a dose rate of 0.4 Gy/s, the model predictions can be summarized as follows:

1) pure water: $k_{HD} = 0$ after about 80 Gy;

2) O_2-saturated: $k_{HD} = +1.8\%$ (endothermic by 1.8%);

3) 50/50 H_2/O_2: $k_{HD} = -2.1\%$ (exothermic by 2.1%).

Our calculations agree with those of Fletcher, although we note that the dose rate labelling on his figure relating to the H_2/O_2 system (Figure 7) is backwards. Also, the O_2 concentration which he used in obtaining Figure 7 is only about one fifth of ours and accounts for the rather strong dependence on accumulated dose which he obtained.

The model predicts approximately the same heat defect for O_2- or air-saturated water, since oxygen is assumed to be the only active component in air. This suggests that the discrepancy observed by Domen is really about 5.5%, since his measurements were done with air-saturated water.

III Calorimeter Design

There were a number of considerations which established the design of our calorimeter. Firstly, the calculations based on MACKSIM showed that rather small product concentrations could lead to significant heat defects. For example, a 90 s irradiation at a dose rate of 0.4 Gy/s of water saturated with a 50/50 mixture of H_2 and O_2 gases leads to the production of about 250 molecules of H_2O_2 for every 10^9 water molecules. This concentration of H_2O_2 is sufficient to cause the H_2/O_2 system to be exothermic by 2.1%. This result suggests that water calorimetry may be sensitive to any reactive impurities in the water, and so we wanted a calorimeter in which water quality could be carefully controlled.

Since we wanted to test the response of water containing various dissolved gases, it was essential that our calorimeter be gas-tight. In addition, it must incorporate the necessary hardware to fill, drain and bubble the water with various gases. In order to minimize the bubbling time, the volume of water should not be too large.

As for all calorimeters, the sensitive volume must be well isolated thermally from the environment. In order to improve the thermal response characteristics of the calorimeter, we stir the water in the sensitive volume of the calorimeter. Some of our early work was done with an unstirred system, but the time required to establish satisfatory drift rates was very long. Changing to a stirred system was one of the most important steps in developing a practical calorimeter to test the response of a wide range of systems.

Our calorimeter has undergone a number of design changes over the past several years, but the main characteristics are now fairly well established. The details of an early version have already been published (Ross et al (1984)). Figure 1 is a cross-sectional view of the present version. Apart from a small polyurethane-varnish seal associated with the thermistor probes, all of the surfaces in contact with the water are glass. The glass vessel has a total volume of about 190 ml, and is filled with 100 ml of water. Although only one thermistor is shown, there are in fact two, and each is connected to its own sensing circuit.

The sensitive volume of the calorimeter is isolated from the environment by a temperature regulated shroud. The temperature of the shroud is controlled to about ±1 mK by water flowing through channels within the shroud. The thermal drift of the sensing volume is controlled by varying the shroud temperature, thus dispensing with a control element within the water. The temperature of the water to be put in the calorimeter is brought close to the operating temperature (21°C) before being poured in. Under these conditions, runs can begin within about 10 minutes of filling and bubbling the calorimeter. A few minutes between runs is usually sufficient to reestablish a satisfactory drift rate.

Each of the two 0.51-mm diameter sensing thermistors (about 13 kΩ at 21°C) is connected to its own Wheatstone bridge. The electrical power dissipated in each thermistor is about 2 μW. The output from each bridge is connected to its own sensitive voltmeter, and the analog output from each voltmeter is monitored by a

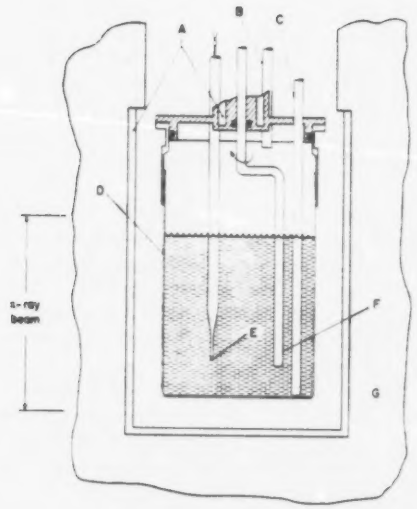

Figure 1. Cross-sectional view of the water calorimeter. The drawing is not to scale, but the water occupies a cylindrical volume about 5 cm in diameter and 5 cm high. The key elements are identified by letters: (A) channels for temperature-regulated water. The flow of water through these channels establishes a temperature-stabilized shroud which almost completely surrounds the sensitive volume of the calorimeter. (B) outlet tube for gas flow; (C) glass filling and bubbling tube; (D) thin-walled (0.040 g cm^{-2}) glass (Pyrex) calorimeter vessel; (E) one of two thermistors; (F) glass stirring paddle; (G) styrofoam insulation.

multipen chart recorder. A typical calibration and irradiation run is shown in Figure 2.

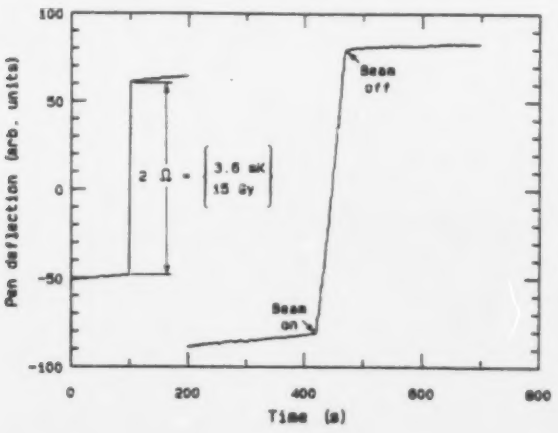

Figure 2. Chart recorder output showing a typical calibration and irradiation run. The thermistor power level was about 2 μW.

IV Relative Heat Defect Measurements

Water from two different sources has been used for the work described in this report, the purification process being somewhat different for each. However, both processes featured a deionizer, at least one stage of distillation, and a step to remove organic contaminants.

All the irradiations were done using 20 MV x-rays, produced by allowing a beam of 20 MeV electrons to impinge on a fully-stopping aluminum target. As indicated in Figure 1, the field size of the x-ray beam was slightly larger than the cross-sectional area presented by the water volume.

In the first phase of our work, the objective was to test the relative response of pure water, water saturated with O_2 gas, and water saturated with a 50/50 mixture of H_2 and O_2 gases. The model predictions for these three systems have been summarized in Section II. Since the details of these measurements have already been published (Ross et al (1984)), only the main features will be reproduced here.

Pure water was simulated by bubbling with either Ar or N_2 gas, neither of which participates in the radiation chemistry. Since we measured only the relative response of the three systems, we chose to normalize our measured response for the H_2/O_2 system to the calculated exothermicity of 2.1%. This system was chosen as the reference since it exhibited the least sensitivity to preparation technique.

The results of our measurements are summarized in Figure 3. After an accumulated dose of about 100 Gy, the relative response of the three systems is in reasonable agreement with the calculated values. We note that for the pure water, and the O_2-saturated system, the first couple of points tend to be high. This is a general feature which we have observed, and one which tended to become smaller the more effort we devoted to achieving a clean system. A similar effect has been reported by Barnett (1986) using a large calorimeter of a design similar to that of Domen. He noted that his calorimetric response decreased by several per cent, eventually becoming stable, as the accumulated dose increased. This effect is probably due to the radiation-induced removal of reactive impurities in the water, and emphasizes the importance of constructing a clean system.

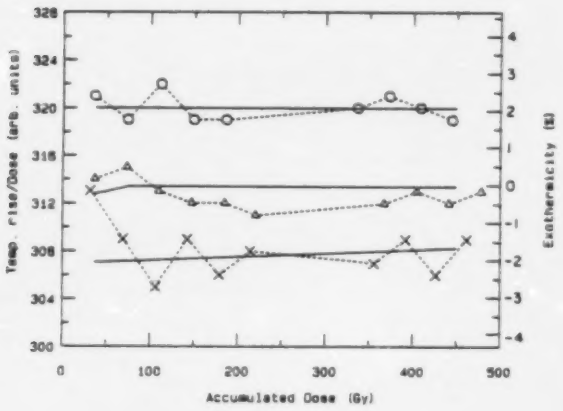

Figure 3. Temperature rise per unit dose for water containing different dissolved gases. The measured values are identified by the following symbols: Δ N_2-saturated; X O_2-saturated; O 50/50 H_2/O_2-saturated (50/50 by pressure). The results of the model calculations are shown by the solid lines and are plotted as percent exothermicity (right-hand ordinate). The measurements have been tied to the exothermicity axis by assuming that the measured and calculated exothermicity for the 50/50 H_2/O_2 system agree.

V Fricke Comparison

Our measurements of the relative response of water containing various dissolved gases supported the calculated heat defects based on MACKSIM. This result suggested that there was a problem with the first generation of large water calorimeters, and it was probably due to impurities in the water. However, our measurements did not establish an absolute absorbed dose scale, and it was possible that the absolute response was wrong, even though the relative response was correct.

We note however, that there is independent evidence to indicate that this is very unlikely. The model of Boyd et al predicts that pure water reaches a steady state condition after an accumulated dose of about 80 Gy. By definition, steady state implies that the concentration of stable products does not change, and thus that the heat defect must be zero. Measurements of product concentrations by Schwarz (1962) in water saturated with He gas showed that indeed a steady state was reached. The dose rates used for this work were much higher (400 Gy/s to 14,000 Gy/s) than we use, but MACKSIM calculations are able to reproduce very well the product concentrations measured by Schwarz. His results, if they can be extrapolated to lower dose rates, provide strong support for the prediction that the heat defect of pure water confined to a closed system should be zero.

Nevertheless, a test of the absolute absorbed dose scale established by our calorimeter seemed desirable. The basic approach we used was to replace the water in our calorimeter with Fricke solution, and determine the dose using Fricke dosimetry techniques.

The Fricke dosimetry system which we used is part of the NRC calibration service. It has excellent precision (about 0.1% for in-house work), it is based on the Sevensson and Brahme (1976) value of εG (3.515×10^{-3} ℓ/cm/J), and it agrees to about 0.2% with the NRC standard based on graphite calorimetry for the absorbed dose to water due to ^{60}Co γ-rays. The optical density is read at 303 nm using a Cary model 210 spectrophotometer.

Although the radiation absorption characteristics of Fricke solution are quite similar to water, there are small differences which must be considered. Once the dose to Fricke solution per monitor unit averaged over the volume occupied by the solution $(\bar{D}_F/M)$ is determined, the corresponding dose to water per monitor unit $(\bar{D}_w$ (via Fricke)$/M)$ is given by

$$\frac{\bar{D}_w(\text{via Fricke})}{M} = \frac{\bar{D}_F}{M} R_F^w k_{dis}, \qquad (2)$$

where R_F^w is the ratio of mass energy absorption coefficients for water to Fricke solution, and k_{dis} is a correction factor to account for the fact that the dose distribution in the Fricke solution may be slightly different from that in water. The evaluation of these factors is discussed in detail by Ross et al (1988), and they obtain $R_F^w = 1.001$ for 20 MV x-rays, and $k_{dis} = 1.000$.

The dose to water was determined calorimetrically using water saturated with a 50/50 mixture of H_2 and O_2 gases. As discussed in Section II, the heat defect for this system is expected to be -0.021. Then the dose to water per monitor unit averaged over the volume occupied by the water is given by

$$\frac{\bar{D}_w(\text{via cal})}{M} = c \cdot \frac{dT}{dR} \cdot f \cdot d \cdot (1+k_{HD}) \cdot k_{FM}, \qquad (3)$$

where

c = specific heat of water;

$\frac{dT}{dR}$ = thermistor sensitivity;

f = overall sensitivity of the detection system;

d = measured chart recorder deflection per monitor unit;

k_{HD} = heat defect;

k_{FM} = correction for foreign mass in contact with the water.

The specific heat of water at 21°C is 4.181×10^3 J/kg/deg. The factors f and d are determined from runs similar to those shown in Figure 2. The factor k_{FM} accounts for the fact that the specific heat of glass is only about one fifth that of water, and so, much of the radiation-induced heat energy in the glass will be transferred to the water. The mass of glass in direct contact with the water is approximately 5.5 g, so k_{FM} is expected to represent a correction of a few percent.

We measured k_{FM} by repeating the calorimetric and Fricke dosimetric measurements with varying amounts of glass in contact with the water. Measurements were made using glass vessels with masses approximately twice and four times the mass of the standard vessel. As well, measurements were made with approximately twice and four times the mass of glass immersed in the water. Each set of Fricke measurements consisted of four separate irradiations with the dose varied from about 10 to 40 Gy. The corresponding calorimetric measurements consisted of five or six calorimetric runs using a single fill of water.

In Figure 4 the calorimetric response (obtained using equation (3) but with k_{FM} set to unity) divided by the dose to water derived from Fricke dosimetry is plotted versus the mass of glass. If these results are extrapolated to zero mass, the ratio of the dose to water based on calorimetry to the dose to water based on Fricke dosimetry is obtained. The result is

$$\frac{\bar{D}_w(\text{via calorimetry})}{D_w(\text{via Fricke})} = 1.006 \pm 0.004, \qquad (4)$$

where the uncertainty represents the statistical uncertainty and corresponds to one standard deviation.

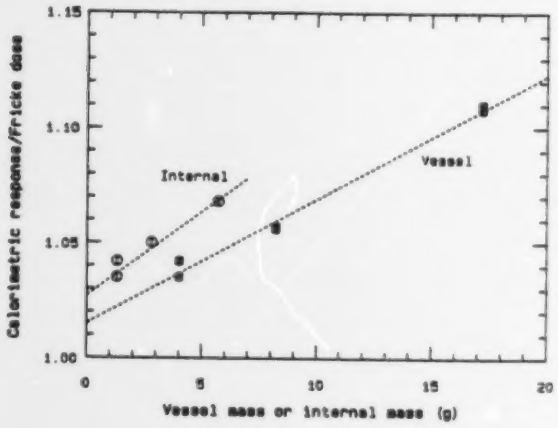

Figure 4. Data used to obtain the correction (k_{FM}) to the calorimetric response due to the glass in contact with the water. The data are represented as follows: □ - effect of varying the mass of the vessel; ○ - effect of varying the internal mass. The error bars showing the statistical uncertainties are roughly the same size as the symbols used to locate the data points. Note that the two data points corresponding to the least internal mass are the same as the two corresponding to the least vessel mass. The dashed lines represent the best linear fit to the data.

In obtaining equation (4), we have assumed that the ferric ion yield ($G(Fe^{+++})$) is independent of beam quality. Although some dependence on LET is expected, the work of Nahum et al (1980) suggests that the variation from ^{60}Co γ-rays to 20 MV x-rays is probably not much greater than 0.5%.

Equation (4) gives further support to our present understanding of the heat defect of water containing various dissolved gases.

VI Work in Progress

Recently, we have concentrated on further tests and refinements of the reaction set for the radiolysis of water and related systems. Klassen et al (1988) have pointed out that a recent reexamination of the reactions of importance in the radiolysis of water has resulted in some changes to the model as proposed by Boyd et al (1980). In the case of water saturated with a 50/50 mixture of H_2 and O_2 gases, these changes lead to a change in the heat defect from -2.1% to -2.4%.

We have recently studied three additional dilute aqueous systems for which the reaction set is fairly well known. One system is formed by bubbling water with a mixture of N_2O and O_2 gases, another by bubbling with a mixture of CO and O_2 gases, and the third by adding millimolar quantities of sodium formate and bubbling with O_2 gas. For details of the radiation chemistry of these systems, see Klassen et al (1988). The heat defects of these systems are predicted to be:

$$k_{HD}(N_2O/O_2) = -2.0\%,$$

$$k_{HD}(CO/O_2) = -3.3\%,$$

$$K_{HD}(\text{formate}/O_2) = -2.6\%.$$

All three systems are exothermic.

We have measured the response of these systems relative to our standard H_2/O_2 system, and the results are shown in Figure 5. The

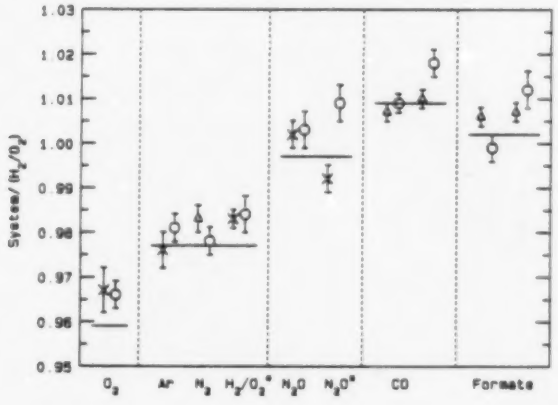

Figure 5. Comparison of the measured and calculated calorimetric response for a number of systems relative to the H_2/O_2 system. The systems labelled Ar, N_2 and H_2/O_2* are all believed to simulate pure water (the asterisk on the H_2/O_2 system indicates that the concentration of H_2 and O_2 was very low, corresponding to the steady state values predicted by MACKSIM for pure water). The asterisk on the N_2O/O_2 system indicates that the gas mixture was diluted using Ar. The solid horizontal lines are the MACKSIM predictions. Each set of runs has two data points associated with it, corresponding to the two thermistors. The various symbols serve to identify different thermistor probes.

solid horizontal lines are the MACKSIM predictions, based on the new value of k_{HD} for the H_2/O_2 system, namely -2.4%. Agreement between the measured and calculated values is within about 0.5%, with a suggestion that the calculated ratio is too small.

Our early measurements (Figure 3) on the relative response of water containing various dissolved gases suggested that the pure water system was endothermic by about 0.5%. Our recent measurements (Figure 5), if referenced to the same value of $k_{HD}(H_2/O_2)$ as used in Figure 3, namely -2.1%, show good agreement between the measured and calculated heat defect. Efforts are continuing to refine the precision of our measurements so that we may identify the reason for this 0.5% discrepancy.

One of the limitations of our calorimeter is that we must operate with low thermistor power (about 2 μW) or else the noise level increases. We interpret this effect as being due to the irregular movement of the thermal gradient established around the thermistor because of the stirring. The low thermistor power restricts our sensitivity, and would make measurements on our ^{60}Co unit difficult. In order to reduce this effect, we attempted to increase the surface area of the thermistor, and thereby decrease the thermal gradient, by using flake thermistors. However, these units did not have acceptable stability, a fact recognized by the manufacturer. However, we have recently begun using a probe consisting of six conventional thermistor beads in series, having about the same overall resistance as our single-bead detectors. This approach has permitted us to operate with ten times the power level (one expected an improvement of at least six) and thus increase the sensitivity of our calorimeter by over a factor of three. The data shown by triangles in Figure 5 have been taken with this new detector.

We have also shown that it is possible to actively cool a thermistor using a thermoelectric cooler coupled to its leads. Although we do not yet have a workable probe based on this approach, it should permit operation at power levels as high as 1 mW.

References

Barnett, R.B. (1986). Water Calorimetry for Radiation Dosimetry, Ph.D. thesis, University of Calgary, Calgary, Alberta.

Boyd, A.W., Carver, M.B. and Dixon, R.S. (1980). Computed and Experimental Product Concentrations in the Radiolysis of Water, Radiat. Phys. Chem. 15, 177-185.

Domen, S.R. (1982). An Absorbed Dose Water Calorimeter: Theory, Design and Performance, J. Res. Nat. Bur. Stand. (U.S.) 87, 211-235.

Fletcher, J.W. (1982). Radiation Chemistry of Water at Low Dose Rates - Emphasis on the Energy Balance: A Computer Study, Chalk River Nuclear Laboratories, AECL-7834.

Galloway, G., Greening, J.R. and Williams, J.R. (1986). A Water Calorimeter for Neutron Dosimetry, Phys. Med. Biol. 31 397-406.

Klassen, N.V., Ross, C.K., Shortt, K.R. and Smith, G.D. (1988). The Chemical Heat Defect of Water, see the index of these proceedings.

Kubo, H. (1983). Absorbed Dose Determination with a Water Calorimeter in Comparison with an Ionization Chamber, Phys. Med. Biol. 28, 1391-1399.

Nahum, A.E., Svensson, H. and Brahme, A. (1980). The Ferrous Sulfate G-Value for Electron and Photon Beams: A Semi-empirical Analysis and its Experimental Support, Proc. Seventh Symp. on Microdos. (Harwood Academic Publishers Ltd.), 841-851.

Pettersson, C. (1967). Calorimetric Determination of the G-Value of the Ferrous Sulfate Dosimeter with High-Energy Electrons and Co-60 Gamma-Rays, Arkiv för Fysik 34, 385-400.

Ross, C.K., Klassen, N.V. and Smith, G.D. (1984). The Effect of Various Dissolved Gases on the Heat Defect of Water, Med. Phys. 11, 653-658.

Ross, C.K., Klassen, N.V., Shortt, K.R. and Smith, G.D. (1988). A Direct Comparison of Water Calorimetry and Fricke Dosimetry, submitted to Phys. Med. Biol.

Schwarz, H.A. (1962). A Determination of Some Rate Constants for the Radical Processes in the Radiation Chemistry of Water, J. Phys. Chem. 66, 255-262.

Svensson, H. and Brahme, A. (1979). Ferrous Sulfate Dosimetry for Electrons. A Re-evaluation, Acta Radiol. Oncol. 18, 326-336.

Discussion

Fletcher: Are the solid lines in your last figure based on Fricke dosimetry?

Ross: No, the Fricke measurements do not enter into the results presented here.

-

Klassen: You might comment on how the calculated results in your last figure change depending on whether Model I or Model II is used.

Ross: In Model II the H_2/O_2 system is about 0.3% more exothermic than in Model I. If this were the only effect, it would move the solid lines up by 0.3%. However, the calculated heat defect for the other systems may also change slightly.

-

Schulz: Are the chart recorder deflections measured using a ruler and a pencil?

Ross: Yes, Klassen does the analysis. We also have one detector interfaced to our computer.

-

Kubo: In your comparison of calorimetry and Fricke, you quote a standard deviation of 0.4%. What contributes to this uncertainty?

Ross: It arises from about equal contributions from our calibration and irradiation runs.

-

Kehoe: You quote a factor of three increase in sensitivity for the series probe. What does that mean?

Ross: The sensitivity goes roughly as the square root of the thermistor power. With the series probe we can operate at about ten times the power level and still have about the same noise level. This is what I meant by a factor of three increase in sensitivity.

-

Roos: You said that Cerenkov radiation might contribute to the heat defect. I believe that it contributes to the absorbed dose and should not be included in the heat defect.

Ross: Are you saying that Cerenkov radiation should not be included in the definition of absorbed dose, the same as rest mass changes are not to be included?

Roos: According to ICRU, I believe it should influence the absorbed dose, but not the relationship between absorbed dose and temperature rise.

Cormack: I would agree with that.

Ross: The question of molecular deexcitation may be more straightforward. If a large fraction of optical emission escapes from the calorimeter, it will not be measured, although chemical or biological changes have occurred.

Henry: But that isn't included in the absorbed dose either.

MEASUREMENT OF THE HEAT DEFECT OF WATER CAUSED BY HIGH-ENERGY ELECTRONS

M. Roos
Physikalisch-Technische Bundesanstalt
D-3300 Braunschweig, Federal Republic of Germany

ABSTRACT - The establishment of the water calorimeter as a primary standard for water absorbed dose demands the determination of the heat defect of water by a method which does not include the absorbed dose. A method is being developed based on the total absorption of high energy electrons in a water absorber. The method is outlined, preliminary measurements are reported, the necessary corrections being discussed.

L'établissement du calorimètre à eau comme étalon primaire pour la mesure de la dose absorbée par l'eau impose qu'on détermine la valeur du déficit thermique de l'eau par une méthode qui ne fait pas intervenir la dose absorbée. Une méthode est mise au point qui est basée sur l'absorption totale d'électrons très énergétiques dans un absorbeur aqueux. La méthode est décrite, les résultats préliminaires sont présentés et les corrections qui s'imposent sont analysées.

INTRODUCTION

In order to realize a more accurate determination of the water absorbed dose - the measurand in dosimetry for radiotherapy - water absorbed dose calorimeters are being developed (references can, for example, be taken from the review article of Domen 1987). This dosimeter type allows the dose to be measured according to its definition, requiring, however, the knowledge of that portion of the mean energy imparted to water by radiation which is converted to heat. The deviation of that portion from unity - the "heat defect" - depends critically on impurities in the water but it should be independent of radiation energy for low LET radiation (Fletcher 1982, Ross, Klassen and Smith 1984). The model calculations underlying these results show that the heat defect of pure water is zero, raising the question: when is water in a calorimeter pure enough to reveal a zero heat defect? Relative measurements verify the results of the model calculations with regard to the dependence of the heat defect on impurities (dissolved gases) to within several parts in a thousand (Ross et al. 1984, Schulz et al. 1987).

Considering the results of water calorimetric measurements by Domen (Domen 1982), Mattsson (Mattsson 1984) or Kubo (Kubo 1983), for instance, one could conclude that the heat defect of water, including organic impurities (introduced through contact of the water with parts of the calorimeter or by using less purified water), is stable. This assumption is also supported by measurements of Ross et al. (Ross et al. 1984) which in addition show that specified impurities - for instance a mixture of H_2 and O_2 - can ensure a stable heat defect.

Hitherto absolute measurements were based on the comparison of dose values measured with the water calorimeter with corresponding values determined using other dosimetric methods, the deviations being attributed to the heat defect. Therefore the uncertainties can amount to several percent and the correction of the water calorimetric results using these values would be a calibration of the calorimeter.

The establishment of the water calorimeter as a primary standard, however, demands the determination of the heat defect of water using a method which does not include the absorbed dose (Roos and Hohlfeld 1987). For the primary standard appropriate impurities, supplying a stable heat defect, should not be a disadvantage. The uncertainty in the determination of the heat defect in any case enters into the total uncertainty of the standard, irrespective if whether the heat defect is zero or amounts to 2 ‰ or 3 ‰.

In the following, the main features

are outlined of a method for the determination of the heat defect for high energy electrons. Together with an experimental method for soft X-rays (Hohlfeld 1988) it paves the way for the application of a water absorbed dose calorimeter (Roos 1987) as a primary standard at the Physikalisch-Technische Bundesanstalt (PTB).

EXPERIMENTAL METHOD

The method is based on the total absorption of the radiation in a water absorber. We essentially take advantage of the high energy stability and the narrow energy spread of the electron beam from our microtron. This allows the determination of the electron energy, which together with the number of electrons gives the energy imparted to the absorber.

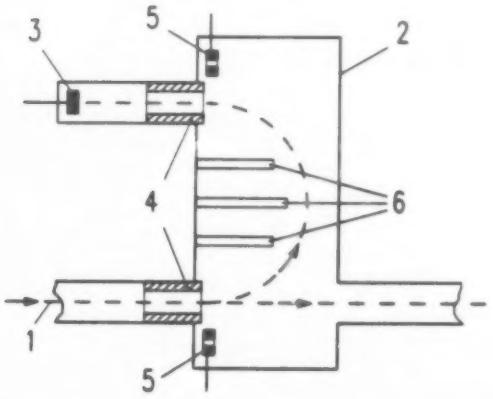

Figure 1

Schematic diagram of the magnet spectrometer for the measurement of the electron energy. (1) electron beam from microtron, (2) 180° deflection chamber, (3) electron beam collector, (4) iron tubes, (5) slit apertures, (6) insertion channels for nuclear magnetic resonance probes.

To determine that portion of the energy imparted which is converted to heat, the temperature rise is measured and the same temperature rise is produced without a heat defect by electrical heating. The difference of the energy imparted by radiation and the electrical energy yields the heat defect.

The microtron supplies energies of about 1.1 MeV, 1.9 MeV and 5.1 MeV with energy spreads less than 10 keV. The mean beam current is typically 10^{-8} A and the pulse repetition frequency can be adjusted to 50 Hz, 100 Hz, 200 Hz or 400 Hz. The pulse length is 1.3 µs, the fine structure of the pulses is given by the magnetron frequency of 3 G Hz. That means every pulse consists of 4300 micropulses of length 0.003 ns.

Fig. 1 shows the magnet spectrometer for the measurement of the electron energy. The magnetic induction of the bending magnet can be measured using nuclear magnetic resonance probes inserted into channels (6). At the end of the entrance and exit tubes of the deflection chamber iron tubes (5) cause the magnetic induction to rapidly fall off inside the tubes. The fluctuations of the magnetic induction inside the deflection chamber amount to less than 0.2 ‰.

To determine the electron energy the slit apertures (5) (of width 0.2 mm) are placed in front of the entrance and the exit tube in the deflection chamber. The exit slit is fixed at a position in the centre of the tube whereas the entrance slit is shifted across the beam. For each position the magnetic induction is varied until the current measured with the collector reaches a maximum value. Then the magnetic induction is measured, the uncertainty being below 0.1 ‰. From the magnetic induction and the separation of the slits the kinetic electron energy can be derived with an uncertainty of 0.2 ‰.

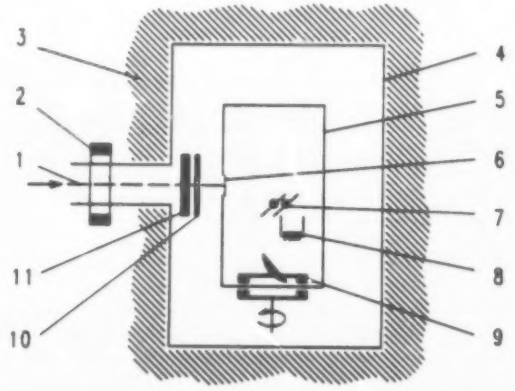

Figure 2

Total-absorption calorimeter at the end of the beam guiding system. (1) electron beam from microtron, (2) calibrated beam monitor, (3) air conditioned enclosure, (4) vacuum container, (5) absorption vessel, (6) entrance window, (7) thermistors, (8) electrical heater, (9) magnetically coupled stirrer, (10, 11) ring shaped detector.

Fig. 2 shows the calorimeter. When the bending magnet is switched off the beam is guided to the entrance window (6) of the absorption vessel (5) by means of a beam handling system. It consists of a 30° deflection magnet and two pairs of quadrupole lenses.

The charge carried to the absorber is measured by means of a calibrated beam monitor (2), realized by a beam current transformer. The uncertainty of the charge measurement is 0.3 %. A ring-shaped detector (10, 11) in front of the entrance window permits the verification that all electrons, their charge being measured, do indeed hit the window. The diameter of the beam is less than 4 mm. The diameter of the window is 8 mm; it consists of Mylar foil 20 µm thick. The inner diameter of the detector is slightly smaller. The detector consists of two rings (10, 11) each connected to an electrometer. The second one (10) prevents backscattered electrons from the window from being detected by the first one (11). In practice it turned out that the fraction of electrons hitting the first detector ring is well below 0.1 %. The dimensions of the vessel (5) ensure that all the electrons entering through the entrance window (6) are stopped completely in the water. So the radiant energy imparted to the absorber is given as the product of the measured parameters kinetic energy of the electrons and charge carried to the absorber, divided by the elementary charge.

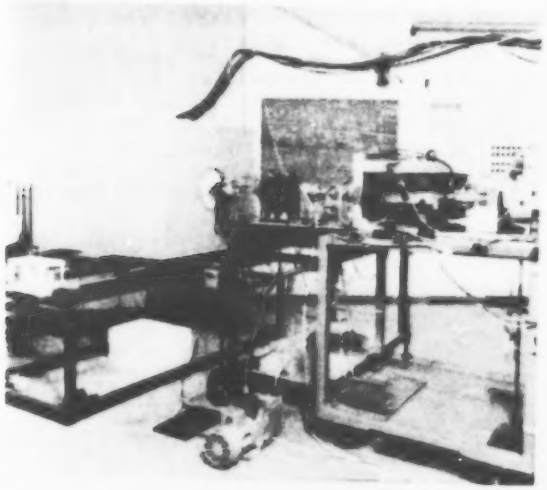

Figure 3

The calorimeter at the microtron.

For the measurement of the heat caused by the absorption of the radiant energy, a magnetically coupled stirrer (9) provides a homogeneous temperature distribution throughout the absorber (5). The temperature rise is measured using two thermistors (7) in opposite arms of a Wheatstone AC bridge. The bridge voltage caused by the temperature change is amplified by a lock-in amplifier and then recorded.

The same rise in temperature as caused by irradiation is then generated - without a heat defect - by electrical heating. The heater (8) is supplied by a constant current generator, the voltage drop is measured by counting the pulses of a calibrated voltage frequency converter. The uncertainty in the determination of the electrical heating energy is below 0.1 %.

In the following some photographs illustrate further details of the experimental setup. Fig. 3 shows the total-absorption calorimeter with its wooden temperature stabilizing enclosure in front of the beam guiding system (with 180° deflection chamber, quadrupole lenses and beam monitor) of the microtron.

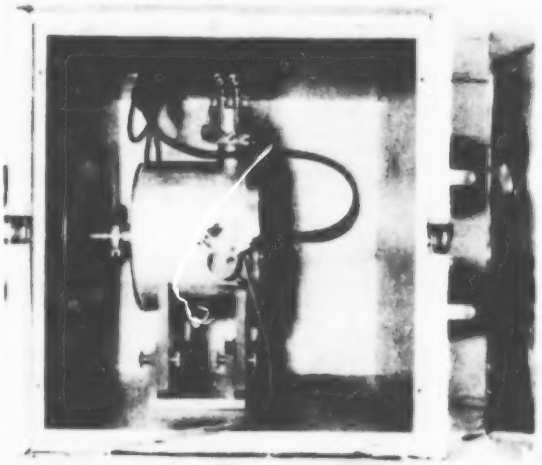

Figure 4

Inner box of the calorimeter, with the lid removed, containing the vacuum container.

Inside the outer enclosure of the calorimeter is a thermally isolating box containing the absorption vessel inside a vacuum container. Fig. 4 shows the inner box.

The air around the inner box is regulated to a temperature of 30° C, well above room temperature. That is accomplished by heaters (2 bulbs on the right-hand side of Fig. 4) and ventilators to cause air circulation.

In order to electrically isolate the calorimeter from the beam-guiding system, and to minimize heat transfer from the room to the vacuum container, we use a lucite tube in front of the calorimeter (on the left hand side of Fig. 4).

Fig. 5 shows a view into the vacuum container from the opposite side of the beam entrance. The absorption vessel is suspended by thin nylon wires to minimize the heat conduction to the supporting ring in the vacuum enclosure.

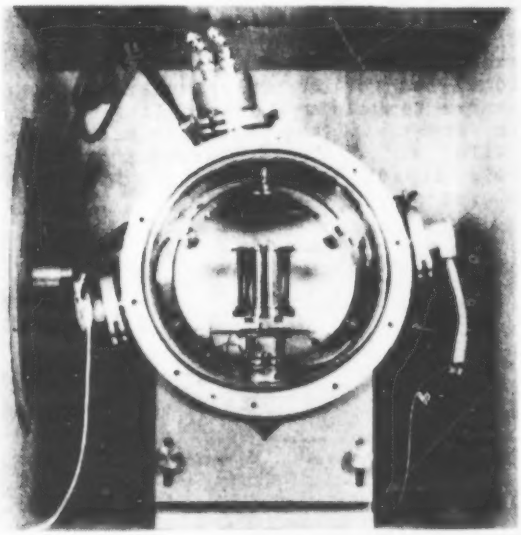

Figure 5

Vacuum container with the lid removed.

Convection heat transfer is avoided by evacuation. So the cooling constant is less than 10^{-4} s^{-1}. Below the absorption vessel a steel plate support for the synchronous motor underneath can be seen; the latter drives a rotor coupled magnetically to a stirrer inside the absorption vessel.

Fig. 6 shows an absorption vessel for 2 MeV electrons from below underside and stirrer being removed. The diameter is about 2 cm. It is made of stainless steel. The stirring method necessitates a circular cross-section. The dimensions of the vessel ensure that the fraction of electron energy transferred to other materials than water is negligible.

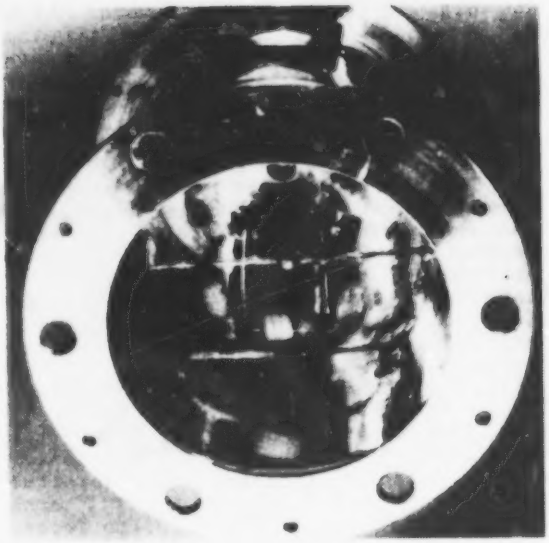

Figure 6

Absorption vessel for 2 MeV electrons with thermistors and heater.

Fig. 7 shows the underside of the absorber, containing the stirrer magnetically coupled to the synchronous motor. The magnets are covered with polyethylene foil to avoid rusting. The sealing consists of Teflon. The material selection is generally guided by the principle that no other materials should be in contact with the water than those used in the case of the water absorbed dose calorimeter. So most of the parts inside the absorption vessel are covered with polyethylene foils.

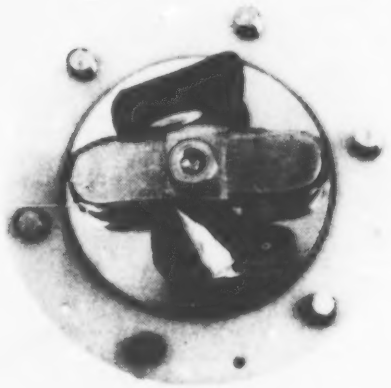

Figure 7

Underside of the absorption vessel from Fig. 6.

The number of revolutions of the stirrer is adjusted to 2 per second by a gear unit. The stirring effect can be enhanced by regularly changing the direction of the revolutions. The power transferred to the absorber by stirring is essentially generated by friction, particularly by friction of the stirrer bearing, which is a ball bearing of stainless steel. This power is kept well below 1 ‰ of the radiation power and the electrical power under non-steady state conditions. In the steady state case it is sufficiently constant so that its influence is negligible.

We use two types of total absorption vessels. One allows the disassembly of the absorber without too much trouble, enabling checking of the internal parts. That is naturally very advantageous during the testing stage. The disadvantage is that the vessel contains more mechanical elements, partly in the form of leads. These cause additional cooling effects at the beginning of the calorimeter post periods, because it takes some time until the heat transferred to the water also reaches the outer parts of the absorber. The absorber shown in Fig. 6 and Fig. 7 is of this type. The second type of absorber has nearly no projecting parts, the mass of the vessel being minimized. Both absorber types, of course, enable the water to be bubbled with gases and then to be sealed, but only during the stage when the vacuum system is ventilated.

PERFORMANCE OF MEASUREMENTS

Several hours before beginning the irradiation the water is stirred with constant power to obtain steady-state conditions, i. e. a constant temperature in the absorber. Then a cycle of measurements is performed as schematically illustrated in Fig. 8.

The measurements start with the recording of the calorimeter pre-period (pp), the amplitude of the signal fluctuations $\delta\vartheta$ being less than 100 µK. Then a rise in temperature $\Delta\vartheta_r$ of about 30 mK is effected in the heating period by irradiation, the irradiation time being about 3 minutes. During the post-period (pp), which is the pre-period of the heating stage of electrical heating, the radiation energy transferred to the absorber is evaluated. Then the electrical heating current is adjusted to produce the same energy transferred to the absorber within the same time, effecting the rise in temperature $\Delta\vartheta_e$.

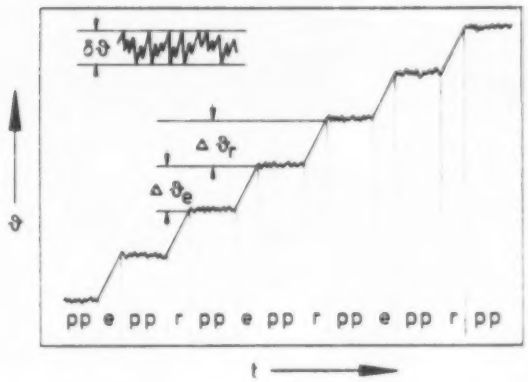

Figure 8

Illustration of the temperature ϑ versus time t program during a cycle of measurements, comprising calorimetric pre- and post periods (pp) respectively, periods of electrical heating (e) with rises in temperature $\Delta\vartheta_e$ and periods of heating by irradiation (r), causing rises in temperature $\Delta\vartheta_r$.

Fig. 9 shows a recorder trace of the temperature vs. time curve of the absorber as reflected by the change in the thermistor resistance. After a pre period at time a, irradiation with 5 MeV electrons was started and at time b it was stopped. The sudden changes in the intervals were caused by manual resistance changes. The charge carried to the absorber was about 7 µC caused by about 10^{13} electrons. The radiation energy imparted was 35 J causing a temperature rise of about 35 mK.

The additional cooling effect immediately after the irradiation period reveals that the absorber used was of the first type. At the time c electrical heating was started and ended at time d. The current was adjusted to about 20 mA to produce a power of about 160 mW, as was the case for the previous irradiation.

It turned out that the temperature vs. time curves during and after the periods of irradiation and of electrical heating are practically the same, the additional cooling effect after the end of the heating periods included. Consequently, small systematical errors, for instance, in the extrapolation of the post-periods, cancel and do not affect the value of the heat defect.

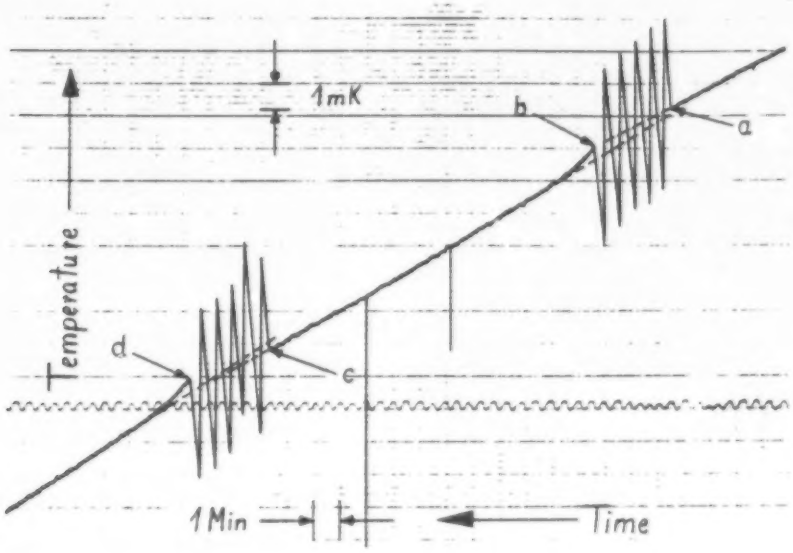

Figure 9

Recorder trace of the temperature vs. time curve of the absorption vessel around the periods of irradiation and of electrical heating. The time increases from the right hand side to the left hand side. At time a irradiation commenced, at time b it ended and at time c electrical heating commenced, ending at time d. Meanwhile the bridge resistance was changed manually.

In order to examine whether the precision of the measurements is sufficient, we took about 20 measurements, as an initial test of the quotients of the electrical energy divided by the corresponding temperature rise and the radiant energy divided by the temperature rise, the measurements extending over a week. Those parameters which could have an influence were kept constant: for instance the electron energy, pulse repetition frequency of the microtron, mean beam current, electrical heating power and the duration of the irradiation period and of the electrical heating period. The standard deviation of the mean value of the quotient above revealed to be smaller than 0.1 % and would seem to be satisfactory.

To calculate the heat defect from the results shown, corrections have to be made for back-scattering of electrons at the entrance window of the absorber and energy lost by bremsstrahlung, produced during the deceleration of the electrons. The correction factors differ only by a few percent from 1 and are determined using a Monte Carlo code (Grosswendt and Roos 1986). The calculations are in progress.

CONCLUSION

The experiment presented here enables the heat defect of water to be measured for electron radiation in the energy range from 1 MeV up to 5 MeV. Together with the experimental method for soft X-rays it allows the heat defect to be studied systematically for low LET radiation, paving the way for the application of the water calorimeter as a primary standard of absorbed dose.

REFERENCES

1. Domen, S.R. 1982. An absorbed dose water calorimeter: theory, design and performance. Journal of Research of the NBS 87, pp. 211-235.

2. Domen, S.R. 1987. Advances in Calorimetry for Radiation Dosimetry. In: The Dosimetry of Ionizing Radiation, Vol. II. Ed. Kase, K., Björngard, B.E. and Attix, F. Academic Press, Orlando.

3. Fletcher, J.W. 1982. Radiation chemistry of water at low dose rates with emphasis on the energy balance: a computer study. AECL-7834 (Chalk River Nuclear Laboratories, Ontario, Canada).

4. Grosswendt, B. and Roos, M. (1986). Zur Bestimmung von Elektronen-Reichweiten in Wasser aus Messungen in Festkörperphantomen. Medizinische Physik pp. 265-274.

5. Hohlfeld, K. 1988. Determination of the heat defect of water by total absorption of soft X-rays. In this volume.

6. Kubo, H. 1983. Absorbed dose determination with a water calorimeter in comparison with an ionization chamber. Phys. Med. Biol. 28, pp. 1391-1399.

7. Mattsson, L. O. 1984. Application of the water calorimeter, Fricke dosimeter and ionization chamber in clinical dosimetry. Thesis, University of Göteborg.

8. Roos, M. and Hohlfeld, K. 1987. A measurement of the heat defect of water caused by high energy electrons. Thermochimica Acta, 119, pp. 95-101.

9. Roos, M. 1987. A water calorimetric determination of absorbed dose to water. Thermocimica Acta, 119, pp. 81-93.

10. Ross, C.K., Klassen, N.V. and Smith, G.D. 1984. The effects of various dissolved gases on the heat defect of water. Med. Phys. 11, pp. 653-658.

11. Schulz, R.J., Wuu, C.S. and Weinhous, M.S. 1987. The direct determination of dose-to-water using a water calorimeter. Med. Phys. 14, 5, pp. 790-796.

Discussion

Ross: I believe your technique to measure the heat defect is the same as used by Feist to measure the G-value of Fricke. The uncertainty on his measurements was about 1%; do you expect to do better?

Roos: We are now able to make more precise Fricke measurements, with an uncertainty of perhaps 0.2%.

-

Rogers: How much of the bremsstrahlung is reabsorbed in the container?

Roos: The bremsstrahlung escaping from the container amounts to about 2% of the energy.

-

Shortt: Is there any problem due to the fact that your calibration heater is essentially a point source?

Roos: No, I don't think so. The water is continuously stirred.

McDonald: Could you use the same apparatus for other beams; low energy x-rays or low energy ion beams?

Roos: No. The differential method we are using for low-energy x-rays could be applied to other beams.

-

Klassen: The system is a bit difficult to model, because the dose rate varies greatly throughout the water volume.

Roos: That is true, and there is also the problem of whether one should consider the dose rate in the electron pulse, or the dose rate during the RF micro pulse.

Ross: What is your schedule?

Roos: We expect to have useful numbers in the next month.

-

Klassen: I would like to follow up on a comment you made early in your talk. For a system in which the heat defect is not zero, the accuracy of the calculated heat defect depends on how good the model is. On the other hand, for a system which is predicted to go to steady state, and therefore have a heat defect of zero, the model parameters are not nearly so important. Then the uncertainty is more likely due to such things as the level of impurities.

Kehoe: How can you be sure that the heat defect you measure with this system will apply to the water in your large calorimeter?

Roos: We will measure the heat defect before and after the water is put in our large calorimeter.

THE ROLE OF WATER PURITY, CONVECTION, AND HEAT CONDUCTION IN A NEW CALORIMETER DESIGN

Steve R. Domen
Center for Radiation Research
National Bureau of Standards, Gaithersburg, MD 20899 U.S.A.

ABSTRACT - A calorimeter suitable for absorbed-dose measurements in high-purity water is described. The purpose of the design is to eliminate effects caused by convection and non-water materials.

On décrit un calorimètre permettant le mesurage de la dose absorbée dans de l'eau de grande pureté. La conception de ce calorimètre élimine les effets de la convection et de la présence de substances autres que l'eau.

Introduction

The purpose of this paper is to describe a new design of an absorbed-dose water calorimeter suitable for containing high-purity water enclosed in glass. Simplicity of design is aided by operating the calorimeter at a regulated temperature above room temperature. The geometric design is aimed at preventing convection and decreasing errors caused by excess heating of materials other than the high-purity water.

Water Purity

Two necessary requirements of a water calorimeter as a standard instrument are (1) the heat defect must be accurately known, and (2) the absorbed-dose measurements must be reproducible. The heat-defect correction depends on the water quality, which changes with types and amounts of impurities including dissolved gases. Results have been reported with the use of three general qualities of water. The first of those results were with once-distilled water (Domen, 1981,1982), high-purity water saturated with nitrogen (Schulz et al., 1987), and high-purity water saturated with nitrogen, oxygen, or a 50/50 mixture of hydrogen and oxygen gases (Ross et al., 1984, 1988).

Before describing present efforts being made at NBS in developing a calorimeter for measuring absorbed dose in high-purity water, it would be worthwhile to point out some original results concerning the use of once- distilled water and its present status. Figure 1 is a plot of apparent absorbed dose rate measurements in a ^{60}Co beam as a function of accumulated absorbed dose up to 150 Gy (Domen, 1982). An absorbed dose of 3.3 Gy was delivered during each 3 minutes of irradiation, 45 being the maximum number of runs made during a day. Curve 1 represents consistent measurements in once-distilled water. New water was drawn from a 100-L still container and used for each day of measurement, and then the water was discarded. This procedure was used on nine days over a period of 120 days. The daily average absorbed dose rate was determined. The standard deviation of those averages is 0.2%. During that period it was noticed that the bottom of the container was covered with a layer of sediment. After the container was cleaned, which resulted in an increase in electrical resistivity of the water from about 100-kΩ cm to 800-kΩ cm, there was no noticeable change in the measured absorbed dose rate.

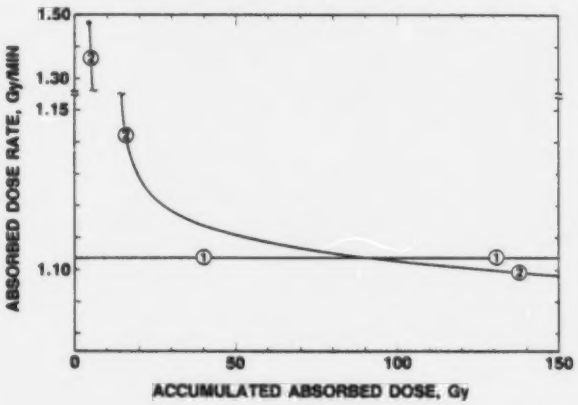

Fig. 1. Measured apparent absorbed dose rates as a function of accumulated absorbed dose in: (1) once-distilled water; (2) tap water.

Would once-distilled water from other laboratories give results sufficiently close to the above results? It was impractical to make a direct comparison test at NBS, because of the large water volume of the calorimeter, a 30-cm cube. But it was assumed that the use of once-distilled water in other laboratories would give results closer to those indicated by curve (1) than to results measured in the tap water used at NBS. This water

had properties which were drastically different from the once-distilled water. In contrast, the tap water was gassy, as revealed by many bubbles which were formed on the immersed surfaces (this did not happen with the once-distilled water). Also, as a result of more impurities, the electrical resistivity of the tap water was about 100 times lower than that of the once-distilled water. Results obtained with the use of the tap water are shown by curve 2 in figure 1. Curve 2 represents the average of reproducible results measured on three different days. The first calorimeter measurement was 35 percent higher than that in the once-distilled water; but the measurements rapidly decreased to within one percent of the measurements between 60 Gy and 150 Gy in distilled water. Therefore, one could assume that in other laboratories using once-distilled water, if there were an initial variation with accumulated absorbed dose, that variation would be much smaller than that shown by curve 2 and would soon disappear to give a response like curve (1) over a sufficiently great accumulated absorbed dose. If this were the case, then a sufficiently large number of irradiation runs could be made during a day before a further variation would occur.

The advantages of using once-distilled water are that it is easily prepared and that the calorimeter container does not need to be meticulously clean compared to a high-purity system. A disadvantage of its use is that there appears to be an apparent exothermic heat defect of 3.5%, compared with results determined with a graphite calorimeter, which has no heat defect. Therefore, this type of water calorimeter requires a correction based on comparisons with other detectors. Exothermic heat defects, for low LET radiation, ranging from 2 to 5% have been reported (Barnett, 1986; de Marles, 1981; Domen, 1981,1982; Kubo, 1983; Mattsson, 1984). It is difficult to determine how much this variation can be attributed to the other detectors in the comparison because they themselves have uncertainties. A fairer judgment concerning the reproducibility between laboratories of measured results in once-distilled water would be in a calorimetric system which would require only a small amount of water sent by other laboratories.

Because such a test has not been made, a judgment concerning the reproducibility between laboratories of measurements in once-distilled water cannot be made. But even if such comparisons were close, some doubt would still exist concerning its use. Furthermore, for the 18-mGy/s dose rates which were used, an exothermic effect is contrary to what is expected on the basis of what is known of the radiolysis of pure water saturated with air or oxygen (Boyd et al., 1980). Therefore, use of a water system in which the radiolysis of water is known would at least initially appear to be a more acceptable and assuring system to use. But more importantly, the heat defect can be (or is assumed to be) zero or is known from calculations on the basis of the radiolysis of water. Such a system would circumvent comparisons with other detectors, except as an initial test to determine if the two systems are giving results which are in agreement within experimental uncertainties.

Schulz et al. (1987) described a calorimeter containing high-purity water saturated with nitrogen. Good agreement over a six-month period was obtained when compared with results determined with an ionization chamber. Ross et al. (1984, 1988) also describe such a calorimeter including saturation of the water with a 50/50 mixture of hydrogen and oxygen gases. This latter system results in a calculated negative heat defect (exothermicity) of -2.1 percent, which is supported by their experimental measurements.

The remainder of this paper is a description of recent studies and present efforts being made at NBS in constructing a simple high-purity water calorimeter.

Convection

Since simplicity of design is a desirable feature, a high-purity water calorimeter is being designed for operation at several degrees above room temperature. Operation at such temperatures raises concerns about the role of convection, particularly during horizontal irradiations (Schulz and Weinhous, 1985; Domen, 1986). The former authors have eliminated those concerns by operating the calorimeter at 4°C. The latter author suggests the use of convective barriers, when needed (Domen, 1982).

The onset of convection is determined by the Rayleigh number (Ra), (McLaughlin, 1964; Domen, 1982, 1987). It is most strongly dependent on the cube of a geometric distance. This is the parameter of most importance in the calorimeter design. The driving force of convection is temperature gradients which may create buoyant volume elements of water. Temperature gradients can arise from two causes. Large temperature gradients result from heat conduction between the calorimeter and an uncontrolled environmental temperature, and gradients can be caused by successive irradiation runs. The former can be controlled within 0.1°C by use of an enclosure placed over the calorimeter (Domen, 1982), and the latter can be largely eliminated by circulating the water.

An important practical question is: what is the maximum convective velocity which could be encountered in practice and what is its effect on a measurement? The only published calorimeter data which aid in answering this question are in reports by Schulz and Weinhous (1985) and Domen (1987, 1988a, 1988b). The former authors' figure 4(b) and figure 5 show runs when the calorimeter was operated at 30°C. The runs were made with the proximal thermistors located close to a vertical entrance wall heated by a horizontal beam. The thermistors were calculated to be directly in an upward convective stream caused by the temperature difference between the wall and adjacent water (Domen, 1987). The electrical power dissipated in the thermistors was 80 μW and there were no convection barriers near the thermistors. Their figures clearly show the existence of convection and its effects. The convective velocities were estimated from results of an investigation described below.

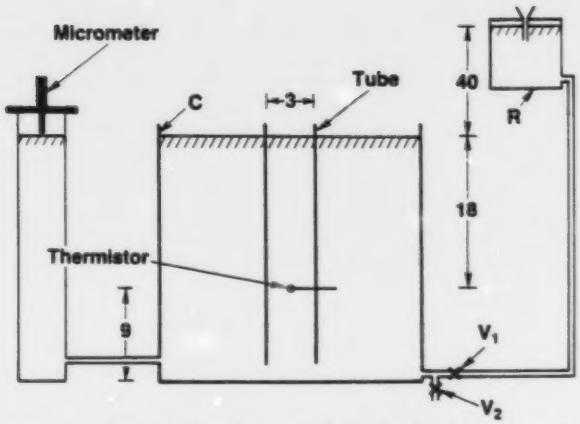

Fig. 2. Experimental setup for simulating natural convection by forced convection to study its effect on a thermistor initially at an equilibrium temperature above that of the surrounding water. The drawing is not to scale. The dimensions are in centimeters.

Figure 2 shows an experimental setup (not to scale) for investigating the effects of natural convection simulated by forced convection (Domen, 1988a). An electrically insulated calibrated thermistor (0.25 mm in diameter) was positioned on the axis of a tube. Its equilibrium temperature rise (ΔT) above the stagnant and uniform temperature water was:

$$\Delta T = 1.41P \text{ mK} \qquad (1)$$

where P = power in microwatts.

The average upward surface velocity was determined from micrometer measurements (to the water surface) made prior to and after V_1 was suddenly opened and then closed at the end of a measured time interval. It is well-known that the water velocity within the tube builds up to a parabolic distribution. Detailed theoretical calculations were made by Szymanski (1932) and are summarized in a more available reference (Bird et al., 1960). The results were used with the measured surface velocity to calculate an average axial water velocity ($\bar{A}_v$), along the tube axis, during a time interval ($t_{50\%}$) where the temperature drop in the thermistor reached 50% of its equilibrium temperature drop. A measurement was made of the average rate of temperature drop in this time interval and related to $\bar{A}_v$. A rate of temperature drop is equivalent to a "negative" absorbed dose rate ($\dot{D}^-$). The results are summarized in figure 3 for thermistor powers from 5 to 100 μW.

Application of these results is described by Domen (1988b). They were used in estimating the convective velocities which produced the effects (in the proximal thermistors) in figure 4(b) and figure 5 in the report by Schulz and Weinhous (1985). The estimated velocities (at the end of irradiation) as a result of horizontal irradiations with 25-MV x-rays and 19-MeV electrons are 3.3 mm/min and 5.7 mm/min, respectively. Therefore, even maximum convective velocities should be expected to be small. Nevertheless, the results

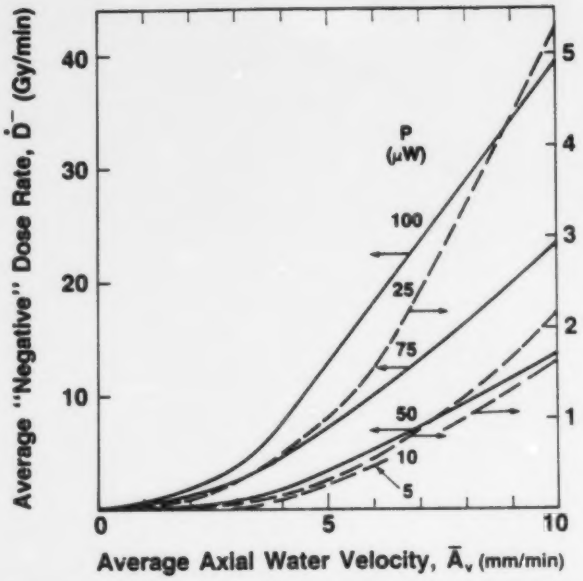

Fig. 3. Summary of the measurements of the average "negative" absorbed dose rate ($\dot{D}^-$) as a function of the average axial water velocity ($\bar{A}_v$) during the time interval of $t_{50\%}$.

shown in figure 3 indicate that velocities varying from zero to such small values and back to zero, combined with the use of high thermistor powers, can easily distort the normal shape of calorimeter runs as recorded and observed by Schulz and Weinhous (1985). The results shown in figure 3 also indicate that the effect can be reduced or eliminated by decreasing uninhibited convection (by the use of a convective barrier near the vicinity of a thermistor) and by operating the thermistor at a low electrical power. If the velocity is zero, then the background temperature of the water need not be uniform. If this is not the case, then an additional effect may be significant which could be caused by a temperature difference (in the background water temperature) leaving and entering the region of the thermistor. It was pointed out above how the background temperature gradients can be decreased, which will also decrease observed temperature drifts in a Wheatstone bridge output signal.

The internal diameter of the original Schulz-Weinhous calorimeter is about 140 mm. The calorimeter being developed at NBS is to have a glass cylindrical container, 30 mm in diameter. This convective barrier represents (under identical temperature gradient patterns) a reduction of the Rayleigh number by a factor of $(140/30)^3 \approx 100$. Its effectiveness can be tested particularly by observing the afterdrifts of absorbed-dose measurements at different thermistor powers and background temperature drifts.

The chosen 30-mm diameter is a compromise based mainly on considerations (other than convection) of conductive effects caused by the glass cylindrical wall, which is overheated during irradiation. This is discussed below.

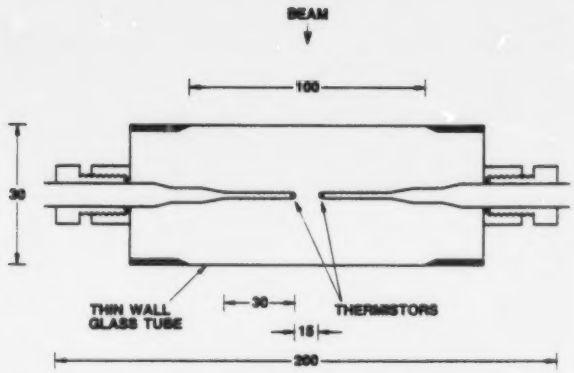

Fig. 4. Detector assembly for containing high-purity water. The dimensions are in millimeters.

The Calorimeter

Figure 4 is a drawing (not to scale) of the internal structure of the calorimeter constructed of Pyrex glass. A relatively thick-walled glass tube, 30 mm inside diameter, was drawn out to result in the thin wall shown, about 0.25-mm thick. The other dimensions shown are approximate and are in millimeters. High-purity water is enclosed in the glass tube, which is then immersed in a large volume of once-distilled water, electrically grounded. The glass tube also encloses two temperature probes, where each consists of a 0.25-mm diameter calibrated thermistor embedded as close as practical to the end of a thin glass capillary. The support sections are 7 mm in diameter and pass through soft (low density) polyethylene bushings. Initially, the glass tube is filled by first partially unscrewing the bushings. Gases (N_2 or 50/50 H_2/O_2) or water can then be made to flow between the loose machine threads. After the tube is filled, the bushings are tightened to make a vacuum-tight polyethylene-to-glass seal (the details shown at the ends of the tube are only for illustration). About 15 mm^2 of polyethylene is in contact with the pure water. Storing water overnight in the presence of polyethylene (or polymethyl methacrylate) did not affect measurements made using water saturated with O_2 or a mixture of 50/50 H_2/O_2 (Ross et al., 1984).

Not shown in figure 4 is a platinum lead fused through the glass wall, to permit electrical grounding or ungrounding of the pure water. Also not shown is a small amount of gas within the tube, to prevent fracturing of the tube if it is subject to excessive internal pressure.

Three temperature probes were constructed. They differ in the detailed embedment and enclosure of the thermistor. Figure 5 shows two preliminary types. The dimensions shown are in millimeters. The type chosen to be used in the calorimeter is discussed below and is shown in figure 9. The probe assemblies were fabricated from commercially available pipettes. The 0.32-mm inside diameter of the probe was formed by drawing the thin end of the pipette over a #28-gauge wire. The wire had been blackened over a candle flame. This prevented the glass from fusing onto the wire, so that it could be withdrawn.

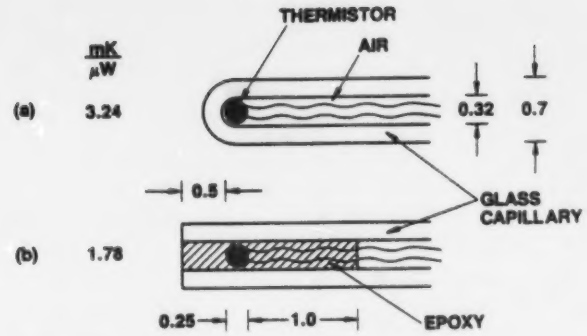

Fig. 5. Measurements of the temperature rise in a thermistor per microwatt of its electrical power dissipation, for a thermistor surrounded directly by: (a) air; (b) epoxy resin. The dimensions are in millimeters.

Figure 5(a) shows a thermistor surrounded immediately by air, which resulted in a measured value of $\Delta T = 3.24$ mK/μW with the probe immersed in water. The thermistor was then removed, and the end of the glass probe was ground off. The thermistor was then re-inserted and embedded in epoxy resin as shown in figure 5(b), which shows a measured value of $\Delta T = 1.78$ mK/μW. This lower value is an improved feature, and is attributed mainly to the higher thermal conductivity from the thermistor and its leads. Solid insulating materials have a thermal conductivity about 10 times that of air. The measured thermistor "material constant" (β) was 3249 K, when the thermistor was surrounded by the air and when it was embedded in the epoxy resin. The measured values of β and ΔT were determined from measurements of the thermistor resistance as a function of the water temperature and thermistor power (Domen, 1982).

Heat Conduction

It is assumed that the entire calorimeter is uniformly irradiated. Therefore, this section does not deal with possible measurement errors caused by conduction due to variations in axial absorbed dose rates, reported by Roos (1987) and by Nath and Rothman (1988). This section is concerned with conduction as it is related to avoiding errors caused by calorimetric materials other than high-purity water. It was convenient for the calculations to assume a zero heat defect and a relative absorbed dose rate of one for the water enclosed in the tube shown in figure 4. An exothermic effect of 3.5 percent is assumed for the once-distilled water outside the tube. Therefore, this water has a relative absorbed dose rate of 1.035. This will cause excess heat to be conducted cylindrically toward the axis where the thermistors are located. The irradiated glass will rise higher in temperature than that of the water. The amount of excess heat generated and conducted away from the glass varies as the amount of glass, which must be as small as possible. A glass wall thickness of 0.25 mm is assumed for the calculations. The properties of the glass and water and also their mass energy-absorption coefficients were taken into

consideration. The result is that a good approximation can be made by viewing the glass as being replaced with water where the relative absorbed dose rate is 2. This excess heat is conducted cylindrically toward (and away from) the axis.

A complicated situation exists at the probe ends where the thermistors are located. Approximate calculations for this situation have yet to be made (a theoretical solution could not be found). However, a simple and practical geometry was assumed which resulted in easy calculations and gave an upper limit to the effect of the probes. This was done by assuming that a thermistor is located at a point in the middle of a long solid glass rod along the axis. Therefore, there is only cylindrical flow of heat away from the glass rod. The glass rod is assumed to have a radius of 0.25 mm. A temperature probe can be constructed where the glass cross-sectional area of the capillary is approximately the same as that of the assumed rod.

Numerical calculations in this case require the calorimeter to be viewed as consisting of concentric cylindrical shells of equal thickness, inside and outside the tube. The thickness of each shell is chosen to be 0.25 mm. The numerical method is well-known and was illustrated recently by Domen (1987). The beam duration is imagined to consist of a series of pulses, where conduction takes place after each pulse. The duration of each pulse is $(0.025\ cm)^2/(2\alpha) = 0.22$ s, where $\alpha = 0.00144\ cm^2/s$ (the thermal diffusivity of the water).

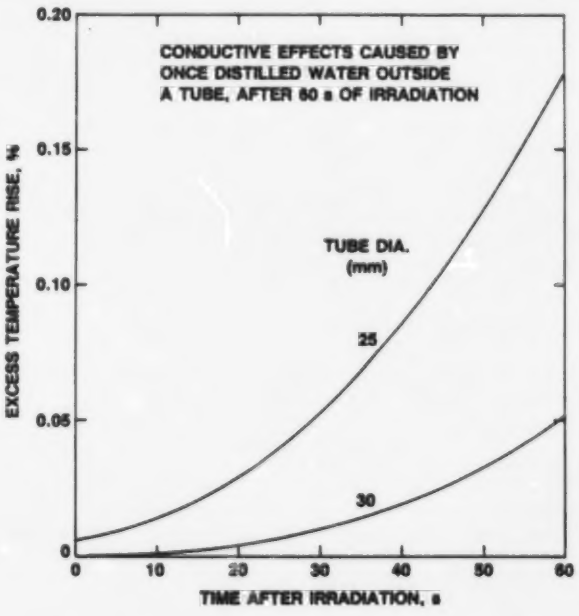

Fig. 6. Excess thermistor temperature rise caused by conduction from once-distilled water outside a tube, 25 mm and 30 mm in diameter, as a function of time after a 60 s irradiation run.

Figures 6, 7, and 8 show, respectively, the excess temperature rise (in percent), at the thermistor position along the axis, caused by the once-distilled water outside the tube, by the thin glass wall, and by a long solid glass rod, 0.25 mm radius, along the axis. The excess temperature rise is plotted as a function of time after irradiation for the indicated durations from 30 s to 60 s. Attempts should be made to limit the duration of a run within one minute, which can be easily accomplished when measuring high-dose rates available with accelerators. This would also make the measurements more accurate in cases where the radial or axial dose rates are changing rapidly.

Figures 6 and 7 show reductions to negligible effects when the tube diameter is increased from 25 mm to 30 mm. A larger tube diameter will result in disadvantages of increasing the Rayleigh number and increasing the minimum depth at which a measurement is made. A computer can be used to automatically subtract the above effects (fitted to empirical equations) from the observed calorimeter signals.

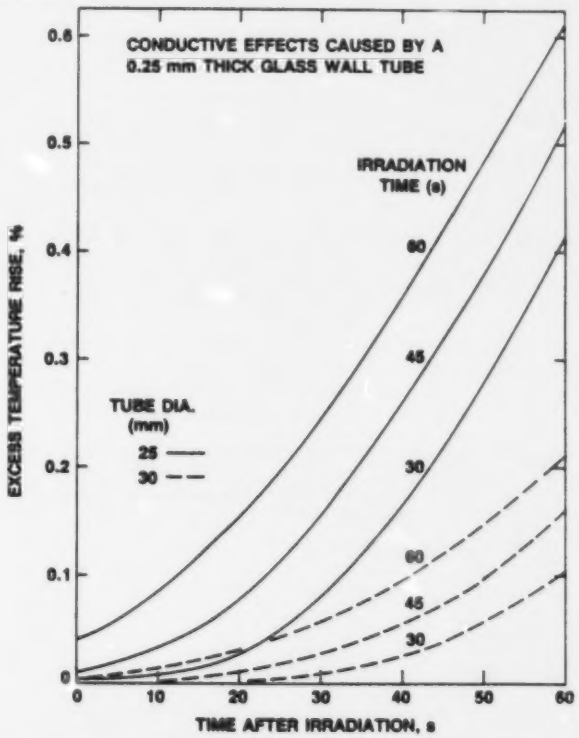

Fig. 7. Excess thermistor temperature rise caused by conduction from a 0.25-mm-thick glass wall tube, 25 mm and 30 mm in diameter, as a function of time after irradiation.

Figure 8 shows that the largest effect will be caused by the glass rod along the axis. The curves show, after irradiation, a rapid initial decrease in excess temperature. The results shown in figure 8 will be reduced by making the cross-sectional area of the glass as small as practical. Schulz et al. (1987) observed it necessary to ignore about 8 s of the initial afterdrift signal.

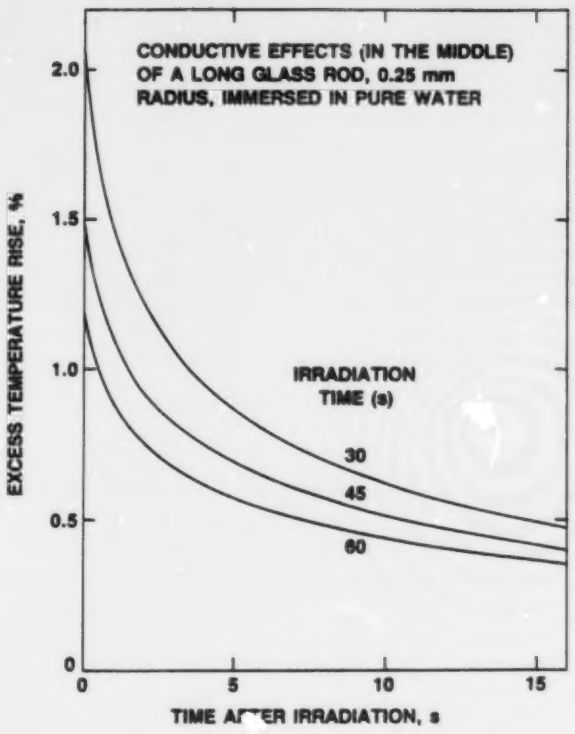

Fig. 8. Excess temperature rise (in the middle) of a long glass rod, 0.25-mm radius, immersed in pure water as a function of time after an irradiation run.

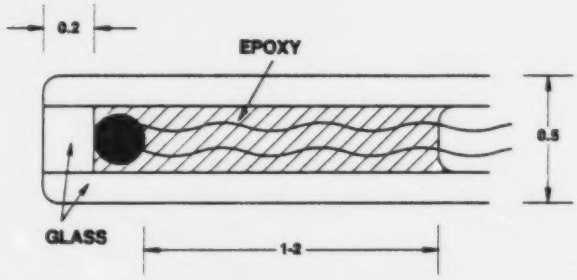

Fig. 9. Constructional details of a thermistor probe enclosed in glass. The approximate dimensions are in millimeters. This structure is intended to have a minimum excess temperature rise in the thermistor as a result of electrical power dissipation and irradiation of non-water materials.

Figure 9 shows a drawing (dimensions in millimeters) of a temperature probe in a glass capillary which has a cross-sectional area of 60% of that of the 0.25-mm-radius solid rod assumed in calculating the effects shown in figure 8. This will cause some excess heat from the epoxy region to flow toward the right, away from the thermistor. A much further reduction in excess heat is attained because the thermistor is located near the capillary end from which heat is conducted spherically, a more rapid rate of heat flow than that of the cylindrical flow from the lateral surface of the capillary. Because the end of the capillary is coolest, the thermistor should be as near to that position as practical. Figure 9 shows a thermistor 0.2 mm from the end of the probe. A glass rod was epoxied into the end of the probe and both were ground down to give that dimension. The maximum capillary diameter can be limited to approximately 0.5 mm, as shown in figure 9. The epoxy length shown (1-2 mm) is a compromise based on a possible further reduction of the value 1.78 mK/μW shown in figure 5 while only slightly increasing the excess heat generated.

Some capillaries were drawn down to outside diameters as small as 0.38 mm, wall thicknesses of about 0.03 mm, and lengths of about 40 mm. It was necessary to construct a simple fixture to prevent these fragile probes from being broken while the ends were ground to the appropriate dimension. The fixture supported the probe assembly along a vertical axis. The weight of the probe assembly was supported by the thin end of the probe, which rested on a microscope slide containing a mixture of abrasive and water. The grinding was accomplished by moving the slide.

Three test probes were immersed in water for about 6 weeks. Leakage resistances between the leads and water were in the range of 10 GΩ to 100 GΩ. The resistances appeared stable, but occasionally small changes were observed. It was calculated that this would result in a signal well within the noise level, during the duration of a calorimeter run.

Summary

A calorimeter suitable for absorbed-dose measurements in high-purity water is described. The water is enclosed within a glass tube immersed in a large volume of once-distilled water. The purpose of the design is to eliminate convection at the measurement position and also effects caused by materials other than the high-purity water.

Acknowledgment

The author is indebted to J.T. Weaver for his computer programming assistance.

References

Barnett, R.B. (1986). Water calorimetry for radiation dosimetry. Ph.D. Thesis, Faculty of Graduate Studies, Univ. of Calgary, Calgary, Alberta.

Bird, R.B., Stewart, W.E. and Lightfoot, E.N. (1960). Transport Phenomena. New York: John Wiley & Sons, p. 129.

Boyd, A.W., Carver, M.B., and Dixon, R.S. (1980). Computed and experimental product concentrations in the radiolysis of water. Radiat. Phys. Chem. 15, 177-185.

de Marles, A.E.M. (1981). Comparison of measurements of absorbed dose to water using a water calorimeter and ionization chambers for clinical radiotherapy photon and electron beams. Ph.D. Thesis, Graduate School of Biomedical Sciences, Univ. of Texas, Houston, Texas.

Domen, S.R. (1981). An improved absorbed dose water calorimeter. Med Phys. 8, 552-553.

Domen, S.R. (1982). An absorbed dose water calorimeter: Theory, design, and performance. J. Res. Nat. Bur. Stand. (U.S.) 87, 211-235.

Domen, S.R. (1986). Letter: Comment on 'Convection currents in a water calorimeter'. Phys. Med. Biol. 31, 1166-1168.

Domen, S.R. (1987). Advances in calorimetry for radiation dosimetry. Chapter 4 in The Dosimetry of Ionizing Radiation, Vol. II, K.R. Kase, B.E. Bjarngard and F.H. Attix, eds., Academic Press, Orlando, Florida.

Domen, S.R. (1988a). Convective velocity effects on a thermistor in water. J. Res. Nat. Bur. Stand. (U.S.), in press.

Domen, S.R. (1988b). Letter: Further comments on convection currents in a water calorimeter. Phys. Med. Biol., in press.

Kubo, H. (1983). Absorbed dose determinations with a water calorimeter in comparison with an ionisation chamber. Phys. Med. Biol. 28, 1391-1399.

Mattsson, O. (1984). Application of the water calorimeter, Fricke dosimeter and ionization chamber in clinical dosimetry. Ph.D. Thesis, Department of Radiation Physics, Univ. of Goteborg, Goteborg, Sweden.

McLaughlin, E. (1964). Thermal conductivity of liquids and dense gases. Chem. Rev. 64, 389-428.

Nath, R., and Rothman, A. (1988). A model of heat production and transport in a water calorimeter. Med. Phys. 15, 370-374.

Roos, M. (1987). A water calorimetric determination of absorbed dose to water. Thermochimica Acta, 119, 81-93.

Ross, C.K., Klassen, N.V. and Smith, G.D. (1984). The effect of various dissolved gases on the heat defect of water. Med. Phys. 11, 653-658.

Ross, C.K., Klassen, N.V., Shortt, K.R. and Smith, G.D. (1988). A direct comparison of water calorimetry and Fricke dosimetry. Submitted to Phys. Med. Biol.

Schulz, R.J. and Weinhous, M.S. (1985). Convection currents in a water calorimeter. Phys. Med. Biol. 30, 1093-1099.

Schulz, R.J., Wuu, C.S., and Weinhous, M.S. (1987). The direct determination of dose-to-water using a water calorimeter. Med. Phys. 14, 790-796.

Szymanski, P.P. (1932). Quelques solutions exactes des équations de l'hydrodynamique du fluide visqueux dans le cas d'un tube cylindrique. J. Math. Pures Appl., Series 9, 11, 67-107.

Discussion

Ross: I would like to encourage you to add the necessary plumbing so that you can easily change the water and saturate it with various gases.

Domen: I think my proposed arrangement is adequate to do that.

-

Domen: I would like to comment on the water I used for my measurements. I found consistent results with once-distilled water obtained from a 100-litre still. However, I noticed the still was dirty inside, so I cleaned it out. The electrical resistivity of the water increased by a factor of 8. Using water from the clean still I got the same consistent results. This result suggests that once-distilled water, no matter how it is prepared, will give the same result.

Kubo: If you feel that once-distilled water gives consistent results, perhaps those who are measuring the heat defect could measure it for your water.

Rogers: Your results may be consistent, but aren't they consistently wrong?

Domen: Water calorimetry requires consistency, and a knowledge of the corrections. If people require more than that, I don't have too much sympathy for them.

Klassen: Are you planning to use high purity water in your calorimeter?

Domen: I will try different systems.

-

Schulz: It appears that your whole design, which is very clever, is based on the requirement that you want to run at room temperature. Why not drop down to 4°C?

Domen: The system becomes more complicated; I would like to try to operate at room temperature.

-

Loevinger: What kind of water will you use?

Domen: I will look for advice from the experts.

CALORIMETRY IN 1913

D V Cormack
Tom Baker Cancer Centre, Calgary, Alberta, Canada

Calorimetry was one of the methods for measuring x-rays considered by Theophil Christen and discussed briefly in a monograph which appeared in 1913. This method was however, not thought to be useful in an x-ray laboratory because of the difficulty in detecting the extremely small temperature differences involved.

La calorimétrie est une des méthodes de mesure des rayons X que Theophil Christen a considérée et décrite brièvement dans une monographie parue en 1913. Cette méthode n'a toutefois pas été jugée utile dans un laboratoire des rayons X parce qu'il était trop difficile de déceler les écarts de températures extrêment faibles en jeu.

Many of the concepts and terms which we use today in describing ionizing radiations were developed in the first few years following Roentgen's discovery of x-rays in 1895. For several of these ideas we are indebted to Theophil Christen, a Swiss physician, scientist and mathematician. Christen's major contributions are reported in a 122-page monograph in German (Christen, 1913) and summarized in a paper in English (Christen, 1914). He introduced and defined half-value layer (Trout, 1962), tissue-equivalent materials (White, 1978) and dose (Greening, 1981).

In the monograph noted above, Christen considered several methods for measuring x-rays including phosphorescence, fluorescence, "radioelectrical" methods (including ionization in gases), chemical effects and heat. His short section on heat is reproduced in Fig. 1. He notes that, in principle, the measurement of heat offers an excellent indirect way of determining forms of energy that are not measurable directly since all forms of energy are efficiently transformed into random molecular motion, i.e. there is little or no "heat defect".

e) Wärme.

Auf den meisten Gebieten ist diejenige indirekte Energiemessung die beste, bei welcher die nicht direkt meßbare Energieform in Wärme umgewandelt wird. Dies hat seinen Grund darin, daß hierbei in der Regel die Forderung der Restlosigkeit am besten gewahrt bleibt, d. h. der Nutzeffekt ist meist bei der Transformation in Wärme am größten, wenn nicht geradezu gleich Eins. Es geht ja überhaupt am Ende aller Dinge jede Energie in Wärme, d. h. in ungeordnete Molekularbewegung über.

Für die Röntgenenergie trifft dies aber nicht zu. Es ist im Gegenteil bei allen bisherigen Versuchen die Ausbeute an Wärmeenergie so gering gewesen, daß man sich lange darum gestritten hat, ob sie überhaupt nachweisbar sei. Dorn, Rutherford und Clung haben die durch Absorption von Röntgenstrahlen erzeugte Wärme gemessen. Leininger hat ein negatives Resultat erhalten. Angerer hat die Resultate Dorns wieder bestätigt.

Begreiflicherweise sind die auf solchen subtilen Messungen beruhenden Methoden im Röntgenlaboratorium nicht verwendbar.

Figure 1
Excerpt from page 62 of Reference 1

With x-ray energy, however, the experimental evidence available in 1913 indicated that the heat produced by the action of x-rays was barely detectable. Dorn, Rutherford, Clung and Angerer had reported measurements of a heating effect whereas Lehninger had obtained a negative result.

In view of the uncertainty as to whether the heat produced was detectable at all Christen concluded that energy determinations based on such subtle measurements were not applicable in an x-ray laboratory. The present workshop provides us with an excellent opportunity to test Christen's hypothesis.

Figure 2
Dr. med. et phil. Theophil Christen

REFERENCES

1. Christen, Th. 1913. MESSUNG UND DOSIERUNG DER ROENTGENSTRAHLUNG. Lucas Graefe & Sillem, Hamburg.

2. Christen, Th. 1914. RADIOMETRY. Archives of the Roentgen Ray. Vol. 19, pp. 210-218

3. Greening, J.R. 1981. FUNDAMENTALS OF RADIATION DOSIMETRY. Adam Hilger, Bristol.

4, Trout, E. Dale. 1962. Private communication

5. White, D.R. 1978. TISSUE SUBSTITUTES IN EXPERIMENTAL RADIATION PHYSICS. Medical Physics Vol. 5, pp. 467-479.

Discussion

Ross: The extract indicates that some people saw an effect and some didn't. Did you look at any of those references?

Cormack: No, no, no! Christen published a paper in English in 1914 in the Archives of the Roentgen Ray, the predecessor of the British Journal of Radiology. This paper is quite readable. I have tried to read Bragg's 1912 paper on cavity theory, and didn't know he was talking about the same subject.

THE RADIATION CHEMISTRY OF WATER AT HIGH LET

N.V. Klassen and C.K. Ross
Division of Physics, National Research Council of Canada, M-35, Ottawa, Canada, K1A 0R6

The radiation chemistry of dilute aqueous solutions is examined for low, intermediate, and high LET. Calculated values for the dose required to achieve a stationary state with pure water and the heat defect predicted for air-saturated water are given. The predicted values are compared to water calorimetry measurements using neutron irradiation.

La chimie des radiations de solutions aqueuses diluées est examinée au transfert linéaire d'énergie (LET) à des niveaux faible, intermédiaire et élevé. Les valeurs calculées de la dose requise pour réaliser un état stationnaire avec de l'eau pure et le déficit thermique prévu pour l'eau saturée d'air sont donnés. Les valeurs prévues sont comparées aux valeurs obtenues au calorimètre à eau par irradiation neutronique.

INTRODUCTION

Most of the work on water calorimetry has been with low LET (0.2 eV/nm) radiation. However, the technique can be applied to higher LETs and Galloway, Greening and Williams (1986) and Williams, Galloway and Greening (1987) used a water calorimeter to measure neutron dose rates. Water calorimetry can only be useful if the heat defect of the system is known and a knowledge of the heat defect of the system depends on a knowledge of the radiation chemistry. Two existing publications apply radiation chemistry to the heat defect of water and various aqueous solutions subjected to low LET radiation (Ross, Klassen and Smith, 1984; Fletcher, 1982). The subject is also dealt with in our earlier presentation at this Workshop. What is lacking is the application of radiation chemistry to the whole range of LET, from very low to very high. This is done briefly in this presentation. In order to present some useful numbers, we present the predictions of simulations using the same dose rate (2.6×10^{16} eV L^{-1} s^{-1}) used by Williams, Galloway and Greening (1987) in their water calorimeter determination of the absorbed dose in neutron beams.

LOW LET

The passage of ionizing radiation through a medium deposits energy in discrete amounts in discrete volumes. The deposited energy produces chemical species in these volumes. These regions of highly concentrated reactive species are called spurs for 6-100 eV events, blobs for 100-500 eV events, and short tracks for 500-5000 eV events. The proportion of spurs, blobs and short tracks depends on the LET of the radiation, and the chemistry which ensues depends on these proportions, but the dependence is not strong at low LET. For example, the mean LET in water for 2 MeV electrons is lower than that of Co-60 (ICRU Report 16, 1970), but there is little difference in the chemistry produced by these radiations. This is because, in going from low LET to yet lower LET, the main effect is to space the spurs further and further apart. At 1 mM concentrations of solute there is a reasonably clear separation between spur reactions and reactions which take place in the bulk solution, and the latter predominate over interspur reactions. Hence, the effect of spacing the spurs yet further apart has little effect on the chemistry.

We have simulated the radiolysis of pure water and air-saturated water using model I (Boyd, Carver and Dixon, 1980) and model II (based on the recent compilation of Buxton et al., 1988) at a dose rate of 2.6×10^{16} eV L^{-1} s^{-1}. The same G-values for the yields after spur reactions was used for models I and II ($G(e^-_{aq}) = 2.7$, $G(H^+) = 2.8$, $G(OH^-) = 0.1$, $G(H) = 0.55$, $G(H_2) = 0.45$, $G(OH) = 2.75$ and $G(H_2O_2) = 0.7$). Using model I, the time to reach a stationary state was 13 min. and the H_2O_2 concentration at stationary state was 0.04 μM. Using model II, it took 5.6 hrs. to reach a stationary state and the H_2O_2 concentration was 0.2 μM. The stationary state is the result of a delicate balance between the production of stable products and the back-reactions destroying them and the time to arrive at the stationary state is very sensitive to the model. For air-saturated water, at an accumulated dose of 20 Gy, both model I and II predict 1.8% endothermicity.

INTERMEDIATE LET

The radiation chemistry for higher LET radiation can be simulated using the same model as used for low LET radiation. However, the G-values needed as input are less well known at high LET. As the LET is increased, more chemistry takes place in spur (and inter-spur) reactions, thus reducing the chemistry in the bulk solution. This makes the measured heat defect less sensitive to impurities in the solution.

Using a water calorimeter to measure the dose to water from a d(16) + Be neutron beam, Galloway, Greening and Williams (1986) measured an endothermicity of 4% on the basis of the dose measured by an ion chamber. Using a p(62) + Be neutron beam (Williams, Galloway and Greening, 1987), the result was 2% endothermicity. For a 14.6 MeV neutron, about 70% of the dose is deposited at an LET $\leq$ 50 eV/nm and the mean LET decreases as the neutron energy is increased (ICRU Report 16,

1970). We estimated the yields after spur reactions from reports by Burns and Sims (1981) and Burns, May, Buxton and Wilkinson-Tough (1981) for an LET of 30 eV/nm. The estimated values are $G(e^-_{aq}) = 0.5$, $G(H^+) = 0.5$, $G(OH^-) = 0.0$, $G(OH) = 1.2$, $G(H_2) = 0.8$, $G(H_2O_2) = 0.9$ and $G(H) = 0.9$. Both models required about 70 hours of irradiation to reach a stationary state with a H_2O_2 concentration at stationary state of 6 μM predicted by model I and 10 μM predicted by model II. The rate of change of product concentrations decreases as the stationary state is approached and, at about 6 hours, model I predicts an endothermicity of 0.6% while model II predicts 0.8%. Two other comments are in order about these long irradiation times. When the time to achieve a stationary state is very long, the diffusion of gaseous products out of the water may actually preclude a stationary state from being reached. If the solution is not irradiated uniformly, the diffusion of products from the region of higher dose rate into the region of lower dose rate may also make a stationary state impossible to achieve.

Simulations were also done for air-saturated water. At an accumulated dose of 20 Gy, both models I and II predict an endothermicity of 2.9%, i.e., a value intermediate between the two measurements with neutrons (Galloway, Greening and Williams, 1986; Williams, Galloway and Greening, 1987)

HIGH LET

At high LET (300 eV/nm and higher), such as found for heavier charged particles and at the Bragg peak of alpha particles, most radicals react in the spur. One additional difference is that some reactions may occur at very high LET which do not occur at low LET. For example, small, but measureable yields of O_2 and HO_2 escape the spur at high LET (Burns, May and Baverstock, 1981) whereas, at low LET, they are not produced in the spur. One explanation given for this is that, in the spur at very high LET, the concentration of radicals is so high that presolvated electrons react with H_2O^+ (i.e. recombination) to produce H_2O^*. Then $2H_2O^* \rightarrow 2H_2 + O_2$, followed by $H + O_2 \rightarrow HO_2$.

In the LET range of 200-300 ev/nm, G(OH) is reported to be about 0.3 (LaVerne, 1988; Burns and Sims, 1981). Combining this value with values for other species (Appleby and Schwarz, 1969), and choosing $G(e^-_{aq})$ and $G(H^+)$ to get a material balance, we used $G(H_2) = 1.1$, $G(H) = 0.3$, $G(H_2O_2) = 1.1$, $G(HO_2) = 0.07$, $G(e^-_{aq}) = 0.2$ and $G(H^+) = 0.2$ for our simulations. Both models I and II failed to reach a stationary state by 11 days of irradiation. For air-saturated water after 20 Gy of accumulated dose, both models predict 4.3% endothermicity.

At very high LET, only H_2, O_2, HO_2 and H_2O_2 exist after the spur reactions. For our input at very high LET, we selected $G(H_2) = 1.4$, $G(H_2O_2) = 1.0$ and $G(HO_2) = 0.3$ (see Burns and Sims, 1980) with small adjustments for a material balance. Using pure water, a stationary state is unattainable. With air-saturated water, the endothermicity after 20 Gy was predicted by both models to be 5.2%. This can be considered the limiting case for the practical purposes of water calorimetry.

REFERENCES

Appleby, A. and Schwarz, H.A., *J. Phys. Chem.*, 73, 1937 (1969).

Boyd, A.W., Carver, M.B. and Dixon, R.S., *Radiat. Phys. Chem.*, 15, 177 (1980).

Burns, W.G., May, R. and Baverstock, K.F., *Rad. Res.*, 86, 1 (1981).

Burns, W.G., May, R., Buxton, G.V. and Wilkinson-Tough, G.S., *J. Chem. Soc., Faraday Trans. I*, 77, 1543 (1981).

Burns, W.G. and Sims, H.E., *J. Chem. Soc., Faraday Trans. I*, 77, 2803 (1981).

Buxton, G.V., Greenstock, C.L., Helman, W.P. and Ross, A.B., Radiation Chemistry Data Center, Radiation Laboratory, University of Notre Dame, 1988.

Galloway, G., Greening, J.R. and Williams, J.R., *Phys. Med. Biol.*, 31, 397 (1986).

Fletcher, J.W., Atomic Energy of Canada Ltd. Document No. AECL7834 (1982).

ICRU Report 16, (1970), International Commission on Radiation Units and Measurements, 7910 Woodmont Ave., Washington, D.C.

LaVerne, J.A., Abstract Em-6, 36th Annual Meeting of the Radiation Research Society, Philadelphia, April, 1988.

Ross, C.K., Klassen, N.V. and Smith, G.D. *Med. Phys.*, 11, 653 (1984).

Williams, J.R., Galloway, G. and Greening, J.R., *Phys. Med. Biol.*, 32, 403 (1987).

Discussion

Rogers: What is the LET for x-rays?

Klassen: I can't tell you offhand. I've dealt with neutrons since they fit into the range of intermediate LETs.

Cormack: I don't think LET has much meaning for x-rays. The spurs are isolated, and so the LET should be thought of as being low.

CONCEPTS TO IMPROVE WATER CALORIMETER SENSITIVITY AND ACCURACY

J.W. Fletcher, Atomic Energy of Canada Limited
Chalk River Nuclear Laboratories, Chalk River, Ontario, Canada, K0J 1J0

ABSTRACT - Impurities can affect the accuracy of the water calorimeter. Additives could be used to not only improve the accuracy but also the sensitivity of the calorimeter. A one-hundred fold increase in sensitivity has been obtained by catalytically (Cu^{2+}) initiating the chain decomposition of hydrogen peroxide.

La présence d'impuretés peut nuire à la précision du calorimètre à eau. Des additifs pourraient permettre non seulement d'améliorer la précision, mais aussi la sensibilité de l'appareil. Une sensibilité centuplée a été obtenue en déclenchant catalytiquement (Cu^{2+}) la décomposition en chaîne du peroxyde d'hydrogène.

In water calorimetry a non-linear temperature rise is normally observed during the initial irradiation period. The non-linearity is due to the presence and subsequent removal of impurities and the establishment of steady-state[1] concentrations of radiolytic products (H_2, H_2O_2, O_2).

Pre-irradiation techniques have proven to be most effective in improving water quality. Hydrogen saturation could also reduce impurity effects and lead to steady-state conditions at a lower dose.

The addition of hydrogen peroxide leads to an increase in sensitivity due to exothermic decomposition (reaction [1]) by a chain removal step (reactions [2], [3]). The

[1] $2H_2O_2 \longrightarrow O_2 + 2H_2O$
[2] $OH + H_2O_2 \longrightarrow HO_2 + H_2O$
[3] $HO_2(O_2^-) + H_2O_2 \longrightarrow OH + O_2 + H_2O$

experimentally measured chain decomposition rates of hydrogen peroxide in hydrogen saturated aqueous solutions are less than predicted from computer simulation. This is presumably due to impurities which could reduce the chain length which is very impurity sensitive due to the slowness of reaction [3].

Transition metals such as copper can be used to increase the rate of the chain step (reactions [4], [5]) and thus reduce impurity effects. To

[4] $O_2^- + Cu^{2+} \longrightarrow Cu^+ + O_2$
[5] $Cu^+ + H_2O_2 \longrightarrow OH + Cu^{2+} + OH^-$

be suitable as a radiation sensitive system the lower valence state (Cu^+) must not be stable and thus lead to continued decomposition in the absence of radiation. Initial experiments indicate that the decomposition of hydrogen peroxide is quite small (approx. 10^{-7} $mol.L^{-1}.s^{-1}$) in the absence of radiation.

A G value of approximately 10,000 has been observed for a solution containing 8×10^{-2} $mol.L^{-1}$ hydrogen peroxide and 10^{-3} $mol.L^{-1}$ copper ion irradiated at a dose rate of 4×10^{16} $eV.L^{-1}.s^{-1}$.

REFERENCE

[1] Fletcher, J.W. (1982). Radiation Chemistry of Water at Low Dose Rates - Emphasis on the Energy Balance: A Computer Study, Chalk River Nuclear Laboratories, AECL-7834.

Discussion

Ross: I believe in one of your progress reports you indicated a possible sensitivity enhancement of about 1000. How stable, how reproducible, would you expect this system to be?

Fletcher: A factor of 100 is certainly possible. I think the copper system should be quite stable, but not the peroxide system. One wants to add something that you know is going to remove the reactive species so that the system can be simulated. This is the advantage of the H_2/O_2 or formate systems.

Rogers: Do you think the enhancement can be calculated well enough to allow the system to be used as a primary standard?

Fletcher: No, I would think it would be more useful as a secondary standard. However, I would think that the system should be reproducible and not affected by impurities. It may be somewhat dependent on dose rate or accumulated dose.

WATER CALORIMETRY IN MEDIUM ENERGY X-RAY BEAMS

J. Seuntjens, H. Thierens, A. Poffyn and O. Segaert
Standard Dosimetry Laboratory, Faculty of Medicine, Ghent State University,
Proeftuinstraat 86, B-9000 Ghent, Belgium

The values of the absorbed dose to water obtained with a water calorimeter are compared with the results deduced from in-phantom ionization chamber measurements for medium energy X-rays. The water calorimeter results are 11.6%, 11.0%, 10.8% and 9.7% higher than the ionization chamber results for 150 kV (HVL:0.59 mm Cu), 200 kV (HVL:1.14 mm Cu), 250 kV (HVL:2.05 mm Cu) and 350 kV (HVL:3.97 mm Cu) respectively.

Les valeurs de la dose absorbée par l'eau obtenues au moyen d'un calorimètre à eau, sont comparées aux résultats déduits des mesures effectuées par chambre d'ionisation dans un fantôme, pour une exposition à des rayons X d'énergie moyenne. Les résultats du calorimètre à eau sont 11,6 %, 11,0 %, 10,8 % et 9,7 % plus élevés que ceux de la chambre d'ionisation pour des tensions de 150 kV (HVL: 0,59 mm Cu), 200 kV (HVL: 1,14 mm Cu), 250 kV (HVL: 2,05 mm Cu) et 350 kV (HVL: 3,97 mm Cu) respectivement, où HVL s'entend de la couche de demi-atténuation.

1. INTRODUCTION

The determination of absorbed dose to water for medium energy X-rays is generally based on the working procedure proposed by the ICRU report 23 (ICRU, 1973). The absorbed dose D due to X-rays with energy above 150 keV at reference depth in a reference field can be determined from an "in-phantom" exposure measurement with an "in-air" calibrated ionization chamber by the formula (ICRU, 1973) :

$$D = R\, k_1\, k_2\, N\, F \qquad (1)$$

where R represents the chamber reading at the specified point, k_1 the correction factor for difference in temperature and pressure at the time of measurement and calibration. The factor k_2 accounts for a correction of the exposure calibration factor N at a specified radiation quality due to differences between the ionization chamber response in the radiation field used for calibration and that at the reference depth in water-phantom. The conversion coefficient F relates the exposure at the ionization chamber position to the absorbed dose to the undisturbed waterphantom with the chamber removed. This conversion factor incorporates a "displacement correction" necessary to account for the change of the radiation field due to the displacement of the water volume by the chamber. According to the report the magnitude of the displacement effect is negligible.

The results of dose measurements using the outlined working procedure were compared with the water calorimetric determination of the quantity by Kubo (Kubo, 1985) and Mattsson (Mattsson,1985). Kubo performed measurements at a depth of 5 cm in water with a field of 20 x 20 cm^2 at three medium energy X-ray qualities. The calorimeter results were 7 to 9 % higher than the ionization chamber results at a tube potential of 280 kV with HVL 1.7 0.625 and 0.5 mm Cu respectively. Mattsson made the same experiments for 100 keV (HVL:3.9 mm Al) and 200 kV (HVL:1.2 mm Cu) X-ray beams, but for a field size of 17.5 x 17.5 cm^2 and at depths of 2 cm and 3 cm respectively. His calorimeter results were also higher by respectively 7.6 % and 5.6 %.

Based on Monte-Carlo calculations of photon fluence spectra at different depths and fieldsizes Cunningham (Cunningham et al, 1986) suggests that the discrepancies between the results of mentioned authors can be attributed to differences in mass energy absorption coefficient ratios for different in fieldsizes and depths.

The international protocol for the determination of absorbed dose in photon and electron beams (IAEA, 1987) proposes the same working procedure as the ICRU (ICRU, 1973) for medium energy X-rays. Here the correction for the displacement effect is specified explicitly as a perturbation correction factor p_u. The value of this factor is greater than unity and varies from 1.10 to 1.01 in the HVL range 0.17 to 3.37 mm Cu. Using these perturbation factors a better agreement is obtained between water calorimeter and ionization chamber results. The results of a new formalism for absorbed dose determination for medium energy X-rays based on a single ^{60}Co calibration as proposed by Mijnheer (Mijnheer and Chin, 1988) support the results adopted in the IAEA protocol.

On the other hand Kristensen (Kristensen et al, 1988) compared a dose measurement with a Farmer type chamber using the ICRU formalism with LiF and alanine detectors. His investigation did not confirm the numerical value of the stated perturbation factors. In a previous paper (Seuntjens et al, 1988), present authors evaluated the air kerma-dose to water conversion factor, quality correction factor and perturbation correction factor as a function of HVL and tube potential for medium energy X-rays. The resulting perturbation correction factors are also found to be less than 1 %.

The aim of present work is the comparison of the results of previous work, extented to larger field sizes, with the water calorimetric determi-

nation of absorbed dose to water at a depth of 5 cm.

2. EXPERIMENTAL SET-UP

a. Irradiation equipment

All measurements were made using a constant potential Philips MG 420 system coupled to a MCN 421 tube with inherent filtration of 2.2 mm Be. A removable monitor with a filter holder is mounted at the exit window of the tube for normalization of the measurements. The stability and response of the monitor are investigated prior to the measurements. The source-detector distance is 40 cm corresponding to a field size of 14 x 14 cm^2 at the point of measurement. The water calorimeter and the phantom are irradiated horizontally. The measuring depth was set to 5 cm water equivalent in both cases taking into account the density of the PMMA windows. Further measuring conditions and the characteristics of the radiation qualities used are summarized in table 1.

b. Water calorimeter

A schematic diagram of the water calorimeter is shown in figure 1. The water phantom has 5 mm thick PVC walls and a 8 mm thick PMMA front window. A second window allowing alignment is provided in the rear wall of the phantom. The wall is thermally isolated by glass wool and the lid is of styrofoam. During the measurement the front window is covered with a 4 cm thick styrofoam plate. The phantom wall and water can be warmed up by a teflon insulated resistance wire (not shown). A magnetic stirring system is provided for homogenisation. At the time of measurement the phantom was filled with doubly distilled water. The water temperature is recorded to a resolution of 0.01K by means of a calibrated PT100 platina probe.

The detector system used is slightly different from the system developped by Domen (Domen, 1982). For use in horizontal photon beams the detector system is mounted to a rail above the water tank. Two PMMA spacer rods guarantee a constant distance from the front window. The detector contains only one thermistor (Le Carbone, type LC2) which is calibrated in the same setup prior to the measurements.

The thermistor is connected to a one arm AC bridge as shown in figure 2. The amplitude of the positive oscillator (f = 73 Hz) may be adjusted continuously with stable precision potentiometers from 0 to 1 V effective. The thermistor power depends on the bridge setting but amounts typically to 25 µW. The mean temperature rise above the water temperature due to the electrical dissipation is measured in a temperature range 16°C, 28°C to be 1.30 mK/µW. For stability purpose the lock-in amplifier contains a phase sensitive network with the same architecture and electronic components as the oscillator. The offset drift for short time periods is negligible and the amplifier input noise amounts to 100 nV peak to peak. The output of the demodulator is coupled to a chart recorder and a digital voltmeter which is connected to a PC for signal analysis. For each set of measurements at a given offset voltage the bridge response is calibrated using a 5 Ω precision resistor.

The absorbed dose to water (assuming no chemical defect) is calculated using the equation (Domen, 1980) :

$$D_w(Gy) = c_w \frac{\Delta R}{R} S^{-1} \qquad (2)$$

where

$\frac{\Delta R}{R}$ the fractional change in thermistor resistance which is derived from extrapolation of the fore- and afterdrift to mid run. For this purpose fore- and afterdrift are fitted with least square fits;

S the measured sensitivity of the thermistor (in K^{-1}) and

c_w the specific heat capacity of water (in $Jkg^{-1} K^{-1}$) at the operating temperature.

c. Ionization chamber dosimetry

The ionization chamber used in present work is the 0.6 cm^3 Farmer NE 2571 graphite walled cylindrical chamber. In a previous paper (Seuntjens et al, 1988) the response of this chamber in comparison to free air ionization chambers for an extensive set of X-ray qualities was investigated.

The water phantom for the ionization chamber measurements is made of PMMA and has the same dimensions as the water calorimeter. For the measurements in water the chamber is insulated in a PMMA holder with a wall thickness of 0.5 mm. The measuring depth is set to 5 cm water equivalent. The same styrofoam plate as used in the calorimeter measurements is used here. The standard deviation on the ionization chamber measurements is indicated in table 3.

The ionization chamber reading is converted to absorbed dose to water using the equation (IAEA, 1987) :

$$D_w = M_u N_K k_u (\bar{\mu}_{en}/\rho)_{w,air} P_u \qquad (3)$$

In this formula N_K represents the air kerma calibration factor for an arbitrary quality. In this case we used calibration factors of the primary quality at which the measurements are carried out. They are also summarized in table 1.

The factor $(\bar{\mu}_{en}/\rho)_{w,air}$ is the air kerma - absorbed dose to water conversion factor at the given depth for the given field size and defined as :

$$\left(\frac{\bar{\mu}_{en}}{\rho}\right)_{w,air} = \frac{\int_0^{E_{max}} (\mu_{en}/\rho)_{water} (d\Phi_E/dE)\, EdE}{\int_0^{E_{max}} (\mu_{en}/\rho)_{air} (d\Phi_E/dE)\, EdE} \qquad (4)$$

where $d\phi_s/dE$ represents the photon fluence spectrum at the depth and field size of interest due to a primary X-ray beam with end-point energy E_{max}. The spectra $d\phi_s/dE$ for the qualities used in this study are obtained by Monte-Carlo calculation starting from measured primary photon fluence spectra. The resulting conversion factor $(\bar{\mu}_{en}/\rho)_{w,air}$ is then obtained using formula 4 and the mass-energy absorption coefficients of Hubbell (Hubbell, 1982). Table 2 contains values for field sizes 100 cm^2, 200 cm^2 and 400 cm^2 at a depth of 5 cm. The differences between results for different fieldsizes at the same quality are limited to 1 %.

The quality correction factor k_u takes into account differences in the response between the radiation quality of the users beam in free air and at the reference depth in the water phantom. The response of the chamber was studied in detail in a previous paper (Seuntjens et al, 1988). It was seen that the response of the ionization chamber could be adequately described by HVL in mm Cu. The quality correction arising from the modification of the primary spectral distribution by 5 cm water was deduced from the HVL change. The results of this calculation for different field sizes are also presented in table 2.

The perturbation correction factor p_u accounts for the effect of the water volume displaced by the chamber. In a previous paper (Seuntjens et al 1988) the perturbation correction factor is calculated as a weigthed sum of perturbation factors from mono-energetic photon beams. This factor, in turn, was obtained from an extrapolation procedure of air-kerma calculations for different chamber sizes to zero radius. Table 2 shows that p_u does not exceed 1 % for the qualities of interest.

3. RESULTS AND DISCUSSION

Two problems were encountered in making measurements using a water calorimeter with medium energy X-ray beams.

The first problem is the relatively low dose rate at distances which are achievable for calorimetry. In our case the dose rate amounted approximately to 0.5, 0.8, 0.9 and 1.5 Gy/min for the 150 keV, 200 keV, 250 keV and 350 keV beams respectively at a distance of 40 cm (200 cm^2 field size). Further reduction of the distance was impossible due to the large cooling drifts (Mattsson, 1985).

A second problem is the direct effect (figure 3) of medium energy X-rays on the thermistor bead. An onset of the X-ray beam causes a sudden increase in calorimeter response while a sudden decrease at the end of the irradiation is observed. Tests showed that a collimated pencil beam aligned just besides the thermistor bead does not cause such effect. Tests with the calorimeter in a ^{60}Co beam showed also that the effect is typical for medium energy X-rays. The effect is probably a warm-up of the thermistor bead above the water temperature due to the thermal insulation by the poly-ethylene films. The self heating persists as long as the calorimeter is irradiated but disappears as the beam is turned off. For the composition of our thermistor it was calculated that :

$$\left(\frac{\overline{\mu_{en}}}{\rho}\right)_{thermistor,water} = 4.6,$$

the ratio of the mean energy absorption coefficients of the thermistor and water, at medium energy X-rays (250 kV; HVL : 2.05 mm Cu) while for ^{60}Co this quantity equals 0.87. The energy absorbed in the thermistor bead and appearing as heat is a factor of 5 higher for medium energy X-rays than for ^{60}Co. Measurements with low tube potential and small filtration show a larger relative "jump" than measurements with high tube potential and large filtration. Principally, the jumps do not affect the absorbed dose determination although they may influence the extrapolation procedure and therefore the standard deviation of a set of measurements.

Table 3 summarizes the results of the absorbed dose determination with the water calorimeter and the ionization chamber using the conversion and correction factors given in table 2 (field size 200 cm^2) together with the ratio calorimeter-ionization chamber. The water calorimeter gives 11.6 % $\pm$ 5.3 %, 11.0 % $\pm$ 2.9 %, 10.8 % $\pm$ 2.9 % and 9.7 % $\pm$ 1.8 % higher absorbed dose values than the ionization chamber for the 150 kV (HVL:0.59 mm Cu), 200 kV (HVL: 1.14 mm Cu), 250 kV (HVL:2.05 mm Cu) and 350 kV (HVL: 3.97 mm Cu) beams respectively.

4. CONCLUSIONS

The aim of the present work was a comparison of the absorbed dose determination by a water calorimeter with the results obtained with an ionization chamber using reevaluated conversion and correction factors for medium energy X-rays.

Our study shows that the water calorimeter results are systematically 10 % higher than the ionization chamber values. The observed discrepancy between both methods for medium energy X-rays is also observed by other authors (Mattsson, 1985; Kubo, 1985) although not as large as in our work. Furthermore our study shows that an unsatisfactory knowledge of the correction and conversion factors involved in ionization chamber dosimetry is not responsible for the observed difference.

The influence of self heating of the thermistor during irradiation by medium energy X-rays on the determination of the absorbed dose remains to be investigated further.

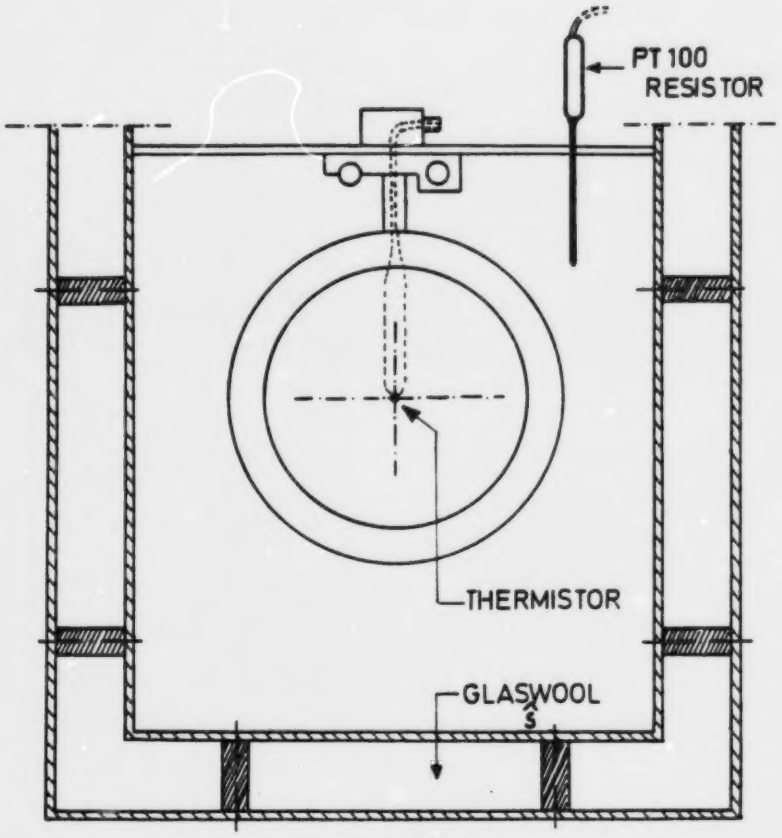

Figure 1: Schematic diagram of the water calorimeter.

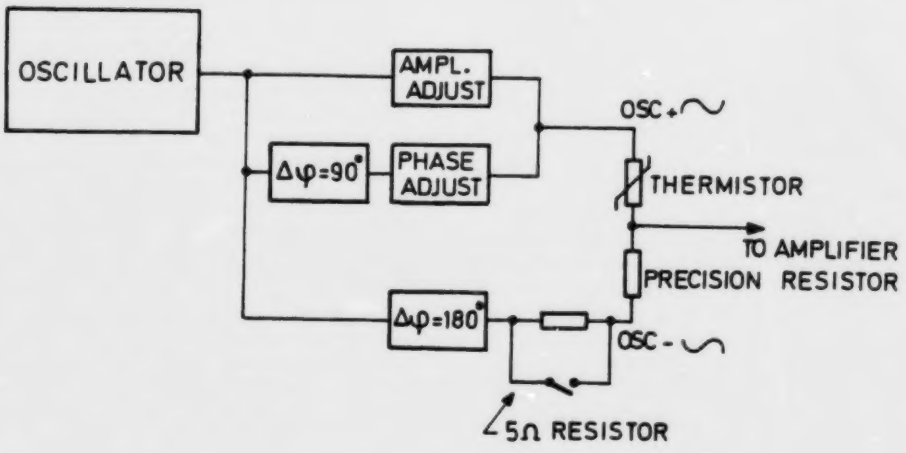

Figure 2: Electronic circuit diagram.

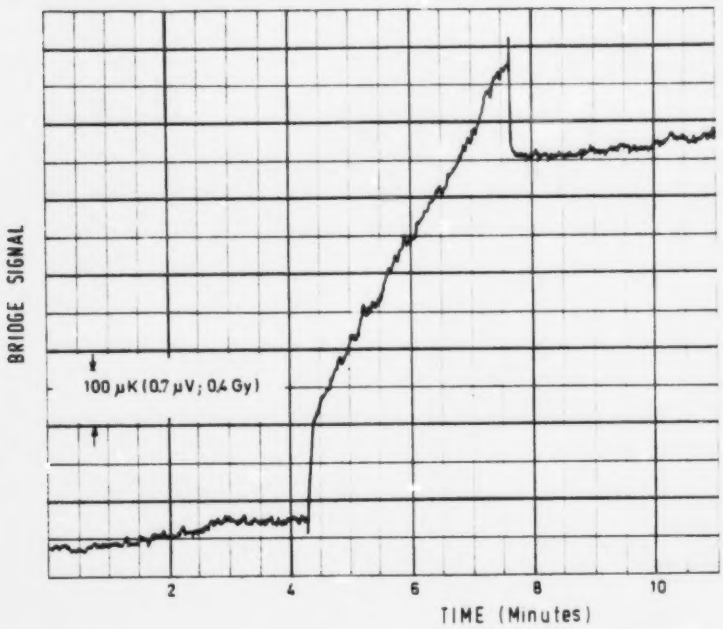

Figure 3: Typical calorimeter run for 250 kV (HVL: 2.05 mm Cu; dose-rate 0.8 Gy/min).

Table 1: Radiation qualities and measuring conditions.

kV_p (kV)	added filtration (mm)	HVL (mm)	air kerma calibration factor N_K (Gy/reading)	tube current (mA)	irr. time (s)
150	1.02 Al + 0.30 Cu	0.59 Cu	0.951	6	200
200	1.02 Al + 0.53 Cu	1.14 Cu	0.957	7	200
250	1.02 Al + 1.11 Cu	2.05 Cu	0.952	8	200
350	1.02 Al + 2.89 Cu	3.93 Cu	0.954	12	100

Table 2: Results of calculated conversion and correction factors for the determination of absorbed dose to water from "in phantom" measurements.

Radiation quality (kV_p HVL mm)	field size 100 cm^2			200 cm^2		400 cm^2	
	$(\bar{\mu}_{en}/\rho)_{w,air}$	k_u	p_u	$(\bar{\mu}_{en}/\rho)_{w,air}$	k_u	$(\bar{\mu}_{en}/\rho)_{w,air}$	k_u
150kV (0.59 Cu)	1.058	0.9958	1.008	1.049	0.9954	1.047	0.9948
200kV (1.14 Cu)	1.069	0.9969	1.006	1.066	0.9960	1.064	0.9954
250kV (2.05 Cu)	1.082	0.9987	1.004	1.079	0.9982	1.077	0.9976
350kV (3.93 Cu)	1.100	0.9997	1.001	1.097	0.9995	1.095	0.9996

Table 3: Results of the comparison ionization chamber - water calorimeter.

Radiation quality kV_p/ HVL(mm)	water calorimeter (Gy/monitor unit) x 10^{-5}		ionization chamber (Gy/monitor unit) x 10^{-5}		ratio (calo./ ion.)	σ(%)
	D_w/M	σ(%)	D_w/M	σ(%)		
150 kV 0.59 Cu	2.771	5.3	2.482	0.1	1.116	5.3
200 kV 1.14 Cu	9.167	2.9	8.255	0.1	1.110	2.9
250 kV 2.05 Cu	8.806	2.9	7.951	0.2	1.108	2.9
350 kV 3.93 Cu	8.262	1.8	7.513	0.4	1.097	1.8

5. REFERENCES

1. Cunninham J.R., Woo M., Rogers D.W.O. and Bielajew A.F. 1986. THE DEPENDENCE OF MASS ENERGY ABSORPTION COEFFICIENT RATIOS ON BEAM SIZE AND DEPTH IN A PHANTOM. Med. Phys. 13 (1986), 496.

2. Domen S.R. 1980. ABSORBED DOSE WATER CALORIMETER. Med. Phys. 7 (1980), 157.

3. Domen S.R. 1982. AN ABSORBED DOSE WATER CALORIMETER : THEORY, DESIGN AND PERFORMANCE. Journal of Research of the NBS 87 (1982), 211.

4. Hubbell J.H. 1982. PHOTON MASS ATTENUATION AND ENERGY-ABSORPTION COEFFICIENTS FROM 1 keV TO 20 MeV. Int. J. Appl. Radiat. Isot. 33, 1269.

5. IAEA 1987. ABSORBED DOSE DETERMINATION IN PHOTON AND ELECTRON BEAMS, An International Code of Practice. International Atomic Energy Agency, Vienna, 1987, report 277.

6. ICRU 1973. MEASUREMENT OF ABSORBED DOSE IN A PHANTOM IRRADIATED BY A SINGLE BEAM OF X OR GAMMA RAYS, Report 23 (ICRU Publications, P.O.Box 30185, Washington, D.C.20014, USA)

7. Kristensen M., Hjortenberg P., Hansen J.W. and Wille M. DETERMINATION OF IONIZATION CHAMBER KERMA CORRECTION FACTORS FOR MEASUREMENT IN MEDIA EXPOSED TO ORTHOVOLTAGE X-RAYS 1988, Dosimetry in Radiotherapy (Proc. Symp. Vienna, 1987), IAEA, Vienna (1988) 149.

8. Kubo H. 1985. WATER CALORIMETRIC DETERMINATION OF ABSORBED DOSE BY 280 kV_p ORTHOVOLTAGE X-RAYS. Radioth. Oncol. 4, 275.

9. Mattsson O. 1985. COMPARISON OF WATER CALORIMETRY AND IONIZATION CHAMBER DOSIMETRY IN 100 AND 200 kV X-RAY BEAMS. Report CCEMRI (I) 185-15, Offilib, Paris.

10. Mijnheer B.J. and Chin L.M. 1988. DOSIMETRY OF ORTHOVOLTAGE X-RAY BEAMS. Dosimetry in Radiotherapy (Proc. Symp. Vienna, 1987), IAEA, Vienna (1988) 129.

11. Seuntjens J., Thierens H., Van der Plaetsen A. and Segaert O. 1988. DETERMINATION OF ABSORBED DOSE TO WATER WITH IONIZATION CHAMBERS CALIBRATED IN FREE AIR FOR MEDIUM ENERGY X-RAYS (in press Phys. Med. Biol. 1988).

Discussion

Kubo: How big is your thermistor?

Seutjens: 0.5 mm in diameter.

Kubo: I wonder if Mattsson has seen a similar anomaly in the thermistor response to what you see?

Mattsson: I did not. What I saw was just a spike, not a shift.

Shortt: Did you see the effect for ^{60}Co?

Seuntjens: No, not at all.

Schulz: It is not a grounding problem. We also saw a similar effect in x-ray beams.

Rogers: If it is a question of beam absorption in the thermistor, why doesn't everyone see the same effect?

Mattsson: It may depend on how much mass you have around the thermistor.

Seuntjens: I was able to model the heat transfer problem, and by using the appropriate ratio of mass energy absorption coefficients I would predict the response I observe.

Schulz: Was the run you showed typical? I would have difficulty extrapolating the rating periods to mid-run.

Seuntjens: The thermal stabilization was not as good as we would have liked.

Mattsson: You had very little thermal insulation around the calorimeter; on the front you had none.

Seuntjens: The measurements were made with a shroud of 4 cm of Styrofoam.

BRIEF REPORT ON THE NEW NPL CALIBRATION SERVICE IN ABSORBED DOSE TO WATER FOR HIGH-ENERGY X- AND GAMMA-RADIATION

D T Burns, J E Burns & B Owen
National Physical Laboratory
Teddington, Middlesex, UK

1. INTRODUCTION

At present, the determination of absorbed dose to water for high-energy radiotherapy is based on measurements in a water phantom using an ionisation chamber whose calibration is traceable to a primary standard of air kerma, and the application of conversion factors contained in codes of practice.

To improve the calibration accuracy NPL are launching a new dosemeter calibration service (Burns *et al* 1988) whose main features are:

(i) the primary standard is a graphite microcalorimeter similar in design to that of Domen (1974),

(ii) calibrations are in ^{60}Co and high-energy X-ray beams typical of those used in radiotherapy,

(iii) secondary standard dosemeters are calibrated in absorbed dose to water, with the chamber in a water phantom.

The possession of a linear accelerator capable of precision radiation metrology (with seven standard energies between 4 and 19 MV) enables secondary standards to be calibrated in the same energy beam as the primary standard. This approach reduces the calibration uncertainty as compared with present procedures.

Two methods were chosen for the conversion from D_c to D_w, one based on the photon-fluence scaling theorem (Pruitt & Loevinger 1982) and the other using cavity ionisation theory. The method used at NBS for ^{60}Co – a thick graphite-walled chamber – is not applicable to high-energy X-radiation.

2. PHOTON-FLUENCE SCALING THEOREM

If two phantoms of different materials are placed successively in the same photon beam such that their dimensions, their distances from the source, the field sizes and the depths of measurement are all scaled in the inverse ratio of the electron densities of the two materials, then the photon-fluence scaling theorem states that the photon spectra at the scaled depths will be identical.

The photon energy fluence Ψ_m at a depth d_m in medium m is given by

$$\Psi_m = \Psi_{(m)} \exp(-\mu_m d_m) S_m(d_m, A_m)$$

where $\Psi_{(m)}$ is the fluence at the same point in space in the absence of the phantom, $\exp(-\mu_m d_m)$ is the narrow-beam attenuation, and $S_m(d_m, A_m)$ is the scatter factor for field size A_m. When the scaling theorem applies, it follows that, for water w and graphite c phantoms,

$$\frac{\exp(-\mu_w d_w)}{\exp(-\mu_c d_c)} = 1 \quad \text{and} \quad \frac{S_w(d_w, A_w)}{S_c(d_c, A_c)} = 1$$

so that, when the inverse square law applies in air,

$$\frac{\Psi_w}{\Psi_c} = \frac{\Psi_{(w)}}{\Psi_{(c)}} = \left(\frac{f_c}{f_w}\right)^2$$

where f is the distance from the source to the point of measurement. Expressing the absorbed dose to material m as

$$D_m = \Psi_m (\mu_{en}/\rho)_m \beta_m$$

where $(\mu_{en}/\rho)_m$ is the mass energy absorption coefficient and β_m is the ratio of absorbed dose to collision kerma, then

$$\frac{D_w}{D_c} = \left(\frac{f_c}{f_w}\right)^2 \frac{(\mu_{en}/\rho)_w}{(\mu_{en}/\rho)_c} \frac{\beta_w}{\beta_c}$$

The inverse square law factor is obtained from measurements in air and the method was checked by carrying out measurements at different pairs of distances. Monte Carlo calculations of the linac X-ray spectra combined with the published mass attenuation coefficients of Hubbell (1977) yield excellent agreement with the attenuations as measured at NPL; this gives confidence in the calculation of the linac spectra and in the mass energy absorption coefficients which have been used for the above formula. The ratio

β_w/β_c is calculated from data published by Attix (1979).

The theory assumes photon interactions by Compton scattering only, and corrections are applied for the effect of pair production. Collimator scatter is negligible for the NPL linac X-ray beam.

The ratio of calibration factors for a chamber calibrated by this method is then given by

$$\frac{N_w}{N_c} = \frac{D_w/Q_w}{D_c/Q_c} = \frac{D_w}{D_c}\frac{Q_c}{Q_w}$$

where Q_c/Q_w is the ratio of responses of the chamber when placed at the points of measurement in the two phantoms at which the ratio of absorbed doses D_w/D_c was determined.

3. CAVITY IONISATION THEORY

The ratio of calibration factors can also be calculated from cavity ionisation theory using

$$\frac{N_w}{N_c} = \frac{K_c}{K_w}\frac{p_w}{p_c}\frac{(\mu_{en}/\rho)_w}{(\mu_{en}/\rho)_c}\frac{\beta_w}{\beta_c}$$

where K_c/K_w is the ratio of the ionisation currents per unit photon energy fluence at the centre of the chamber, and p_w/p_c is the ratio of the perturbation of the photon fluence caused by the displacement of the medium by the chamber.

If photon beams at the depths of measurement in graphite and water phantoms have the same spectra, a simplified formula can be derived for a graphite-walled chamber which is fitted with a Perspex sheath when used in water:

$$\left(\frac{K_c}{K_w}\right)^{-1} = \alpha_{wall} + \alpha_{sheath}\frac{(\mu_{en}/\rho)_{Perspex}}{(\mu_{en}/\rho)_c}\frac{(L/\rho)_c}{(L/\rho)_{Perspex}}$$

$$+ \alpha_w\frac{(\mu_{en}/\rho)_w}{(\mu_{en}/\rho)_c}\frac{(L/\rho)_c}{(L/\rho)_w}$$

where α is the proportion of secondary electrons entering the chamber cavity that arise from photon interactions in the material indicated by the subscript, and (L/ρ) is the restricted mass stopping power for the secondary electrons (Andreo & Nahum 1985).

Values for the ratio p_w/p_c and for the partition coefficient α can be derived from data given in the TG21 protocol (AAPM 1983).

4. SUMMARY

Agreement between the two conversion methods is excellent (typically 0.2 %). The uncertainty in the scaling theorem method is thought to be less than that using cavity ionisation theory. The first calibration period is scheduled for autumn 1988.

NPL would be interested in comparing transfer standard chambers with those calibrated by any other laboratories having a water calorimeter which is considered to be of primary standard status.

5. REFERENCES

AAPM 1983, Med Phys **10**, p 741

P Andreo & A E Nahum 1985, Phys Med Biol **30**, p 1055

F H Attix 1979, Health Physics **36**, p 347

J E Burns *et al* 1988, *New Calibration Service for High Energy X-Radiation at NPL*, IAEA-SM-298/56 in Proceedings of the International Symposium on Dosimetry in Radiotherapy Volume 2, organised by IAEA/WHO Vienna, Austria, 31 Aug – 4 Sep 1987 (International Atomic Energy Agency, Vienna)

S R Domen & P J Lamperti 1974, J Res Nat Bur Std 78A **5**, p 595

J H Hubbell 1977, Radiation Research **70**, p 58

J S Pruitt & R Loevinger 1982, Med Phys **9**, p 176

DISCUSSION

Mattsson: What type of ionization chamber was used for these measurements?

Burns: It was the 2561.

Mattsson: With an aluminum central electrode?

Burns: As far as I know.

Ross: Some years ago, there was a proposal from NPL to establish a standard using an ionization chamber with high density walls. Why was this approach dropped?

Burns: It was not. The tungsten ionization chamber was used to help establish the standard; I think, in checking the photon fluence scaling theorem.

CONSTRUCTION OF A PROTOTYPE HIGH SENSITIVITY PULSED CALORIMETER

[illegible], Department of Radiation Oncology
University of [illegible] Cancer Center, Rochester, New York 14642

ABSTRACT - A prototype [illegible] was constructed and operated in a Co-60 beam. A basic idea of [illegible] calorimeter is to provide higher excitation voltage to the calorimeter detector to increase bridge output voltage, while containing the self-[illegible] of the thermistor temperature sensor to a reasonably low value. In this report, [illegible] our prototype pulsed calorimeter and future [illegible] results are presented.

Un prototype de calorimètre à [illegible] a été [illegible] et mis en faisceau de Co-60. L'objet premier d'un calorimètre à [illegible] d'excitation plus élevée en [illegible] du calorimètre à une tension raisonnable l'auto-échauffement d'un [illegible] présentons des évaluations de [illegible] à impulsions et traitons d'éventuels facteurs de perfectionnement [illegible]

INTRODUCTION

A water calorimeter has proved to be the most promising device in determining the absolute absorbed dose in radiation beams and has actively been pursued by national calibration laboratories in recent years. A water calorimeter has two major advantages over an ion chamber: 1) The dose to water, reference medium recommended by many international protocols[1-3], can be directly measured; and 2) One major unknown parameter, the heat defect of water, is reported to be resolved[4,5]. This is in contrast to the ion chamber method which requires many correction factors to arrive at the dose to water.

One of the problems associated with the calorimeter is the very low voltage signals generated by a two-thermistor Wheatstone bridge (see Fig. 1). One obvious solution to increase the sensitivity is to raise the bridge excitation voltage (0.2 volts were used in our previous work[6,7]) so that the bridge output voltage rises proportionately. Unfortunately, the higher excitation voltage causes higher self-heating in thermistors, which lowers the thermistor resistance. This decreased resistance has to be separated from the resistance decrease induced by radiation and be corrected. This procedure could add an additional uncertainty against the spirit of simplicity presented by a calorimeter and should be avoided.

Our approach to increase the sensitivity of the Wheatstone bridge detector is to add the pulse excitation technique to our current direct voltage measurement technique on-line with a computer. The on-line computer method permits digital data processing to manipulate the calorimeter data to enhance the sensitivity and also to provide the absorbed dose instantaneously and was reported elsewhere[8,9]. The idea of pulse excitation technique is to keep the amount of self-heating in the detector to be minimum while trying to achieve higher sensitivity. In the following, we will describe in detail our approach to implement pulsing technique to a calorimeter.

METHODS

Electronics

The objective of the present method is to excite a Wheatstone bridge detector for a short period of time during which, the bridge output signal will be read by a 12 bit I/O board+ and stored in the computer++. If necesary, the stored data can be analyzed and the absorbed dose determined directly between the calorimeter measurements. This idea is schematically shown in Fig. 1 and the measurement can proceed as the following. At an interval of one second, a pulse generator simultaneously produces, a bridge input voltage V_{BI} and an external conversion command (EXT CC in the figure). The bridge output voltage V_{BO} is given by the equation 1 as the following:

$$V_{BO} = V_{BI} \left(\frac{T_A}{T_A + R_A}\right) - \left(\frac{R_B}{T_B + R_B}\right) \qquad (1)$$

where T_A and T_B are the values of thermistor resistance and R_A and R_B are the balancing resistors on the Wheatstone bridge and are temperature-independent.

The amplitude and width (W_{BO}) of the bridge input voltage V_{BI} are adjustable. However, the amplitude of 3-5 volts and width 10-100 msec were used in this study. Higher input voltages, thereby higher output voltage signals, will also be implemented and examined very soon.

The falling edge of the EXT CC signal (Fig. 2) is used to initiate successive approximation conversion on the bridge output voltage signal. The width of the EXT CC signal W_{EX} was typically

---

+ RTI 800 I/O Board, Analog Devices, Norwood, MA. 02062

++ PS/2 Model 30, IBM, Boca Raton, FL 33429

selected to be 1 msec, short enough to start conversions at the beginning of bridge output voltage. The number of and the intervals between conversions per one conversion signal are adjustable, depending mainly on the width of the bridge output W_{BO}. In this study, the interval between conversions was set at 1 msec. Therefore, for a 100 msec wide bridge output signal, the I/O board will perform about 100 conversions and waits for the next conversion signal to arrive. The converted digital signals were stored in a computer memory. A Fortran software was developed to add and average the specified number of digital signals, typically 10-20 signals near the falling edge of the bridge signals. The average value was permanently stored in the computer and recorded on the diskette for further data manipulation.

RESULTS AND DISCUSSION

1. Self-heating

The heat P generated in each thermistor of the detector can be calculated by a product of the thermistor resistance T, the square of current I that flows through the thermistor and a fraction of time f that the excitation voltage is on, or $P = T \cdot I^2 \cdot f$. For a Wheatstone bridge of approximately equal resistance among resistors and thermistors (which is indeed the most common case), the current I is approximately equal to $V_{BI}/(2T)$. Therefore, for excitation voltage of 5 volts, 50 msec pulse duration, 1 second repetition, and the bridge resistance of 4,000 ohms, the generated heat in each thermistor is approximately 80 microwatts. This is in contrast to 1600 microwatts of heat which would otherwise be generated by a DC excitation method. The merit of using the pulse excitation is that the bridge output is now 25 times larger (5 volts vs. 0.2 volts input voltage, though the power consumptions are 80 microwatts vs. 2.5 micro watts).

According to Domen[10], 300 μW of heat lowered the resistance value of a thermistor from approximately 2900 ohms to 2810 ohms (or 3% change) whereas 80 μwatts of heat lowered the resistance from 2900 to 2870 ohms (or approximately 1% change). No data exists for heat greater than 300 μW. A relationship between the thermistor power and thermistor resistance value of the pulse calorimeter will be established in the near future. Another possibility to minimize the self-heat corrections is to use a thermistor of higher resistances.

2. Calorimeter Signals

The calorimeter signals obtained in a Co-60 beam using the prototype setup (Fig. 1) are shown in Fig. 3. This data was the result of 4 minute irradiation of the polystyrene detector and shows considerable data scatter, almost $\pm$ 20 μV over one minute period. This large data scatter was observed only when the I/O board was operated on external conversion command mode and was not observed on a continuous read mode. This observation led us to believe that the noise was created in the I/O board. Incidentally, we are looking into alternative boards to minimize the data scatter.

3. Further Considerations

Future considerations for this promising pulsed calorimeter will include improvements in:

1) I/O board performance, in particular, to minimize the noise associated with the external trigger mode. Another alternative is look for other I/O boards. There are several I/O boards available on the market. The specs of several 16 bit resolution boards are reported to have much smaller noise levels.

2) Pulse generator performance - A possible source of noise other than that by the I/O board may be a pulse generator. At this point, the pulse generator noise may be masked by large noises generated by the I/O board and is hard to estimate. As seen in eq. (1), the output voltage is directly proportional to the input voltage. Any noise (or fluctuations) on the input voltage will propagate and could add to the measurement uncertainties. To improve this portion of the performance, two options are available; one is to use a battery instead of a pulse generator. The pulse generator will be used only to switch on and off the battery power supply. In this way, the bridge excitation voltage is pulsed and is stable to the extent of the stability of battery. Another option is to read bridge output and input voltages simultaneously and store the ratios. The ratio will absorb fluctuations of the input voltage. This second option can be useful for both pulse generator and battery operations. The implementation of these improvements is already underway and will be reported in the near future.

SUMMARY

A calorimeter based on pulsing technique was successively operated. Of several problems that were identified with our prototype model, the noise generated by the I/O board was considered to be the major one. The observed noise level $\pm$ 20 μV was too high to deduce accurate absorbed dose, even though this level of noise was within the specs of the I/O board. In the near future, a new board with a much smaller noise level will be installed together with an implementation of voltage ratio technique to minimize the effects on the output voltage fluctuation caused by the input voltage fluctions.

REFERENCES

1. Nordic Association of Clinical Physics (NACP), Acta. Rad. Oncol. 19, 55(1980); also Supplement, Acta. Rad. Oncol. 20, 401(1981).

2. ICRU Report 35, Bethesda, MD. (1984).

3. Task Group 21 of American Association of Physicists in Medicine. Med. Phys. 10,741 (1983).

4. J.W. Fletcher, Report No. AECL-7834 (Atomic Energy of Canada Ltd.), Chalk River, Canada, 1982.

5. J.R. Schulz, C.S. Wuu and M. Weinhous, Med. Phys. 14,790 (1987).

6. H. Kubo, Phys. Med. Biol. 28,1391 (1983).

7. H. Kubo, Phys. Med. Biol. 31,251 (1986).

8. H. Kubo and D.E. Brown, Phys. Med. Biol., 29,885 (1984).

9. H. Kubo and D. Mento, Phys. Med. Biol., 29, 1436 (1984).

10. S.R. Domen, J. Res. Nat. Bur. Stand. 87,211 (1982).

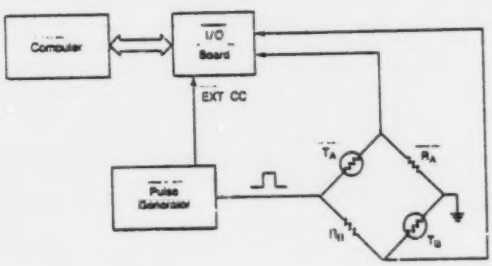

Fig. 1

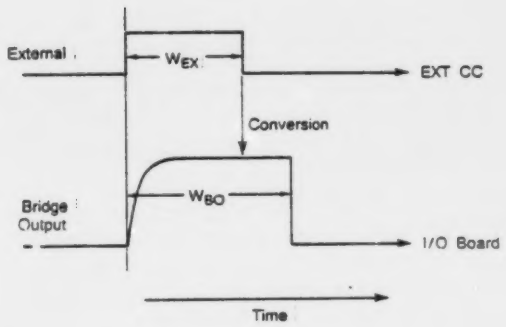

Fig. 2

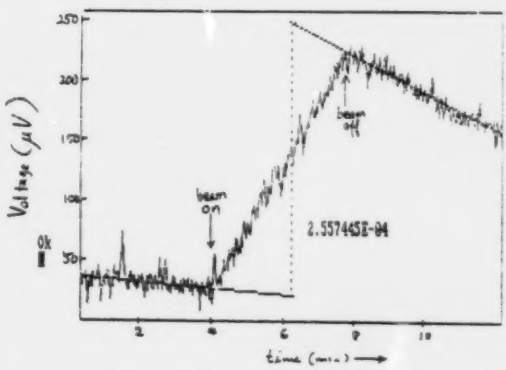

Fig. 3

Acknowledgement

This investigation was supported by PHS Grant No. R01-CA44054 awarded by the National Cancer Institute, DHHS.

Discussion

Shortt: What dose rate were you using?

Kubo: I think it was about 300 rads per minute, but I haven't calculated it yet.

-

Schulz: It seemed to be cooling off very rapidly.

Kubo: This is a polystyrene detector.

-

Ross: What is the stability on the pulse generator?

Kubo: Right now we are using a battery. I think it is better than 1/10 of 1%.

Ross: So this is a linear gate that opens and not a digital to analog converter?

-

Klassen: The power per pulse does not show the variation you see in your measured results.

Kubo: I didn't measure power. These are just the calculations.

MEASUREMENT OF THE THERMAL DEFECT OF WATER EXPOSED TO PROTONS IN THE RANGE 0.9-40 MEV[a]

R. J. Schulz and N. Venkataramanan
Department of Therapeutic Radiology
Yale University, New Haven, CT 06510

ABSTRACT - This paper describes apparatus which is under development for the measurement of the thermal defect of water and tissue-equivalent liquids exposed to protons in the range 0.9-40 MeV.

La présente communication décrit un appareil prototype pour mesurer le déficit thermique d'eau et de liquides équivalents à des tissus pendant leur exposition à des protons de 0,9 à 40 MeV.

INTRODUCTION

The experimental determination of the thermal defect of water exposed to x-ray and electron beams is complicated by the dual requirements of a) measuring the absolute temperature change of the irradiated water and b) by a combination of measurements and calculations, to determine the fraction of incident energy absorbed by the water. Using a variety of experimental strategies, Hohlfeld et al (1) are actively engaged in a project to determine the thermal defect of water exposed to low linear-energy transfer (LET) radiations. Recognizing that the thermal defect may be LET dependent but also that any and all data relating to this phenomenon are likely to be of value to the development of the absorbed-dose water calorimeter, the present authors have undertaken to measure the thermal defect of water and tissue-equivalent liquids (TEL) exposed to protons in the range 0.9-40 MeV. The advantages of protons over x-rays and electrons for thermal defect measurements are that they are completely absorbed in thin layers of test materials, they produce essentially no bremsstrahlung, they are not backscattered, and delta rays that may be scattered out from the absorber are readily returned by relatively weak electric fields. Another distinct advantage is gained by using the experimental technique described by Fleming and Glass (2) in which relative temperature changes are recorded in an absorber consisting of both the test and reference materials. The absorber, described below, has copper as a reference material (assumed zero thermal defect) on one side, and water behind a thin Mylar film on the other side. As these two materials contribute to a common heat capacity, only relative temperature change measurements need be made thus obviating the problems associated with absolute temperature measurements.

METHODS AND MATERIALS

The heart of the thermal-defect calorimeter is the absorber or core shown in figure 1. To obtain rapid temperature equilibrium, the core is made mainly of copper. A Mylar window will be chosen such that 1 MeV protons lose less than 20% of their energy in it before reaching the water. So as to facilitate heat transfer from the water to the copper, and thus to the thermistors, the thickness of the water behind the Mylar is 1.0 mm (thus limiting this particular core to protons of less than 9 MeV). Water, whose gas content is controlled, is passed into and out from the core through small-guage copper tubing. After about 15 minutes of flushing to remove contaminants, the core is sealed by crimping the tubes with a conventional wire cutter whose blades were purposely made dull. (To subsequently open the core, the copper tubing is cut through with a fine-toothed saw. This procedure may be repeated four or five times before new tubes must be soldered into place.) Three thermistors, imbedded in threaded, copper rods, are mounted near the periphery of the core. Two of these are connected to opposite arms of a Wheatstone Bridge, and the third is used as a heater for bench testing of the apparatus. The electrical charge carried into the core by the proton beam is brought to an electrometer by a signal lead attached to one of the studs holding the Mylar window in place.

The core is supported within the vacuum container, shown in figure 2, by a Delrin ring. So as to minimize heat transfer, this ring is machined to make contact with the core at only three points. The ring, in turn, is supported by Delrin rods, one of which exits the vacuum container through a rotating seal. Not shown in figure 2 is a stepping motor which rotates the core through 180° on command from the control area of the accelerator. The core is surrounded by a copper shield which may be alternately grounded, connected to a -300V bias battery, or

connected to an electrometer. Coaxial with a window in the shield and the center of the core is an aluminum disk with a 3 mm aperature. The charge collected from this disk is compared with the charge collected from the core so as to provide assurance that the proton beam is centered. All electrical leads are brought out of the vacuum container through two feed-thrus located at the dashed-line ellipses shown in figure 2. The vacuum container is coupled directly to a beam line from the accelerator. Preliminary, bench-top experiments clearly demonstrated that temperature regulation of the vacuum container is necessary for stable, consistent operation. To achieve this, electrical heater wire, commonly used to prevent pipes from freezing, was wrapped around the container, and a silicon-diode temperature sensor imbedded into the backplate. These are connected to a Lakeshore Cryogenics temperature controller which is set to 303.0 K. To further assure temperature stability, the vacuum container is supported inside of a 9.5-inch ID aluminum tube by Delrin disks, and all remaining air space filled with Styrofoam packing chips.

As an aid to beam centering, and to permit the uninterupted operation of the accelerator during a series of experiments, a beam-centering/proton-valve assembly is mounted prior to the vacuum container on the beam line. This device, which has proven to be essential to our experiments, is shown in figure 3. When the valve is closed, the proton beam may impinge upon one of the four pie-shaped brass electrodes or the small, circular electrode at the center. Generally, the beam hits only one of the electrodes, and its signal drives one of five LED bar graphs located at the accelerator control console. The accelerator operator steers the beam until it impinges upon the 2-mm diameter central electrode which lights up the central bar graph. To irradiate the core, the valve is turned 90° upon command from the control area, and the proton beam passes through the hole that runs side-to-side in the Delrin cyclinder which supports the centering electrodes.

Instrumentation for the thermal-defect calorimeter, in addition to the temperature regulator, motor controls and beam-centering bar graphs, includes a Wheatstone bridge whose degree of unbalance is measured by either a Keithley 180 or 181 nanovoltmeter, a Keithley 617 electrometer with an external capicitor for extended-range charge measurements, and a Keithley 610 electrometer for measuring the proton current collected from the aluminum aperature. The Keithley 180 nanovoltmeter has a standard analogue output which is used to drive a strip-chart recorder. The Keithley 181 stability of the core, and the general operational status of the equipment. As described below, acquisition and analysis of experimental data are carried out by the Compaq computer.

Computerized data acquisition and analysis are done with software called Labtech Notebook (3); file management is provided by Lotus 1,2,3 (4). The Keithley 181 is monitored at the rate of 20 times per minute for about two minutes prior to and for two minutes after irradiation which lasts about 30 seconds. Data points are displayed on the computer terminal in the form of a graph of signal (mV) versus time. At the end of a run, these data are transferred to Lotus 1,2,3 where the experimenter selects the beginning and ending of the rating and irradiation periods thus establishing three files. These files are then transferred back to Labtech Notebook where each is fitted by a first-order polynomial, intercepts established, extrapolations made to the irradiation midpoint, and the bridge unbalance (mV) calculated. A comparison of five runs made with the strip-chart recorder and five runs made with the computer demonstrated a 0.9% standard deviation for the bridge unbalances obtained from the recorder compared with a 0.6% standard deviation for those from the computer.

Utilizing the potential drops measured at four locations in the Wheatstone bridge and the bridge unbalance determined by Labtech Notebook, a supplementary program will calculate the thermistor resistance and power levels, the change is thermistor resistance caused by irradiation, and the temperature change of the core.

Protons in the range 0.9-1.0 MeV are obtained from a Van de Graaff generator located in the Sloan Physics Laboratory. This machine, which is used mainly for undergraduate and graduate student experiments, includes an energy-analysing magnet, focusing coils, and a switching magnet for diverting the beam to any one of three beam lines. Beam energy is maintained within $\pm$ 2 keV.

Protons, and heavier charged particles, in the range of 2-40 MeV/nucleon are currently available from a tandem Van de Graaff accelerator located at the Wright Nuclear Structure Laboratory. Within the year a 4 MeV Van de Graaff will also be brought into operation which will greatly alleviate scheduling problems that exist on the tandem machine.

RESULTS

At this writing, only preliminary testing of the thermal defect apparatus has been done using charge collected by the core and the unbalance of the Wheatstone bridge caused by the temperature change (0.6% standard deviation for five runs). The physical parameters pertinent to these runs were: 20 nanaspares beam current; 0.900 MeV beam energy; 20 seconds irradiation time. This testing also demonstrated the necessity of the beam-centering/proton-valve assembly which, in addition to beam centering, allows a series of irradiation to be carried out without interrupting the operation of the accelerator.

DISCUSSION

At present, our efforts are directed principally toward the mounting and testing of thin (5-10 micron) Mylar windows which can separate water from vacuum. These windows will absorb between 10% and 20% of the energy of 1 MeV protons, and will be used for our first thermal defect measurements using the 1 MeV Van de Graaff. The problem of window thickness will become less severe when we move our experiment to the tandem Van de Graaff, however, as access time to this machine is severely limited, we want to have a good deal of experience, and a great deal of confidence in our equipment, before using its higher-energy protons.

Following our studies on the thermal defect of water, we do similar studies on tissue-equivalent liquids. The goal of these experiments is the development of a TEL calorimeter for neutron and heavy-charged-particle dosimetry.

REFERENCES

[a]This work supported by Grant No. CA38563 awarded by the National Cancer Institute.

1. Hohlfeld, K. Kramer, H.M., Roos, M. and Selbach, H. J., Two Experimental Methods for Determining the Heat Defect of Water, IAEA-SM-298/29 (1987).

2. Fleming, D.M. and Glass, W.A., Rad. Res., 37, 316-322 (1969).

3. Labtech Notebook, Laboratory Technologies Corporation, Wilmington, MA (1986).

4. Baras, Edward M., The Advanced Guide to Lotus 1,2,3, (1987).

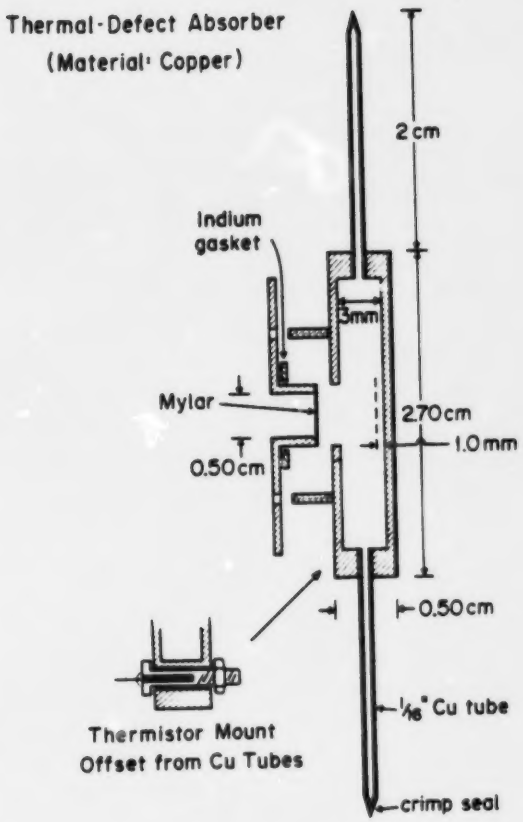

Figure 1

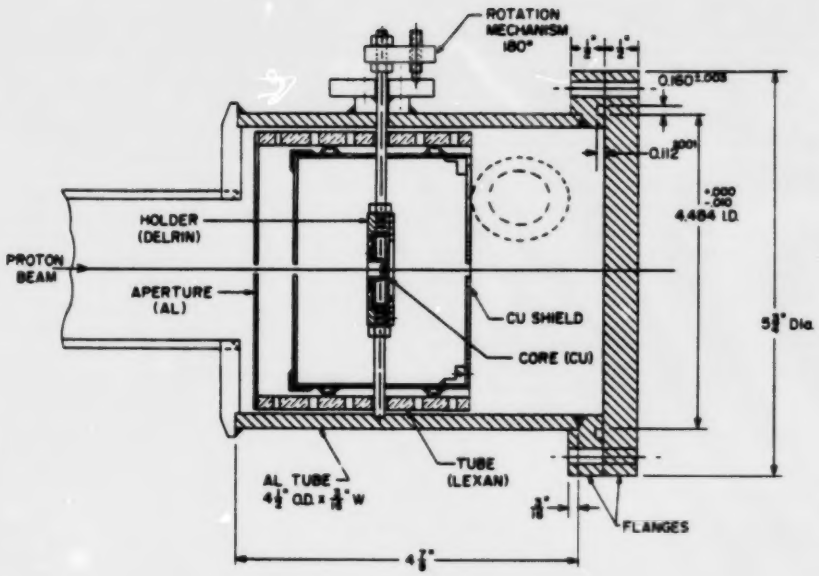

Figure 2

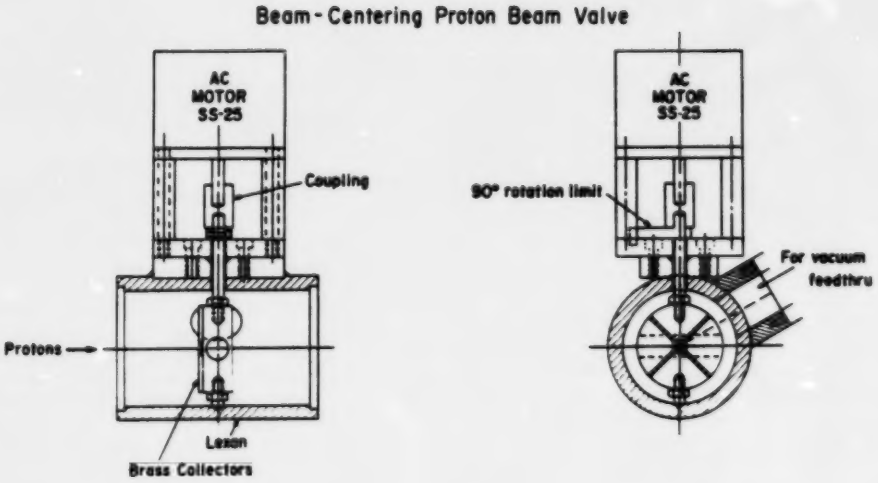

Figure 3

Discussion

Rogers: As I understand it, the target gets rotated, so that in one case the beam enters the copper directly, while in the other it enters the water through the Mylar window. Do you have to make corrections for the Mylar?

Schulz: Yes; we have not worked out the details yet.

Hohlfeld: Perhaps you can use a nickel foil. It could be made very thin.

Klassen: Presumably you need a small diameter since there is a pressure differential across the window.

Schulz: We have vacuum on one side, and the chamber is filled at atmospheric pressure. The window bulges considerably.

McDonald: Yes, I think you will need nickel foils. That's what we had to use for our work. There were two problems we worried about. One was to equalize the emissivity of both surfaces, the other was potential heat sources shining down the beam pipe.

Schulz: You were using 4 MeV protons?

McDonald: Most of our work was done with 4 MeV protons. What dose rates do you expect to use? It is difficult to get stable low currents.

Schulz: Our beam current was 20 nA. The temperature rise was not great because of the fairly large heat capacity.

-

Rogers: It is difficult to measure the current accurately because of backstreaming electrons.

Schulz: We are still working on that problem.

-

Ross: In view of Fletcher's presentation, is copper a poor choice as an absorber?

Fletcher: I don't think it's a problem.

-

[At this point, Hohlfeld made a brief presentation on their work to measure the heat defect using protons.]

Hohlfeld: We plan to use protons with energies from 5 to 20 MeV. The beam power is 250 W. The protons enter the water through a 5 μm nickel foil, which gives an energy loss of 250 keV at 5 MeV and about 100 keV at 20 MeV. We will use two methods. One is a differential measurement, like that of Schulz, for which we do not need to know the beam energy or current. In the second method, we will measure the beam energy and current so that we know the energy deposited in the absorber. Activation of the metal could be a problem and maybe the heat defect of the metal because the particle has enough energy to cause displacements in the metal.

Klassen: Clearly, there are many calculations still to be done with people going to higher LETs, high dose rates and metal surfaces in contact with thin layers of water.

-

Rogers: Would the chemists comment on whether the heat defect of ice is considerably different from that of water?

Klassen: I have never tried to calculate the heat defect for ice. Some reactions might be slower in ice due to reduced diffusion, so the heat defect might depend on the time at which you make the measurement.

Fletcher: There is less decomposition in ice isn't there?

Klassen: Yes.

FERROUS SULPHATE DOSIMETRY AND ITS ROLE IN ESTABLISHING AN ABSORBED DOSE TO WATER STANDARD FOR THE NATIONAL RESEARCH COUNCIL OF CANADA

K.R. Shortt, N.V. Klassen, C.K. Ross and G.D. Smith
National Research Council of Canada
Ottawa, Ontario K1A 0R6 CANADA

ABSTRACT: The absorbed dose measured by water calorimetry (H_2/O_2 saturated water) agrees to ±0.6% with the absorbed dose measured by Fricke dosimetry ($\varepsilon \cdot G = 3.515 \times 10^{-3}$ l $cm^{-1}J^{-1}$), corroborating our calculated value of the heat defect. We intend to use the Fricke system as a transfer standard to determine the absorbed dose to water at the reference point in a large water phantom. Following this process, we expect the uncertainty in the absorbed dose to water for 20 MV photons to be about ±0.8%.

La dose absorbée mesurée au moyen d'un calorimètre à eau (eau saturée, H_2/O_2) concorde à ± 0,6 % près à la dose absorbée mesurée par dosimétrie de Fricke ($\varepsilon \cdot G = 3{,}515 \times 10^{-3}$ l $cm^{-1}J^{-1}$), ce qui confirme notre valeur calculée du déficit thermique. Nous avons l'intention d'utiliser le système de Fricke comme étalon de transfert afin de déterminer la dose absorbée dans l'eau au point de référence dans un grand fantôme constitué d'eau. Nous prévoyons dans ce cas l'incertitude de la dose absorbée dans l'eau pour des photons de 20 MV d'être ± 0,8 %.

1. Introduction

In general, two different approaches to water calorimetry have been used in the attempt to establish an absorbed dose to water standard: the large volume water calorimeter initially proposed by Domen and the small volume water calorimeter as used in our laboratory. The purity of water in the large volume calorimeters which are open to the atmosphere is difficult to ascertain and maintain. Neither is it possible, with any degree of certainty, to reproduce the heat defect independently if the impurities are not known.

Our sealed, stirred-water, small volume calorimeter was used initially to compare the heat defect of several different aqueous solutions with theoretical calculations based on a model of water radiolysis (Ross et al. (1984)). With respect to establishing an absorbed dose standard, the difficulty with our calorimeter is that it measures the average dose over a 100 cm^3 volume which is large compared to the central element of a classical calorimeter. In other words, our calorimeter is too big to measure the dose directly at the reference point in a water phantom. Therefore, we intend to use our water calorimeter to measure $\varepsilon \cdot G$ for Fricke solution (by replacing the water in the calorimeter with Fricke solution) and in a separate experiment to use the calibrated Fricke solution in small vials to determine the dose to water at the reference point. This transfer process is attractive because the precision of the Fricke system (roughly ±0.1%) will make only a minor contribution to the overall uncertainty which is dominated by the precision of the water calorimeter response (roughly ±0.5%) and the uncertainty in our estimate of the heat defect (roughly ±0.5%). It will be necessary to make an estimate of the correction for the effect of the walls of the Fricke vials at the transfer step but no wall effect correction is required for the determination of $\varepsilon \cdot G$ since the water of the calorimeter is simply replaced by the Fricke solution.

Since there is an internationally accepted value for $\varepsilon \cdot G$ (Svensson and Brahme (1979)) and since our spectrophotometer has been calibrated absolutely, we can use the Fricke system itself to determine the average dose to water in the calorimeter. By comparing the dose determined by Fricke dosimetry to that measured by our water calorimeter, we have additional confidence that our estimate of the heat defect is correct.

2. Fricke Dosimetry at the NRCC

2.1 The fundamental equation

The fundamental equation of Fricke dosimetry is given by

$$D_{water} = \frac{\Delta OD}{\varepsilon \cdot G \cdot \rho \cdot L} \times F^{water}_{Fricke} \times k_{wall} \qquad (1)$$

D_{water} is the absorbed dose to water averaged over the volume of the solution. ΔOD is the radiation induced change in optical density measured spectrophotometrically at 303 nm. We use $\varepsilon \cdot G = 3.515 \times 10^{-3}$ l $cm^{-1}J^{-1}$ as recommended by Svensson and Brahme (1979). Both ε and G increase as the temperature increases. We use +0.69%/°C for the temperature coefficient of ε. We have measured the temperature coefficient of G to be +0.12(±0.01)%/°C and we have standardized all our measurements to 25°C. Since Fricke measurements in the calorimeter vessel were done at 21°C, the correction to G

amounts to 0.5% and is therefore quite important. The density of our Fricke solution at 25°C is $\rho = 1.0227$ g/cm^3. We use cuvettes whose path length, L, is either 2 or 4 cm and the uncertainty in L is negligible. F^{water}_{Fricke} is the ratio of dose to water and dose to Fricke. For photon beams, F is calculated by averaging the mass energy absorption coefficient over the photon spectrum. $F^{water}_{Fricke} = 1.003$ for cobalt-60 and $F^{water}_{Fricke} = 1.001$ for 20 MV photons. The uncertainty in F is about ±0.1%. Finally, k_{wall} is the factor required to correct for the effect of the walls of the vials used to measure the dose at the reference point. This factor will be discussed more fully below.

2.2 Materials

Using ultra high purity components, our Fricke solution is made according to the standard prescription (Fricke and Hart (1966)): 1 mM ferrous ammonium sulphate, 1 mM sodium chloride and 0.4 M sulphuric acid. Evidence indicating that pretreatment of the acid is unnecessary is given below.

We prepare our water in a three step process. Tap water is mechanically filtered and fed to a Barnstead Nanopure II four column deionizer which has a recirculating pump. After deionization, about 2 litres of water is batch-processed (30 minutes) in a Barnstead Organicpure UV photolysis unit. The ozone produced by this unit oxidizes any organic compounds which may be present. This water is fed to an automatic double quartz still manufactured by Quartz and Silica Ltd. The distillate is stored in quartz flasks for use in the water calorimeter or for making Fricke solution, which is also stored in quartz.

Water quality is of great importance in achieving good reproducibility for Fricke dosimetry and it may also have a significant effect on the magnitude of the heat defect in water calorimetry. There is no simple analytical procedure to test the suitability of water for water calorimetry. Water which gives reproducible results for Fricke dosimetry is probably of sufficient purity to be used for water calorimetry. There are two additional tests which can be carried out to test water quality. In a series of careful studies, Cottens et al (1982) studied how the addition of NaCl to Fricke solution caused G to be suppressed. For pure water, the suppression is 0.65% for solutions containing 1 mM NaCl. A larger effect would imply the presence of organic contaminants. Another test is to use the spectrophotometer to compare the UV absorption spectrum of water taken at various stages of the water preparation process to the spectrum of pure water. We find absorption peaks in deionized water which are not present after subsequent ozone treatment. Unfortunately, the spectra are not reproducible over the long term and we have not tried to identify the contaminants. As an illustration, figure 1 shows the absorption spectrum for our best quality water after storage in a clean high density polyethylene bottle for a period of three hours compared to the same quality of water after two days storage in a quartz vessel. Other than increasing the baseline optical density, the impurities responsible for the absorption peak at 220 nm may not be a problem in determining the radiation induced change in optical density at the ferric ion absorption peak at 224 nm. On the other hand, the presence of these molecules in solution (if we assume $\varepsilon = 100$ litre mole^{-1}cm^{-1}, their concentration would be 0.01 mM) might catalyze reactions or take part in chain reactions which could lead to a change in the sensitivity of Fricke solution response and in the magnitude of the heat defect. In summary, water, whose UV spectrum is free of absorption peaks and which can be used to produce Fricke solution whose reproducibility is good and for which the effect of adding sodium chloride is as expected, is probably of sufficient purity for water calorimetry.

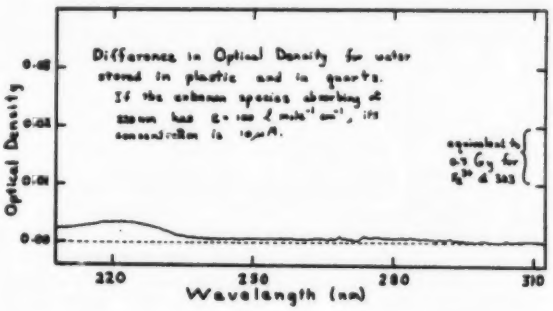

Figure 1. Differences in optical density versus wavelength

2.3 Intercomparisons

At the NRCC, Fricke dosimetry has been used since the early 1970's as the basis for a calibration service offered to radiotherapy centres (Lévesque (1977)). In 1981, a Cary model 210 spectrophotometer was purchased and a program was started to make Fricke dosimetry an in-house research tool. In 1982, an intercomparison of the optical density scale for our spectrophotometer and that of the NPL was carried out based upon potassium dichromate samples prepared according to an NBS formula (NBS 260-54 (1977)). In 1984, an intercomparison of the Fricke systems of the NRCC and the NPL was carried out and the results were reported to the BIPM (CCEMRI(I)/85-20) and are summarized in table 1 below. For each Fricke measurement, 15 vials were irradiated and the precision (one standard deviation) was ±0.1%. The over-all agreement between the Fricke results and the graphite calorimeter confirms the values used in equation (1). The agreement between items 2 and 3 for which the NRCC's spectrophotometer was used to measure the

Table 1: NRCC - NPL Intercomparison of 1984

Item	Conditions	Dose Rate to Water (cGy/min as of 1982-01-01)
1	graphite calorimetry by W.H. Henry + ionometric transfer to water	15.70 ± 0.6%
2	NRC Fricke solution with NaCl converted to dose using equation (1)	15.72
3	NPL Fricke solution read by NRC converted to dose using a modified form of equation (1)	15.69
4	NPL Fricke solution read by NPL converted to dose as for 3 above	15.71

optical density of both NPL and NRC Fricke solution, confirms that the two Fricke systems agree. It should be noted that since the NPL solution did not contain NaCl, G was increased by 0.65% compared to the value stated in section 2.1. The NRCC quartz vials are pancake shaped with a diameter of 3 cm, a height of 9 mm and a flat wall thickness of about 0.8 mm. The NPL flame sealed pyrex vials have a cylindrical volume 3 cm long and 1.2 cm in diameter with an air space at the neck. The wall correction factor k_{wall} was taken to be unity for both vial types. The agreement between the Fricke dosimetry and graphite calorimetry implies that the correction to G due to the sodium chloride and the assignment of k_{wall} equal to unity for both vials is correct unless these various effects happen to cancel fortuitously. Finally, the agreement between items 3 and 4 confirms that the spectrophotometer calibration is the same for both laboratories.

2.4 The value of $\varepsilon \cdot G$ based on calorimetry

Svensson and Brahme (1979) reviewed the value of $\varepsilon \cdot G$ for electrons of different energies and recommended the value of 3.515×10^{-3} $\ell\ cm^{-1} J^{-1}$. The paper by Mosse et al (1982) lists the relevant references including their own contribution. Values for $\varepsilon \cdot G$ are plotted in figure 2. Although all of the data published since 1980 are somewhat below the recommended value, only three of the fifteen data points deviate from the recommended value by more than 1%. Given the apparent independence of G on electron energy and the agreement between Fricke dosimetry and graphite calorimetry for cobalt-60 photons, it seems reasonable to expect $\varepsilon \cdot G$ to be within ±1% of the recommended value for all high energy radiations. If we consider only those experiments reported since 1980, namely the graphite calorimetry values of Mosse et al (1986) and Cottens et al, the total absorption value of Feist and our value (Ross et al. (1988)) using water calorimetry for 20 MV photons, the total spread in the 8 data points is less than ±0.5%. It appears reasonable to assign an uncertainty (1 standard deviation) of ±1% to the value of $\varepsilon \cdot G$ recommended in section 2.1.

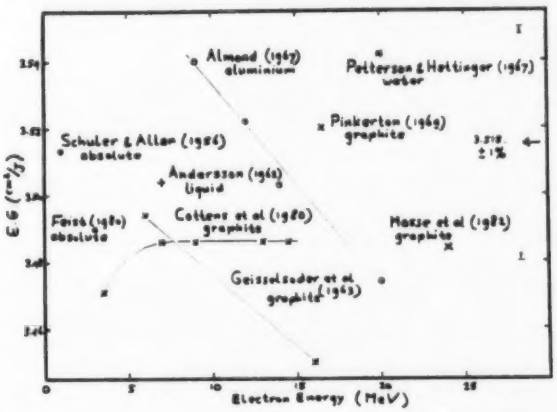
Almond (1967) aluminium
Petterson & Hettinger (1967) water
Pinkerton (1965) graphite
Schuler & Allen (1984) absolute
Anderson (1965) liquid
Feist (1980) absolute
Cottens et al (1980) graphite
Mosse et al (1984) graphite
Geissdoerfer et al (1963) graphite
Electron Energy (MeV)

Figure 2. $\varepsilon \cdot G$ versus energy for electron beams based on calorimetry. The original survey of these data was conducted by Svensson and Brahme (1979). The values shown here are taken from Mosse et al (1982) which also lists the references. All but three of the points are within ±1% of the recommended value of 3.515 $cm^2\ J^{-1}$. Our value of $\varepsilon \cdot G$ for 20 MV photons is 3.494 $cm^2\ J^{-1}$ which is in excellent agreement with the values of Feist, Cottens and Mosse, all of which were published since 1980.

3. Intercomparison of Water Calorimetry and Fricke Dosimetry

We have recently reported (Ross et al. (1988)) our results for the intercomparison of water calorimetry and Fricke dosimetry. In this experiment, we used the recommended value of $\varepsilon \cdot G$ for Fricke solution to determine the dose to water. The Fricke solution was placed in the calorimeter vessel so the average dose to the entire solution (100 cm^3) was determined in either case. A critical part of the experiment was the determination of the effect of the "foreign" mass (i.e. non-water) on the response of the calorimeter. The results are summarized in table 2 and demonstrate clearly some of our checks of self-consistency. The first column lists the mass of the vessel being used.

To start, each vessel was cleaned in hot chromic acid and rinsed with water. After assembling the calorimeter, a series of irradiations of water saturated with a

Table 2: Summary of Water Calorimetry/Fricke Dosimetry

Conditions	F_2 at 303 nm	OD Ratio 224/303 V	OD Ratio 224/303 VI	Ratio of Slopes V/VI 1.9984	Intercept (cGy)	Slope	Precision 1 σ 8 data	Difference in Control Readings
5g	0.3549	2.064	2.065	1.9982 ± 7	2.4±3.3	7.788	0.12%	0.0000
11g	0.3550	2.066	2.064	1.9931 ± 17	-3.5±3.6	7.987	0.12%	0.0000
20g	0.3549	2.064	2.063	1.9984 ± 11	3.5±2.7	7.938	0.10%	0.0006
5g, 2X[1]	0.3552	2.063	2.062	1.9988 ± 5	-4.7±5.0	7.847	0.12%	-0.0001
5g	0.3550	2.065	2.065	1.9980 ± 9	-2.6±2.7	7.915	0.10%	-0.0002
11g	0.3550	2.064	2.064	1.9973 ± 13	-8.5±1.6	7.972	0.06%	-0.0001
20g	0.3550	2.066	2.062	1.9952 ± 12	0.1±9.3	7.903	0.34%[3]	0.0001
5g, 4X[2]	0.3550	2.066	2.069	1.9979 ± 29	-1.3±3.5	7.886	0.13%	0.0001
mean	0.3550 ± 1	2.065 ± 1	2.064 ± 2	1.9971 ± 20	-1.8±3.9			

[1]the regular 5g vessel was used with the internal mass doubled

[2]the regular 5g vessel was used with the internal mass quadrupled

[3]linac was unstable

50/50 mixture of H_2 and O_2 was carried out in order to determine the thermal response per unit monitor signal. In situ, the vessel was rinsed with water and rinsed with Fricke solution following the same protocol each time. Before and after completing all the Fricke irradiations, control solutions were put into, and removed, from the vessel. The optical density difference of these unirradiated controls is shown in column 9. In spite of all the solution manipulations and rinsing required, the difference in optical density was usually no larger than twice the least significant figure displayed by the spectrophotometer (i.e. 2 × 0.0001).

Each time a sequence of readings was taken by the spectrophotometer, the optical density of a reference filter F_2 was measured. Its mean value at 303 nm recorded during these runs is given in column 2. Monthly readings in the last two years have a mean and standard deviation of 0.3549 ± 0.0001. Clearly, the spectrophotometer is maintaining its calibration.

The Fricke solution was given nominal doses of 10, 20, 30 and 40 Gy. Aliquots from every solution were read in both a 2 cm path length cuvette (#VI) and a 4 cm cuvette (#V). Optical densities were measured at 224 nm as well as 303 nm. In every case, the radiation induced change in optical density versus monitor chamber counts was fitted to a straight line. Previously it was found that the ratio of the slopes at 224 and 303 nm (2.064 ± 0.005) was very sensitive to solution contamination. Columns 3 and 4, for cuvettes V and VI respectively, show that all solutions were well behaved. The ratio of the slopes for cuvette V and VI is given in column 5. The mean value is 1.9971 ± 20 which is in good agreement with the value 1.9984 expected on the basis of mechanical measurements of the cuvette path lengths.

The intercept, slope and precision given in columns 6, 7 and 8 respectively are based on 8 data points, 4 with each cuvette. The intercept is not significantly different from zero. Based on this evidence, it was decided that no pretreatment of the sulphuric acid was required in contradistinction to most other groups who treat the acid with hydrogen peroxide or radiation. Since each entry in the table represents an entirely new experimental set-up, we do not necessarily expect the slope of Fricke response versus monitor to display good reproducibility. In each case, it is the water calorimeter and Fricke that are to be

compared using the monitor as a reference. The precision in the slope is typically ±0.1% which is sufficiently small so as to make a negligible contribution to the uncertainty in the comparison of Fricke and water calorimetry.

The contributions to the uncertainty have been summarized in table 3 where all the systematic uncertainties for the calorimeter (such as that due to the heat capacity of water) have been included in item 7 and the statistical uncertainties in the calorimeter/Fricke intercomparison have been included in item 8. We can treat the intercomparison between water calorimetry and Fricke dosimetry in two ways: taking the Fricke as having been calibrated by using $\varepsilon \cdot G$ from the literature enables a determination to be made of the heat defect for the calorimeter; using the heat defect as calculated from a knowledge of the radiation chemistry enables an estimate to be made of $\varepsilon \cdot G$ for Fricke solution. Using the first approach, the uncertainty contributions come from items 2 through 5 plus number 8 giving ±1.1% overall. Clearly, the 1% uncertainty in $\varepsilon \cdot G$ makes the largest contribution to the uncertainty in the heat defect. Using the second approach, the uncertainty in $\varepsilon \cdot G$ for Fricke for 20 MV photons comes from items 3 through 5 plus 7 and 8, giving ±0.6%. In order to transfer that dose to the dose at a point, we estimate that the uncertainty in k_{wall} will be less than ±0.4% which would make the uncertainty for 20 MV photons at the reference point ±0.8%. In summary, if we take Fricke as already having been calibrated, the uncertainty on the heat defect is ±1.1%. If we use the calorimeter measurements to estimate $\varepsilon \cdot G$ for 20 MV photons, we get the value 3.494×10^{-3} J cm^{-1}J^{-1} with an the uncertainty of ±0.6%. We will be able to transfer this dose to the reference point with an uncertainty of ±0.8%.

Table 3: Summary of Uncertainties

Item	Element	Uncertainty as %
1	Δ OD	0.1
2	$\varepsilon \cdot G$	1.0
3	ρ	0.01
4	L	0.01
5	F	0.1
6	k_{wall}*	0.4
7	heat defect	0.5
8	calorimetry/Fricke	0.4

*provisional value

4. Future Work

In order to establish the dose at the reference point, it is necessary to estimate the wall effect correction, k_{wall}. Preliminary experiments for cobalt-60 and 10 MV photons found no measurable effect as a result of decreasing the quartz wall thickness by one third. Sets of Fricke vials made of lucite and of graphite have been constructed and it has been shown that contact time between solution and vial of less than three hours does not cause an overwhelming growth in optical density of the unirradiated control solutions. These vials will also be used in estimating k_{wall}.

One of the attractive features of Fricke dosimetry is its seemingly energy independent response for high energy radiations. It is our plan to evaluate $\varepsilon \cdot G$ for cobalt-60 photons and for electrons from 10 to 30 MeV by comparing Fricke dosimetry to our water calorimeter for those radiations.

References

1. BIPM: CCEMRI (I)/85-20 (1985). Fricke intercomparison between NPL and NRC Canada.

2. E. Cottens, A. Janssens, G. Eggermont and J. Buysse (1982). Study of the effect of chloride ion on the ferric ion yield of the Fricke dosemeter in the absence of impurities, Phys. Med. Biol. 27, 597-602.

3. H. Fricke and E.J. Hart (1966). Chemical Dosimetry, chapter 12 of Radiation Dosimetry, Second Edition, Volume II, Instrumentation, edited by F.H. Attix and W.C. Roesch (Academic Press), 187.

4. R. Lévesque (1977). Results of a comparison of the measurement of absorbed dose using ferrous sulphate dosimetry, Phys. Med. Biol. 22, 278-283.

5. D. Mosse, M. Cance, K. Steinschaden, M. Chartier, A. Ostrowsky and J.P. Simoen (1982). Determination of the yield of a ferrous sulphate dosemeter in a 35 MeV electron beam, Phys. Med. Biol. 27, 583-596.

6. NBS Special Publication 260-54 (1977) entitled: "Certification and use of acidic potassium dichromate solutions as an ultraviolet absorbance standard - SRM 935".

7. C.K. Ross, N.V. Klassen and G.D. Smith (1984). The effect of various dissolved gases on the heat defect of water, Med. Phys. 11, 653-658.

8. C.K. Ross, N.V. Klassen, K.R. Shortt and G.D. Smith (1988). A direct comparison of water calorimetry and Fricke dosimetry, Phys. Med. Biol. accepted for publication.

9. H. Svensson and A. Brahme (1979). Ferrous sulphate dosimetry for electrons: a reevaluation, Acta Radiologica Oncology 18, 326-336.

Discussion

Schulz: Are you using the standard 0.8 N Fricke system?

Shortt: Yes, along with 1 mM ferrous ammonium sulfate and 1 mM sodium chloride.

-

Klassen: Ken has given a possible answer to the question of how to judge water quality; look at its absorption spectrum in the vicinity of 200 nm.

Domen: I was interested in your results on storing water in Nalgene containers. For my calorimeter, I tried returning the water used in the calorimeter to the large Nalgene container. I did this over about 220 days and found the result was a bit lower, although not more than 1%, than when I used water stored in glass vessels and discarded the water at the end of the day.

-

Schulz: Do you know if you could eliminate any of the steps in purifying your water without affecting your results?

Shortt: I have looked at the absorption spectrum at various stages in the processing. Sometimes I see absorption peaks and sometimes I don't. There have been reports on resin coming off the ion exchange columns. Sometimes I think that I can taste differences in the water at various stages in the purification. I have never observed any peaks in the water coming from the still.

Klassen: I would note that Ken's system is in fact very simple to use, and largely runs unattended.

Ross: What is the cost of your system?

Shortt: Somewhere between ten and twelve thousand dollars, including the quartz vessels used to store the water.

Concluding Remarks

C.K. Ross
National Research Council
Ottawa, Canada

I. Introduction

Yesterday, Loevinger pointed out that for radiation therapy purposes water is the reference material in which the absorbed dose is to be specified. Although there is no single compelling reason for this choice, it is by now well-established, so an absorbed dose standard should give the dose to water. The most direct way of establishing such a standard is via a water calorimeter, and much effort has been devoted to establishing an absorbed dose standard based on water calorimetry.

There are several reasons why water calorimetry is considerably more difficult than the more conventional graphite calorimetry. First of all, it is necessary to establish the heat defect of water. This is not an easy task, since the heat defect may be strongly influenced by the presence of reactive impurities. This means that water quality must be carefully controlled. Secondly, the problem of heat transfer to and from the point of measurement in large calorimeters filled with stagnant water must be carefully studied. In solid calorimeters this problem is resolved by carefully isolating a small mass surrounding the point of measurement from the rest of the phantom, but this approach is not practical for a liquid medium. Finally, because the specific heat of water is about five times that of most other common materials, the sensitivity of a water calorimeter is only one fifth that of a graphite calorimeter. This means that extra care must be taken with the temperature-sensing circuitry, especially in view of the fact that thermistor power levels need to be kept fairly low.

II Recent Progress

Presentations at this Workshop have indicated progress in all of the problem areas outlined above.

On the problem of the heat defect, Schulz and collaborators have reported on the construction and operation of a calorimeter in which care was taken to carefully control the water quality. By comparing their calorimetric measurements with measurements using ionization chambers, they get results which by and large are consistent with the predictions of the radiation chemistry of water. This is to be contrasted with the results obtained with most large water calorimeters, where the apparent absorbed dose is a few percent greater than expected. Hohlfeld, Roos and their collaborators, as well as Schulz and his collaborators, have several experiments underway which should provide a direct measurement of the heat defect. If these measurements can achieve adequate precision, they will provide an important test of our present understanding of the heat defect of water. Finally, Ross et al have reported on measurements made using a small calorimeter containing stirred water. They used water saturated with a 50/50 mixture of H_2 and O_2 gases, for which the heat defect is calculated to be -2.1%. They find that the dose measured with their calorimeter is consistent with the dose obtained using Fricke dosimetry.

In what might be termed general technical progress, Domen has reported on the development of a new, large stagnant-water calorimeter. Somewhat similar in concept to that of Schulz, the Domen design would incorporate a small sealed vessel in which the water quality would be carefully controlled. This small vessel would be embedded in a larger water phantom. Provision would be made for saturating the high-quality water with various gases. Schulz, as well as Roos, have emphasized the advantages of operating a water calorimeter at 4°C. At this temperature the density of water is maximum, so any problems due to convection are eliminated. Finally, Ross and collaborators have taken advantage of the fact that water is a liquid to construct a small calorimeter containing stirred water. This approach also eliminates the problem of convection, and allows water quality to be carefully controlled.

Finally, we note progress reported in sensing techniques. In stagnant-water calorimeters, it is important to minimize the thermistor power so as to minimize the thermal gradients established in the water near the thermistor. Kubo has reported on the possibility of operating a pulsed system in which the thermistor power is repeatedly turned on and off. This approach might permit operation at relatively high peak power (and therefore high sensitivity) while keeping the average power low. Fletcher reported on the possibility of using chain reactions to chemically enhance the sensitivity of a water calorimeter. This essentially amounts to creating a system with a very large (negative) heat defect, and Fletcher suggested that amplification factors as large as 100 might be achievable. Finally, Ross reported on Smith's development of series thermistor probes. These probes consist of six beads in series over a length of about 1 cm. By effectively increasing the area of a single bead by six times, this approach allows the probe to be operated at power levels at least six times that of a single bead.

III The Future

The work reported at this meeting suggests that absorbed dose standards based on water calorimetry should be available within the next few years. The application of water calorimetry to high energy photon and electron beams should provide more reliable dosimetry for these beam qualities. However, access to high energy photon and electron beams is considerably more difficult and expensive than to a ^{60}Co source, so it is interesting to speculate as to how the standards laboratories can best disseminate the new absorbed dose standards.

One possibility is that it will prove to be too expensive and difficult for the standards laboratories to offer routine calibrations of users' ionization chambers. Instead, the standards laboratories would use water calorimetry to test and refine the existing protocol procedures and the only direct calibration of the user chamber would be for ^{60}Co (or equivalent).

A second possibility is that the user will be prepared to cover the cost of ionization chamber calibrations at high energies. Then the user would specify the beam qualities for which he requires an absorbed dose calibration. Under this scenario, there would seem to be little or no need for the various dosimetry protocols which have been developed in the past few years.

Another possibility (there are probably many more) is that a few representative ionization chambers would be calibrated by the standards laboratories. These would then be shipped out to any users who requested the service, and used to calibrate their field instruments.

General Discussion

Shortt: With respect to practical ways to disseminate the standard; the NPL proposal to calibrate a few in-house ionization chambers at a number of beam qualities is an approach which we could also use. That is, we could use the Fricke as a transfer from the water calorimeter to calibrate some in-house ion chambers, which are easier to use on a routine basis.

Ross: Another question is whether we routinely calibrate users' chambers.

Shortt: If we could give a calibration factor for 10, 15 and 20 MV photons, how would people in the clinics like to have the standard disseminated?

Schulz: I don't think that protocols are going out of business. I think that you can only calibrate at some finite number of energies. You can't calibrate for every commercial machine which appears. They all have different target thicknesses, different scattering foils, etc. Calibrating for a span of energies will limit the uncertainties but you will still need a way to get from your 13 MeV electron beam to the user's 14 or 15 MeV beam. Custom tailored calibrations would be very expensive.

Ross: Would one foresee the development of a certain set of beam qualities as now applies to x-rays that the standards labs would provide?

Schulz: I think it will turn out a little like we do for orthovoltage calibrations in terms of exposure where we send a chamber to the Bureau and get about four or five spots and then interpolate from one quality to the next.

Cormack: I agree. I think the ionization ratio is a perfectly adequate way to describe your beam and it would be satisfactory to have calibrations covering the range you want.

Ross: How much are the clinics prepared to pay for high energy calibrations?

Shortt: Suppose it cost $1,000 a quality?

Schulz: Does that include development costs?

Ross: No. That would be roughly the cost of providing a calibration.

Schulz: Hospitals in the United States have become very cost conscious and would balk at $1,000 a point. There is the TG21 protocol and it's not all that bad as far as we can tell.

Kubo: A hospital administrator would have some problems with $1,000.

Ross: I guess people are saying that the crucial first step is to point out the problems in the existing protocols and then hospitals will be more prepared to pay the cost of having a routine calibration.

Rogers: I presume that, in practice, routine calibrations will not be done, the new standards will be used to define a new protocol which starts only with an absorbed dose calibration, which will then get modified by less than 2 or 3% for all of their beams. There will still be a protocol industry because there are a lot of other things than beam quality that are involved in protocols, such as position in the beam and recombination corrections.

Ross: Recombination corrections are a technical correction like temperature and pressure.

Rogers: Yes, but they represent a potentially significant problem in clinical situations. Hopefully, protocols will be relegated to much simpler correction factors than currently in place.

Shortt: Are you suggesting the equivalent of C_λs and C_ϵs for a handful of defined chambers?

Schulz: For the user's chamber.

Rogers: In England they have said that everyone will have the same chamber. In Canada, we can potentially talk about three or four.

Ross: Isn't that the collapse of the protocol industry if we have one chamber for which we define the response for a range of beam qualities?

Rogers: The protocol will then be used to define the beam quality. The calibration factor will be much simpler.

Ross: I think of the protocol as these twelve factors that Bob mentioned.

Schulz: Most of those will go.

McDonald: I wonder how the AAPM accredited dosimetry calibrations in the United States would fit into these proposed schemes? Could we get such things going with the ADCLs?

Loevinger: We can't expect them to have a source any more expensive than a ^{60}Co source but they may have access to accelerators after hours.

McDonald: Would you want them to have water calorimeters?

Loevinger: OK, but if it's for high energy calibrations, then they need to carry out the calibration in a high energy beam. Using an instrument for calibration which is designated for clinical work is a poor way to run a calibration laboratory.

McDonald: Could we do something in the States like a measurement quality assurance program where you would have calibrations done for one chamber for the laboratory at one time and then there would be subsequent checks by the NBS to see if there is consistency? That way, you would avoid having to pay that $10,000 every year. You would pay it once and after that, as long as you had a consistency that was demonstrable, you could continue. That method would involve sending in a chamber and have it calibrated as a function of beam quality and, in subsequent years the NBS would send you a chamber and ask you to demonstrate all of your qualities and see if your readings are consistent with theirs.

Ross: Essentially like my last approach.

Loevinger: At NBS we do send chambers out, but that's for testing calibration labs and not hospitals. Calibration laboratories are in the calibration business and you test them by sending them chambers but hospitals are in the irradiation business and you test them by sending them something to irradiate, not something to calibrate. You could send out chambers to calibration labs or rent them out to institutions whereby they would calibrate their own instruments. But how would you know if they were doing it properly? That's important now in the USA from a medical-legal viewpoint. In general, in the USA, they all want to be traceable to NBS if for no other reason than legal protection in the event of a lawsuit.

-

Klassen: Has it been defined how frequently an instrument should be calibrated?

Loevinger: It has been defined, but only arbitrarily. The NRC (USA) used to require a calibration every two years but this was stretched out to every four years because NBS couldn't handle it all. Then the five secondary calibration labs got going and they didn't have enough business to keep going. As discussed at the AAPM meetings, one calibration of a chamber which is handled properly could last a lifetime if you establish a good redundant constancy check system, that is, multiply redundant. You must check out your chamber by this redundant system before it's calibrated at the Standards Lab, then again after it comes back from the Standards Lab. You use a three- or four-fold redundancy, checking it against a ^{60}Co machine, against other ion chambers and the chance that all of these will be in error in the same way, at the same time, is too small to be considered. As to how long between calibrations, even a week with a bad instrument is too long. However, chambers do not go bad slowly. They go bad through trauma, something happens to them, or as a result of bad design, like the head coming loose.

Rogers: Once we have calibrated Fricke, we can send vials of Fricke solution out to the clinic and ask them to irradiate it in their own beams, so that we don't have to duplicate their beam qualities here, and then send them back an answer with an accuracy more or less equivalent to the standard. At the moment we quote ±3%, because that's the uncertainty the ICRU quotes for ϵG, but our precision is much better than that and we ought to be able to quote 1% accuracy.

Cormack: In the clinic, I would rather have an instrument in my possession that I knew about, even one calibrated by you at ^{60}Co rather than rely on a measurement at one spot and then to ship Fricke for a different range of energies.

-

Kubo: In the United States we have a large number of small clinics with only one dosimetrist and one clinician. It took a long time to establish the use of the TG21 protocol. Other methods are much less convenient.

Ross: I sense a conflict for the standards labs. On the one hand, you don't want to pay to have your own chamber calibrated here. On the other hand, you're not happy about getting Fricke or one of our chambers because it is not a standard setup.

Kubo: If we need five or six beam qualities, then I see $5,000 right there. Then I have to side with Bob Schulz that we have the TG21 protocol to provide the beam quality other than cobalt. We are used to paying $1,000 every two years to have calibration against cobalt.

Schulz: There is a pattern. People will send their chambers to get calibrated. It would be nice to maintain that, but you would have to do it for a number of beam qualities. Could the cost be brought down, by automation or some other way?

Ross: Ken and I have discussed this, and it would make a difference in cost if we were calibrating three user chambers at the same time versus only one. But the simple fact is that, if our standard existed, it would take most of a morning for Ken and I to calibrate for one quality on the linac. When that cost is added up, it comes to the sort of cost that Ken mentioned. But Eugenio Cecatti spent six months with us a while ago when we initiated a program which is basically the step to compare Fricke dosimetry with primarily the AAPM protocol for a range of ion chambers and a range of beam

qualities. We have had a complete pass at the measurements from ^{60}Co to 30 MV x-rays. We want to finish that project and do it for electrons as well. So from the user's point of view, you would still get the cheap calibration on ^{60}Co and you would have some confidence in the uncertainty you assign to whatever protocol you are using at the higher energies.

-

Rogers: Klaus (Hohlfeld), what will happen in Germany once yours is in place?

Hohlfeld: We have a standard, the Fricke dosimeter,which we can use at high energies and in Germany we only provide calibrations at ^{60}Co in terms of absorbed dose in the water phantom. Beyond that, we type test all types of ionization chambers to higher energies and we provide these correction factors for beam quality and they are stated in the German standard as experimentally derived factors. It is not possible for us to calibrate all chambers of the customer at higher energies, even if they are willing to pay, because we wouldn't have the time. We have about 200 clinics in Germany and it wouldn't be possible to calibrate their chambers every two years. We don't have a system as maybe in the U.K. where they have hospitals which can act as standards hospitals, and they have linear accelerators. Then, the NPL can calibrate their chambers at higher energies and the dissemination can go from the secondary standards.

-

Shortt: On one occasion in the last four years we had six chambers of the same design in the lab and I tested my ability to predict the calibration factor as a function of beam quality, knowing the factor at cobalt. Five of the chambers fell on the same curve to within 0.25% but one was out by 2.5% at the minimum of the curve. So the calibration can type test at the higher energies, but there is no way to guarantee that the manufacturer didn't make a mistake on a particular chamber.

Kehoe: Remember that the user will have more than one electrometer-ion chamber combination.

Klassen: What if that particular chamber is calibrated for different beam qualities at a standards lab and the chamber is regularly checked at ^{60}Co? Is there any reason to worry about changes at other beam qualities if nothing has changed at ^{60}Co?

Hohfeld: No.

Loevinger: In the orthovoltage x-ray regions, you cannot take ^{60}Co as a guarantee but presumably you can for the high energy region.

-

Hohlfeld: In Germany, we run our Fricke calibration service twice a year and we are limited to fifteen participants for each run. We cooperate with the NPL and they give us all their vials but we still can't cover everyone interested in this calibration service.

-

Loevinger: Carl, you seemed to imply that refining the protocols was the same as checking to see that the protocols gave the right answer. I think that refining the protocols means looking at all the correction factors in the protocols and deciding whether they are really necessary, could some be lumped together, or be made a simple function of beam quality, and then the question is how do you specify beam quality. The British are doing in terms of the TPR 20/10, the ratios of the depth doses at these two depths at a constant distance. So, in my mind, refining the protocols means simplifying them. In writing these protocols, each one of these correct'on factors was handled separately. If you know the absorbed dose, if you know the ^{60}Co calibration factor, you should find some path between them that's simpler than these protocols.

Ross: The British have refined it to the ultimate where there is just one number that the user has to know.

Loevinger: Not quite, because it's energy dependent, and they are facing the question of how shall they define the quality of their high energy beams in terms that their users will understand and they have temporarily decided on this TPR 20/10.

Ross: Right. But it seems to me that the AAPM protocol, which attempted to be as general as possible, actually gets more complicated as times goes on, and necessarily so. Dave has been pointing out this electrode correction for some chambers. As long as you want it to apply to as wide a range of chambers as possible it is inevitably going to get more complicated, not simpler.

-

Rogers: I would like to see some discussion of the jumps that some people have seen on their chart recordings.

Ross: They seem to come in two varieties. There was the sensor problem which the person felt was technical, as for example we see from time to time and which we attribute to some sort of leakage, probably with the seal in our probe. On the other hand, Seuntjens attributed a spike to a true physical effect. Clearly, one doesn't want to struggle with effects like ones due to electrical noise when the shutter moves or interference from RF systems. However, if there are real physical processes involved, it deserves more consideration.

Rogers: There were two comments during the meeting. Olof (Mattsson) mentioned that he sees an initial decrease and a corresponding increase at the end, which he attributed to charging in an electron beam but someone else said that they didn't see it in electron beams. Someone else said that when they didn't see it, it was due to the thermistor being in a glass tube.

Domen: I suspect that your (Seuntjens) signal jumps when you turn the beam on and off are due to the machine itself, that is, when you turn it on there is a current produced in your bridge circuit. Is your machine on all the time?

Seuntjens: I start the machine and, after some time the relay turns the high voltage on and then I have a jump which takes 5-6 seconds and then I have a temperature increase due to the absorbed dose in water.

Ross: Have you looked at that with the calorimeter being near the machine but not being irradiated?

Seuntjens: Using the same setup, but with the beam aligned to irradiate only the leads of the thermistor, I did not see anything.

Domen: Did your bridge have a loop where you could be picking up some kind of current which would go in one direction when the beam was on and disappear when you turned it off? I make my leads close together so they don't enclose a big area.

Mattsson: The jump I saw with electrons was not there when I irradiated with photons, even using the same machine for electrons on one day and for photons the next day without moving the calorimeter.

Ross: I believe that Schulz reported electron irradiations which did not show that effect.

Kehoe: We don't see that in Edinburgh.

-

[There followed a lengthy discussion of experimental conditions which led or did not lead to spikes on turning the beam on, with or without a complimentary spike in the opposite direction at the end of the irradiation. No grand unified theory evolved.]

-

McDonald: What was the range of the thermal defect measurements for low LET and high LET? Generally the low LET measurements may show a few percent exothermic?

Klassen: The measurements done with neutrons on air-saturated water showed 2 and 4% endothermic. My calculation, using my best guess for the G-values for that LET, gave me 3% endothermic. For low LET radiation with air-saturated water, the calculations predict 1.6% endothermic. As the LET increases, it tends to become more endothermic.

McDonald: You mean there's no indication of exothermicity at high LET?

Klassen: I have only simulated air-saturated water and pure water at high LET. Both of these are endothermic. Air-saturated water is endothermic and pure water strives to get to zero heat defect. That is not to say that someone using impure water might not start out by measuring an exothermicity. A system like water saturated with hydrogen and oxygen is exothermic at low LET is presumably exothermic at high LET.

McDonald: When Steve Domen measures a higher dose with the water calorimeter than with the ionization chamber, is that due to a negative thermal defect?

Klassen: It is well established that water calorimeters can show a negative heat defect at low LET. Chain reactions with impurities in the water may lead to a negative heat defect. Impurities catalyzing hydrogen peroxide decomposition, in the manner which Wally Fletcher described, might also do the same. We have no problem with such results. We measured about 2% exothermic initially for oxygen-saturated water when had been purified by reverse osmosis. We consider this to be dirty water. But, as we irradiated it, the radiation removed the reactive impurities, creating other, non-reactive, impurities and we finally got down to the value we expected. We measured an initial exothermicity for pure water and air-saturated water, just like the people with large calorimeters, but as we cleaned our system up, the initial exothermicity we measured got smaller and smaller.

Kehoe: However, after repeated runs in everybody's open-to-atmosphere calorimeters, they don't see any downward trend at all. Are you saying that their dose was too small?

Klassen: Well, Barnett and Schulz did see an effect by irradiating. As well, with a large calorimeter you have to irradiate the whole thing or impurities can drift in from weakly irradiated portions. They might also come in from the atmosphere or from materials in contact with the water.

-

Mattsson: In which direction should development go now from the chemical point of view? Is it the large calorimeter or the sealed type which is the future?

Ross: We share the view expressed yesterday by Bob Loevinger that the more ways people try to do it the better. For example, the approach of Schulz and the approach that Steve (Domen) is now proposing of an isolated clean system in a larger phantom all look hopeful and it is nice to have duplicate approaches that try to solve the problem. However, we suggest that the first

generation of calorimeters are such that the impurity levels cannot be controlled in a satisfactory way to lead to a primary absorbed dose standard.

Mattsson: Not even with additives for scavenging?

Klassen: It is a possibility, but we don't have the experience with the large calorimeters to be able to tell. But, there is an intrinsic attractiveness to be able to work with something which you believe should have a heat defect of zero. Those two situations are quite different. For situations when it isn't zero, you have the uncertainty in the model, whereas theory says that pure water should go to zero and the problems are really experimental, not theoretical. I am sure that, in the end, people will be happier if they have the capability of using what they consider to be the best water so they can do the pure water situation. Then how do you prove that you have reached zero? That's when the capability of being able to put in something else comes in.

DETECTION OF INDIVIDUAL VARIATION IN RADIOSENSITIVITY IN HUMAN POPULATIONS: POSSIBLE CONSEQUENCES FOR RADIOGENIC CANCER RISK AND FOR RADIOTHERAPEUTIC TUMOUR MANAGEMENT

N.E. Gentner and D.P. Morrison, Radiation Biology Branch, Atomic Energy of Canada Limited, Chalk River Nuclear Laboratories, Chalk River, Ontario KOJ 1J0, Canada.

ABSTRACT - This report details the existence, within a human population, of ostensibly normal individuals whose cultured cells, when assayed in vitro, exhibit increased sensitivity to the cytotoxic effect of ionizing radiation exposure. Study of strains derived from a cancer patient population indicates a significant association between hypersensitivity and increased probability of developing cancer.

RESUME - Ce rapport detaille l'existence, dans une population humaine, d'individus qui sont ostensiblement normaux, mais dont les cellules en culture, demontrent une sensibilite augmentee a l'effet cytotoxique de la radiation ionisante. Des etudes similaires sur des cellules derivees d'une population de patients ayant le cancer indiquent une association marquee entre l'hypersensibilite et l'augmentation de la probabilite de developper un cancer.

Background

The implication of environmental agents in cancer induction, being very amenable to study, has received considerable attention (Doll, 1977; Higginson and Muir, 1979). Increasingly, however, there is recognition of the very appreciable role played in cancer causation by genetic susceptibility factors. Many of these may be related to DNA repair competence. Persons who repair DNA damage less well may have a greater level of residual damage -- and hence of the consequences known as "late biological effects" (such as cancer) -- than do normal persons, after exposure to a given amount of a carcinogenic agent. Hence the resultant risk, which society attempts to control by setting limits on exposure, may not be equally distributed in exposed persons. Clinical epidemiologists currently recognize some two hundred Mendelian traits associated with neoplasia, as either a feature or a complication (Mulvihill, 1985), and a clear inborn susceptibility to known environmental carcinogens is known or inferred in a number of these. Abnormal susceptibility *in vitro* to particular DNA-damaging agents (carcinogens) has been demonstrated to be associated with various "cancer susceptible" genetic disorders, using tissue culture techniques and cultured cell lines derived from donors manifesting the heritable condition. Such abnormality is usually described as increased sensitivity to the cytotoxic action of the agent in question; this is deemed attributable to diminished DNA repair competence. There is wide acceptance of the principles that DNA repair protects humans against carcinogens (Arlett, 1985) and that persons with deficiencies in DNA repair are more susceptible to carcinogens and more likely to develop cancer (Lynch *et al.*, 1985).

Ataxia-telangiectasia (A-T), a severely debilitating autosomal recessive disorder which results in death by an average age of 20y, is the prototypical ionizing radiation sensitive, cancer-prone, heritable condition. Compared to an age-matched control population, the excess cancer risk in A-T patients (homozygotes; possess two copies of the defective allele) is several hundred-fold (Morrell *et al.* 1986). It turns out that this model condition is not entirely recessive, however, since a predisposing effect in asymptomatic heterozygotes (who possess one copy of the affected allele) is known. (It may therefore be more correct to call A-T an autosomal dominant disorder with a gene dosage effect). The relative risk of cancer for such A-T carriers is 2.3 for males and 3.1 for females (Swift *et al.*, 1987), the higher factor for females reflecting in part inclusion of a risk factor of 6.8 for female breast cancer specifically. A-T carriers are much more numerous (most probable value: 2.8% of the U.S. white population) than A-T patients, who represent only 3-11 of each million live-births (Swift *et al.*, 1986). A-T patients make only a minute contribution to the total cancer burden (Gentner *et al.*, 1988), and the major ill-health effect due to the existence in the human population of the A-T allele hence may be attributable to its cancer-predisposing effect when present in single copy in clinically normal carriers: the product of their relative risk and probable frequency in the population suggests that they may account for 7-8% of all cancers. These carriers appear to exhibit a small degree of increased radiosensitivity (Chen *et al.*, 1978, Paterson *et al.*, 1985).

Other heritable disorders and certain familial conditions exist that also associate cancer proneness *in vivo* with abnormal radiosensitivity *in vitro* (Paterson *et al.*, 1984; Arlett, 1985). It may be that much of this sort of variation is hidden (i.e. not related to any overt disease condition) and that an appreciable proportion of humans exhibits abnormal radioresponse. Arlett (1988) has reported that there clearly exist apparently normal individuals whose cultured cells exhibit significantly greater sensitivity to the cytotoxic action of ionizing radiation than do those from most normal persons. Our own laboratory has also identified persons, within a clinically normal cohort, whose cultured fibroblasts and/or lymphoblastoid cells exhibit substantial radiation

hypersensitivity (Gentner *et al.*, 1988; Morrison *et al.*, 1988).

The question of the range and extent of variation in radiosensitivity that exists in human populations is an exceedingly important one that should be addressed experimentally. One major reason is related to potential impact on future improvements in radiation protection (Gentner *et al.*, 1988), *viz.*:

> "The purpose of defining standards for radiation protection is to allow regulations to be promulgated to achieve the desired degree of safety. Since standards defined on the basis of existing biological data may achieve an acceptable average degree of protection but fail to adequately protect sensitive subgroups, identification of individuals with abnormal radiosensitivity, their frequency in the population at large and, ultimately, the extent of their increased risk, will provide new information relevant to advancing radiation-protection goals."

> "Traditionally, risk has been reduced linearly in the area of radiation effects by reducing exposure. The ability to identify persons of abnormal radiosensitivity and to minimize their exposure could support a disproportionate reduction".

Various national and international bodies that grapple with radiation protection concerns have been aware of this problem. The difficulty has been in an appropriate assay for putative radiosensitivity and cancer proneness. The U.S. National Academy of Sciences Committee on the Biological Effects of Ionizing Radiations (BEIR,1980) refers to the "....increasing recognition that there are human genotypes that confer both increased susceptibility or resistance to DNA damage and increased cancer risk after exposure to carcinogenic agents, including ionizing radiation", and also that "If population subsets can be identified as being at substantially greater risk of radiation carcinogenesis, their risk will require separate estimation."

The United Nations Scientific Committee on the Effects of Atomic Radiation (UNSCEAR,1988) makes a number of comments relevant to these concerns:

> "Given the genetic variability that exists between individuals .... it is reasonable to presume that the risk of cancer may vary among individuals .... when exposed to the same amount of ionizing radiation. A number of relatively rare, largely recessive disorders are known in which fibroblasts from trait-bearers are unable to repair radiation damage *in vitro*; it is also known that these individuals are at increased risk of a number of malignancies, especially malignant lymphoma and leukemia .... Some cell lines from patients with heritable diseases, including cancer-prone ones, have shown cell-killing sensitivity after such radiation ...."

> "Given the genetic variability that exists between individuals .... it is reasonable to presume that the risk of cancer may vary among individuals .... when exposed to the same amount of ionizing radiation. A number of relatively rare, largely recessive disorders are known in which fibroblasts from trait-bearers are unable to repair radiation damage *in vitro*; it is also known that these individuals are at increased risk of a number of malignancies, especially malignant lymphoma and leukemia .... Some cell lines from patients with heritable diseases, including cancer-prone ones, have shown cell-killing sensitivity after such radiation ...."

> "Data .... are sparse but suggest that there may be a small but non-trivial fraction of the human population which is prone to develop cancer and, as a consequence, may be much more liable to develop radiation-related cancers. This may mean that the average dose response pattern is a relatively poor indication of individual risk .... However, to improve the estimation of risk one must be able to identify the susceptible individuals which is not practicable at present."

Our approach

It is to this salient question that our activities have been addressed. We might expect that persons prone to 'spontaneous' or radiogenic cancer would be found within a cohort exhibiting abnormal sensitivity to ionizing radiation when assayed *in vitro*. The data base on what constitutes a "normal response" is surprisingly limited, however (Arlett,1988); most post-radiation survival analyses have been performed on strains associated with some genetic disorder. A large number of different strains from individual donors must be assayed in order to properly evaluate the range of variation in ostensibly normal persons and to determine what proportion might reasonably be regarded as showing abnormal radiation sensitivity. Conventional "survival of colony-forming ability" assays are too labour-intensive and costly, especially if fibroblasts are used; a more rapid and inexpensive screening assay is needed to ascertain the size of this susceptible sub-group. To accomplish this, we developed a novel *in vitro* assay using lymphoblastoid cell lines (Gentner *et al.*, 1988). In principle, this "grow-back assay" is akin to conventional post-irradiation "survival of colony forming ability" approaches, in that the response measured is basically one of whether irradiated cells survive the test γ-ray exposure sufficiently to sustain a reasonable subsequent period of reproductive cell division. Briefly, the re-growth curves for unirradiated (control) and irradiated cells are established using a Coulter Counter; the ratio of the slopes of the exponential portions of the irradiated to the control re-growth curves furnishes a "grow-back ratio" (GBR) which is used as one estimator of radioresponse. Use of this ratio corrects for intrinsic differences in growth rate between different strains (Gentner *et al.*, 1988), and is analogous to the 'viability ratio' approach which Tarone *et al.* (1984) concluded was the most suitable parameter to use in

growth-response assays. The ability of our assay to discriminate abnormal radiosensitivity has been validated using A-T strains and other lymphoblastoid cell strains for which significant radiosensitivity has been demonstrated using cultured fibroblasts obtained from the same donors (Gentner *et al.*, 1988; Morrison *et al.*, 1988).

We employed a "chronic γ-exposure" regime (4 Gy delivered at a dose ratio of 0.003 Gy·min^{-1}) in our testing, because such dose delivery more likely reflects the real-life situation. (In contrast, acute dose delivery is employed nearly universally elsewhere, for such screening purposes). This arose from a suggestion by Cox (1982) that a chronic exposure protocol might "....resolve differences in radiosensitivity that are masked in the response of cells to acute doses". We have demonstrated the increased discrimination of protracted compared to acute γ-exposure in detecting moderately radiosensitive responses in cultured fibroblast strains (Paterson *et al.*, 1985; Myers and Gentner, 1987).

Results & Discussion

The accompanying figure depicts the distribution of radioresponse for 270 different lymphoblastoid cell strains (upper panel) derived from ostensibly normal donors and assayed 'blind'; the inset bar, covering the 25th- to 75th-percentile responses, represents a dose range of about 1.4 (derived from GBR versus dose curves for normal strains; Morrison *et al.*, 1988). A discrete sub-set of strains, representing ~12% of the total number assayed, is evident at low GBR values (from negative values up to -0.06); these may be considered to represent highly radiosensitive responses, as they fall within the distribution of radioresponses for 11 different A-T (homozygote) strains that were assayed blind as part of the same series (middle panel). GBR's from about 0.08-0.18 include an additional 7-8% of strains, which may be of lesser but still appreciable radiosensitivity. The majority of responses (~80%) are spread over a broad range above a GBR value of 0.18 or so.

This high proportion of hypersensitive (A-T-level) radioresponses is remarkable. Since A-T comprises only 0.0003-0.0011% of live-births (Swift *et al.*, 1986), this sub-group must represent other conditions. These hypersensitive responses also do not likely include contributions from possible A-T carriers: all A-T heterozygote strains assayed to date fall above the 25th-percentile of the range of normal responses.

The question of the degree to which the A-T model predicts the cancer proneness of persons exhibiting abnormal radiation sensitivity *in vitro* thus becomes crucial. To test this, we have embarked on a similar study of the radioresponses of strains derived from freshly-presented, non-selected cancer patients. This study is in its early stages; of the strains established to date, 27 have been assayed. The distribution of their radioresponses is presented in the lower panel of the figure. Responses consonant with elevated radiosensitivity represent a higher proportion of cancer patient strains than of ostensibly normal

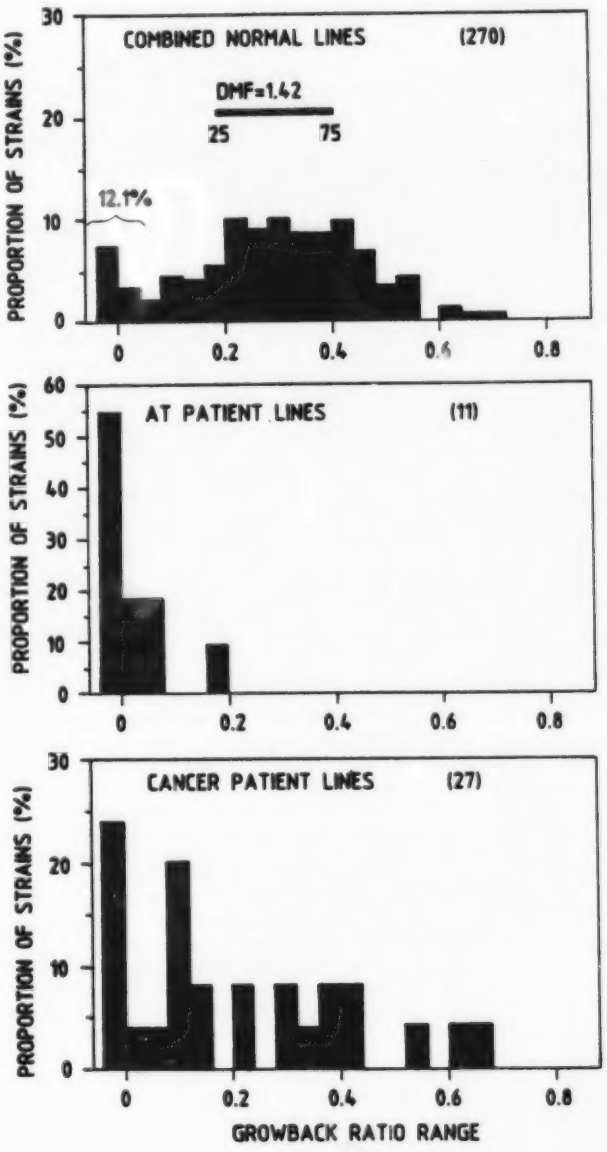

Legend to Figure:

Distributions of radioresponse, as measured by the "grow-back" assay, in three populations of lymphoblastoid cell line strains; percent of the total number of strains versus GBR in increments of 0.04. All GBR's less than zero are included in the lowest range. Upper panel: 270 strains from apparently normal donors. Middle panel: 11 strains derived from A-T patients (homozygotes); purchased from the Human Genetic Mutant Cell Repository, Camden, NJ. Lower panel: 27 cancer patient strains.

strains. The 25th-percentile (about GBR=0.18) of the normal distribution may be taken as a division point between "radiosensitive" and "more radioresistant" responses: using this, the difference between the two distributions is significant ($p < 0.05$, χ^2 test). For "radiosensitive" responses (GBR $\leq$ 0.18), the ratio of cancer patient to normal responses is 2.3; for responses of GBR $\geq$ 0.18, this ratio is 0.58. Therefore, the relative risk of cancer in donors whose cultured cells exhibit a sensitive response is 4-fold greater (i.e. 2.3 ÷ 0.58) than in the remainder of donors whose cultured cells exhibit greater radioresistance.

Whether environmental ionizing radiation exposure or "ionizing radiation-like" DNA damage may be responsible for the increased incidence of cancer in A-T patients or carriers is not known (Arlett,1985). The same holds with respect to the hypersensitive responses described here. But it would seem prudent to assume that the relative risk for radiogenic cancer in donors associated with such responses would be at least as great as shown here for "spontaneous" cancer.

Radiation protection is predicated on an implicit assumption of "equal exposure -- equal risk"; so is occupational health protection in general. Our data indicate that this assumption may not be tenable: our *in vitro* tests suggest that a significantly-sized sub-group of persons exist who are abnormally sensitive to the cytotoxic effects of ionizing radiation and who account for a substantial portion of spontaneous cancers. This information is not likely to change the total risk incumbent on exposure of human populations to ionizing radiation, since present risk estimates are based on whole populations as constituted and would therefore already include the contribution of putative susceptible sub-groups. But this new knowledge certainly indicates that the distribution of this risk may be substantially skewed. It would seem useful to consider minimizing the potential exposure of those who may be more susceptible. Even without change in present exposure limits, this would seem likely to provide a net reduction of total risk. This may be the most prudent immediate course of action. Other novel strategies for reducing risk are also possible.

Another major finding deserves mention. In a separate but related study, we have observed highly radiosensitive responses in strains from two radiotherapy patients who were clinically observed to exhibit marked radioreaction *in vivo*. One was a breast cancer patient who had a marked reaction after only 20 Gy in 8 fractions; the other was a woman with rectal cancer who exhibited a severe bowel reaction after 26 Gy and had to have treatment stopped. These results indicate that our assay may serve as a useful prognostic indicator for adverse radioreaction *in vivo*. Moreover, the concordance between extreme hypersensitivity using our *in vitro* assay and the marked radioreaction in the patients themselves provides strong supporting evidence that our screening assay estimator does indeed mirror donor radioresponse. Perhaps of greater import, the prematurely terminated treatment in the rectal cancer patient was reported by our colleague Dr. C. Danjoux (Head, Radiation Oncology) at the Ottawa Regional Cancer Clinic to result in one of the most rapid regressions they have observed for such a tumor. The GBR for this patient indicates that, in fact, she received a highly aggressive treatment relative to the intrinsic ability of her cells to repair such damage. This suggests that "tailor-made" radiotherapy protocols based on an individual's particular radiosensitivity may allow the development of more effective procedures for tumor treatment. Certainly no one level of treatment would seem appropriate for all cancer patients, given the substantial variation they exhibit in radioresponse.

Thus while our initial goal was to demonstrate how improved protection (prevention of cancer) may be accomplished, as far as achievable, application of this *in vitro* assay in the future may have societal benefit in improved cancer cure rates as well.

References

Arlett, C.J., 1985, In Familial Cancer, edited by Hj. Müller and W.Weber (Basel: Karger), pp.234-237.

Arlett, C.F., 1988, In Proceedings of the 8th International Congress of Radiation Research, Vol.2, edited by E.M. Fielden, J.F. Fowler, J.H. Hendryand D. Scott (London: Taylorand Francis), pp.424-430.

BEIR,1980, The Effects on Populations of Exposure to Low Levels of Ionizing Radiation. Committee on the Biological Effects of Ionizing Radiations (Washington:National Academy of Sciences).

Chen, P.C., Lavin, M.F., Kidson, C. and Moss, D., 1978, Nature, 274, 484-486.

Cox, R., 1982, In Ataxia-telangiectasia: A Cellular and Molecular Link Between Cancer, Neuropathology, and Immune Deficiency, edited by B.A. Bridges and D.G. Harnden (Chichester:Wiley), pp.141-153.

Doll, R., 1977, In Origins of Human Cancer, edited by H.H. Hiatt, J.D. Watson and J.A. Winstein (New York:Cold Springs Harbor Laboratory), pp.1-5.

Gentner, N.E., Morrison, D.P. and Myers, D.K., 1988, Health Physics, 55, 415-425.

Higginson,J. and Muir, C.S., 1979, Journal of the National Cancer Institute, 63, 1291-1298.

Lynch, H.T., Lynch, J.F. and Fusaro, R.M., 1985, In Familial Cancer, edited by Hj. Müller and W. Weber (Basel:Karger), pp.6-12.

Morrell, D., Cromartie, E. and Swift, M., 1986, Journal of the National Cancer Institute, 77, 89-92.

Morrison, D.P., Gentner, N.E. and Marko, A.M. (1988), In Proceedings of the International Conference on Risk Assessment of Energy Development and Modern Technology (Japan: Health Research Foundation), in press.

Mulvihill, J.J., 1985, In Familial Cancer, edited by Hj. Müller and W. Weber (Basel:Karger), pp.13-16.

Myers, D.K. and Gentner, N.E., 1987, Radiation and Environmental Biophysics, 26, 263-273.

Paterson, M.C., MacFarlane, S.J., Gentner, N.E. and Smith, B.P., 1984, Journal of Cellular Physiology, Supplement 3, 45-62.

Paterson, M.C., MacFarlane, S.J., Gentner, N.E. and Smith, B.P., 1985, In Ataxia-telangiectasia: Genetics, Neuropathology, and Immunology of a Degenerative Disease of Childhood, edited by R.A. Gatti and M. Swift (New York:Liss), pp.111-121.

Swift, M., Morrell, D., Cromartie, E., Chamberlin, A.R., Skolnick, M.H. and Bishop, D.T., 1986, American Journal of Human Genetics, 39, 573-583.

Swift, M., Reitnauer, P.J., Morrell, D. and Chase, C.L., 1987, New England Journal of Medicine, 316, 1289-1294.

Tarone, R.E., Scudiero, D.A. and Robbins, J.H., 1984, Mutation Research, 111, 79-96.

UNSCEAR, 1988, Annex G: Radiation Carcinogenesis in Man (Vienna:United Nations Scientific Committee on the Effects of Atomic Radiation, Thirty-seven session, 6-17 June 1988).